

University of Alberta

Multirate Nonlinear Sampled-Data Systems: Analysis and Design

by

Hossein Beikzadeh

A thesis submitted to the Faculty of Graduate Studies and Research
in partial fulfillment of the requirements for the degree of

Doctor of Philosophy

in

Control Systems

Department of Electrical and Computer Engineering

© Hossein Beikzadeh

Spring 2014

Edmonton, Alberta

Permission is hereby granted to the University of Alberta Libraries to reproduce single copies of this thesis and to lend or sell such copies for private, scholarly or scientific research purposes only. Where the thesis is converted to, or otherwise made available in digital form, the University of Alberta will advise potential users of the thesis of these terms.

The author reserves all other publication and other rights in association with the copyright in the thesis and, except as herein before provided, neither the thesis nor any substantial portion thereof may be printed or otherwise reproduced in any material form whatsoever without the author's prior written permission.

*To my beloved parents,
Tahereh and Mahmood
for their unconditional encouragement and support*

Abstract

This thesis concerns with a common practical problem in the area of sampled-data control systems where the plant is described by nonlinear dynamics and input and output signals are sampled at different rates. We first follow the continuous-time (emulation) approach to propose a general stabilization framework for multirate nonlinear systems in presence of disturbances. This provides a multirate H_∞ synthesis scheme which can be used to tackle the intrinsic difficulty of unknown exact discrete-time model in nonlinear sampled-data control systems. Moreover, an alternative performance criterion is introduced based on the \mathcal{L}_2 incremental gain as a stronger form of the usual \mathcal{L}_2 gain that quantifies whether or not small changes in exogenous inputs such as disturbances or noise will result in small changes at the output.

The second part of the thesis investigates the discrete-time approach based on model approximation to the problem of multirate nonlinear sampled-data systems. First, we establish prescriptive design principles for single-rate sampled-data nonlinear observer that is input-to-state stable in the presence of unknown exact discrete-time model as well as disturbance inputs. Our results are then applied to the so-called one-sided Lipschitz nonlinearities to develop constructive design techniques via tractable (linear matrix inequalities) LMIs. Taking the idea of input-to-state stable observer into account, we propose a general framework for multirate observer design that exploits a single-rate observer working at the base sampling period of the system together with modified sample and hold devices to reconstruct the missing intersample signals.

Finally, in order to verify the advantages of multirate sampling we extend our results to the area of networked-control systems (NCSs). A general output-feedback structure is developed which utilizes the same idea as that of our multirate observer to predict the missing outputs between measured samples. The proposed multirate network-based con-

troller is shown to be capable of preserving the dissipation inequality slightly deteriorated by some additive terms, in spite of network-induced uncertainties and disturbance inputs. By this means a stable NCS can be obtained under much lower data rate and a significant saving in the required bandwidth.

Acknowledgements

First and foremost, I would like to express my sincere gratitude to my supervisor Prof. Horacio J. Marquez for his valuable advice and generous support in all aspects of this research. His strong enthusiasm and skillful ideals in control theory together with patience and understanding in guiding my effort were essential from the beginning to the final stage of my journey in pursuing my PhD. Horacio's high standard and rich expertise have helped me not only to deeply understand my own research topic but also the qualifications of an engineer and researcher in large. It has been my great pleasure and an enjoyable time to work with him.

I would like to appreciate all the great friends I met here at University of Alberta. I am indebted to my colleagues at the Advanced Control Systems Laboratory for the endless friendship and valuable discussions that we had throughout the years.

Last but not least, my deepest thanks go to my lovely parents Tahereh and Mahmood, to whom I have dedicated this thesis, for their endless support and encouragement at all times. Parents, you are the most prestigious belongings in my life. I will never forget the sacrifice you made. I also dedicate this thesis to my sister, Elham, and my brother, Hamid, who have been great sources of energy for me to accomplish this thesis. For this, I am forever grateful to them.

Finally, this work was financially supported by the Natural Sciences and Engineering Research Council of Canada (NSERC) and the Informatics Circle of Research Excellence (iCORE).

Hossein Beikzadeh
Edmonton, Alberta
Canada

Notation

\mathbb{R}, \mathbb{Z}	The sets of real and integer numbers
$\mathbb{R}^+, \mathbb{Z}^+$	The sets of nonnegative real and integer numbers
\mathbb{R}^n	The set of real n -dimensional vector
$\mathbb{R}^{n \times m}$	The set of real $n \times m$ matrices
\mathcal{L}_p	Function space with well-defined p -norm
$\mathcal{L}_{p,T}$	Extended \mathcal{L}_p space of truncated signals
\exists	Existential quantifier
\forall	Universal quantifier
$x \in X$	x is an element of set X
$X \subset Y$	X is a subset of Y
A^\top or A'	Transpose of matrix or vector A
A^{-1}	Inverse of matrix A
A^\perp	Orthogonal complement of a matrix A , i.e., $A^{\perp\top}A = 0$
I	Identity matrix of appropriate dimension
$\ \cdot\ $ or $ \cdot $	Euclidean norm of a vector or matrix
$\langle \cdot, \cdot \rangle$	Natural inner product, i.e., $\langle x, y \rangle = x^\top y$
$\lfloor \cdot \rfloor$	Floor of a real number
$\lceil \cdot \rceil$	Ceiling of a real number
$B(r)$	Open ball of radius r around origin
$a \circ b$	Composition operation of a and b

Abbreviations

A/D	Analog to Digital
D/A	Digital to Analog
CTD	Continuous-Time Design
DTD	Discrete-Time Design
MSD	Multirate Sampled-Data
ISS	Input-to-State Stability
LMI	Linear Matrix Inequality
NMI	Nonlinear Matrix Inequality
NCS	Networked-Control System
SER	Signal-to-Error Ratio
R-SER	Relative Signal-to-Error Ratio

Table of Contents

1	Introduction	1
1.1	Nonlinear Sampled-Data Systems	1
1.1.1	Controller Emulation	3
1.1.2	Direct Discrete-Time Design	4
1.2	Multirate Sampled-Data Systems	6
1.3	Research Motivation and Objectives	9
1.3.1	Emulation-Based Results	9
1.3.2	Discrete-Time Approximation-Based Results	12
1.4	Thesis Outline	17
2	Mathematical Background	20
2.1	Notation and Fundamental Tools	20
2.2	Basic Definitions	21
2.2.1	Dissipativity	21
2.2.2	Input-to-State Stability	22
2.2.3	Consistency of Discrete-Time Approximate Models	24
2.2.4	One-Sided Lipschitz Condition	28
3	Multirate Nonlinear Control via Emulation Method	30
3.1	Preliminaries and Controller Setup	31
3.2	Preservation of Dissipativity in Multirate Setup	34
3.2.1	Static Feedback Case	34
3.2.2	Dynamic Feedback Case	38
3.3	Application: Multirate Nonlinear H_∞ Control	41

3.4	Summary	44
4	Nonlinear H_∞ Control Using Incremental Gain	46
4.1	State Feedback Control for Lipschitz Systems	48
4.1.1	Preliminaries and System Description	48
4.1.2	Incremental H_∞ Controller Synthesis	52
4.1.3	Uncertain Nonlinear Plants	58
4.1.4	Robust Controller Design	59
4.1.5	Robustness Analysis	61
4.2	Observer-Based Control for One-Sided Lipschitz Systems	62
4.2.1	System Model	62
4.2.2	Observer-based Controller Design	63
4.3	Simulation Results	70
4.4	Summary	77
5	Input-to-Error Sampled-Data Nonlinear Observer	79
5.1	Definitions and Problem Setting	80
5.2	Observer Design via Approximation and Input-to-State Stability	82
5.3	Observer Design via Emulation and Input-to-State Stability	85
5.4	Application: One-Sided Lipschitz Systems	86
5.4.1	DTD Method:	86
5.4.2	Emulation Method:	92
5.5	Illustrative Examples	94
5.6	Summary	99
6	Multirate Observer Design via Discrete-Time Approximation	101
6.1	Multirate System and Preliminaries	102
6.2	Multirate Nonlinear Observer	105
6.3	Simulation Examples	113
6.3.1	PVTOL	113
6.3.2	A One-Sided Lipschitz System	115
6.4	Summary	118

7	Multirate Output Feedback NCS via Discrete-Time Approximation	119
7.1	Multirate Nonlinear NCS: Modelling and Problem Setting	121
7.2	Multirate Networked Output-Feedback Stabilization	125
7.2.1	Controller Design	125
7.2.2	Dissipativity of the Multirate NCS	126
7.3	Stability of the Multirate NCS	134
7.3.1	Input-to-State Stability	134
7.3.2	Exponential Stability	135
7.4	Case Study	140
7.5	Summary	143
8	Conclusions and Future Works	144
	Bibliography	149

List of Figures

1.1	Sampled-data control system	2
1.2	General multirate sampled-data system	7
1.3	The standard setup of an NCS	15
3.1	Standard multirate sampled-data control configuration	32
3.2	The sampled-data inferential control system	33
3.3	The performance of the continuous-time H_∞ controller with sinusoidal disturbance	45
3.4	The performance of multirate and single-rate H_∞ controller under emulation with sinusoidal disturbance for $T_i = 0.4$ sec and $T_m = 2$ sec	45
4.1	(a) glow tube characteristic, (b) A one-port \mathcal{N} driven by an independent current source in series with a glow tube.	49
4.2	Disturbance nonlinearity	71
4.3	States responses in presence of the disturbance input with variable operation region	72
4.4	Norm of the penalty output	72
4.5	Time responses of the system states using the proposed robust incremental controller	74
4.6	Phase portrait of the controlled Oscillator	74
4.7	Reference tracking using the incremental H_∞ controller in presence of disturbance input	76
4.8	Phase portrait of the controlled Lorenz system	76
4.9	The simulation results for incremental observer-based H_∞ controller	78

5.1	Estimated states for different values of T under uniformly random disturbance	96
5.2	Estimated states for a fixed T and different values of h under uniformly random disturbance	96
5.3	(a) Schematic of a Chua's circuit with cubic nonlinearity, (b) A chaotic behaviour of the circuit called double-scroll attractor	97
5.4	Sampled-data state estimation of a chaotic circuit from noisy measurements using DTD and CTD observers	99
5.5	Comparison of the estimation error for two sampled-data observers	100
6.1	A schematic of the multirate nonlinear sampled-data observer.	106
6.2	Sampled-data state estimation of PVTOL with different sampling rates using single-rate and multirate observers	115
6.3	Norm of the estimation error for single-rate and multirate observers	115
6.4	Estimate of x_4 and norm of the observer error for different values of T under uniformly random disturbance	117
6.5	Estimate of x_4 and norm of the observer error for a fixed T and different values of h under uniformly random disturbance	117
6.6	Estimate of x_4 and norm of the observer error for single-rate and multirate observer under uniformly random disturbance and multirate sampling	117
7.1	Structure of the multirate NCS with output feedback controller	121
7.2	Channels model	122
7.3	Output feedback multirate controller	126
7.4	State evolution of the multirate NCS (a) under different network uncertainties and $N = 100$ (b) under different values of integration period $h = T/N$ and $\mathcal{C} = 4.33$	142
7.5	Bounds on the channel uncertainty for exponential stability under SER and R-SER models	142

Chapter 1

Introduction

This thesis explores controller and observer design for nonlinear sampled-data systems under multirate sampling. While it is a common practical problem in the area of sampled-data control systems that the input and output signals are constrained to be sampled at different rates, the analysis and design tools for nonlinear multirate systems are still limited. The purpose of this research is to cover a range of several open issues by providing different analysis and design techniques for multirate nonlinear sampled-data systems. The thesis also presents various applications of the theoretical results through simulation based studies.

In this chapter the preliminary background, the thesis objectives, the thesis contributions, and a short overview of the literature will be given.

1.1 Nonlinear Sampled-Data Systems

The significance of digitally implemented controllers in today's industry together with the fact that most systems of reasonable complexity are often described by nonlinear dynamics, motivate the area of *nonlinear sampled-data control* systems. A sampled-data system involves both continuous-time system and digital controller which is implemented by the computer. Although a linear approximation around a prescribed operating point may be used to analyze some nonlinear plants, in many situations the nonlinearities can not be neglected. This become more critical considering the fact that most practical systems and processes are nonlinear in nature. There is a wide area of applications for sampled-

data control systems, where nonlinear phenomena cannot be avoided. These applications range from the manoeuvre control of an aircraft, such as a VTOL aircraft systems, ship or submarine vehicle control, position control for robotic systems in a precision manufacturing process, autonomous vehicle systems, biochemical reactors, power plants and many others.

A general configuration of a sampled-data feedback system is shown in Figure 1.1. A continuous-time plant (process) is connected to a digital controller via analog-to-digital (A/D) and digital-to-analog (D/A) converters that are often referred to as *sample* and *hold* devices, respectively. The A/D converter samples the plant output $y(t)$ at the sampling instants t_k and sends it to a control algorithm. The controller processes the measured output $y(t_k)$ and produces a suitable sequence of control inputs $u(t_k)$. This sequence is then converted through the D/A converter into a piecewise continuous control signal $u(t)$ that is applied to the plant. This is usually done by holding the value of the control signal constant during the sampling intervals (zero-order-hold). In a single-rate setup, the sampling instants t_k are equidistant, i.e., $t_k = kT$, $k = 0, 1, 2, \dots$, where $T > 0$ is the *sampling period*.

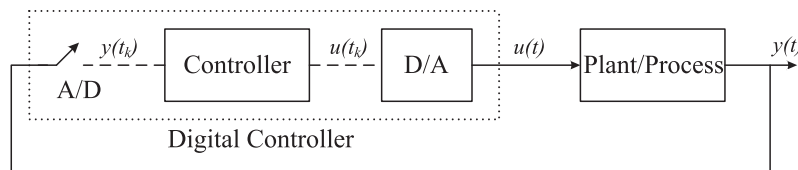


Figure 1.1: Sampled-data control system

In general, we can identify three main approaches for designing the digital controller in Figure 1.1 (see e.g., [1]):

1. The continuous-time design (CTD) method: Design based on a continuous-time model of the plant and then controller discretization (this method is often referred to as the *controller emulation* design).
2. The discrete-time design (DTD) method: Design based on a discrete-time model of the plant
3. The sampled-data design (SDD) method: Design based on the sampled-data model of the plant which also takes into account the inter-sample behaviour in the design procedure.

While the SDD method has been successfully developed for linear systems, only the first two approaches, namely CTD and DTD methods, have brought about rigorous results for nonlinear systems (see [2,3] for a survey on some recent results). This is mainly due to mathematical complexities of nonlinear equations. Sampled-data design method uses exact sampled-data model of the system and controller is designed using this model. However, the major difficulty arising when designing a controller for a sampled-data nonlinear plant is that, the exact discrete-time/sampled-data model of the plant cannot be found [4]. This is in contrast to linear systems where the exact model is usually available. The absence of such a model has lead to several schemes that use different types of discrete-time approximate models for this purpose. We now overview some of the results on single-rate nonlinear sampled-data control systems.

1.1.1 Controller Emulation

This method consists of the following steps:

continuous-time plant \Rightarrow continuous-time controller \Rightarrow discretize controller \Rightarrow implement the controller

Clearly, in this case controller design is the topic of the area of continuous-time nonlinear control. Therefore, the CTD method is well-established since a wide range of continuous-time strategies can be directly used for design of digital controllers. The main question in this method is whether the desired properties of the continuous-time closed-loop system will be preserved, and if so, in what sense for the closed-loop sampled-data system obtained by emulation.

As a starting point, we are interested in the stability of the sampled-data nonlinear system. Asymptotic stability and input-to-state stability within the emulation design framework have been addressed in [5]- [6] and [7], respectively. However, other important theoretic properties such as passivity or L_p stability may be also center of attention in some applications. In [8] Nesić and Teel propose a rather general notion of dissipativity which covers most of these properties. Precisely, two different forms of dissipation inequalities, called the “weak” and the “strong” forms, are introduced and it is shown that the exact discrete-time model of the closed-loop sampled-data system preserves the dissipation inequalities under emulation in a semiglobal practical sense [9]. The cases of static and

dynamic state feedback controllers are studied in [8] and [10], respectively. It should be noted that each of the forgoing dissipation inequalities is useful in certain situations.

There are some advantages of emulation design. First, there are many tools for controller design in continuous-time domain. Second, the sampling is taken into account at the implementation stage. Therefore, the controller design problem is separated from the problem of choosing a sampling period. However, some disadvantages may arise during the application of this method. Since the performance of the continuous-time controller can only be recovered under very fast sampling condition, because of hardware restrictions it may be impossible to reduce sampling period to a sufficiently small value to ensure desired performance. Therefore, in these cases direct discrete-time design is a better alternative which is based on discrete-time model of the plant.

1.1.2 Direct Discrete-Time Design

The design procedure of the DTD method is as follows:

continuous-time plant \Rightarrow discretize plant model \Rightarrow discrete-time controller \Rightarrow implement the controller

In this method, one first derives a discrete-time model of the plant, then designs a digital controller for the discretized plant and finally implements the designed controller using a sampler and hold device. Despite the difficulties encountered in the DTD approach for nonlinear systems, there is a strong motivation for pursuing this method since it deals with the sampling directly and effectively. Besides, as illustrated by [11] it may yield better results than the corresponding emulation design.

As mentioned earlier, the exact discrete-time model of a nonlinear plant is inaccessible in most cases. Moreover, the exact discrete-time model of a linear system is linear while the exact discrete-time model for a sampled-data nonlinear system does not usually preserve important structures of the underlying continuous-time plant, like control affine structure. Consequently, whenever we refer to the DTD method, it is always reasonable to assume that only an approximate discrete-time model is available for the controller design. The key question in the approximate DTD scheme is whether or not the properties of the closed-loop system containing the exact discrete-time model and the digital controller will be similar to those of the closed-loop system containing the approximate discrete-time

plant model and the digital controller. Several research has been done in the literature to answer this question [12,13].

One may come to believe that to obtain a stabilizing controller via the DTD method, it is sufficient to design a stabilizer for an approximate discrete-time plant model with adequately small sampling time $T > 0$. However, this reasoning is wrong as can be seen by the following counterexample.

Example 1.1. [2] Consider the sampled-data control of the triple integrator

$$\dot{x}_1 = x_2, \quad \dot{x}_2 = x_3, \quad \dot{x}_3 = u$$

Although the exact discrete-time model of this system can be computed, we base our control design on the its Euler approximate model

$$x_1(k+1) = x_1(k) + Tx_2(k), \quad x_2(k+1) = x_2(k) + Tx_3(k), \quad x_3(k+1) = x_3(k) + Tu(k)$$

a minimum-time dead-beat controller for the Euler approximation is given by

$$u(k) = -\frac{x_1(k)}{T^3} - \frac{3x_2(k)}{T^2} - \frac{3x_3(k)}{T}$$

The closed-loop system consisting of the Euler model and the dead-beat controller is asymptotically stable for all $T > 0$. On the other hand, the closed-loop system consisting of the exact discrete-time model of the triple integrator and the dead-beat controller has a pole at ≈ -2.644 and, hence, is unstable for all $T > 0$!

Therefore, no matter how small the sampling period is, we may always find a controller that stabilizes the approximate model but destabilizes the exact model for the same sampling period. Extra conditions are needed. These conditions have been characterized by [4] using the notion of *consistency*, which is a criteria for closeness of the solutions within the numerical approximation analysis. Then, the stabilization conditions for the static state feedback controller under the DTD method is investigated. The dynamic feedback case is also treated in [12]. Indeed, these results provide a unified framework for sampled-data stabilization of nonlinear plants based on the approximate discrete-time models (see also [13]).

In general, there are some advantages of the direct discrete-time design. First, the sampling is considered from the beginning of the design process. Therefore, better performance can be achieved by the controller obtained by direct discrete-time design comparing

to emulation controller. Second, larger sampling periods may be applied to the controller designed by direct discrete-time design. However, there also exist some disadvantages of this method. Since the continuous-time model is discretized at the beginning of the design process, the discretization may destroy some important properties of the continuous-time model such as feedback linearizability and minimum phase properties. Therefore, analysis and design using this method are usually harder. This disadvantage can be overcome by careful design and the choice of sampling period.

1.2 Multirate Sampled-Data Systems

The sampling period is an important design parameter in the design of digital controllers. Usually, increasing the sampling frequency enhances the performance of a sampled-data control system. However, the computer costs will also increase because less time is available to process the controller equations. Furthermore, faster sampling rates require faster A/D converters which may also increase system overall costs. Apart from costs, the selection of the sampling rates depends on many factors such as hardware restriction.

The literature overviewed in the previous section are restricted to single-rate systems where the A/D and D/A converters are applied at the same sampling rate. However, in some practical cases hardware restrictions on input and measurement sampling rate can be essentially different. For example, the D/A converters are generally faster than A/D converters, thus the measurements are often sampled at slower rates compared to the control input. This situation where the system has several sample and hold devices operating at different rates is called *multirate sampled-data (MSD)* system (see e.g., [1] and [14]). Figure 1.2 displays a general MSD system. Such cases can be seen in systems with special data transmission links or special sensors and actuators and are useful for improving the system performance. *Networked control systems* (NCS) is a good example for this type of systems. Also, use of multirate sampling is natural in multiprocessor applications.

Indeed, since the pioneering work of Kranc [15], multirate sampled-data (MSD) systems has been a topic of constant research with multiple applications, including estimation and control [16–23], fault detection and isolation [24, 25], communications and sensor

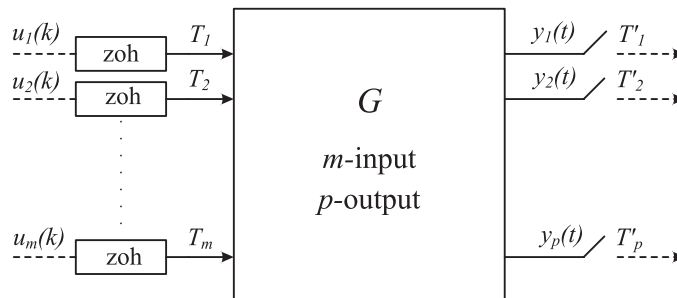


Figure 1.2: General multirate sampled-data system

networks [26,27], and digital signal processing [28–30] (see also [31,32] and the references therein for some earlier applications). Multirate systems arise when signals comprising the system are sampled at different rates, a situation that often occurs when there exist different dynamics and hardware restrictions associated with different input and output channels.

Handling the MSD system necessitates a certain type of controllers called *multirate controllers*. Indeed, if we want to control the output not only at the sampling instants but also between the sampling instants, then a multirate controller would be helpful. As classified by [33], three common approaches can be distinguished:

1. Single slow-rate method: downsample the multirate measurements to a lower sampling rate, i.e., representing the MSD system by an equivalent single-rate model whose sampling period is the least common multiple of all sampling periods in the systems. The main drawback of this method is that it doesn't use all the available information!
2. Single fast-rate method: the sampling period is the greatest common divisor of all the sampling periods of the multirate plant. Note that, this technique is applicable if all the signals are available at a faster rate than that in the original multirate system.
3. Lifting method: stacking of fast-rate measurements of a signal during one repetition period from a slow-rate signal (see e.g., [1]). This method which is the most popular approach in this context, uses all the available information in the multirate data. Roughly speaking, it involves converting the multirate system into a single-rate system (with slower sampling rate and higher dimension) using the lifting operators.

Extensive research on development and analysis of linear multirate control systems has been carried out (see e.g., [1, 34, 35] and the references therein). For instance, Longhi [36] analyzes some structural properties such as reachability, controllability and stabilizability of linear MSD plants. Linear multirate controllers for a given MSD are parameterized in [37]. After pioneering works developed by Chen and Qiu [34] on multirate H_2/H_∞ control, many researchers try to solve this problem using various methodologies, e.g., [35] and [38]. A performance comparison of the linear single-rate and multirate sampled-data systems was accomplished in [33].

Nonlinear multirate systems, however, have received comparatively much less attention and a general theory of multirate (controller and observer) design of nonlinear plants does not exist. This is mainly due to intrinsic complexity accompanied with nonlinear equations. One specific situation treated in the literature is the “low measurement rate” constraint where D/A convertors are much faster than A/D convertors. In particular, nonlinear MSD stabilization is addressed by [17–21], when the output is measured at a slower rate compared to the control input. Their main idea is to employ an inferential control setup which uses a fast-rate numerical integration scheme to reconstruct the intersample state trajectories and then supply them to a fast-rate digital controller. More explicitly, [17] studies practical asymptotic stability of the multirate setup in the presence of measurement delay for both the controller emulation and DTD strategies. This reference ignores the effect of disturbances which can have a destabilizing effect given that actual measurements are substituted with model predictions. The authors in [18] and [19] consider input-to-state stability (ISS) of the multirate system driven by disturbance inputs. These references show that the proposed inferential setup is capable of input-to-state stabilizing the nonlinear sampled-data plant in both the CTD and DTD methods, respectively, in a practical sense. In [20], we investigate the dissipativity of multirate nonlinear plants using “emulation” with emphasis on the design of \mathcal{L}_2 gain nonlinear controllers for MSD plants.

The aforementioned work consider the full-information case where all state-variables are available for feedback, a situation that may be unrealistic in many practical cases. To overcome this difficulty, [21] considers dual-rate output feedback stabilization low measurement rate. Reference [22] employs a discrete-time high-gain observer and proposes a

multirate observer-based controller for a class of nonlinear systems where, unlike [17–21], the measurement sampling rate is faster than the control update rate. Another interesting work on the subject is [23] which presents a recursive multirate approach to decrease the computational load on the classical nonlinear mode-based predictive controllers.

1.3 Research Motivation and Objectives

The purpose of this section is to briefly introduce and highlight the main contributions of this thesis. More in-depth arguments can be found in the related chapters. Although significant achievements have been obtained for multirate nonlinear systems, there still remain many unanswered questions. For instant, most of the existing results are confined to the analysis problem and less efforts have been paid to the design problem for nonlinear MSD plants. In particular, there is no systematic algorithm for multirate nonlinear observer design and most of the literature on this topic assume a full information state feedback that is unrealistic in practical situations. Moreover, stabilization has been studied only under either the “low measurement rate” constraint or the dual-rate case, hence development a theory for general multirate systems is necessary. This work is aimed at addressing some of these problems. Our main focus is on the design problem, meanwhile, we will provide some extensions and modifications to the analysis results. In general, the results in this thesis can be categorized into the emulation-based and direct discrete-time design methods. The continuous-time design is the center of attention in Chapters 3-4 and the discrete-time design based on approximation models will be pursued in Chapters 5-7.

1.3.1 Emulation-Based Results

Our disability to exactly compute the discrete-time model of nonlinear plants is the major obstacle in controlling nonlinear sampled-data systems. Nonlinear MSD plants will naturally inherit this problem with more complexities due to the existence of different sampling rates. The open-loop estimators used in [17–19, 21] to reconstruct the inter-sample state trajectories are model-based. Therefore, the robustness properties of their proposed schemes needs further investigations. These facts motivate us to develop an H_∞ strategy, that is the first choice to deal with the uncertainties and unknown plant model (see e.g., [39]), to stabilize multirate nonlinear systems. Since the continuous-time results

reported by several researchers (e.g., [40] and references quoted therein), successful results have been obtained regarding the nonlinear H_∞ control problem for discrete-time [41] as well as single-rate sampled-data systems [42, 43]. The problem of nonlinear H_∞ control is entirely based on the notion of differential games and the theory of dissipativity.

Dissipativity is a general property (see Chapter 2 for fundamental definitions) that covers several system theoretic properties including stability, input-to-state stability, passivity, L_p -stability, etc. [44]. In Chapter 3, using the idea of inferential setup utilized in [18] and the theory of dissipativity, we propose a general framework for stabilization of nonlinear MSD plants under the emulation method. Our result is applicable for both the static and dynamic state feedback case. As a special case with practical importance, it is shown that an approach to the problem of multirate H_∞ control is obtained from the proposed framework.

As mentioned before, the design procedure of the emulation method is basically performed in the continuous-time domain ignoring the effect of sampling. Hence, the main effort should be devoted to presenting a continuous-time controller with great capabilities. Following this objective, in Chapter 4 we introduce an alternative approach to nonlinear H_∞ control based on the \mathcal{L}_2 incremental gain with promising results. System *gain* is a concept that has played a crucial role in control theory. System gains were formally introduced in the control literature by Zames [45] and Sandberg [46] (see also [47], [48], [49]), and are the central tool in the input-output theory of systems that has been a cornerstone of major advances in control theory over the past three decades, including the development of the H_∞ and \mathcal{L}_1 optimal control theories and all of the robustness results that rely on the use of small gain theorems. Also proposed in those papers is the notion of *incremental gain*. For an operator $\Gamma : w \mapsto z(\mathcal{L}_{2,T} \rightarrow \mathcal{L}_{2,T})$, the induced and incremental \mathcal{L}_2 gains from the input $w \in \mathcal{L}_{2,T}$ to the output $z \in \mathcal{L}_{2,T}$ are respectively defined as follows

$$\begin{aligned} \|\Gamma\|_{i,2} &= \sup_{w \in \mathcal{L}_{2,T}, w \neq 0} \frac{\|(\Gamma w)_T\|}{\|w_T\|} \\ \|\Gamma\|_{\Delta,2} &= \sup_{w, \tilde{w} \in \mathcal{L}_{2,T}, w \neq \tilde{w}} \frac{\|(\Gamma w)_T - (\Gamma \tilde{w})_T\|}{\|w_T - \tilde{w}_T\|} \end{aligned}$$

where the extended space $\mathcal{L}_{2,T}$ contains all truncated signals with bounded 2-norm. Roughly speaking, the incremental gain is a stronger form of system gain that measures *continuity* of the input-output map and has important properties that can be of interest in con-

trol problems. In particular, incremental gains quantify whether or not small changes in exogenous inputs such as disturbances or noise will result in small changes at the output. Moreover, incremental forms of the small gain theorem ensure not only closed loop stability but also existence and uniqueness of the solution of the system equations (see e.g., [47]).

Despite these important features, incremental gains have received comparatively less attention than regular gains in the control literature. Several reasons probably contribute to this. First and foremost, when restricted to linear systems, both standard and incremental gains are identical and can be computed using the so-called *operator* norm or *induced* norm of the system. Thus, for linear systems the popular H_∞ and \mathcal{L}_1 theories enjoy all of the properties associated with the incremental gain mentioned above. When dealing with nonlinear systems, however, these similarities disappear and great care must be exercised when extending familiar concepts and theories from linear systems to the nonlinear case. The H_∞ theory, originally proposed in [50] for linear-time invariant systems, in particular, has been extended to the nonlinear case based on the fact that the concept of “induced norm” carries over to the nonlinear case without changes. The extension has led to a comprehensive body of literature of unquestionable value, but does not carry the same properties encountered in the linear case. In particular, the notion of continuity, attenuation of disturbance changes and existence and uniqueness of the system of equations in feedback systems, are all lost.

More than 20 years after [45,46], Georgiou [51] employs the incremental gain to measure the distance between nonlinear dynamical systems applicable in robust control and to introduce the notion of differential stability (see [52–54] for recent results). Incremental gains have also been employed in the input-output analysis of linear feedback loops with saturation [55–58]. In [55] the authors examine the regularity properties of this type of systems, while [56] considers the characterization and approximate computation of the incremental gain via matrix inequalities. A comparison of the induced norm and incremental gain for low-order saturating systems is presented in [57], and an approach for estimating the \mathcal{L}_2 incremental gain of piecewise linear systems with application to the anti-windup problem is provided in [58].

Motivated by the specifications discussed above, in this thesis we first synthesis a state

feedback incremental H_∞ controller for Lipschitz nonlinear plants. Then, considering a more general class of nonlinearities, namely *one-sided Lipschitz*, we tackle the problem of H_∞ output feedback control design using the incremental gain. The details are given in Chapter 4. These continuous-time techniques are cast into tractable LMIs and can be readily applied in the general multirate framework developed in Chapter 3.

One-sided Lipschitz systems were inspired by recent advances in the mathematical literature on numerical analysis and can be viewed as a generalization of the popular Lipschitz condition that has received much attention in the control literature for the past 4 decades. The one-side Lipschitz condition reduces the intrinsic conservatism in the Lipschitz approach and relaxes the assumption of linear dominance associated with classical Lipschitz based results. Explicit mathematical definition is given in Chapter 2. [59, 60] present a complete analysis of the observer convergence problem for one-sided Lipschitz systems. Existence conditions are discussed in [61] and the stabilization problem is formulated in [62]. See also [63–65] for some other recent works. In this thesis, the one-sided Lipschitz condition will be exploited to examine our general frameworks by constructing systematic design methods (Chapters 4 and 5).

1.3.2 Discrete-Time Approximation-Based Results

Direct discrete-time approach to the problem of nonlinear sampled-data systems is followed in Chapters 5 and 6 to establish single-rate and multrate nonlinear observers, respectively. Precisely, in Chapter 5 we study sampled-data nonlinear observers, understood as observers for continuous-time systems implemented using a digital computer via sample and hold devices. Observers, or state estimators, are well accepted as one of the fundamental building blocks in system theory and extensive research has been done concerning continuous-time and discrete-time nonlinear observers (see, for example, [66] and the references therein). Discrete-time observers are of particular importance because, in practice, most observers are implemented using a digital computer. Most of the literature dealing with discrete-time observers assumes the existence of a discrete-time model of the plant and proceed with the design in discrete-time. An alternative is to first design a continuous-time observer and then proceed to discretize the resulting observer using one of several discretization techniques (this is the so-called *emulation* approach). As men-

tioned earlier, the discrete-time design is usually preferred to the emulation approach as it can typically render similar performance at lower sample rates. The main difficulty encountered in the discrete-time design, however, is that finding the discrete-time model of a nonlinear plant requires solving the system's differential equation between two samples. Most nonlinear differential equations of interest do not have a closed-form solution and therefore the designer is forced to rely on approximate models.

Despite advances in nonlinear sampled-data control, sampled-data observers have received much less attention and there remain several challenging open issues. Significant results in this context include the Newton observers proposed by [67], which assumes that only sampled measurements are available, [68] that resolves the problem of unknown exact discrete-time models in [67], [69] that studies discretized high-gain observers, and [70] that proposes a general framework for sampled-data observer design along the lines in [2, 4, 13].

One important element not discussed in the existent literature on sampled-data observers is the effect of disturbances on the estimation error. Incorporating disturbance action in observers is nontrivial given that in the presence of external disturbances the reconstructed observer cannot converge to that of the true plant and therefore the notion of state convergence and analysis based on Lyapunov theory cannot be employed. One way to tackle this problem is to consider the mapping from disturbance to observer error and employ the notion of input-to-state stability to characterize the error. This analysis provides a measure of the deviation from the origin of the error dynamics that is directly proportional to the norm of the disturbance action. We mention in passing that the effect of disturbance action has typically been studied in the context of state estimation or filtering, where the primary focus is on disturbance or noise attenuation either in statistical sense (such as in Kalman filtering) or in terms of operator norms (such as in the H_∞ problem). Our primary interest is in observer convergence in the ISS sense, which can also be viewed as an L_∞ bound on the estimation error, in some sense. The use of ISS in the observer context is not new and has been applied to observer design of continuous-time plants with slope-restricted nonlinearities [71] and Lipschitz systems [72].

In Chapter 5 we present two general estimation procedures for general nonlinear systems based on (i) discrete-time design (DTD), and (ii) continuous-time design (CTD) or emulation. We show that, given a continuous-time nonlinear plant model, then under some

standard assumptions and Lyapunov-ISS conditions, the proposed observers converge to the true plant state at each sampling instant in an input-to-state stable, semiglobal practical sense. Then we confine our attention to *one-sided Lipschitz* condition to obtain constructive algorithms for a special class of systems. We present two DTD and CTD (emulation)-based schemes that ensure *input-to-error stability* in terms of LMIs. Both of the proposed observers introduce refined Euler models by incorporating an integration parameter together with the sampling period to approximate the exact discrete-time models.

Inspired by the single-rate input-to-error stable observer introduced in Chapter 5, in Chapter 6 we tackle the observer design problem for nonlinear MSD systems under the effect of disturbance inputs. Our main purpose is to layout a general framework for multirate observer synthesis. The main idea is to introduce a fast-rate sampler that reconstructs the inter-sample outputs between measured samples using an approximate discrete-time model of the plant together with the system output function and a modified hold device that assigns each control input to its previous measured value during the corresponding sampling interval. The outputs of the modified sample and hold devices are then fed to a single-rate observer working at the base sampling period of the plant. Taking the disturbances as the input and the estimation error as the state, the notion of input-to-state stability (ISS) is adopted to analyze the convergence of the estimation error. We show that if the single-rate observer is input-to-state stable, under some standard assumptions and Lyapunov-ISS conditions, the proposed multirate observer is input-to-state stable in the semiglobal practical sense.

Our approach deals explicitly with (i) the model mismatch introduced by the discrete-time approximation (discussed in [70] for single-rate sampled-data observers), and (ii) the effect of disturbances and consequent deviations of the model estimates from true plant outputs. Our proposed sampled-data scheme is not restricted to either the high gain observers used in [22] or to the dual-rate case studied by [21] and covers the “low measurement rate” case addressed in [17–21] as a special case.

Finally, in Chapter 6 we will study a practical application of multirate sampling by proposing a general output feedback framework for nonlinear networked-control systems (NCSs) based on discrete-time approximation. Unlike the emulation results of Chapter 3,

in this chapter all of the state variables are not necessarily available for measurement that is a more realistic assumption.

Feedback control loops in which system components (sensors, controller, actuators, etc.) are exchanging data over a wired or wireless communication network constitutes an attractive and challenging research area in control theory that is called Networked Control Systems (NCSs) (see Figure 1.3). The main motivation behind the recent increasing interest in NCSs is to offer great advantages, such as low cost, simple diagnosis and maintenance, high reliability and flexibility compared with the conventional control systems [73]. Moreover, capabilities of NCSs have been demonstrated in numerous applications including mobile sensor networks [74], automated highway systems [75], unmanned aerial vehicles [76], and multi-agent systems [77]. However, the insertion of a network in the control loop is accompanied with different kind of imperfections and uncertainties such as quantization, packet dropout, communication delay, and limited data rate, etc., which are potential resources of performance degradation and/or instability. Therefore, in order to exploit the benefits of the network-based control systems by preserving the closed-loop stability (and performance) in the face of these constraints imposed by networks, several specific control techniques have been reported in the literature. The current status and overview of available NCS structures can be found in special issues [78,79] and many survey papers, e.g., [80,81].

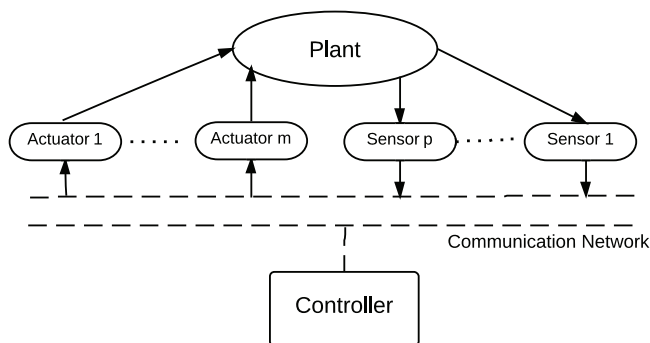


Figure 1.3: The standard setup of an NCS

The efforts on NCSs are mostly devoted to the modelling, stability analysis and controller synthesis of linear NCSs (see e.g., [81] and the references cited therein). Significant results have also been presented for the nonlinear counterpart problem, however, with relatively less expansion. Among others, continuous-time approach toward NCS by consider-

ing networked-induced effects is pursued in [82, 83] to stabilize a certain class of nonlinear systems based on Lyapunov-Krasovskii functions, in [84] to develop model predictive control strategy, in [85, 86] to address the output feedback problem using Riccati inequalities, and in [87–89] to analyze stability within general frameworks which make use of controller discretization (emulation). On the other hand, there exist only a limited number of works on discrete-time approach for nonlinear NCSs. Inspired by the theory of nonlinear sampled-data systems (see e.g., [4, 13]) based on discrete-time approximation, [90] proposes a model-based communication protocol to deal with time varying delays and packet losses in nonlinear NCSs. Very recently, [91] extends the same theory to the case of time varying and uncertain sampling intervals and delays (that are not enforced to be multiple of the sampling interval like what assumed in [90]), to derive sufficient conditions for the global exponential stability of the nonlinear discrete-time NCSs. It is worth noting that discrete-time design usually preferred to emulation-based controllers due to direct incorporation of the sampling period and providing better performance. Besides, it is shown by [92] that in the case of linear NCSs, discrete-time approach may reduce conservatism.

In practice, since there exist different dynamics and hardware restrictions associated with different input and output channels, it is often unrealistic to sample all the signals comprising the system uniformly at one single rate. Therefore, multirate systems, in which different sampling rates coexist, has found prominent importance in control applications. Aside from the physical limitations, multirate sampling brings specific advantages to NCSs:

- It can often decrease the required storage space or computational complexity for signal processing,
- Not only it does not violate the finite bandwidth constraint in NCSs, but also can increase overall efficiency by effective usage of the available data rates,
- Multirate controllers are generally time varying, hence they can achieve what single-rate systems cannot [1].

The objective of the model-based NCSs recently presented by e.g., [90, 93, 94] is also to reduce the communication bandwidth requirement by creating more dependence on the plant model rather than the actual measurements. However, the restrictive assumption of single-rate sampling rates was always made in these works. Inclusion of multirate

operations in NCSs can be seen in [95], where a subband coding scheme is proposed to efficiently use the limited bit rates and to account for message losses. The problem of model predictive control for networked-based multirate systems is studied in [96] via a switched Lyapunov function approach. The ideas of channel resource allocation and topological entropy of the plant are adapted in [97] to obtain necessary and sufficient condition for stabilization of linear continuous-time system NCSs with imperfect multirate input channels, in pursuit of [98] which focuses on discrete-time systems with imperfect single-rate input channels. To the best of the author’s knowledge, nothing has been reported on the nonlinear multirate NCSs and usually full information state feedback is assumed in the existing linear multirate NCSs.

In Chapter 6, we employ the theory of dissipativity to stabilize multirate nonlinear NCSs in the face of network-induced constraints and disturbance inputs. A general sampled-data framework is proposed which utilizes a numerical prediction scheme together with an output feedback controller to preserve a certain dissipation inequality. This work generalizes the results of Chapter 3 to output feedback stabilization of multirate nonlinear sampled-data systems via discrete-time design and in presence of a communication network. Then, as special cases with practical importance explicit conditions in terms of different sampling rates and network uncertainties are derived to guarantee, respectively, the input-to-state stability and exponential stability of the disturbance driven and disturbance free multirate NCS.

1.4 Thesis Outline

The organization of this research can be summarized as below:

Chapter 2: In this chapter, technical preliminaries are provided. Common notation and definitions which will be used throughout the thesis are also presented.

Chapter 3: This chapter deals with a common practical problem where the output of a nonlinear sampled-data system is constrained to be measured at a relatively lower sampling rate. Designing a continuous-time controller that satisfies a specific dissipation inequality, it is shown that the closed-loop sampled-data system obtained by digitally implementation of the emulated controller in a multirate scheme preserves similar dissipation inequality in a semiglobal practical sense. Moreover, we address multirate nonlinear H_∞ control via

emulation method as an important application.

Chapter 4: The \mathcal{L}_2 incremental gain is proposed as an alternative to the usual gain for designing nonlinear H_∞ controllers. Considering a class of plants with Lipschitz nonlinearities and using LMIs, a state feedback controller is designed such that the closed-loop system is exponentially stable in the absence of disturbance inputs and has \mathcal{L}_2 incremental gain less than or equal to a minimized number in the presence of disturbances as well as model uncertainties. Moreover, a norm-wise robustness analysis of the proposed technique against nonlinear uncertainties has been accomplished. Our result is verified through stabilization of both certain and uncertain systems in an incremental sense and also input tracking of a chaotic plant.

In the second part, an H_∞ output feedback controller is presented for one-sided Lipschitz systems, which consists of a state feedback control together with a nonlinear observer. By proposing the \mathcal{L}_2 incremental gain as an alternative H_∞ performance measure to the usual gain, we develop a design technique that guarantees an asymptotically stable closed-loop system in the absence of disturbance inputs and further minimizes the incremental gain from disturbances to the controlled output. This method is based on the Lyapunov function parametrization and is formulated in terms of LMIs. Our result is then validated via numerical example of a discontinuous plant exposed to disturbance inputs with numerous variations.

Chapter 5: In this chapter the design of sampled-data state observer for nonlinear plants is investigated under the effect of system and measurement disturbance signals. We establish general design principles using the standard approaches of (i) direct discrete-time design via approximation and (ii) discretization of a continuous-time observer (emulation). By interpreting the disturbances as exogenous inputs affecting the error dynamics, sufficient conditions are derived which ensure input-to-state stability (ISS) of the proposed sampled-data observers with respect to the estimation error in a semiglobal practical sense, in the presence of unknown exact discrete-time model as well as disturbance inputs. Our results are then applied to the so-called one-sided Lipschitz nonlinearities to develop constructive design techniques via tractable LMIs. Simulations of an academic example and a chaotic attractor validate the effectiveness of the proposed sampled-data estimators based on the approximation and emulation methods.

Chapter 6: This chapter is devoted to the problem of nonlinear state estimation under multirate sampling in presence of disturbance inputs. Considering a general description of a nonlinear sampled-data system, we establish a prescriptive framework for multirate observer design via an approximate discrete-time model of the plant. This framework is shown to be input-to-state stable in a semiglobal practical sense with respect to the estimation error for the unknown exact discrete-time model. A numerical example of an aerospace vehicle with input and output channels of various sampling rates demonstrates how the multirate observer can drastically improve performance compared with the single-rate observer.

Chapter 7: This chapter studies the problem of output feedback stabilization of nonlinear networked control systems (NCSs) with multirate sampling. Modeling the network induced constraints as multiplicative or relative uncertainties to the input and output channels a general framework for the multirate nonlinear NCS design is established that exploits a dynamic sampled-data output feedback together with a numerical integration scheme based on discrete-time approximate models to predict the missing intersample measurements. The behavioral analysis is performed in the context of dissipativity theory. We show that given an output feedback control satisfying a certain dissipation inequality for the single-rate NCS, under standard continuity and consistency assumptions the proposed multirate network-based structure is also dissipative with respect to similar supply rate slightly deteriorated by some additive terms, in spite of channels uncertainties and disturbance inputs. These terms are closely related to the sampling rates and the integration period and can be modified elaborately to preserve the input-to-state stability (ISS) in a semiglobal practical sense. Moreover, sufficient conditions are provided which guarantee the exponential stability of the uncertain multirate NCS in the absence of disturbances. A simple simulation example exhibits some important features of the design approach by rendering a stable closed-loop system under low rate of data transmission.

Chapter 8: The concluding remarks and future work related to the research are discussed in this chapter.

Chapter 2

Mathematical Background

This chapter provides technical preliminaries and definitions and fixes some standard notation that will be used throughout the thesis.

2.1 Notation and Fundamental Tools

For a given function $d : \mathbb{R}^+ \rightarrow \mathbb{R}^q$, $d(k)$ indicates the value of $d(\cdot)$ sampled at $t = kT$, $k \in \mathbb{Z}^+$ and $\bar{d} = d[k] := \{d(t) : t \in [kT, (k+1)T], k \in \mathbb{Z}^+\}$ with the norm $\|d[k]\|_\infty = \text{ess sup}_{\tau \in [kT, (k+1)T]} |d(\tau)|$.

The classes of functions defined below play an important role in characterizing stability of nonlinear systems.

Definition 2.1. *A continuous-time function $\alpha : [0, a) \rightarrow [0, \infty)$ is said to belong to class \mathcal{K} if it is strictly increasing and $\alpha(0) = 0$. It is of class \mathcal{K}_∞ if, in addition, $a = \infty$ and $\lim_{t \rightarrow \infty} \alpha(t) = \infty$. Functions of class \mathcal{K}_∞ are invertible.*

Definition 2.2. *A continuous-time function $\beta : [0, a) \times [0, \infty) \rightarrow [0, \infty)$ is said to belong to class \mathcal{KL} if for each fixed t , $\beta(\cdot, t)$ is of class \mathcal{K} with respect to t and for each fixed s , $\beta(s, \cdot)$ is decreasing with respect to s and $\lim_{t \rightarrow \infty} \beta(s, t) = 0$.*

Two basic mathematical theorems that are useful in this thesis are provided below.

Theorem 2.1. (Mean Value Theorem) *Assume that $f : \mathbb{R}^n \rightarrow \mathbb{R}$ is continuously differentiable at each point x of an open set $S \subset \mathbb{R}^n$. Let x and y be two points of S such*

that the line segment $L(x, y) \subset S$. Then there exists a point $z \in L(x, y)$ such that

$$f(y) - f(x) = \frac{\partial f}{\partial x} \Big|_{x=z} (y - x) \quad (2.1)$$

The line segment $L(x, y)$ joining two distinct points x and y in \mathbb{R}^n is

$$L(x, y) = \{z | z = \theta x + (1 - \theta)y, 0 < \theta < 1\} \quad (2.2)$$

Theorem 2.2. (Gronwall-Bellman Inequality) Let $\lambda : [a, b] \rightarrow \mathbb{R}$ be continuous and $\mu : [a, b] \rightarrow \mathbb{R}$ be continuous and nonnegative. If a continuous function $y : [a, b] \rightarrow \mathbb{R}$ satisfies

$$y(t) \leq \lambda(t) + \int_a^t \mu(s)y(s)ds \quad (2.3)$$

for all $a \leq t \leq b$, then on the same interval

$$y(t) \leq \lambda(t) + \int_a^t \lambda(s)\mu(s)e^{\int_a^s \mu(\tau)d\tau} ds \quad (2.4)$$

In particular, if $\lambda(t) = \lambda$ is a constant, then

$$y(t) \leq \lambda e^{\int_a^t \mu(\tau)d\tau} \quad (2.5)$$

if, in addition, $\mu(t) = \mu \geq 0$ is a constant, then

$$y(t) \leq \lambda e^{\mu(t-a)} \quad (2.6)$$

2.2 Basic Definitions

2.2.1 Dissipativity

The notion of dissipativity is a broad system theoretic property which allows us to study connections between input-output stability and classical Lyapunov stability of state space realizations. Roughly speaking, it indicates there can be no “internal creation” of energy. Therefore, the stored energy in a dissipative system at time $t = t_1$ is, at most, equal to the energy initially stored at time $t = t_0$, plus the total energy externally supplied during the interval $[t_0, t_1]$.

Consider a dynamical system given by the following state space realization

$$\Sigma : \begin{cases} \dot{x}(t) = f(x, u), & u \in \mathcal{U}, x \in \mathcal{X} \\ y(t) = h(x, u), & y \in \mathcal{Y} \end{cases} \quad (2.7)$$

where $\mathcal{X} \subset \mathbb{R}^n$, $\mathcal{U} \subset \mathbb{R}^m$, $\mathcal{Y} \subset \mathbb{R}^p$ are, respectively, the state, input and output spaces. Associated with (2.7) we define a function $w(t) = w(u(t), y(t)) : \mathcal{U} \times \mathcal{Y} \rightarrow \mathbb{R}$, called *supply rate* (*dissipation rate*), that is a locally integrable function of the input u and output y of the system Σ .

Definition 2.3. [49] *A dynamical system Σ is said to be dissipative with respect to the supply rate $w(t)$ if there exists a function $\phi : \mathcal{X} \rightarrow \mathbb{R}^+$, called the storage function, such that for all $x_0 \in \mathcal{X}$, all $t_1 \geq t_0$, and all inputs $u \in \mathcal{U}$*

$$\phi(x(t_1)) \leq \phi(x(t_0)) + \int_{t_0}^{t_1} w(u(t), y(t)) dt \quad (2.8)$$

where $x(t_0) = x_0$ and $x(t_1)$ is the state of Σ at time t_1 resulting from initial condition x_0 and input function $u(\cdot)$.

The inequality (2.8) is called the *dissipation inequality*. In general, the storage function ϕ need not be differentiable. However, the most widely used form of (2.8) upon which several important results can be obtained, is the *differential dissipation inequality* which further assumes a continuously differentiable storage function. More explicit definition is given in Chapter 3. Also, the discrete-time form of dissipativity will be reviewed and applied in Chapter 7.

There are several interesting candidates for the supply rate $w(t)$ each of which implicates a certain property such as input-to-state stability, passivity, small gain, \mathcal{L}_p stability, etc. One common type known as *QSR-dissipativity* in the literature is obtained by considering $w(t) = y^\top(t)Qy(t) + 2y^\top(t)Su(t) + u^\top(t)Ru(t)$, that covers different kinds of passivity as well as the finite-gain stability as special cases of interest for specific choices of the parameters Q , S , and R . The interested reader is referred to [40, 49, 99] for more details.

2.2.2 Input-to-State Stability

The concept of *input-to-state stability* (*ISS*) was firstly introduced by [100] as a natural generalization of asymptotic stability to fill the gap between stability in the sense of

Lyapunov on one hand and input-to-output stability on the other hand of the spectrum. ISS is basically utilized to analyze stability of systems described by state space realization with variable input functions by investigating whether or not *bounded inputs* results in *bounded states*. Although for linear time-invariant (LTI) systems where all notions stability coincide, input-to-state stability is equivalent to asymptotic stability of the unforced plant, the nonlinear case is a lot more subtle. One can easily find simple counterexamples showing that, in general, these implications fail for nonlinear systems.

Consider a nonlinear system with input

$$\dot{x}(t) = f(x(t), u(t)) \quad (2.9)$$

where $f : D \times D_u \rightarrow \mathbb{R}^n$ is continuously differentiable in x and u , and the sets D and D_u is defined by $D = \{x \in \mathbb{R}^n : \|x\| < r\}$, $D_u = \{u \in \mathbb{R}^m : \text{ess sup}_{t \geq 0} \|u(t)\| = \|u\|_\infty < r_u\}$. Note that these assumptions guarantee the local existence and uniqueness of the solutions of the differential equation (2.9). The input-to-state stability is defined as follows.

Definition 2.4. *The system (2.9) is said to be locally input-to-state stable (ISS) if there exists a class \mathcal{KL} function $\beta(\cdot, \cdot)$ and a class \mathcal{K} function $\gamma(\cdot)$ such that*

$$\|x(t)\| \leq \beta(\|x_0\|, t) + \gamma(\|u\|_\infty) \quad (2.10)$$

for all $x_0 \in D$, $u \in D_u$, and $t \geq 0$. It is said to be input-to-state stable, or globally ISS if $D = \mathbb{R}^n$ and $D_u = \mathbb{R}^m$.

Remark 2.1. *The input vector u of the system may have two different interpretations; first, it can be a control, which is free to be designed to satisfy specific performance criteria of the system and second, it can be an internal or external perturbation of the model like exogenous disturbances. This case is considered Chapters 5-7*

Remark 2.2. *For the unforced system $\dot{x} = f(x, 0)$, ISS implies that the origin is uniformly asymptotically stable.*

Remark 2.3. *An alternative way to Definition 2.4 is to replace (2.10) by*

$$\|x(t)\| \leq \max\{2\beta(\|x_0\|, t), 2\gamma(\|u\|_\infty)\} \quad (2.11)$$

The equivalence comes from the fact that given $\beta > 0$ and $\gamma > 0$, $\max\{\beta, \gamma\} \leq \beta + \gamma \leq \max\{2\beta, 2\gamma\}$.

Lyapunov-like conditions can be stated to characterize the input-to-state stability.

Definition 2.5. *A continuous and differentiable function $V : \mathbb{R}^n \rightarrow \mathbb{R}$ is called an ISS Lyapunov function for the system (2.9) if there exists class \mathcal{K}_∞ functions $\alpha_1, \alpha_2, \alpha_3$ and σ such that the following conditions are satisfied:*

$$\alpha_1(|x|) \leq V(x) \leq \alpha_2(|x|) \quad (2.12)$$

$$\frac{\partial V(x)}{\partial x} f(x, u) \leq -\alpha_3(|x|) + \sigma(|u|) \quad (2.13)$$

for all $x_0 \in \mathbb{R}^n, u \in \mathbb{R}^m$.

Theorem 2.3 gives necessary and sufficient conditions for ISS.

Theorem 2.3. *The nonlinear system (2.9) is input-to-state stable if and only if there exists an ISS Lyapunov function for the system.*

We mention that input-to-state stability is a special case of dissipativity. Moreover, the discrete-time form of ISS that is the central analysis tool in Chapters 5-7 will be introduced later.

2.2.3 Consistency of Discrete-Time Approximate Models

Throughout this thesis the discrepancy between the exact and approximate discrete-time models is measured via the concepts one-step and multi-step consistency. Consider again the continuous time nonlinear system (2.9) with the control input u that is realized through a zero-order hold device, i.e., $u(t) = u(kT) := u(k), \forall t \in [kT, (k+1)T), k \in \mathbb{Z}^+$, where T is the sampling period. The difference equation corresponding to the exact discrete-time model of (2.9) and its approximate model are, respectively, represented by

$$x(k+1) = x(k) + \int_{kT}^{(k+1)T} f(x(\tau), u(k)) d\tau := F_T^e(x(k), u(k)) \quad (2.14)$$

$$x(k+1) = F_T^a(x(k), u(k)) \quad (2.15)$$

As mentioned earlier in Chapter 1, F_T^e is not usually available for nonlinear systems and hence, the approximation F_T^a will be used in our analysis and design. We employ two notions adopted from the numerical analysis literature to measure the closeness of solutions of (2.14) and (2.15). The first type of closeness guarantees that the error between solutions starting from the same initial condition is small over *one step*, relative to the size of the step.

Definition 2.6. (One-Step Consistency) [13] *The family $F_T^a(x, u)$ is said to be one-step consistent with the exact discrete-time model $F_T^e(x, u)$ if, for each compact set $\Omega \subset \mathbb{R}^n \times \mathbb{R}^m$, there exist a class- \mathcal{K} function $\rho(\cdot)$ and a constant $T^* > 0$ such that for all $(x, u) \in \Omega$ and $T \in (0, T^*]$ we have*

$$|F_T^e(x, u) - F_T^a(x, u)| \leq T\rho(T) \quad (2.16)$$

A sufficient condition for one-step consistency is the following whose proof is given in [4, 9].

Lemma 2.1. *If*

1. F_T^a is one-step consistent with F_T^{Euler} where $F_T^{Euler} = x + Tf(x, u)$,
2. given any strictly positive real numbers (δ_x, δ_u) , there exists $\rho_1 \in \mathcal{K}_\infty$, $M > 0$, $T^* > 0$ such that for all $T \in (0, T^*)$ and $|x_1| \leq \delta_x$, $|u| \leq \delta_u$

- $\max_{|x| \leq \delta_x, |u| \leq \delta_u} |f(x, u)| \leq M$
- $|f(x_1, u) - f(x_2, u)| \leq \rho_1(|x_1 - x_2|)$

then, F_T^a is one-step consistent with F_T^e .

By Lemma 2.1, it can be shown that the Euler approximate model is one-step consistent with the exact model. The second type of closeness guarantees that the error between solutions starting from the same initial condition is small over *multi steps*, relative to the size of the step.

Definition 2.7. (Multi-Step Consistency) [4] *The family $F_T^a(x, u)$ is said to be multi-step consistent with the exact discrete-time model $F_T^e(x, u)$ if, for each $L > 0$, $\mu > 0$ and each compact set $\Omega \subset \mathbb{R}^n \times \mathbb{R}^m$, there exist a function $\alpha : \mathbb{R}^+ \times \mathbb{R}^+ \rightarrow \mathbb{R}^+ \cup \{\infty\}$ and $T^* > 0$ such that for all $T \in (0, T^*]$, we have*

$$\{(x_1, u) \in \Omega, (x_2, u) \in \Omega, |x_1 - x_2| \leq \delta\} \Rightarrow |F_T^e(x_1, u) - F_{T,h}^a(x_2, u)| \leq \alpha(\delta, T) \quad (2.17)$$

and

$$k \leq L/T \Rightarrow \alpha^k(0, T) := \overbrace{\alpha(\dots \alpha(\alpha(0, h), h) \dots, h)}^k \leq \eta \quad (2.18)$$

A sufficient condition for multi-step consistency is the following whose proof is given in [4].

Lemma 2.2. *If for each compact set $\Omega \subset \mathbb{R}^n \times \mathbb{R}^m$ there exist $K > 0$, $\rho \in \mathcal{K}_\infty$ and $T^* > 0$ such that for all $T \in (0, T^*]$ and all $(x_1, u) \in \Omega$, $(x_2, u) \in \Omega$ we have*

$$|F_T^e(x_1, u) - F_T^a(x_2, u)| \leq (1 + KT)|x_1 - x_2| + T\rho(T), \quad (2.19)$$

then F_T^a is multi-step consistent with F_T^e .

Remark 2.4. *It can be inferred that the condition of Lemma 2.2 is guaranteed by one-step consistency plus a Lipschitz condition on either F_T^e or the family F_T^a .*

In general, one-step and multi-step consistency do not imply each other. This issue is clarified by means of the following example [4, Remark 3, Example 2].

Example 2.1. *Consider the linear system*

$$\begin{aligned} \dot{x}_1 &= x_1 + u_1 \\ \dot{x}_2 &= u_2 \end{aligned} \quad (2.20)$$

with the exact discretization

$$\begin{aligned} \dot{x}_1(k+1) &= e^T x_1(k) + [e^T - 1]u_1(k) \\ \dot{x}_2(k+1) &= x_2(k) + Tu_2(k) \end{aligned} \quad (2.21)$$

and the Euler approximate model

$$\begin{aligned} \dot{x}_1(k+1) &= [1 + T]x_1(k) + Tu_1(k) \\ \dot{x}_2(k+1) &= x_2(k) + Tu_2(k) \end{aligned} \quad (2.22)$$

which is controlled by

$$u(x) = \begin{cases} [-2x_1 \ 0]^\top & \text{if } 0 < 0.1x_1 < x_2 < 10x_1 \\ [-2x_1 \ -x_2]^\top & \text{otherwise} \end{cases} \quad (2.23)$$

It follows from Lemma 2.1 that (u_T, F_T^a) is one-step consistent with (u_T, F_T^e) . However, (u_T, F_T^a) is not multi-step consistent with (u_T, F_T^e) . Indeed, consider the initial condition $(\xi_1, \xi_2) = (1, 0.1)$. It is easy to see that, in this case, $(x_1^a(k, \xi), x_2^a(k, \xi)) = (1 - T)^k(1, 0.1)$, i.e., the positive ray $x_2 = 0.1x_1 > 0$ is forward invariant for all $T \in (0, 1)$. On the other

hand, $(x_1^e(1, \xi), x_2^e(1, \xi)) = ((2 - e^T)1, (1 - T)0.1)$, i.e., for all small $T > 0$, $x_2^e(1, \xi) < 10x_1^e(1, \xi)$ and $x_2^e(1, \xi) > 0.1x_1^e(1, \xi)$ since $e^T > 1 + T$. It follows that, for $k \geq 1$, $x(k, \xi)$ will take values on the horizontal line given by $x_2 = (1 - T)0.1$ moving in the direction of decreasing x_1 until it crosses the positive ray $x_2 = 10x_1$. Let \bar{k} denote the number of steps required to cross the positive ray $x_2 = 10x_1$. It is easy to put an upper and lower bound on $\bar{k}T$ that is independent of T . Then since, for all $k \leq \bar{k}$, we have $x_2^e(k, \xi) = (1 - T)0.1$ while $x_1^e(k, \xi) = (1 - T)^k 0.1 \leq e^{-kT} 0.1$, it is clear that the conclusion of Lemma 2.2 is not satisfied. Hence, (u_T, F_T^a) cannot be multi-step consistent with (u_T, F_T^e) .

The fact that one-step consistency may not hold when multi-step consistency does hold can be seen from the plant $\dot{x} = x + u$ with Euler approximation $x(k + 1) = x(k) + T(x(k) + u(k)) = F_T^a(x(k), u(k))$ and controller $u_T(x) = -(\frac{1}{T} + 1)x$. The exact discrete-time model is $x(k + 1) = e^T x(k) + (e^T - 1)u(k)$ and we have $F_T^a(x, u_T(x)) = 0$ and $F_T^e(x, u_T(x)) = (1 - \frac{e^T - 1}{T})x$. Since, for x in a compact set, $F_T^e(x, u_T(x))$ is of order T we do not have one-step consistency. On the other hand, it follows from $F_T^a(x, u_T(x)) = 0$ and the fact that $F_T^e(x, u_T(x))$ is of order T that we do have multi-step consistency. Indeed, for each compact set $\mathcal{X} \in \mathbb{R}$ and each $\eta > 0$ there exist strictly positive numbers K, T^* such that, for all $x, z \in \mathcal{X}, T \in (0, T^*), k \geq 0$,

$$|F_T^e(x, u_T(x)) - F_T^a(z, u_T(z))| = |F_T^e(x, u_T(x))| \leq KT := \alpha(\delta, T) = \alpha^k(0, T) \leq \eta$$

Since in this thesis we will consider the effect of disturbance inputs as well and we deal with multirate systems, more general definitions of consistency properties are needed. Assume that the nonlinear system (2.9) is affected by exogenous disturbances $d(t)$ as $\dot{x} = f(x, u, d)$. Then, consistent with the literature on nonlinear sampled-data control systems we denote the exact discrete-time plant model by $F_T^e(x(k), u(k), d[k])$ and its approximate model by $F_{T,h}^a(x(k), u(k), d[k])$. Note that the discrete-time approximate model is here parametrized by the integration period h of the numerical method upon which it is generated. The following definition of one-step consistency, that appears to be much more reasonable for multirate systems, will be widely used throughout the thesis. The analogous multi-step consistency condition is given in Definition 7.1.

Definition 2.8. *The approximate model $F_{T,h}^a$ is said to be one step consistent with F_T^e if there exist a class- \mathcal{K} function $\rho(\cdot)$ and $T^* > 0$ such that given any strictly positive numbers*

$(\delta_1, \delta_2, \delta_3)$ and each fixed $T \in (0, T^*]$, there exists $h^* \in (0, T]$ such that

$$|F_T^e(x, u, \bar{d}) - F_{T,h}^a(x, u, \bar{d})| \leq T\rho(h) \quad (2.24)$$

for all $x \in B(\delta_1)$, $u \in B(\delta_2)$, $\|d\|_\infty \leq \delta_3$ and $h \in (0, h^*)$.

2.2.4 One-Sided Lipschitz Condition

As mentioned in Chapter 1, the one-sided Lipschitz systems is known as a broad family of nonlinear plants with practical significance (e.g., *stiff* dynamical systems [63]) which generalizes the classical Lipschitz systems as an special case. In this thesis, particularly Chapters 4 and 5, we examined our general frameworks on this important class of nonlinearities to illustrate the effectiveness of the results and to obtain some systematic design approaches.

Definition 2.9. [63] *The nonlinear function $\Phi(x, u)$ is said to be Lipschitz with respect to x in a region \mathcal{X} around the origin if there exists a constant $\lambda > 0$ such that $\forall x_1, x_2 \in \mathcal{X}$*

$$\|\Phi(x_1, u^*) - \Phi(x_2, u^*)\| \leq \lambda \|x_1 - x_2\| \quad (2.25)$$

where u^* is any admissible control signal. This nonlinearity is called *one-sided Lipschitz* if there exists $\rho \in \mathbb{R}$ such that $\forall x_1, x_2 \in \mathcal{X}$

$$\langle \Phi(x_1, u^*) - \Phi(x_2, u^*), x_1 - x_2 \rangle \leq \mu \|x_1 - x_2\|^2 \quad (2.26)$$

the smallest $\lambda > 0$ and μ satisfying (2.25) and (2.26) are known as the Lipschitz and the one-sided Lipschitz constants, respectively.

The properties of Definition 2.9 might be local or global. Note that unlike the Lipschitz constant, the one sided Lipschitz constant is not necessarily positive. This is a significant feature of the one-sided Lipschitz nonlinearities which removes the need to rely on the dominance of the linear terms in the classical Lipschitz approach. It is well known that every Lipschitz function is continuous, one-sided Lipschitz functions on the other hand may be discontinuous.

For any Lipschitz function $\Phi(x, u)$, we have

$$|\langle \Phi(x_1, u^*) - \Phi(x_2, u^*), x_1 - x_2 \rangle| \leq \|\Phi(x_1, u) - \Phi(x_2, u)\| \|x_1 - x_2\| \leq \lambda \|x_1 - x_2\|^2$$

Thus, any Lipschitz function is also one-sided Lipschitz. The converse, however, is not true. For continuously differentiable nonlinear functions it is well-known that the smallest possible constant satisfying (2.25) (i.e., the Lipschitz constant) is the supremum of the norm of Jacobian of the function over region \mathcal{X} , that is

$$\lambda = \limsup \left(\left\| \frac{\partial \Phi}{\partial x} \right\| \right), \quad \forall x \in \mathcal{X} \quad (2.27)$$

Alternatively, the one-sided Lipschitz constant is associated with the *logarithmic matrix norm* (*matrix measure*) of the Jacobian. The logarithmic matrix norm of a matrix A is defined as [48]

$$\mu(A) = \lim_{\epsilon \rightarrow 0} \frac{\|I + \epsilon A\| - 1}{\epsilon}, \quad (2.28)$$

where the symbol $\|\cdot\|$ represents any matrix norm. Then, we have [101]

$$\mu = \limsup \left[\mu \left(\frac{\partial \Phi}{\partial x} \right) \right], \quad \forall x \in \mathcal{X} \quad (2.29)$$

If the norm used in (2.28) is indeed the induced 2-norm (the spectral norm) then it can be shown that $\mu(A) = \lambda_{\max}(\frac{A+A^T}{2})$ [48]. On the other hand, from the Fan's theorem we know that for any matrix, $\lambda_{\max}(\frac{A+A^T}{2}) \leq \sigma_{\max}(A) = \|A\|$. Therefore, $\mu \leq \lambda$. Usually one-sided Lipschitz constant can be found to be much smaller than the Lipschitz constant [101]. It is well-known in numerical analysis that for stiff ODE systems, $\mu \ll \lambda$.

Remark 2.5. *There is an alternative definition for one-sided Lipschitz condition as follows*

$$\langle P\Phi(x_1, u^*) - P\Phi(x_2, u^*), x_1 - x_2 \rangle \leq \mu_1 \|x_1 - x_2\|^2 \quad (2.30)$$

for some symmetric positive definite matrix P . This definition has been already considered by several authors to study one-sided Lipschitz systems (see e.g., [59–62]). However, the main drawback with (2.30) is that it adds additional constraint to the controller or observer synthesis and affects the value of the one-sided Lipschitz constant.

In this thesis the original definition of one-sided Lipschitz condition governed by (2.26) is employed without any scaling matrix like (2.30).

Chapter 3

Multirate Nonlinear Control via Emulation Method

The primary interest of this chapter¹ is the study of dissipativity preservation under multirate sampling. The theory of dissipativity was initiated by [44] and has become a fundamental tool in control systems analysis and design. See for example [40, 49, 99]. We will concentrate on controller emulation when the output is measured at a slower rate compared to the control input. Assuming that the closed-loop system with disturbances satisfies certain form of dissipation inequality, we study the dissipativity of a closed-loop MSD system implemented by emulating the continuous-time controller. We make use of the inferential control setup proposed by [18] and show that under mild assumptions the dissipation inequality is preserved for the nonlinear multirate plant in a semiglobal practical sense.

Essentially, this chapter is a multirate version of the work of [9]- [8], and guarantees the preservation of dissipation inequalities for a closed-loop sampled-data system when the input and output sampling rates are different. Our results are applicable to static and dynamic state feedback controllers and can be used to cover a wide range of important system theoretic properties, including stability, input-to-state stability, passivity, L_p -stability, etc that are special cases of dissipativity. Hence, in the present work we provide a rather general and unified framework for MSD design via CTD method that can be regarded as

¹The results of this chapter have been published in the article: H. Beikzadeh and H. J. Marquez, "Dissipativity of nonlinear multirate sampled-data systems under emulation design," *Automatica*, vol. 49, no. 1, pp. 308-312, 2013.

a generalization of the papers by [17] and [18]. Moreover, it is shown how this framework captures the important case of multirate nonlinear H_∞ control (see e.g., [39] on nonlinear H_∞ control problem) as a special case.

The chapter is organized as follows. In Section 3.1, the multirate controller setup together with the relevant notations and definitions are introduced. Section 3.2 states and proves the main results for both the static and dynamic state feedbacks. We employ an appropriate example to illustrate our results in Section 3.3. It can be seen that if we design a continuous-time nonlinear H_∞ controller, then similar H_∞ performance criterion is preserved for the MSD control system under emulation. Furthermore, simulations reveal that the multirate case outperforms the corresponding single rate case using a prominent slower output sampling rate. Finally, Section 3.4 concludes and summarizes the chapter.

3.1 Preliminaries and Controller Setup

Consider the general nonlinear plant governed by

$$G : \begin{cases} \dot{x}(t) = f(x(t), u(t), d(t)) \\ z(t) = g(x(t), u(t), d(t)) \end{cases} \quad (3.1)$$

initiated by $x(0) = x_0$, where $x \in \mathbb{R}^n$ is the state, $u \in \mathbb{R}^m$ the control input, $d \in \mathbb{R}^q$ the exogenous disturbance to the system, and finally $z \in \mathbb{R}^l$ the penalty output (tracking errors, cost variables, etc). Also, it is assumed that f is locally Lipschitz in all of its arguments, g is continuous and $f(0, 0, 0) = 0$. The state feedback controller will be studied and therefore, all the states are available for measurement. Representing the measured output by y , we will often write $y = x$.

The continuous-time plant (3.1) is connected to a digital controller K_d via sample and hold devices with different sampling rates S_s and H_f , respectively, as shown in Figure 3.1. In this setup, the input sampling period defined by the fast hold H_f is denoted by $T_i = T$ and the measurement sampling period determined by the slow sampler S_s is $T_m = lT$ for some integer $l \geq 1$. This assumption was made before in the literature on multirate plants (see e.g., [17]). Note that T is the basic sampling period of the system and can be assigned arbitrarily.

As a starting point in the emulation design, it is assumed that the state feedback

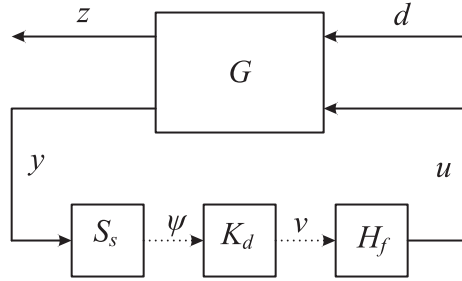


Figure 3.1: Standard multirate sampled-data control configuration

controller has been designed to stabilize or to fulfill certain property of the closed-loop continuous-time system. Differential dissipation defined below is such a broad property that is the centre of attention in this work (see [44]- [99] for more general definitions). We focus on the static controller $u(t) = u(x)$ while the dynamic feedback case may be also handled in a similar fashion in Section 3-2-2.

Definition 3.1. *The continuous-time system (3.1) with the control input $u = u(x)$ is said to be dissipative with respect to a continuous function w , called supply rate, if there exists a continuously differentiable function V , called storage function, such that for all $x \in \mathbb{R}^n$, $u \in \mathbb{R}^m$, $d \in \mathbb{R}^q$, $z \in \mathbb{R}^l$*

$$\dot{V}(t) = \frac{\partial V}{\partial x} f(x(t), u(t), d(t)) \leq w(d(t), z(t)) \quad (3.2)$$

Remark 3.1. *It should be noted that the dissipation rate w is usually expressed as a function of the input and output signals [40], i.e., $w(u, d, y, z)$ for the general representation (3.1). However, since we have considered a state feedback case in a closed-loop configuration, it can be simplified as in (3.2).*

Let

$$x(k+1) = x(k) + \int_{kT}^{(k+1)T} f(x(\tau), u(k), d(\tau)) d\tau := F_T^e(x(k), u(k), d[k]) \quad (3.3)$$

represent the exact discrete-time model of the plant (3.1) with the sampling period $T > 0$. Finding F_T^e requires solving the differential equation in (3.1) which in most practical cases cannot be done analytically. Consistent with the literature on sampled-data systems, F_T^e will be assumed to be unknown and instead, a family of approximate discrete-time models

of the plant will be used

$$x(k+1) = F_{T,h}^a(x(k), u(k), d[k]) \quad (3.4)$$

where h is the period of the numerical integration used to generate the approximate model and may be different from the sampling period T (see [18] for an informative discussion on choosing h different from T). The approximate models can be obtained using any of several well known numerical integration methods.

With these prerequisites, we are able use the sampled-data inferential control setup proposed by [18] with zero disturbance, shown in Figure 3.2, to stabilize the multirate non-linear plant in Figure 3.1. Indeed, the control algorithm K_d is described by the following periodic switch

$$x_c(k+1) = \begin{cases} y(k+1), & \text{if } \exists i \in \mathbb{Z}^+ : k+1 = il \\ F_{T,h}^a(x_c(k), u(k), 0), & \text{otherwise, with initialization } x_c(il) = x(il) \end{cases} \quad (3.5)$$

along with the discretized emulated controller $u(k) = u(x_c(k))$. The basic idea is to compensate for the missing states by means of the switch output which is fed to the fast rate controller.

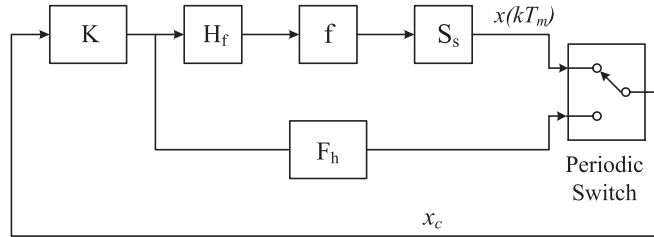


Figure 3.2: The sampled-data inferential control system

Thus, the discrete-time model of the closed-loop sampled-data system consists of the exact discrete-time model of the plant and the multirate controller is given by

$$\begin{aligned} x(k+1) &= F_T^e(x(k), u(k), d[k]) \\ u(k) &= u(x_c(k)) \\ z(k) &= g(x(k), u(k), d(k)) \end{aligned} \quad (3.6)$$

To shorten our notation we write $x := x(k)$, $x_c := x_c(k)$, $u := u(k)$, $d := d(k)$, and $f := f(x(k), u(k), d(k))$ in the sequel. For completeness the following definition and lemma are introduced.

Definition 3.2. (*Uniform Lipschitz*) $F_{T,h}^a$ is said to be uniform locally Lipschitz if given any strictly positive numbers $(\delta_1, \delta_2, \delta_3)$ there exist $L_1 > 0$ and $T_1 > 0$ such that for each fixed $T \in (0, T_1]$, there exists $h_1 \in (0, T]$ such that

$$|F_{T,h}^a(x_1, u, \bar{d}) - F_{T,h}^a(x_2, u, \bar{d})| \leq L_1|x_1 - x_2| \quad (3.7)$$

for all $x_1, x_2 \in B(\delta_1)$, $u \in B(\delta_2)$, $\|d\|_\infty \leq \delta_3$ and $h \in (0, h_1)$.

Lemma 3.1. Suppose that $F_{T,h}^a$ is constructed by a recursive routine on the Euler model as below

$$f_h(i, x, u, d) := x + hf_1(x, u, d_1) + \int_{kT+ih}^{kT+(i+1)h} f_2(x, u, d_2(\tau))d\tau \quad (3.8)$$

$$f_h^{i+1}(x, u, d) := f_h(i+1, f_h^i, u, d) \quad (3.9)$$

where $f(x, u, d) = f_1(x, u, d_1) + f_2(x, u, d_2)$ with the sampled disturbance d_1 and the non-sampled disturbance d_2 . Then, $F_{T,h}^a(x(k), u(k), d[k]) := f_h^N(x, u, d)$, in which $N = T/h$, is one-step consistent with F_T^e .

Remark 3.2. In the single-rate case, a sufficient condition for one-step consistency is established via the Euler approximate model [4, Lemma 1]. Lemma 3.1 provides a similar condition for the multirate case. The proof is immediate from [4, Lemma 1 and Remark 2] together with [13, Corollary 4 and Remark 14].

3.2 Preservation of Dissipativity in Mutilate Setup

3.2.1 Static Feedback Case

The central question is whether the desired property of the closed-loop continuous-time system described in terms of the dissipation inequality (3.2) will be preserved and, if so, in what sense for the closed-loop MSD system (3.6). This section endeavours to answer this question.

Assumption 3.1. The close-loop continuous time system (3.1) with the control input $u = u(x)$ is dissipative as stated by Definition 3.1.

Assumption 3.2. $F_{T,h}^a$ is one-step consistent with F_T^e according to Definition 2.8 and is uniform locally Lipschitz based on Definition 3.2.

Theorem 3.1. *Under Assumptions 3.1-3.2, given positive real numbers $(\delta_x, \delta_d, \nu)$ there exists $T^* > 0$ such that for any fixed $T \in (0, T^*]$, all $|x(0)| \leq \delta_x$ and Lipschitz disturbances that satisfy $\|d\|_\infty \leq \delta_d$, there exists $h^* \in (0, T]$ such that the exact discrete-time model of the closed-loop MSD system (3.6) satisfies the following dissipation inequality*

$$\frac{\Delta V}{T} := \frac{V(x(k+1)) - V(x(k))}{T} \leq w(d(k), z(k)) + \nu \quad (3.10)$$

for each $h \in (0, h^*]$.

Proof: First the results provided in [18, Lemma 1] imply that under Assumption 3.2, given positive real numbers $(\delta_x, \delta_d, \epsilon)$ there exists $T_2 > 0$ such that for any fixed $T \in (0, T_2]$, there exists $h_2 \in (0, T]$ such that for each $|x(0)| \leq \delta_x$, $\|d\|_\infty \leq \delta_d$ and $h \in (0, h_2]$ the following satisfies: If $\max_{i \in \{0, 1, \dots, k\}} |x(i)| \leq \delta_x$ for some $k \in \mathbb{Z}^+$ then

$$|x(k) - x_c(k)| \leq \epsilon \quad (3.11)$$

with $x_c(\cdot)$ as the output of the periodic switch (3.5). Define $\delta = \delta_x + 1$. Let L be the Lipschitz constant of f , and $b > 0$ be a number that satisfies $\max\{|\partial V/\partial x|, |f(x, u, d)|\} \leq b$ on the sets $|x| \leq \delta$ and $\|d\|_\infty \leq \delta_d$. It is easy to see that such $b > 0$ always exists because of the continuous differentiability of V , the local Lipschitz property of f and the fact that they are in a closed set.

Let $T_2 > 0$ and $h_2 > 0$ as generated above for some $\epsilon < 1$, and choose a positive number T_3 such that $T_3 L b (b + L_d) \leq \nu/2$, where L_d is the Lipschitz constant of the disturbance input defined as

$$|d(t_1) - d(t_2)| \leq L_d |t_1 - t_2|, \quad \forall t_1, t_2 \in \mathbb{R}^+ \quad (3.12)$$

Moreover, by the continuity of $\partial V/\partial x$, it follows that given any $\theta > 0$ there exists $T_\theta > 0$, such that $|(\partial V/\partial x)_{x_1} - (\partial V/\partial x)_x| \leq \theta$ for any $T \in (0, T_\theta]$, $|x_1 - x| \leq T b$. Take $\theta = \nu/2b$ and denote $T_4 := T_\theta$ such that for all $T \in (0, T_4]$, $|x| \leq \delta$ and $\|d\|_\infty \leq \delta_d$ the following holds:

$$\left| \frac{\partial V}{\partial x}|_{x_1} - \frac{\partial V}{\partial x}|_x \right| \leq \frac{\nu}{2b} \quad (3.13)$$

Finally, take $T^* = \min\{T_1, T_2, T_3, T_4, 1/2b\}$ and for any $T \in (0, T^*]$ we define $h^* = \min\{h_1, h_2, T\}$. To shorten the notation we symbolize $x := x(k)$, $x_c := x_c(k)$, $u := u(k)$,

$d := d(k)$ and $f_k := f(x(k), u(k), d(k))$ in the sequel. Now consider

$$\begin{aligned} \frac{V(x(k+1)) - V(x(k))}{T} &= \underbrace{\frac{\partial V}{\partial x|_x} f}_1 + \underbrace{\frac{1}{T}\{V(x(k+1)) - V(x + Tf_k)\}}_2 \\ &+ \underbrace{\frac{1}{T}\left\{V(x + Tf_k) - V(x) - \frac{\partial V}{\partial x|_x} f\right\}}_3 \end{aligned} \quad (3.14)$$

in which $T \in (0, T^*]$ and $x + Tf_k$ is the Euler approximate model of the state equation in (3.1). We proceed by imposing some bounds on each term on the right hand side of (3.14).

Term 1: By Assumption 3.1, it follows that

$$\frac{\partial V}{\partial x|_x} f \leq w(d, z) \quad (3.15)$$

Term 2: Using the mean value theorem, we get

$$\frac{1}{T}\{V(x(k+1)) - V(x + Tf_k)\} \leq \frac{1}{T} \frac{\partial V}{\partial x|_{x_2}} |x(k+1) - x - Tf_k| \quad (3.16)$$

where $x_2 = x + Tf_k + \theta_1\{x(k+1) - x - Tf_k\}$, $\theta_1 \in (0, 1)$. Regarding the term $|x(k+1) - x - Tf_k|$ two situations may occur. If $\{x(k+1) - x - Tf_k\} \leq 0$, then by our choice of T^* , in particular $T^* \leq 1/2b$ we obtain $|x_2| \leq |x + Tf_k| \leq \delta_x + 1/2 \leq \delta$. Otherwise, we have $|x_2| \leq |x(k+1)|$, and noting that here $x(t)$ is the solution of initial value problem $\dot{x} = f(x(t), u, d(t))$, $\forall t \in [kT, (k+1)T]$ with the initial value $x(k)$, it implies $|x_2| \leq |x(k+1)| \leq \delta_x + 1 = \delta$. Consequently, in both cases x_2 belongs to our region of interest. Furthermore, by virtue of (3.11), it follows that $|x_c| \leq \delta_x + \epsilon \leq \delta$ which indicates that the switch output also remains inside the region defined by δ . Since $|x_2| \leq \delta$, it yields that $|(\partial V/\partial x)_{x_2}| \leq b$. Using the mean value theorem, triangle inequality and local Lipschitz property of f and also d , i.e., inequality (3.12), it can be concluded

$$\begin{aligned} |x(k+1) - x - Tf_k| &\leq T|f(x(kT + \theta_2T), u, d(kT + \theta_2T)) - f(x, u, d)| \\ &\leq T|f(x(kT + \theta_2T), u, d(kT + \theta_2T)) - f(x, u, d(kT + \theta_2T))| \\ &+ T|f(x, u, d(kT + \theta_2T)) - f(x, u, d)| \\ &\leq TL\{|x(kT + \theta_2T) - x| - |d(kT + \theta_2T) - d|\} \\ &\leq \theta_2LT^2|f(x(kT + \alpha\theta_2T), u, d(kT + \alpha\theta_2T))| + L_dLT^2 \\ &\leq LT^2b + L_dLT^2 \end{aligned} \quad (3.17)$$

with $\theta_2, \alpha \in (0, 1)$. Hence, we can write

$$\text{term 2} \leq TLb(b + L_d) \quad (3.18)$$

By the choice of T_3 and h^* , it yields

$$\frac{1}{T} \{V(x(k+1)) - V(x + Tf_k)\} \leq \frac{\nu}{2} \quad (3.19)$$

Term 3: Let $x_3 = x + \theta_3 Tf$ with $\theta_3 \in (0, 1)$, using the mean value theorem we get

$$\frac{1}{T} \left\{ V(x + Tf_k) - V(x) - \frac{\partial V}{\partial x|_x} f \right\} \leq \frac{\partial V}{\partial x|_{x_3}} f - \frac{\partial V}{\partial x|_x} f \leq b \left| \frac{\partial V}{\partial x|_{x_3}} - \frac{\partial V}{\partial x|_x} \right| \leq \frac{\nu}{2} \quad (3.20)$$

for $|x_3 - x| \leq Tb$. Combining the bounds obtained in (3.15), (3.19)-(3.20) the dissipation inequality (3.10) can be verified. This completes the proof. \blacksquare

The importance of Theorem 3.1 is that, it shows how specifications of a continuous-time controller design based on dissipation inequalities can be preserved in a multirate sampled-data setup (special cases are practical asymptotic stability in [17] and semiglobal ISS stability [18]). As an application, we may obtain a multirate H_∞ design derived from the emulation method (see next section).

Remark 3.3. *For simplicity, Theorem 3.1 was proved for the case of “dual” rate, i.e., when all the components x_i of the state x are sampled at the same slow rate. Picking the largest output sampling as T_m , it can be shown that the theorem is still valid when each state x_i is sampled at a different rate $l_i T$ ($l_i \geq 1$).*

Remark 3.4. *This theorem is analogous to the weak form of dissipation inequalities considered in [8] for the single-rate emulation design. A multirate version of the strong form of dissipation in that paper may be also developed in a similar way.*

Remark 3.5. *The Lipschitz continuity condition imposed on the disturbance input is common in the literature (see e.g., [9, Theorem 3.1]). However, it can be shown that this condition can be eliminated by considering a stronger form of dissipation inequality.*

Remark 3.6. *Assumption 3.2 is made to guarantee the practical ISS stability of the closed-loop system and the boundedness of the periodic switch output x_c but is otherwise unnecessary in the proof of Theorem 3.1. Conversely, this assumption plays a crucial role in preservation of dissipation inequality for the dynamic feedback structure.*

3.2.2 Dynamic Feedback Case

This section extends our result to the case of dynamic state feedback. Assume that the system (3.1) is controlled by

$$\begin{aligned} \dot{v}(t) &= s(x(t), v(t)) \\ u(t) &= u(x(t), v(t)) \end{aligned} \quad (3.21)$$

where $v \in \mathbb{R}^r$ is the state of the controller and s, u are continuous, locally Lipschitz functions and zero at zero. Similar to (3.4), an approximate discrete-time model of the dynamic controller (3.21) will be applied

$$\begin{aligned} v(k+1) &= S_{T,h}^a(x(k), v(k)) \\ u(k) &= u(x(k), v(k)) \end{aligned} \quad (3.22)$$

corresponding to the exact model S_T^e . For the sake of brevity, set $v := v(k)$, $s := s(x(k), v(k))$ and $\tilde{x} = [x^\top \ v^\top]^\top$.

Clearly, for the dynamic controller (3.21) the dissipation inequality in Definition 3.1 has the following form

$$\dot{V}(t) = \frac{\partial V}{\partial x} f(x, u, d) + \frac{\partial V}{\partial v} s(x, v) \leq w(d(t), z(t)). \quad (3.23)$$

Assumption 3.3. *The approximation $S_{T,h}^a$ is one-step consistent with S_T^e .*

Theorem 3.2. *Under Assumptions 3.1-3.3 with $u(x,v)$ and the dissipation inequality (3.23), given positive real numbers $(\delta_x, \delta_d, \nu)$ there exists $T^* > 0$ such that for any fixed $T \in (0, T^*]$, all $|\tilde{x}(0)| \leq \delta_x$ and Lipschitz disturbances that satisfy $\|d\|_\infty \leq \delta_d$, there exists $h^* \in (0, T]$ such that for each $h \in (0, h^*]$ the exact discrete-time model of the closed-loop MSD system containing (3.1), (3.5) and (3.22) fulfills the following dissipation inequality*

$$\frac{\Delta V}{T} := \frac{V(\tilde{x}(k+1)) - V(\tilde{x})}{T} \leq w(d(k), z(k)) + \nu \quad (3.24)$$

provided that for some $k \in \mathbb{Z}^+$ $\max_{i \in \{0, 1, \dots, k\}} |\tilde{x}(i)| \leq \delta_x$.

Proof. Define $\delta = \delta_x + 1$. Let $L_f, L_s > 0$ be the Lipschitz constant of f and s respectively, and $b > 0$ be a number that satisfies $\max\{|\partial V/\partial x|, |\partial V/\partial v|, |f(x, u, d)|, |s(x, v)|\} \leq b$ on the sets where $|x| \leq \delta$, $|v| \leq \delta$ and $\|d\|_\infty \leq \delta_d$. It is easy to see that such $b > 0$ always exists because of the continuous differentiability of V , the local Lipschitz properties of f and s , and the fact that they are in a closed set. Let $T_2, h_2 > 0$ be generated as above for

some $\epsilon = \min\{1, \delta/8bL_s\}$, and $T_3, h_3 > 0$ and $\tilde{\rho}(\cdot) \in \mathcal{K}$ be obtained from Assumption 3.3. Moreover, take positive numbers T_4, h_4 and h_5 such that $T_4b^2(L_f + L_s) + T_4bL_fL_d \leq \nu/4$, $T_3\tilde{\rho}(h_4) \leq 1/2$ and $b\tilde{\rho}(h_5) \leq \nu/4$, where L_d is the Lipschitz constant of the disturbance input. By the continuity of $\partial V/\partial x$, it follows that given $\nu/4b$ there exists $T_5 > 0$, such that for any $T \in (0, T_5]$, $|x_1 - x| \leq Tb$, $|v_1 - v| \leq Tb$ and all $|\tilde{x}| \leq \delta$, $\|d\|_\infty \leq \delta_d$

$$\left| \frac{\partial V}{\partial x} \Big|_{(x_1, v_1)} - \frac{\partial V}{\partial x} \Big|_{(x, v)} \right| \leq \frac{\nu}{4b}. \quad (3.25)$$

Likewise, choose $T_6 > 0$ such that for all $T \in (0, T_6]$, $|\tilde{x}| \leq \delta$ and $\|d\|_\infty \leq \delta_d$

$$\left| \frac{\partial V}{\partial x} \Big|_{(x_2, v_2)} - \frac{\partial V}{\partial x} \Big|_{(x, v)} \right| \leq \frac{\nu}{8b}. \quad (3.26)$$

Finally, take $T^* = \min\{T_2, T_3, T_4, T_5, T_6, 1/2b\}$ and for any $T \in (0, T^*]$ we define $h^* = \min\{h_2, h_3, h_4, h_5, T\}$. Now consider

$$\begin{aligned} \frac{V(\tilde{x}(k+1)) - V(\tilde{x}(k))}{T} &= \underbrace{\frac{\partial V}{\partial x} \Big|_{\tilde{x}} f + \frac{\partial V}{\partial v} \Big|_{\tilde{x}} s}_1 \\ &+ \underbrace{\frac{1}{T} \{V(\tilde{x}(k+1)) - V(x + Tf, v + Ts(x_c, v))\}}_2 \\ &+ \underbrace{\frac{1}{T} \{V(x + Tf, v + Ts(x_c, v)) - V(\tilde{x}) - \frac{\partial V}{\partial x} \Big|_{\tilde{x}} f - \frac{\partial V}{\partial v} \Big|_{\tilde{x}} s\}}_3 \end{aligned} \quad (3.27)$$

Term 1: By Assumption 3.1, this term is bounded by (3.23).

Term 2: Using the mean value theorem, we get

$$\begin{aligned} &\frac{1}{T} \{V(x(k+1), v(k+1)) - V(x + Tf, v + Ts(x_c, v))\} \\ &\leq \frac{1}{T} \frac{\partial V}{\partial x} \Big|_{(x_3, v(k+1))} |x(k+1) - x - Tf| \\ &\quad + \frac{1}{T} \frac{\partial V}{\partial v} \Big|_{(x+Tf, v_3)} |v(k+1) - v - Ts(x_c, v)| \end{aligned} \quad (3.28)$$

where $x_3 = x + Tf + \theta_1\{x(k+1) - x - Tf\}$ and $v_3 = v + Ts(x_c, v) + \theta_2\{v(k+1) - v - Ts(x_c, v)\}$, $\theta_1, \theta_2 \in (0, 1)$. Regarding the first term on the right-hand side of (3.28) two situations may occur. If $\{x(k+1) - x - Tf_k\} \leq 0$, then by our choice of T^* , in particular $T^* \leq 1/2b$, we obtain $|x_3| \leq |x + Tf_k| \leq \delta_x + 1/2 \leq \delta$. Otherwise, we have $|x_3| \leq |x(k+1)|$, and noting that here $x(t)$ is the solution of initial value problem $\dot{x} = f(x(t), u, d(t)), \forall t \in [kT, (k+1)T]$ with the initial value $x(k)$, it implies $|x_3| \leq |x(k+1)| \leq \delta_x + 1 = \delta$. Furthermore, by

virtue of (3.11) $|x_c| \leq \delta_x + \epsilon \leq \delta$ and hence, it follows from Assumption 3.3, the triangular inequality as well as the choice of h_4 : $|v(k+1)| = |S_{T,h}^a(x_c, v)| \leq |S_T^e(\bar{x}_c, v)| + |S_T^e(\bar{x}_c, v) - S_{T,h}^a(x_c, v)| \leq \delta_x + 1/2 + T\tilde{\rho}(h) \leq \delta$. Since $|x_3| \leq \delta$ and $|v(k+1)| \leq \delta$, it yields that $|(\partial V/\partial x)_{(x_3, v(k+1))}| \leq b$. Using the mean value theorem, the triangle inequality and the local Lipschitz property of f and d , we conclude

$$\begin{aligned}
|x(k+1) - x - Tf| &\leq T|f(x(kT + \theta_3T), u, d(kT + \theta_3T)) - f(x, u, d)| \\
&\leq T|f(x(kT + \theta_3T), u, d(kT + \theta_3T)) - f(x, u, d(kT + \theta_3T))| \\
&\quad + T|f(x, u, d(kT + \theta_3T)) - f(x, u, d)| \\
&\leq TL_f\{|x(kT + \theta_3T) - x| - |d(kT + \theta_3T) - d|\} \\
&\leq \theta_3T^2L_f|f(x(kT + \alpha\theta_3T), u, d(kT + \alpha\theta_3T))| + \theta_3T^2L_fL_d \\
&\leq T^2L_fb + T^2L_fL_d
\end{aligned} \tag{3.29}$$

with $\theta_3, \alpha \in (0, 1)$. In exactly the same way, $\max\{|v + Ts(x_c, v)|, |v(k+1)|\} \leq \delta$ yields $|v_3| \leq \delta$, which together with $|x + Tf| \leq \delta$ implies $|(\partial V/\partial v)_{(x+Tf, v_3)}| \leq b$. Applying the triangle inequality, Assumption 3.3 and finally the mean value theorem, we have

$$\begin{aligned}
|v(k+1) - v - Ts(x_c, v)| &\leq |S_{T,h}^a(x_c, v) - S_T^e(\bar{x}_c, v)| + |S_T^e(\bar{x}_c, v) - v - Ts(x_c, v)| \\
&\leq T\tilde{\rho}(h) + |S_T^e(\bar{x}_c, v) - v - Ts(x_c, v)| \\
&\leq T\tilde{\rho}(h) + T|s(x_c, v(kT + \theta_4T)) - s(x_c, v)| \\
&\leq T\tilde{\rho}(h) + TL_s|v(kT + \theta_4T) - v| \\
&\leq T\tilde{\rho}(h) + \eta T^2L_s|s(x_c, v(kT + \eta\theta_4T))| \\
&\leq T\tilde{\rho}(h) + T^2L_sb
\end{aligned} \tag{3.30}$$

where $\theta_4, \eta \in (0, 1)$ and we used the local Lipschitz property of s , again the mean value theorem and the bound of s in the last three inequalities, respectively. Thus, based on (3.29)-(3.30) and by our choice of T_4 and h_5 we can write

$$\text{Term 2} \leq Tb^2(L_f + L_s) + TbL_fL_d + b\tilde{\rho}(h) \leq \frac{\nu}{2}. \tag{3.31}$$

Term 3: Let $x_4 = x + \theta_5Tf$ and $v_4 = v + \theta_6Ts(x_c, v)$ with $\theta_5, \theta_6 \in (0, 1)$. Since $|x_4 - x| \leq Tb$ and $|v_4 - v| \leq Tb$, from the choice of T_5 and T_6 , it follows that $(x_4, v + Ts(x_c, v))$ and (x, v_4) satisfy (3.25) and (3.26), respectively. By adding and subtracting $V(x, v + Ts(x_c, v))$ and

then using the mean value theorem we have

$$\begin{aligned}
& \frac{1}{T} \{V(x + Tf, v + Ts(x_c, v)) - V(\tilde{x}) - \frac{\partial V}{\partial x}|_{\tilde{x}} f - \frac{\partial V}{\partial v}|_{\tilde{x}} s\} \\
& \leq \frac{\partial V}{\partial x}|_{(x_4, v+Ts(x_c, v))} f + \frac{\partial V}{\partial v}|_{(x, v_4)} s(x_c, v) - \frac{\partial V}{\partial x}|_{(x, v)} f - \frac{\partial V}{\partial v}|_{(x, v)} s \\
& \leq b \left| \frac{\partial V}{\partial x}|_{(x_4, v+Ts(x_c, v))} - \frac{\partial V}{\partial x}|_{(x, v)} \right| + \frac{\partial V}{\partial v}|_{(x, v_4)} s(x_c, v) - \frac{\partial V}{\partial v}|_{(x, v)} s \\
& \leq \frac{\nu}{4} + \frac{\partial V}{\partial v}|_{(x, v_4)} s(x_c, v) - \frac{\partial V}{\partial v}|_{(x, v)} s
\end{aligned} \tag{3.32}$$

where we used the bounds of f and (3.25). Hence, It can be seen that

$$\begin{aligned}
\text{Term 3} & \leq \frac{\nu}{4} + \underbrace{\frac{\partial V}{\partial v}|_{(x, v_4)} s(x_c, v) - \frac{\partial V}{\partial v}|_{(x, v)} s(x_c, v)}_{3a} \\
& \quad + \underbrace{\frac{\partial V}{\partial v}|_{(x, v)} s(x_c, v) - \frac{\partial V}{\partial v}|_{(x, v)} s(x, v)}_{3b} \leq \frac{\nu}{4} + \frac{\nu}{8} + \frac{\nu}{8} = \frac{\nu}{2}.
\end{aligned} \tag{3.33}$$

Note that in (3.33) Term 3a is bounded by $\nu/8$ due to (3.26). Moreover, from (3.11) and the local Lipschitz property of s , for Term 3b it yields that $(\partial V/\partial v)|_{(x, v)} s(x_c, v) - (\partial V/\partial v)|_{(x, v)} s(x, v) \leq bL_s \epsilon \leq \nu/8$. Combining the bounds obtained for terms 1-3, the dissipation inequality (3.24) can be readily verified. This completes the proof. \blacksquare

3.3 Application: Multirate Nonlinear H_∞ Control

The theory of dissipative systems provides a general framework to analyze several system theoretic properties and also to design controllers with certain specifications. Particularly, the discrete-time dissipation inequality demonstrated in Theorems 3.1-3.2 is an effective tool that can be used to show that the trajectories of the multirate sampled-data system with an emulated controller have a specific property.

In this section, we illustrate the importance of preserving dissipativity under multirate sampling by applying our results to a nonlinear H_∞ control problem. This problem that is entirely based on the notions of dissipativity of nonlinear systems and differential games ([102]- [41]) can be expressed as follows.

Definition 3.3. [39] We say that G in (3.1) has L_2 -gain $\leq \gamma$ provided that

$$\int_0^t |z(\tau)|^2 d\tau \leq \gamma^2 \int_0^t |d(\tau)|^2 d\tau \tag{3.34}$$

for all measurable input functions d and $t \geq 0$ with output $z(\cdot)$ corresponding to the input $d(\cdot)$ from initial state $x_0 \in \mathbb{R}^n$.

The discrete-time counterpart of Definition 3.3 can be found in [41]. For a given prescribed disturbance attenuation level $\gamma > 0$, the H_∞ control problem consists of finding a controller K_d such that, in the closed-loop configuration of Figure 3.1, the L_2 -gain from exogenous inputs d to the cost variable z is less than or equal to γ . Definitions of dissipativity and finite L_2 -gain declares that the system G has L_2 -gain $\leq \gamma$ if and only if it is dissipative with respect to the supply rate $w(d, z) = \frac{1}{2}\gamma^2|d(t)|^2 - \frac{1}{2}|z(t)|^2$. Consequently, designing an H_∞ controller $u = u(x)$ for the continuous-time plant (3.1) renders to finding a suitable storage function V such that the closed-loop system is dissipative with respect to $\frac{1}{2}\gamma^2|d(t)|^2 - \frac{1}{2}|z(t)|^2$. Then based on the results in the previous section, the proposed multirate structure will preserve similar H_∞ performance in a semiglobal practical sense.

The next corollary demonstrates that applying the emulated H_∞ controller in the inferential strategy (3.5) yields a framework for multirate H_∞ synthesis. We remark that although the practical preservation of the H_∞ performance can be granted by Theorem 3.1, Corollary 3.1 shows how the additive term ν is cancelled for multirate H_∞ control via emulation. It should be mentioned that in this section, the state feedback controller is static.

Corollary 3.1. *Suppose that an H_∞ controller $u(x)$ is designed for system (3.1) with $\gamma > 0$, and storage function V with a locally Lipschitz gradient $\partial V/\partial x$ and $(\partial V/\partial x)(0) = 0$. Then under Assumption 3.2, given any pair of positive real numbers (δ_x, δ_d) there exists $T^* > 0$ such that for any fixed $T \in (0, T^*]$, there exists $h^* \in (0, T]$ such that for each $|x(0)| \leq \delta_x$, Lipschitz disturbances with $\|d\|_\infty \leq \delta_d$ and $h \in (0, h^*]$, the closed-loop MSD system controlled by $u(k) = u(x_c(k))$ ensures the following H_∞ performance criterion*

$$\sum_{k=0}^N |z(k)|^2 \leq \gamma^2 \sum_{k=0}^N |d(k)|^2 \quad (3.35)$$

for all $N \in \mathbb{Z}^+$ and all $d(k) \in \ell_2(\{0, \dots, N\}, \mathbb{R}^q)$ with the output $z(k)$ resulting by $d(k)$ from initial state x_0 .

Sketch of the Proof: First by modifying the proof of Theorem 3.1 based on the arguments carried out in the proof of [9, Proposition 3.4] we get

$$\frac{\Delta V}{T} \leq \frac{1}{2}\gamma^2|d|^2 - \frac{1}{2}|z|^2 + T(K_1|d|^2 + K_2|z|^2) \quad (3.36)$$

for all $T \in (0, T_1^*]$ and some positive real constants K_1, K_2 . Using the quadratic and positive definiteness properties of the different terms in (3.36), it can be easily deduced that there exists $T^* \leq T_1^*$ such that $\forall T \in (0, T^*]$ the closed-loop MSD system is also dissipative with respect to the same supply rate as the closed-loop continuous-time system, i.e., $(1/2)\gamma^2|d(k)|^2 - (1/2)|z(k)|^2$. The remainder of the proof follows directly from the bounded real lemma in [41, Proposition 1].

Example 3.1. Consider the following control affine nonlinear plant [40, ch. 7]

$$\begin{aligned} \dot{x} &= (1 + x^2)u + d \\ z &= \begin{bmatrix} x \\ u \end{bmatrix} \end{aligned} \quad (3.37)$$

with z as the penalty variable and $y = x$. Following the procedure presented in the same reference, we end up with the Hamilton-Jacobi inequality

$$\left(\frac{dP}{dx}(x)\right)^2 \left((1 + x^2)^2 - \frac{1}{\gamma^2}\right) \geq x^2 \quad (3.38)$$

which has a nonnegative solution for $\gamma > 1$, e.g.,

$$P(x) = \frac{1}{2} \ln \left(1 + x^2 + \sqrt{(1 + x^2)^2 - \frac{1}{\gamma^2}}\right) \quad (3.39)$$

leading to the H_∞ feedback law

$$u = -(1 + x^2) \left((1 + x^2)^2 - \frac{1}{\gamma^2} \right)^{-\frac{1}{2}} \quad (3.40)$$

that stabilizes the system about $x = 0$ with L_2 -gain $\leq \gamma$. Figure 3.3 depicts the performance of the closed-loop continuous-time plant controlled by (3.40) in the presence of a sinusoidal disturbance of amplitude 0.1 and frequency 1 rad/s. The initial condition is set to $x_0 = 1$ and the attenuation level is chosen to be $\gamma = 1.1$.

We now study the sampled-data implementation of the continuous-time controller (3.40) under two different assumptions via the emulation method. First a single-rate case is treated. Originating from the same initial condition, our simulations show that the single-rate sampled-data controller stabilizes the system only when the sampling period $T_i \leq 0.45$ sec. Second a more practical situation (multirate case) is considered in which the measurements are constrained to be sampled at a lower sampling rate $T_m = 2$ sec. In order to apply the inferential control setup introduced in (3.5), we need an approximation

methodology. For this purpose, similar numerical integration scheme as that of [19] is utilized (Euler model integration)

$$f_h(i, x, u, d) := x + h(1 + x^2)u + \int_{kT+ih}^{kT+(i+1)h} d(\tau) d\tau \quad (3.41)$$

$$f_h^{i+1}(x, u, d) := f_h(i + 1, f_h^i, u, d)$$

where $f_h = f_h^1(x, u, d) := x + h(1 + x^2)u + \int_{kT}^{kT+h} d(\tau) d\tau$ represents the first step of the numerical integration routine on the sampling interval $[kT, (k + 1)T)$ and finally, $F_{T,h}^a(x(k), u(k), d[k]) := f_h^N(x, u, d)$ is chosen to be our approximate discrete-time model. In addition, h denotes the integration period, T is the sampling period and $N = T/h$.

Lemma 3.1 implies the one-step consistency of $F_{T,h}^a$ constructed above with the exact discrete-time model F_T^e . Therefore, the conditions of Corollary 3.1 are verified readily. The simulation results for both of the foregoing sampled-data systems are shown in Figure 3.4. Here, we choose the input sampling period $T_i = 0.4$ sec and the integration step $h = 0.001$ sec.

From [8] and using the same discussions carried out in this section, it can be inferred that if the sampling rate is fast enough, then the single-rate emulated controller also preserves the H_∞ performance index. However, a large sampling period, here $T_i = 0.4$ sec, will bring about large oscillations and the performance of the single-rate sampled-data system may deviate from that of the continuous-time system. This situation can be seen by dashed lines in Figure 3.4 compared with the solid lines in Figure 3.3. On the other hand, the MSD control system (3.5) stabilizes the system more successfully than the fast single-rate scheme with a guaranteed H_∞ performance criterion. For the same input sampling employed in the single-rate case, the stability is maintained with better performance using much lower measurement sampling rate. Our tests reveal that for the selected value of T_i , if $l \in \{2, 3, \dots, 10\}$ then this maintenance will be still valid but obviously with different performances.

3.4 Summary

In this chapter the dissipativity of nonlinear sampled-data control systems under multirate sampling and “low rate measurement” constraint based on the CTD method is investigated. We show that if a closed-loop continuous-time system satisfies a certain dissipation

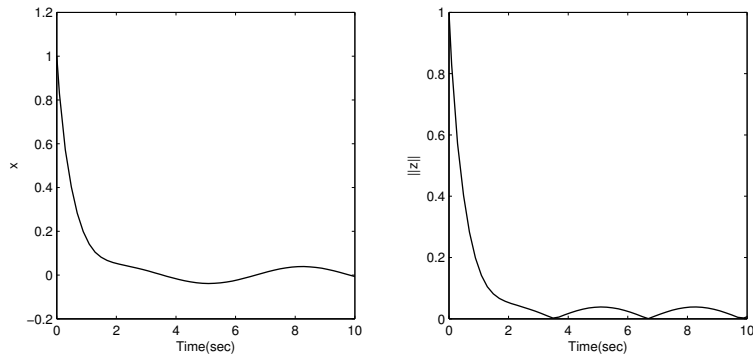


Figure 3.3: The performance of the continuous-time H_∞ controller with sinusoidal disturbance

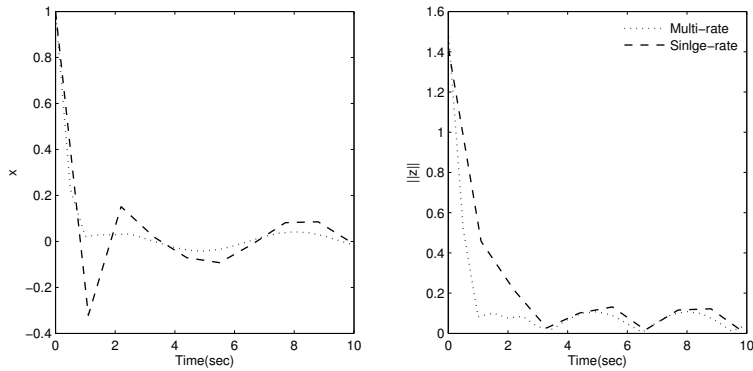


Figure 3.4: The performance of multirate and single-rate H_∞ controller under emulation with sinusoidal disturbance for $T_i = 0.4 \text{ sec}$ and $T_m = 2 \text{ sec}$

inequality via a continuous-time controller, then similar dissipation inequality is preserved in a practical sense for the closed-loop multirate plant that is digitally implemented using the emulated controller and multirate sampler and hold devices. Moreover, a general framework for designing multirate nonlinear H_∞ control in presence of disturbance inputs is offered. The significance of this framework as a perspective result is illustrated through a simulation example where the multirate setup achieves the H_∞ performance criterion and outperforms the fast single-rate scheme using a prominent slower output sampling rate.

Chapter 4

Nonlinear H_∞ Control Using Incremental Gain

Motivated by the important properties of the incremental gain mentioned in Chapter 1, in this chapter¹ we consider an incremental \mathcal{L}_2 -type performance criterion to design H_∞ controllers for nonlinear plants. The first part of the chapter is dedicated to the full information state feedback problem for the Lipschitz nonlinear plants while the second part studies the output feedback problem for more general nonlinearities satisfying the one-sided Lipschitz condition where only some states are measurable.

More precisely, in the first part we propose a stabilizing control law such that the closed loop trajectories converge exponentially with a prespecified decay rate, and also the incremental gain from disturbance to controlled output is less than a prespecified value. Since this problem in its general form brings about partial differential inequalities (PDIs) that are difficult to solve, we restrict our attention to nonlinear systems that satisfy a Lipschitz continuity condition. With these assumptions, the synthesis of the control law can be cast using linear matrix inequalities (LMIs) that can be easily solved using commercial software packages. We also show that our technique can be extended to uncertain nonlinear plants with optimal disturbance rejection and can be also modified to capture the tracking problem with optimal disturbance rejection in an incremental sense. These control schemes are novel, computationally simple, easy to design and implement

¹The results of this chapter have been accepted for publication in the article: H. Beikzadeh and H. J. Marquez, “Robust nonlinear H_∞ control based on the \mathcal{L}_2 incremental gain,” *International Journal of Robust and Nonlinear Control*, Accepted on Nov. 2013.

and flexible due to utilization of LMIs. Moreover, robustness of the proposed strategy against Lipschitz nonlinear uncertainties and time varying uncertainties is guaranteed.

In the second part we directly consider the one-sided Lipschitz systems without any scaling or quadratically inner bounded assumption to address the problem of output feedback design, where all the state variables are not available for measurement. Our approach consists of a nonlinear observer together with a state feedback gain and is based on the Lyapunov candidate parametrization proposed by [103]. Moreover, since the effect of disturbance inputs has been ignored in the articles on the one-side Lipschitz context, we enrich our contribution by attenuating disturbances through an H_∞ performance index based on the \mathcal{L}_2 incremental gain. More precisely, we design a stabilizing state feedback gain as well as a stable nonlinear observer such that the closed loop trajectories converge asymptotically, and also the incremental gain from disturbances to the controlled output is less than a prescribed value. By assuming a mild geometric condition, our synthesis can be cast into a tractable LMI framework. It should be emphasized that our work is basically different from the observer-based result provided by Arcak and Kokotović [104] which studied different functions called nondecreasing nonlinearities with rather different approach and objectives.

The remainder of this chapter is organized as follows. Section 4.1 contains some background material and formulates the state feedback problem. Then, the design procedure of the incremental H_∞ controller for Lipschitz nonlinear systems without uncertainties is presented in terms of some matrix inequalities. Our result is extended to a class of uncertain nonlinear plants to obtain a robust controller. In Section 4.2, we establish an incremental H_∞ output feedback synthesis for one-sided Lipschitz systems. Our result is demonstrated via appropriate simulation examples in Section 4.3. Finally, Section 4.4 closes the chapter and draws some conclusions.

4.1 State Feedback Control for Lipschitz Systems

4.1.1 Preliminaries and System Description

Consider now an operator $\Gamma : w \mapsto z(\mathcal{L}_{2,T} \rightarrow \mathcal{L}_{2,T})$. The induced and incremental \mathcal{L}_2 gains from the input $w \in \mathcal{L}_{2,T}$ to the output $z \in \mathcal{L}_{2,T}$ are respectively defined as follows

$$\begin{aligned}\|\Gamma\|_{i,2} &= \sup_{w \in \mathcal{L}_{2,T}, w \neq 0} \frac{\|(\Gamma w)_T\|}{\|w_T\|} \\ \|\Gamma\|_{\Delta,2} &= \sup_{w, \tilde{w} \in \mathcal{L}_{2,T}, w \neq \tilde{w}} \frac{\|(\Gamma w)_T - (\Gamma \tilde{w})_T\|}{\|w_T - \tilde{w}_T\|}\end{aligned}$$

The following example emphasizes the difference between induced (usual) and incremental gains.

Example 4.1. *The symbol of a glow tube and its approximate $i-v$ characteristic are shown in Figure 4.1a. As can be seen in this figure, the glow tube is a memoryless nonlinear resistor whose voltage is a “single-valued” function of the current, called a current-controlled resistor [105]. Taking i as the input and v as the output, we can view the glow tube as an operator with system of equations*

$$v = \begin{cases} 2i & \text{if } 0 \leq i \leq 10 \\ -3i + 50 & \text{if } 10 \leq i \leq 15 \\ \frac{2}{3}i - 5 & \text{if } i \geq 15 \end{cases}$$

It can be readily verified that the \mathcal{L}_2 incremental gain of the glow tube is determined by the maximum slope of a secant line to the graph (which occurs for $10 \leq i \leq 15$), while the usual gain is given by the maximum slope of a tangent line to the graph crossing the origin (think of v as a function of i in Figure 4.1a). The resulting values for the usual gain and incremental gain of the glow tube are thus $\|\Gamma\|_{i,2} = 2$ and $\|\Gamma\|_{\Delta,2} = 3$, respectively.

This circuit element is connected to a one-port network designated by \mathcal{N} in Figure 4.1b. The series connection of the independent current source and the glow tube can be regarded as a nonlinear load for the rest of the circuit. Obviously, the incremental gain analysis states that the variations of the regulated voltage v_R can be as much as 3 times the variations of the source i . By contrast, the usual gain result fails to recognize incremental changes in the input and only measures input amplification with respect to the zero input.

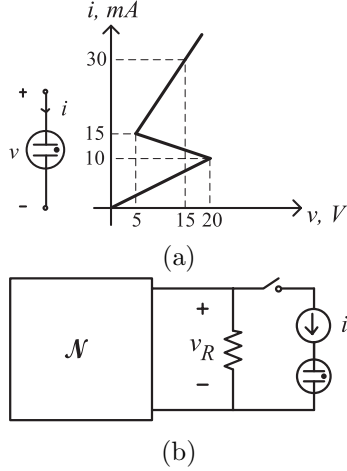


Figure 4.1: (a) glow tube characteristic, (b) A one-port \mathcal{N} driven by an independent current source in series with a glow tube.

In general the incremental gain provides additional detail in the relationship between inputs and outputs.

The operators to be studied in this section are generated by the nonlinear state space realization

$$\Sigma : \begin{cases} \dot{x}(t) = f(x(t), u(t), w(t)) & (4.1) \\ z(t) = h(x(t), u(t)) & (4.2) \end{cases}$$

where $x \in \mathbb{R}^n$, $u \in \mathbb{R}^m$, $z \in \mathbb{R}^l$, and $w \in \mathbb{R}^q$ indicate the state, control input, regulated output (penalty variable), and unknown exogenous disturbance, respectively. We assume that w is piecewise continuous and that the functions f and h are continuously differentiable. Finally, $x = 0$ is an equilibrium point of the unforced system, i.e., $f(0, 0, 0) = 0$.

Definition 4.1. *We say that the relaxed system (4.1)-(4.2), i.e., zero initial conditions, has \mathcal{L}_2 incremental gain $\leq \gamma$ from the disturbance input w to the output z , if there exists a locally integrable control input $u(t) \in \mathbb{R}^m$ such that*

$$\int_0^T \|z_T(\tau) - \tilde{z}_T(\tau)\|^2 d\tau \leq \gamma^2 \int_0^T \|w_T(\tau) - \tilde{w}_T(\tau)\|^2 d\tau \quad (4.3)$$

for all $w, \tilde{w} \in \mathcal{L}_{2,T}$ $w \neq \tilde{w}$ and all $T \geq 0$, where $z(\cdot), \tilde{z}(\cdot) \in \mathbb{R}^l$ are output trajectories corresponding to the disturbances $w(\cdot), \tilde{w}(\cdot)$, respectively.

Remark 4.1. *The incremental gain of the non-relaxed systems can be studied by adding a finite function $\beta(x_0, \tilde{x}_0) \geq 0$ to the right hand side of (4.3), where $x_0, \tilde{x}_0 \in \mathbb{R}^n$ and*

$\beta(0,0) = 0$ [56]. It can be shown that no matter which definition is used, the results obtained thereafter can be translated from one to the other.

Remark 4.2. The usual \mathcal{L}_2 gain is a special case of (4.3) with $\tilde{z} = 0$, $\tilde{w} = 0$.

Our main objective is to design a stabilizing state feedback control law $u = u(x(t))$ such that the inequality (4.3) is satisfied. It is well-known that the concept of \mathcal{L}_p gains is closely related to the theory of dissipative dynamical systems introduced by Willems [44]. A practical form of dissipativity called the *differential dissipation inequality* is given in the following definition.

Definition 4.2. The continuous-time system Σ is said to be dissipative with respect to the supply rate r if there exist a control input $u(t) \in \mathbb{R}^m$ and a positive definite continuously differentiable function V , called storage function, such that

$$\frac{\partial V}{\partial x} f(x, u, w) \leq r(w, z) \quad (4.4)$$

for all $x \in \mathbb{R}^n$ and $w \in \mathbb{R}^q$, with $z = h(x, u)$.

Associated with the system $\Sigma : w \mapsto z$ (4.1)-(4.2), we can define an auxiliary system $\hat{\Sigma} : \hat{w} \mapsto \hat{z}$ as below

$$\hat{\Sigma} : \begin{cases} \dot{\hat{x}}(t) = \hat{f}(\hat{x}, \hat{u}, \hat{w}) & (4.5) \\ \hat{z}(t) = \hat{h}(\hat{x}, \hat{u}) & (4.6) \end{cases}$$

where

$$\hat{x} = \begin{pmatrix} x \\ \tilde{x} \end{pmatrix}, \quad \hat{u} = \begin{pmatrix} u \\ \tilde{u} \end{pmatrix}, \quad \hat{w} = \begin{pmatrix} w \\ \tilde{w} \end{pmatrix}, \quad \hat{z} = \begin{pmatrix} z \\ \tilde{z} \end{pmatrix}$$

and

$$\hat{f} = \begin{pmatrix} f(x, u, w) \\ f(\tilde{x}, \tilde{u}, \tilde{w}) \end{pmatrix}, \quad \hat{h} = \begin{pmatrix} h(x, u) \\ h(\tilde{x}, \tilde{u}) \end{pmatrix}$$

Now we can state the following lemma concerning the \mathcal{L}_2 incremental gain of Definition 4.1.

Lemma 4.1. The nonlinear system Σ has \mathcal{L}_2 incremental gain $\leq \gamma$ if and only if the auxiliary system $\hat{\Sigma}$ is \mathcal{L}_2 dissipative with respect to the supply rate

$$r(\hat{w}, \hat{z}) = \gamma^2 \|w - \tilde{w}\|^2 - \|z - \tilde{z}\|^2 \quad (4.7)$$

i.e., there exist a pair of control inputs $u, \tilde{u} \in \mathbb{R}^m$ and a C^1 function $V : \mathbb{R}^n \mapsto \mathbb{R}^+$ with $V(0) = 0$ such that for all $x, \tilde{x} \in \mathbb{R}^n$, $w, \tilde{w} \in \mathbb{R}^q$

$$\frac{\partial V}{\partial x} \Big|_{x=\tilde{x}} \cdot [f(x, u, w) - f(\tilde{x}, \tilde{u}, \tilde{w})] - \gamma^2 \|w - \tilde{w}\|^2 + \|h(x, u) - h(\tilde{x}, \tilde{u})\|^2 \leq 0 \quad (4.8)$$

Proof: The proof follows directly from the dissipativity theory and Definitions 4.1-4.2 (see Theorem 3 in [58], for sufficiency and Lemma 3.2 in [56] for necessity). \blacksquare

As can be seen in (4.8), finding an stabilizing controller $u = u(x(t))$ that guarantees that the closed-loop system has an \mathcal{L}_2 incremental gain $\leq \gamma$ requires satisfying a partial differential inequality that is difficult to study for the general form of (4.1)-(4.2). Indeed, even by considering a control affine structure for which successful results have been obtained based on the usual \mathcal{L}_2 gain (see [40] and the references cited therein), we can not easily find an explicit control law using the \mathcal{L}_2 incremental gain. Therefore, we will concentrate on the following known structure

$$\dot{x}(t) = Ax + Bu + \Phi(x, u) + Dw \quad (4.9)$$

$$z(t) = h(x, u) \quad (4.10)$$

which enables us to use the powerful LMI optimization tool to design the controller $u(x(t))$. Note that A , B and D are constant matrices of appropriate dimensions, and the nonlinearities Φ and h are assumed to be locally Lipschitz with respect to both arguments in regions \mathcal{D}_x and \mathcal{D}_u containing the origin, i.e., for instance for $\Phi(\cdot, \cdot)$ we have

$$\|\Phi(x_1, u^*) - \Phi(x_2, u^*)\| \leq \lambda_{\Phi_x} \|x_1 - x_2\| \quad (4.11)$$

$$\|\Phi(x^*, u_1) - \Phi(x^*, u_2)\| \leq \lambda_{\Phi_u} \|u_1 - u_2\| \quad (4.12)$$

$\forall x_1, x_2 \in \mathcal{D}_x$, $\forall u_1, u_2 \in \mathcal{D}_u$ and any admissible signals x^* and u^* . Similar equations can be written for $h(\cdot, \cdot)$ with the corresponding Lipschitz constants λ_{h_x} and λ_{h_u} . It is worth noting that if the nonlinear functions Φ and h satisfy the Lipschitz continuity condition globally in \mathbb{R}^n and \mathbb{R}^m , then all the results in the ensuing sections will be valid globally.

Lemma 4.2. *If the function Φ is locally Lipschitz in both arguments, then we get*

$$\|\Phi(x_1, u_1) - \Phi(x_2, u_2)\| \leq \lambda_{\Phi} (\|x_1 - x_2\| + \|u_1 - u_2\|) \quad (4.13)$$

$\forall x_1, x_2 \in \mathcal{D}_x$ and $\forall u_1, u_2 \in \mathcal{D}_u$, where $\lambda_\Phi = \max\{\lambda_{\Phi_x}, \lambda_{\Phi_u}\}$ is called the Lipschitz constant of Φ .

Proof: Adding and subtracting $\Phi(x_1, u_2)$ to the argument of the norm operator on the left hand side of (4.13), it yields by virtue of (4.11)-(4.12)

$$\begin{aligned} & \|\Phi(x_1, u_1) - \Phi(x_1, u_2) + \Phi(x_1, u_2) - \Phi(x_2, u_2)\| \\ & \leq \|\Phi(x_1, u_2) - \Phi(x_2, u_2)\| + \|\Phi(x_1, u_1) - \Phi(x_1, u_2)\| \\ & \leq \lambda_{\Phi_x} \|x_1 - x_2\| + \lambda_{\Phi_u} \|u_1 - u_2\| \end{aligned} \quad (4.14)$$

setting $\lambda_\Phi = \max\{\lambda_{\Phi_x}, \lambda_{\Phi_u}\}$, (4.13) is obtained immediately. ■

Similarly, the Lipschitz constant of h is set to be $\lambda_h = \max\{\lambda_{h_x}, \lambda_{h_u}\}$.

Remark 4.3. Note that we combine λ_{Φ_x} and λ_{Φ_u} in (4.14) only to simplify the formulations. One may consider different Lipschitz constants associated with the state and the control signal to put different emphasises on each of them. Fortunately, the results in the next section can be generalized for this case.

Remark 4.4. There are several works on stabilizing Lipschitz nonlinear systems (see, e.g., [106], [107], [108]). However, most of them assume the nonlinear part to be a function of x only, i.e., $\Phi(x)$. In this section, aside from satisfying a new performance index, the nonlinearity is assumed to be a function of both x and u , which is more general and challenging. Moreover, the penalty variable is assumed to be a nonlinear combination of the state and the control signal.

4.1.2 Incremental H_∞ Controller Synthesis

In this section the problem of disturbance attenuation with internal stability is addressed. More explicitly, we tackle the problem of finding an admissible controller that, in the absence of external inputs yields an exponentially stable closed-loop system with convergence rate $\alpha > 0$, i.e., $\|x\| \leq \eta \|x_0\| e^{-\alpha t}$ (see [48] or [49] for a more formal definition of exponential stability) and in the presence of disturbances satisfies an \mathcal{L}_2 incremental gain less than or equal to a minimized number γ . The state feedback controller is assumed to be $u(t) = -Kx(t)$, where $K \in \mathbb{R}^{m \times n}$, and we first focus on the system (4.9)-(4.10) without uncertainties.

Definition 4.3. *Suppose that the system (4.9)-(4.10) together with $u(t) = -Kx(t)$ has the following properties*

1. *With $w(t) = 0$, the closed-loop system is locally exponentially stable with guaranteed decay rate $\alpha > 0$, i.e. $\exists \alpha, \eta \in \mathbb{R}$: given x_0 in a sufficiently small neighbourhood of $x = 0$, $\|x\| \leq \eta \|x_0\| e^{-\alpha t}, \forall t \geq 0$.*

2. *the signal $z(t)$ satisfies*

$$\int_0^\infty \|z(\tau) - \tilde{z}(\tau)\|^2 d\tau \leq \gamma^2 \int_0^\infty \|w(\tau) - \tilde{w}(\tau)\|^2 d\tau \quad (4.15)$$

for a constant $\gamma > 0$. Under this condition, the control law $u(t)$ is said to be an incremental H_∞ controller for the system (4.9)-(4.10) with convergence rate α and disturbance attenuation level γ .

Strict NMI solution

The design procedure is stated in Theorem 4.1 which brings about a nonlinear matrix inequality (NMI) optimization. We need the following two preparatory lemmas used in the proof of our results.

Lemma 4.3. (*[109]*) *Let U, V and F be real matrices of appropriate dimensions and F satisfying $F^\top F \leq I$. Then for any scalar $\epsilon > 0$ and vectors $x, y \in \mathbb{R}^n$, we have*

$$2x^\top U F V y \leq \epsilon^{-1} x^\top U U^\top x + \epsilon y^\top V^\top V y \quad (4.16)$$

Lemma 4.4. (*Schur's complement formula, [110]*) *For a given matrix $S = \begin{bmatrix} S_{11} & S_{12} \\ * & S_{22} \end{bmatrix}$ with $S_{11} = S_{11}^\top, S_{22} = S_{22}^\top$, then the following statements are equivalent:*

1. $S < 0$,
2. $S_{11} - S_{12} S_{22}^{-1} S_{12}^\top < 0, S_{22} < 0$.

Theorem 4.1. *Consider the Lipschitz nonlinear system (4.9)-(4.10) with the Lipschitz constants λ_Φ, λ_h together with the controller $u(t) = -Kx(t)$. Suppose that for fixed scalars $\alpha, \epsilon_1, \epsilon_2 > 0$ and matrices $P = P^\top > 0$ and G , the following NMI optimization is feasible for a minimum scalar $\gamma > 0$:*

$\min(\gamma)$ s.t.

$$\begin{bmatrix} -Q + \epsilon_1^{-1}I & \sqrt{\epsilon_1}\lambda_\Phi(\|P\| + \|G\|\kappa(P))I \\ * & -I \end{bmatrix} < 0 \quad (4.17)$$

$$\begin{bmatrix} -Q - 2\alpha P + \epsilon_2^{-1}I & \sqrt{\epsilon_2\lambda_\Phi^2 + \lambda_h^2(\|P\| + \|G\|\kappa(P))}I & D \\ * & -I & 0 \\ * & * & -\gamma I \end{bmatrix} < 0 \quad (4.18)$$

where

$$Q = -(AP + PA^\top - BG - G^\top B^\top + 2\alpha P) \quad (4.19)$$

Once the problem is solved

$$K = GP^{-1} \quad (4.20)$$

$$\gamma^* \triangleq \min(\gamma) \quad (4.21)$$

then the closed-loop system with the feedback gain (4.20) is (globally) exponentially stable with decay rate α and minimum incremental disturbance attenuation γ^* of (4.21) according to Definition 4.3.

Note that Theorem 4.1 is a feasibility problem for the minimum value of γ which fulfills matrix inequalities (4.17)-(4.18). Indeed, for a desired decay rate α the parameters ϵ_1 , ϵ_2 and matrices P , G are chosen such that the proposed NMI holds a feasible solution for a minimum incremental gain γ . Alternatively, one may seek to maximize the decay rate for a prescribed incremental gain. In that case it is sufficient to solve (4.17)-(4.18) to maximize α .

Proof of Theorem 4.1: Take the Lyapunov function candidate as

$$V(x(t)) = x^\top \bar{P}x \quad (4.22)$$

where $\bar{P} = P^{-1}$. The time derivative of V along the trajectories of (4.9) is given by

$$\begin{aligned} \dot{V}(t) &= \dot{x}^\top(t)\bar{P}x(t) + x^\top(t)\bar{P}\dot{x}(t) \\ &= [Ax + Bu + \Phi(x, u) + Dw]^\top \bar{P}x + x^\top \bar{P}[Ax + Bu + \Phi(x, u) + Dw] \end{aligned} \quad (4.23)$$

Part I (Exponential stability): Applying $u = -Kx$, we get for the disturbance free plant, i.e., $w = 0$

$$\dot{V}(t) = x^\top [(A - BK)^\top \bar{P} + \bar{P}(A - BK)]x + 2x^\top \bar{P}\Phi(x, u) \quad (4.24)$$

To have exponential stability with guaranteed decay rate, it suffices $\dot{V}(x(t)) \leq -2\alpha V(x(t))$ [48] which yields $\|x(t)\| \leq \sqrt{\lambda_{\max}(P)/\lambda_{\min}(P)}\|x(0)\| \exp(-\alpha t)$. Therefore, it is needed

$$\dot{V}(t) \leq -x^\top \hat{Q}x + 2x^\top \bar{P}\Phi(x, u) < 0 \quad (4.25)$$

in which

$$(A - BK)^\top \bar{P} + \bar{P}(A - BK) + 2\alpha \bar{P} = -\hat{Q} \quad (4.26)$$

The above can be written as

$$A^\top \bar{P} + \bar{P}A - K^\top B^\top \bar{P} - \bar{P}BK + 2\alpha \bar{P} = -\hat{Q} \quad (4.27)$$

that is bilinear with respect to the variables K and \bar{P} and cannot be treated using the existing tractable LMI procedures. This problem will be overcome by pre- and post-multiplying (4.27) by P later on. Using Lemma 4.3, the controller $u = -Kx$ and the Lipschitz property of Φ , we get

$$2x^\top \bar{P}\Phi(x, u) \leq \epsilon_1^{-1} x^\top \bar{P}^2 x + \epsilon_1 \Phi^\top \Phi \leq \epsilon_1^{-1} x^\top \bar{P}^2 x + \epsilon_1 \lambda_\Phi^2 (1 + \|K\|)^2 x^\top x \quad (4.28)$$

Substituting (4.28) into (4.25), a sufficient condition for exponential stability when $w = 0$ can be obtained as

$$\begin{aligned} \dot{V}(t) &\leq x^\top [-\hat{Q} + \epsilon_1^{-1} \bar{P}^2 + \epsilon_1 \lambda_\Phi^2 (1 + \|K\|)^2 I]x \\ &\leq x^\top [-\hat{Q} + \epsilon_1^{-1} \bar{P}^2 + \epsilon_1 \lambda_\Phi^2 (1 + \|G\| \|\bar{P}\|)^2 I]x < 0 \end{aligned} \quad (4.29)$$

which is equivalent to the following matrix inequality by means of Lemma 4.4

$$\begin{bmatrix} -\hat{Q} + \epsilon_1^{-1} \bar{P}^2 & \sqrt{\epsilon_1} \lambda_\Phi (1 + \|G\| \|\bar{P}\|) I \\ * & -I \end{bmatrix} < 0 \quad (4.30)$$

Pre- and post-multiplying (4.30) by $\text{diag}(P, I)$ and then considering $P \leq \lambda_{\max}(P)I = \|P\|I$ and the matrix Q defined by

$$Q = P\hat{Q}P = -(AP + PA^\top - BG - G^\top B^\top + 2\alpha P) \quad (4.31)$$

we arrive at the matrix inequality (4.17). Note that $\kappa(P) = \|P\| \|\bar{P}\|$ denotes the condition number of the matrix P .

Part II (Disturbance attenuation): Now consider the disturbance driven system (4.9)-(4.10).

According to Lemma 4.1 the system (4.9)-(4.10) has \mathcal{L}_2 incremental gain $\leq \gamma$ if

$$\begin{aligned} J \triangleq & 2(x - \tilde{x})^\top \bar{P}[(A - BK)(x - \tilde{x}) + \Phi(x, u) - \Phi(\tilde{x}, \tilde{u}) + D(w - \tilde{w})] \\ & - \gamma^2 \|w - \tilde{w}\|^2 + \|h(x, u) - h(\tilde{x}, \tilde{u})\|^2 \leq 0 \end{aligned} \quad (4.32)$$

where the Lyapunov function of (4.22) is picked as the storage function V in (4.8). Using Lemma 4.3, $u = -Kx$, $\tilde{u} = -K\tilde{x}$ and the Lipschitz property of Φ and h , the following inequalities are derived

$$\begin{aligned} 2(x - \tilde{x})^\top \bar{P}[\Phi(x, u) - \Phi(\tilde{x}, \tilde{u})] & \leq \epsilon_2^{-1}(x - \tilde{x})^\top \bar{P}^2(x - \tilde{x}) + \epsilon_2(\Phi - \tilde{\Phi})^\top(\Phi - \tilde{\Phi}) \\ & \leq \epsilon_2^{-1}(x - \tilde{x})^\top \bar{P}^2(x - \tilde{x}) + \epsilon_2 \lambda_\Phi^2 (\|x - \tilde{x}\| + \|u - \tilde{u}\|)^2 \\ & \leq \epsilon_2^{-1}(x - \tilde{x})^\top \bar{P}^2(x - \tilde{x}) + \epsilon_2 \lambda_\Phi^2 (1 + \|K\|)^2 (x - \tilde{x})^\top (x - \tilde{x}) \end{aligned} \quad (4.33)$$

$$\begin{aligned} \|h(x, u) - h(\tilde{x}, \tilde{u})\|^2 & \leq \lambda_h^2 (\|x - \tilde{x}\| + \|u - \tilde{u}\|)^2 \\ & \leq \lambda_h^2 (1 + \|K\|)^2 (x - \tilde{x})^\top (x - \tilde{x}) \end{aligned} \quad (4.34)$$

Based on (4.33)-(4.34) and the definition of \hat{Q} in (4.27), the performance criterion J in (4.31) can be bounded as below

$$\begin{aligned} J \leq & (x - \tilde{x})^\top [-\hat{Q} - 2\alpha\bar{P} + \epsilon_2^{-1}\bar{P}^2 + (\epsilon_2\lambda_\Phi^2 + \lambda_h^2)(1 + \|K\|)^2](x - \tilde{x}) + 2(x - \tilde{x})^\top \bar{P} \\ & D(w - \tilde{w}) - \gamma^2(w - \tilde{w})^\top(w - \tilde{w}) \end{aligned} \quad (4.35)$$

Hence, it can be deduced from (4.35) and Schur's complement that a sufficient condition for $J \leq 0$ is given as

$$\begin{bmatrix} -\hat{Q} - 2\alpha\bar{P} + \epsilon_2^{-1}\bar{P}^2 & \sqrt{\epsilon_2\lambda_\Phi^2 + \lambda_h^2}(1 + \|K\|)\bar{P} & \bar{P}D \\ * & -I & 0 \\ * & * & -\gamma I \end{bmatrix} < 0 \quad (4.36)$$

In analogy with Part I, pre- and post-multiplying the inequality (4.36) by $\text{diag}(P, I, I)$ together with $P \leq \|P\|I$ and $Q = P\hat{Q}P$ in (4.31) leads to the matrix inequality (4.18). Finally, since the dissipativity of the closed loop system is ensured, Lemma 4.1 implies that

$$\begin{aligned} & \int_0^\infty ((z - \tilde{z})^\top(z - \tilde{z}) - \gamma^2(w - \tilde{w})^\top(w - \tilde{w})) d\tau \leq 0 \\ & \Rightarrow \|z - \tilde{z}\| \leq \gamma \|w - \tilde{w}\| \end{aligned} \quad (4.37)$$

This concludes the proof. ■

Converting NMI to LMI

Due to presence of norm operators in (4.17)-(4.18), the design method provided by Theorem 4.1 is in the form of a nonlinear matrix inequality (NMI). Unfortunately, unlike the case of linear matrix inequalities (LMIs) there is currently no efficient solution in the numerical analysis literature capable of solving NMIs. In order to take advantage of the existent efficient numerical LMI solvers such as Matlab LMI solver, we now show how to convert the NMIs (4.17)-(4.18) into the LMI framework. For this purpose, we need the following assumption.

Assumption 4.1. *Suppose that the nonlinear functions Φ and h are locally Lipschitz with respect to the whole vector $[x \ u]^\top$, i.e.,*

$$\|\Phi(x_1, u_1) - \Phi(x_2, u_2)\| \leq \lambda_\Phi \left\| \begin{bmatrix} x_1 \\ u_1 \end{bmatrix} - \begin{bmatrix} x_2 \\ u_2 \end{bmatrix} \right\| \quad (4.38)$$

$$\|h(x_1, u_1) - h(x_2, u_2)\| \leq \lambda_h \left\| \begin{bmatrix} x_1 \\ u_1 \end{bmatrix} - \begin{bmatrix} x_2 \\ u_2 \end{bmatrix} \right\| \quad (4.39)$$

for all $x_1, x_2 \in \mathcal{D}_x$ and $u_1, u_2 \in \mathcal{D}_u$.

Remark 4.5. *It can be shown that if the function $\Phi(\cdot, \cdot)$ satisfies the inequality (4.38), then the Lipschitz continuity condition (4.13) holds readily. However, the reverse is not true in general. A similar statement can be made about the function $h(\cdot, \cdot)$.*

Corollary 4.1. *Consider the Lipschitz nonlinear system (4.9)-(4.10) satisfying Assumption 4.1 together with the controller $u(t) = -Kx(t)$. Suppose that there exist fixed scalars $\alpha, \epsilon_1, \epsilon_2 > 0$ and a scalar $\gamma > 0$, matrices $P = P^\top > 0$ and G , such that the following LMI optimization is feasible:*

$\min(\gamma)$ s.t.

$$\begin{bmatrix} -Q + \epsilon_1^{-1}I & \sqrt{\epsilon_1}\lambda_\Phi P & \sqrt{\epsilon_1}\lambda_\Phi G^\top \\ * & -I & 0 \\ * & * & -I \end{bmatrix} < 0 \quad (4.40)$$

$$\begin{bmatrix} -Q - 2\alpha P + \epsilon_2^{-1}I & \sqrt{\epsilon_2\lambda_\Phi^2 + \lambda_h^2}P & \sqrt{\epsilon_2\lambda_\Phi^2 + \lambda_h^2}G^\top & D \\ * & -I & 0 & 0 \\ * & * & -I & 0 \\ * & * & * & -\gamma I \end{bmatrix} < 0 \quad (4.41)$$

where Q is given by (4.19). Then $u(t)$ with the feedback gain $K = GP^{-1}$ is an incremental H_∞ controller with exponential decay rate α and minimum disturbance attenuation $\gamma^* = \min(\gamma)$.

Proof: By making use of Assumption 4.1 and Lemma 4.3 we get the critical inequalities shown below

$$\begin{aligned}
2(x - \tilde{x})^\top \bar{P} [\Phi(x, u) - \Phi(\tilde{x}, \tilde{u})] &\leq \epsilon_1^{-1} (x - \tilde{x})^\top \bar{P}^2 (x - \tilde{x}) + \epsilon_1 (\Phi - \tilde{\Phi})^\top (\Phi - \tilde{\Phi}) \\
&\leq \epsilon_1^{-1} (x - \tilde{x})^\top \bar{P}^2 (x - \tilde{x}) + \epsilon_1 \lambda_{\Phi}^2 (\|x - \tilde{x}\|^2 + \|u - \tilde{u}\|^2) \\
&\leq \epsilon_1^{-1} (x - \tilde{x})^\top \bar{P}^2 (x - \tilde{x}) + \epsilon_1 \lambda_{\Phi}^2 (x - \tilde{x})^\top (I + K^\top K) (x - \tilde{x})
\end{aligned} \tag{4.42}$$

$$\begin{aligned}
\|h(x, u) - h(\tilde{x}, \tilde{u})\|^2 &\leq \lambda_h^2 \left\| \begin{bmatrix} x - \tilde{x} \\ u - \tilde{u} \end{bmatrix} \right\|^2 \leq \lambda_h^2 (\|x - \tilde{x}\|^2 + \|u - \tilde{u}\|^2) \\
&\leq \lambda_h^2 (x - \tilde{x})^\top (I + K^\top K) (x - \tilde{x})
\end{aligned} \tag{4.43}$$

instead of (4.33)-(4.34) which enable us to convert the NMIs of Theorem 4.1 to the LMIs of Corollary 4.1. The remainder of the proof is analogous to that of Theorem 4.1, and is omitted. ■

Remark 4.6. An alternative way of converting the NMIs in Theorem 4.1 into an LMI framework is to impose a bound on the feedback gain norm in (4.29) and (4.35) as $\|K\| \leq \|G\| \|P^{-1}\| \leq \sigma_1 \sigma_2$ and then adding the following two matrix inequalities to our LMIs

$$\begin{aligned}
\begin{bmatrix} I & \frac{1}{\sigma_1} G^\top \\ * & I \end{bmatrix} &> 0 \\
\begin{bmatrix} I & \sigma_2 P^\top \\ * & I \end{bmatrix} &> 0
\end{aligned}$$

where $\sigma_1, \sigma_2 > 0$ are prescribed scalars.

4.1.3 Uncertain Nonlinear Plants

This section develops the H_∞ controller design via incremental gain for a class of nonlinear uncertain systems. Moreover, a norm-wise robustness analysis has been carried out to obtain explicit bounds on the nonlinear uncertainty.

4.1.4 Robust Controller Design

Suppose that the nonlinear plant (4.1)-(4.2) can be written into in the following uncertain form

$$\dot{x}(t) = (A + \Delta A(t))x(t) + (B + \Delta B(t))u(t) + \Phi(x(t), u(t)) + (D + \Delta D(t))w(t) \quad (4.44)$$

$$z(t) = h(x(t), u(t)) \quad (4.45)$$

where $\Delta A(t)$, $\Delta B(t)$, and $\Delta C(t)$ are unknown matrices representing time-varying uncertainties, and are assumed to have the structure

$$\begin{aligned} \Delta A(t) &= M_a F(t) N_a & \Delta B(t) &= M_b F(t) N_b \\ \Delta D(t) &= M_d F(t) N_d \end{aligned} \quad (4.46)$$

in which M_a , N_a , M_b , N_b , M_c , and N_c are known real constant matrices of appropriate dimensions and $F(t)$ is an unknown real-valued time-varying matrix satisfying

$$F^\top(t)F(t) \leq I \quad \forall t \in [0, \infty) \quad (4.47)$$

It is worth pointing out that the structure of uncertainties in (4.44)-(4.45) has been widely used in the problems of robust control and robust filtering for both continuous-time and discrete-time systems and can capture the uncertainty in a number of practical situations (see, e.g., [108,111,112]). The following theorem extends the design procedure of Corollary 4.1 to the uncertain case introduced above.

Theorem 4.2. *Consider the Lipschitz nonlinear uncertain system (4.44)-(4.45) satisfying Assumption 4.1 together with the controller $u(t) = -Kx(t)$. Suppose that for fixed scalars $\alpha, \epsilon_1, \epsilon_2 > 0$ and matrices $P = P^\top > 0$ and G , the following LMI optimization is feasible for a minimum scalar $\gamma > 0$*

$\min(\gamma)$ s.t.

$$\begin{bmatrix} R + \epsilon_1^{-1}I & PS_1^\top & G^\top N_b \\ * & -I & 0 \\ * & * & -I \end{bmatrix} < 0 \quad (4.48)$$

$$\begin{bmatrix} R - 2\alpha P + \epsilon_2^{-1}I & PS_2^\top & G^\top S_3 & D \\ * & -I & 0 & 0 \\ * & * & -I & 0 \\ * & * & * & -\gamma^2 I + N_d^\top N_d \end{bmatrix} < 0 \quad (4.49)$$

where

$$R = -Q + M_a M_a^\top + M_b M_b^\top + M_c M_c^\top \quad (4.50)$$

$$S_1 = (\epsilon_1 \lambda_\Phi^2 + N_a^\top N_a)^{\frac{1}{2}} \quad (4.51)$$

$$S_2 = (\epsilon_2 \lambda_\Phi^2 + \lambda_h^2 + N_a^\top N_a)^{\frac{1}{2}} \quad (4.52)$$

$$S_3 = (\epsilon_2 \lambda_\Phi^2 + \lambda_h^2 + N_b^\top N_b)^{\frac{1}{2}} \quad (4.53)$$

and Q is defined by (4.19). Then the controller u with the feedback gain $K = GP^{-1}$ is a robust incremental stabilizer with exponential decay rate α and minimum disturbance attenuation $\gamma^* = \min \gamma$.

Sketch of the Proof: The approach is similar to the proof of Theorem 4.1. In addition to the inequalities used in the proof of Corollary 4.1, we need the following inequalities that are all derived from Lemma 4.3

$$2x^\top M_a F(t) N_a P x \leq x^\top M_a M_a^\top x + x^\top P N_a^\top N_a P x$$

$$2x^\top M_b F(t) N_b G x \leq x^\top M_b M_b^\top x + x^\top G N_b^\top N_b P x$$

$$2x^\top M_d F(t) N_d w \leq x^\top M_d M_d^\top x + w^\top N_d^\top N_d w$$

inserting these inequalities into \dot{V} and J gives rise to the LMIs (4.48)-(4.49). It should be mentioned that in this case, when $w = 0$, a sufficient condition for exponential stability with guaranteed decay rate α is

$$R + (1 + \epsilon_1^{-1})I + P S_1^\top S_1 P + G^\top N_a N_a^\top G < 0$$

that is already included in (4.48) by means of Schur complements. Moreover, since the matrices $\epsilon_1 \lambda_\Phi^2 + N_a^\top N_a$, $\epsilon_2 \lambda_\Phi^2 + \lambda_h^2 + N_a^\top N_a$, and $\epsilon_2 \lambda_\Phi^2 + \lambda_h^2 + N_b^\top N_b$ are positive definite, they have always have a square root. ■

Remark 4.7. We observe that in some cases the optimization problems of Corollary 4.1 and Theorem 4.2 can result in very large or small entries in the gain matrix K . This issue can be resolved by solving the feasibility problem of (4.40)-(4.41) and (4.48)-(4.49) with a prescribed attenuation level γ (see e.g., [106, 107], [110]).

Remark 4.8. By choosing $\lambda = \max\{\lambda_\Phi, \lambda_h, \}$ as the overall Lipschitz constant of the system (4.9)-(4.10), the LMIs (4.40)-(4.41) and (4.48)-(4.49) become linear in both λ and

γ . In this case, the optimizations can be formulated to maximize the admissible Lipschitz constant [108], [111]. As we will see in the next subsection, this maximization adds an extra significant feature to our controller which makes it robust against nonlinear uncertainties.

4.1.5 Robustness Analysis

As mentioned in Remark 4.7, if the overall Lipschitz constant λ is picked as the optimization variable in Theorem 4.2, then maximization of λ makes the proposed controller robust against some Lipschitz nonlinear uncertainty. This feature is studied here through a norm-wise analysis. We find an upper bound on the Lipschitz constant of the nonlinear uncertainty and the norm of the Jacobian matrix of the corresponding nonlinear function.

Assume nonlinear uncertainty as follows

$$\Phi_{\Delta}(x, u) = \Phi(x, u) + \Delta\Phi(x, u) \quad (4.54)$$

where $\Delta\Phi$ is Lipschitz continuous with the Lipschitz constant $\Delta\lambda_{\Phi}$. Inserting (4.54) into (4.44) leads to

$$\dot{x}(t) = (A + \Delta A(t))x(t) + (B + \Delta B(t))u(t) + \Phi(x, u) + \Delta\Phi(x, u) + (D + \Delta D)w(t) \quad (4.55)$$

Let $\lambda = \max\{\lambda_{\Phi}, \lambda_h\}$ and $\Delta\lambda = \Delta\lambda_{\Phi}$.

Proposition 4.1. *Suppose that the actual Lipschitz constant of the system is λ and Theorem 4.2 is rewritten in the form of maximizing the Lipschitz constant with maximum admissible value of λ^* . Then the controller derived from Theorem 4.2 can tolerate any additive Lipschitz nonlinear uncertainty with Lipschitz constant less than or equal to $\lambda^* - \lambda$.*

Proof: Without loss of generality, we can assume that $\lambda = \lambda_{\Phi}$. Based on the Schwartz inequality and Assumption 4.1, we get

$$\begin{aligned} \|\Phi_{\Delta}(x_1, u_1) - \Phi_{\Delta}(x_2, u_2)\| &\leq \|\Phi_{\Delta}(x_1, u_1) - \Phi_{\Delta}(x_2, u_2)\| + \|\Delta\Phi(x_1, u_1) - \Delta\Phi(x_2, u_2)\| \\ &\leq \lambda \left\| \begin{bmatrix} x_1 - x_2 \\ u_1 - u_2 \end{bmatrix} \right\| + \Delta\lambda \left\| \begin{bmatrix} x_1 - x_2 \\ u_1 - u_2 \end{bmatrix} \right\| \end{aligned}$$

Accordingly, $\Phi_{\Delta}(\cdot, \cdot)$ can be any Lipschitz nonlinearity with Lipschitz constant less than or equal to λ^* ,

$$\|\Phi_{\Delta}(x_1, u_1) - \Phi_{\Delta}(x_2, u_2)\| \leq \lambda^* \left\| \begin{bmatrix} x_1 - x_2 \\ u_1 - u_2 \end{bmatrix} \right\|$$

therefore, there must be $\lambda + \Delta\lambda \leq \lambda^* \rightarrow \Delta\lambda \leq \lambda^* - \lambda$. ■

In addition, we know that for any continuously differentiable function $\Delta\Phi$

$$\|\Delta\Phi(x_1, u^*) - \Delta\Phi(x_2, u^*)\| \leq \left\| \frac{\partial \Delta\Phi}{\partial x}(x_1 - x_2) \right\|$$

where u^* is any admissible control signal and $\frac{\partial \Delta\Phi}{\partial x}$ is the Jacobian matrix. So $\Delta\Phi(x, u)$ can be any additive uncertainty with $\left\| \frac{\partial \Delta\Phi}{\partial x} \right\| \leq \lambda^* - \lambda$.

4.2 Observer-Based Control for One-Sided Lipschitz Systems

4.2.1 System Model

Now consider the continuous-time nonlinear dynamical system expressed by

$$\begin{cases} \dot{x}(t) = Ax(t) + Bu(t) + \Phi(x, u) + D_1w(t) \\ y(t) = Cx(t) + h(x, u) + D_2w(t) \\ z(t) = g(x, u) \end{cases} \quad (4.56)$$

where $x \in \mathbb{R}^n$ is the state, $u \in \mathbb{R}^m$ control input, $w \in \mathbb{R}^q$ exogenous disturbance, also $y \in \mathbb{R}^p$ and $z \in \mathbb{R}^l$ stands for the measurement and the regulated output (cost variable), respectively. It is assumed that A, B, C, D_1 and D_2 are constant matrices of appropriate dimensions, and the nonlinear functions Φ, h and g fulfill certain Lipschitz or one-sided Lipschitz conditions, as specified later, based on Definitions 2.9.

The properties of Definition 2.9 might be local or global. We refer the interested readers to [63] for a comprehensive study. Here is an example of a nonlinearity which satisfies the one-sided Lipschitz continuity but not the Lipschitz continuity.

Example 4.2. Consider the discontinuous nonlinear function $f(x) = \frac{1}{\sqrt{x}}$. Clearly, this function is not Lipschitz on any interval like $[0, c]$. Conversely, for any $x_1, x_2 \in [0, c]$ we

get

$$\begin{aligned}\langle f(x_1) - f(x_2), x_1 - x_2 \rangle &= \left(\frac{1}{\sqrt{x_1}} - \frac{1}{\sqrt{x_2}} \right) (x_1 - x_2) \\ &= -\frac{(x_1 - x_2)^2}{(\sqrt{x_1} + \sqrt{x_2})(\sqrt{x_1 x_2})} \leq -\frac{1}{2c\sqrt{c}} (x_1 - x_2)^2\end{aligned}$$

thus, it is locally one-sided Lipschitz with the one-sided Lipschitz constant $-1/(2c\sqrt{c})$.

Remark 4.9. *The one-sided Lipschitz condition is different from the nondecreasing nonlinearities addressed by [104]. For instance, the nonlinear function in Example 4.2 satisfies $(x_2 - x_1)[f(x_2) - f(x_1)] < 0$ with $0 < x_1 < x_2$ and so f is not nondecreasing or slope-restricted.*

4.2.2 Observer-based Controller Design

In this section we tackle the problem of designing an H_∞ stabilizing control law together with a stable observer when only the input u and the output y are available.

Given the dynamical system (4.56), the state feedback controller is assumed to be $u(t) = -K\hat{x}(t)$, where $K \in \mathbb{R}^{m \times n}$ and \hat{x} is the estimated state obtained from a nonlinear observer of the following structure

$$\dot{\hat{x}}(t) = A\hat{x} + Bu + \Phi(\hat{x}, u) + L[y - C\hat{x} - h(\hat{x}, u)] \quad (4.57)$$

with $L \in \mathbb{R}^{n \times p}$. Our purpose is to find the controller gain K and the observer gain L to satisfy our main expectations:

- With $w = 0$, the closed-loop system and the observer (4.57) are asymptotically stable, i.e., $\hat{x} \rightarrow x$ and $x \rightarrow 0$.
- In the presence of disturbances, the closed-loop system satisfies the H_∞ performance index given by the incremental gain condition of (4.3) for a minimized value $\gamma > 0$.

Before stating the main result, we make some important assumptions to the system model (4.56) as below.

Assumption 4.2. *The nonlinear function Φ is one-sided Lipschitz $\forall x \in \mathcal{X}_\Phi$ with the one-sided Lipschitz constant ρ according to Definition 2.9, and also locally Lipschitz with respect to u , i.e.,*

$$\|\Phi(x^*, u_1) - \Phi(x^*, u_2)\| \leq \lambda_u \|u_1 - u_2\| \quad \forall u_1, u_2 \in \mathcal{U}_\Phi \quad (4.58)$$

for any admissible state x^* .

Assumption 4.3. *The nonlinearity Φ can be written as*

$$\Phi(x, u) = E\Psi(x, u) \quad (4.59)$$

where the full-column rank matrix $E \in \mathbb{R}^{n \times s}$ is the corresponding distribution of $\Psi(x, u)$ onto the nonlinear function $\Phi(x, u)$

Assumption 4.4. *The nonlinear functions h and g are locally Lipschitz with respect to both arguments in the regions \mathcal{X}_h , \mathcal{X}_g and \mathcal{U}_h , \mathcal{U}_g with the Lipschitz constants λ_h and λ_g , respectively.*

Remark 4.10. *It is worth mentioning that the Lipschitz continuity in (4.58) is indeed a mild, yet practical assumption. This can be verified by the fact that, most of the results on nonlinear H_∞ design are based on the well-known control affine structure $\Phi(x, u) = a(x) + b(x)u$ that is obviously Lipschitz with respect to u .*

Remark 4.11. *Assumption 4.3 places a geometric condition on the one-sided Lipschitz function Φ . Note that this condition doesn't affect neither the value of the one-sided Lipschitz constant nor the Lyapunov matrix in our synthesis (see Theorem 4.3).*

Theorem 4.3 sums up our main result by proposing an LMI-based technique for optimal output feedback design that satisfies the incremental H_∞ performance criterion.

Theorem 4.3. *Suppose that the nonlinear one-sided Lipschitz system (4.56) satisfies Assumptions 4.2-4.4. The state feedback controller $u = -K\hat{x}$ along with the observer (4.57) asymptotically stabilizes the closed-loop system with minimum \mathcal{L}_2 incremental gain γ^* , if there exists constants $\sigma_1, \sigma_2 > 0$, scalars $\mu, \epsilon_1, \epsilon_2 > 0$ and matrices $X_1 = X_1^\top$, $X_2 = X_2^\top$, $R > 0$, G_1 and G_2 such that the following LMI optimization is feasible*

$\min(\mu)$ *s.t.*

$$(E^\perp X_1 E^{\perp\top} + \epsilon_1 I)B = BR \quad (4.60)$$

$$\begin{bmatrix} I & \frac{1}{\sigma_1} G_1^\top \\ * & I \end{bmatrix} > 0 \quad (4.61)$$

$$\begin{bmatrix} I & \sigma_2 R^\top \\ * & I \end{bmatrix} > 0 \quad (4.62)$$

$$\begin{bmatrix} -Q_1 + 2\epsilon_1 \rho I & BG_1 & 0 \\ * & -Q_2 + (2\epsilon_2 \rho + \lambda_h^2)I & G_2 \\ * & * & -I \end{bmatrix} < 0 \quad (4.63)$$

$$\begin{bmatrix} \Sigma_1 & -\Omega_1 & \Omega_1 & \Omega_2 \\ * & \Sigma_2 & \Omega_3 & \Omega_4 \\ * & * & \Sigma_2 & -\Omega_4 \\ * & * & * & -\mu I \end{bmatrix} < 0 \quad (4.64)$$

where $E^\perp X_1 E^{\perp\top} + \epsilon_1 I > 0$, $E^\perp X_2 E^{\perp\top} + \epsilon_2 I > 0$ and

$$\begin{aligned} Q_1 = & -(A^\top E^\perp X_1 E^{\perp\top} + E^\perp X_1 E^{\perp\top} A + \epsilon_1 A^\top + \epsilon_1 A \\ & - G_1^\top B^\top - BG_1) \end{aligned} \quad (4.65)$$

$$\begin{aligned} Q_2 = & -(A^\top E^\perp X_2 E^{\perp\top} + E^\perp X_2 E^{\perp\top} A + \epsilon_2 A^\top + \epsilon_2 A \\ & - C^\top G_2^\top - G_2 C) \end{aligned} \quad (4.66)$$

$$\Sigma_1 = \begin{bmatrix} -Q_1 + \epsilon_1(2\rho + 3\lambda_u \sigma_1 \sigma_2)I & \lambda_g(1 + \sigma_1 \sigma_2) \\ * & -I \end{bmatrix} \quad (4.67)$$

$$\Sigma_2 = \begin{bmatrix} -Q_2 + (4\epsilon_2 \rho + 2\epsilon_1 \lambda_u \sigma_1 \sigma_2 + 2\lambda_h^2)I & G_2 \\ * & -I \end{bmatrix} \quad (4.68)$$

$$\Omega_1 = \begin{bmatrix} BG_1 & 0 \\ 0 & 0 \end{bmatrix}, \quad \Omega_2 = \begin{bmatrix} (E^\perp X_1 E^{\perp\top} + \epsilon_1 I)D_1 \\ 0 \end{bmatrix} \quad (4.69)$$

$$\Omega_3 = \begin{bmatrix} Q_2 & 0 \\ 0 & 0 \end{bmatrix}, \quad \Omega_4 = \begin{bmatrix} (E^\perp X_2 E^{\perp\top} + \epsilon_2 I)D_1 - G_2 D_2 \\ 0 \end{bmatrix} \quad (4.70)$$

Once the problem is solved

$$K = G_1 R^{-1} \quad (4.71)$$

$$L = (E^\perp X_2 E^{\perp\top} + \epsilon_2 I)^{-1} G_2 \quad (4.72)$$

$$\gamma^* \triangleq \sqrt{\min(\mu)} \quad (4.73)$$

In order to prove this theorem, we need two preparatory lemmas.

Lemma 4.5. [113] For any vectors $x, y \in \mathbb{R}^n$ and any positive definite matrix $P \in \mathbb{R}^{n \times n}$, we have

$$2x^\top y \leq x^\top P x + y^\top P^{-1} y \quad (4.74)$$

Lemma 4.6. For any symmetric matrix $P \in \mathbb{R}^{n \times n}$ and nonzero matrix $M \in \mathbb{R}^{n \times m}$, there exists a symmetric matrix $X \in \mathbb{R}^{m \times m}$ and a positive scalar $\epsilon > 0$ such that P can be parameterized in the form $P = M X M^\top + \epsilon I_n$.

Proof: It is based on the proof of [103, Lemma 4.1], thus omitted. ■

Proof of Theorem 4.3: From (4.56) and (4.57), the error dynamics is

$$\dot{e}(t) = (A - LC)e + \Phi(x, u) - \Phi(\hat{x}, u) + L[h(x, u) - h(\hat{x}, u)] + (D_1 - LD_2)w \quad (4.75)$$

where $e = x - \hat{x}$ is the state estimation error. Let $\mathcal{X} = \mathcal{X}_\Phi \cap \mathcal{X}_h \cap \mathcal{X}_g$ and $\mathcal{U} = \mathcal{U}_\Phi \cap \mathcal{U}_h \cap \mathcal{U}_g$.

Now, Choose the following Lyapunov function candidate for $x \in \mathcal{X}$, $u \in \mathcal{U}$

$$V(x, e) = X^\top \begin{bmatrix} P_1 & 0 \\ 0 & P_2 \end{bmatrix} X = V_1 + V_2 \quad (4.76)$$

where $X = \begin{bmatrix} x^\top & e^\top \end{bmatrix}^\top$ is the augmented state, P_1 and P_2 are symmetric positive definite matrices, and $V_1 = x^\top P_1 x$, $V_2 = e^\top P_2 e$.

Part I (Asymptotic stability): Taking the derivative of V_1 along the trajectories of (4.56) yields

$$\begin{aligned} \dot{V}_1(t) &= \dot{x}^\top(t) P_1 x(t) + x^\top(t) P_1 \dot{x}(t) \\ &= [Ax + Bu + \Phi(x, u) + D_1 w]^\top P_1 x + x^\top P_1 [Ax + Bu + \Phi(x, u) + D_1 w] \end{aligned} \quad (4.77)$$

Applying the control law $u = -K\hat{x}$ and considering $\hat{x} = x + e$ along with Assumption 4.3, we get

$$\begin{aligned} \dot{V}_1(t) &= x^\top [(A - BK)^\top P_1 + P_1 (A - BK)] x \\ &\quad + 2x^\top P_1 E \Psi(x, u) + 2x^\top P_1 D_1 w - 2x^\top P_1 B K e \end{aligned} \quad (4.78)$$

Let

$$(A - BK)^\top P_1 + P_1 (A - BK) = A^\top P_1 + P_1 A - K^\top B^\top P_1 - P_1 B K = -Q_1 \quad (4.79)$$

that is bilinear with respect to the variables K and P_1 . As it will be seen, the equality constraint (4.60) enables us to convert this BMI into an semidefinite programming (SDP) problem. By virtue of Lemma 4.6, assume that the Lyapunov matrix P_1 can be parameterized as

$$P_1 = E^\perp X_1 E^{\perp\top} + \epsilon_1 I_n \quad (4.80)$$

where X_1 is an arbitrary weighting matrix, $\epsilon_1 > 0$ and E^\perp is the orthogonal complement of E , i.e., $E^{\perp\top} E = 0$. Now using (4.80) and the one-sided Lipschitz condition in Assumption 4.2, it follows that $x^\top P_1 E \Psi(x, u) = \epsilon_1 \langle E \Psi(x, u) - 0, x - 0 \rangle \leq \epsilon_1 \rho x^\top x$ and hence

$$\dot{V}_1(t) \leq -x^\top Q_1 x + 2\epsilon_1 \rho x^\top x + 2x^\top P_1 D_1 w - 2x^\top P_1 B K e \quad (4.81)$$

Similarly, the time derivative of V_2 along (4.75) is given by

$$\begin{aligned} \dot{V}_2(t) &= e^\top(t) P_1 e(t) + e^\top(t) P_1 \dot{e}(t) \\ &= e^\top [(A - LC)^\top P_2 + P_2 (A - LC)] e + 2e^\top P_2 [\Phi(x, u) - \Phi(\hat{x}, u)] \\ &\quad + 2e^\top P_2 (D_1 - LD_2) w + 2e^\top P_2 L [h(x, u) - h(\hat{x}, u)] \end{aligned} \quad (4.82)$$

Define

$$(A - LC)^\top P_2 + P_2 (A - LC) = A^\top P_2 + P_2 A - C^\top L^\top P_2 - P_2 LC = -Q_2 \quad (4.83)$$

which can be written as

$$A^\top P_2 + P_2 A - C^\top G_2^\top - G_2 C = -Q_2 \quad (4.84)$$

with $G_2 \triangleq P_2 L$. Assume that P_2 can be also parameterized as $P_2 = E^\perp X_2 E^{\perp\top} + \epsilon_2 I_n$.

Now, using the one-sided Lipschitz property of Φ we have

$$\begin{aligned} e^\top P_2 [\Phi(x, u) - \Phi(\hat{x}, u)] &= \langle P_2 E \Psi(x, u) - P_2 E \Psi(\hat{x}, u), x - \hat{x} \rangle \\ &= \epsilon_2 \langle E \Psi(x, u) - E \Psi(\hat{x}, u), x - \hat{x} \rangle \leq \epsilon_2 \rho e^\top e \end{aligned} \quad (4.85)$$

and the Lipschitz continuity of h together with Lemma 4.5 leads to

$$\begin{aligned} 2e^\top P_2 L [h(x, u) - h(\hat{x}, u)] &\leq e^\top G_2 G_2^\top e + \|h(x, u) - h(\hat{x}, u)\|^2 \\ &\leq e^\top G_2 G_2^\top e + \lambda_h^2 e^\top e \end{aligned} \quad (4.86)$$

Substituting (4.84)-(4.86) into (4.82) we obtain

$$\dot{V}_2(t) \leq -e^\top Q_2 e + 2\epsilon_2 \rho e^\top e + e^\top G_2 G_2^\top e + \lambda_h^2 e^\top e + 2e^\top P_2 (D_1 - LD_2) w \quad (4.87)$$

Then, considering inequalities (4.81) and (4.87), the time derivative of $V(x, e)$ is bounded via

$$\begin{aligned} \dot{V}(t) \leq & x^\top [-Q_1 + 2\epsilon_1 \rho I] x + e^\top [-Q_2 + (2\epsilon_2 \rho + \lambda_h^2) I + G_2 G_2^\top] e \\ & - 2x^\top P_1 B K e + 2x^\top P_1 D_1 w + 2e^\top P_2 (D_1 - LD_2) w \end{aligned} \quad (4.88)$$

Therefore, a sufficient condition for asymptotic stability ($\dot{V} < 0$) when $w = 0$ is given by the matrix inequality

$$\begin{bmatrix} -Q_1 + 2\epsilon_1 \rho I & P_1 B K & 0 \\ K^\top B^\top P_1 & -Q_2 + (2\epsilon_2 \rho + \lambda_h^2) I & G_2 \\ 0 & G_2^\top & -I \end{bmatrix} < 0 \quad (4.89)$$

that is obtained by means of the Schur complement [110]. Using (4.60) and the change of variables $G_1 = RK$ we have $P_1 B K = B R K \triangleq B G_1$. Having G_1 and inserting the geometric parametrization of P_1 and P_2 into (4.89), we arrive at the LMI (4.63). Note that the positiveness of R ensures the nonsingularity of R , and hence, the existence of a unique solution for K .

Part II (Performance criterion): According to Lemma 4.1, the closed-loop system (4.56) with the observer (4.57) and the controller $u = -K\hat{x}$ has \mathcal{L}_2 incremental gain $\leq \gamma$ if

$$J \triangleq \left. \frac{dV}{dX} \right|_{X=\tilde{X}} \cdot [\mathcal{F}(X, u, w) - \mathcal{F}(\tilde{X}, \tilde{u}, \tilde{w})] - \gamma^2 \|w - \tilde{w}\|^2 + \|g(x, u) - g(\tilde{x}, \tilde{u})\|^2 \leq 0 \quad (4.90)$$

in which, the storage function V is chosen the same as the Lyapunov function (4.76), $X = [x^\top \ e^\top]^\top$ and $\mathcal{F} = [\mathcal{F}_1^\top \ \mathcal{F}_2^\top]^\top$ with

$$\begin{aligned} \mathcal{F}_1 &= (A - BK)x + \Phi(x, u) + D_1 w \\ \mathcal{F}_2 &= (A - LC)e + \Phi(x, u) - \Phi(\hat{x}, u) + L[y - C\hat{x} - h(\hat{x}, u)] + (D_1 - LD_2)w \end{aligned} \quad (4.91)$$

For simplicity denote $\tilde{e} = \tilde{x} - \hat{x}$, $\bar{\Phi}(x, \hat{x}, u) \triangleq \Phi(x, u) - \Phi(\hat{x}, u)$, and $\bar{h}(x, \hat{x}, u) \triangleq h(x, u) -$

$h(\hat{x}, u)$. With these notations, calculating (4.90) yields

$$\begin{aligned}
J &= \frac{\partial V_1}{\partial x} \Big|_{X-\tilde{X}} \cdot [\mathcal{F}_1(x, u, w) - \mathcal{F}_1(\tilde{x}, \tilde{u}, \tilde{w})] + \frac{\partial V_2}{\partial e} \Big|_{X-\tilde{X}} \cdot [\mathcal{F}_2(x, \hat{x}, u, w) - \mathcal{F}_2(\tilde{x}, \tilde{\hat{x}}, \tilde{u}, \tilde{w})] \\
&\quad - \gamma^2 \|w - \tilde{w}\|^2 + \|g(x, u) - g(\tilde{x}, \tilde{u})\|^2 \\
&= 2(x - \tilde{x})^\top P_1 [(A - BK)(x - \tilde{x}) - BK(e - \tilde{e}) + \Phi(x, u) - \Phi(\tilde{x}, \tilde{u}) + D_1(w - \tilde{w})] \\
&\quad + 2(e - \tilde{e})^\top P_2 [(A - LC)(e - \tilde{e}) + \bar{\Phi}(x, \hat{x}, u) - \bar{\Phi}(\tilde{x}, \tilde{\hat{x}}, \tilde{u}) \\
&\quad + L\bar{h}(x, \hat{x}, u) - L\bar{h}(\tilde{x}, \tilde{\hat{x}}, \tilde{u}) + (D_1 - LD_2)(w - \tilde{w})] \\
&\quad - \gamma^2 \|w - \tilde{w}\|^2 + \|g(x, u) - g(\tilde{x}, \tilde{u})\|^2 \leq 0
\end{aligned} \tag{4.92}$$

From the geometric parametrizations of P_1 and P_2 and Assumption 4.3, we get $P_i \Phi = P_i E \Psi = \epsilon_i \Phi$ for $i = 1, 2$. Now using Assumptions 4.2-4.4 together with Lemma 4.5, the triangle and Cauchy-Schwarz inequalities, the followings can be derived

$$\begin{aligned}
2(x - \tilde{x})^\top P_1 [\Phi(x, u) - \Phi(\tilde{x}, \tilde{u})] &= 2\epsilon_1 \langle \Phi(x, u) - \Phi(\tilde{x}, \tilde{u}), x - \tilde{x} \rangle \\
&= 2\epsilon_1 [\langle \Phi(x, u) - \Phi(\tilde{x}, u), x - \tilde{x} \rangle + \langle \Phi(\tilde{x}, u) - \Phi(\tilde{x}, \tilde{u}), x - \tilde{x} \rangle] \\
&\leq 2\epsilon_1 \rho \|x - \tilde{x}\|^2 + 2\epsilon_1 \|x - \tilde{x}\| \|\Phi(\tilde{x}, u) - \Phi(\tilde{x}, \tilde{u})\| \\
&\leq 2\epsilon_1 \rho \|x - \tilde{x}\|^2 + 2\epsilon_1 \|x - \tilde{x}\| \lambda_u \|K\| \|\hat{x} - \tilde{\hat{x}}\| \\
&\leq 2\epsilon_1 (\rho + \lambda_u \|K\|) \|x - \tilde{x}\|^2 + 2\epsilon_1 \lambda_u \|K\| \|x - \tilde{x}\| \|e - \tilde{e}\| \\
&\leq \epsilon_1 (2\rho + 3\lambda_u \|K\|) \|x - \tilde{x}\|^2 + \epsilon_1 \lambda_u \|K\| \|e - \tilde{e}\|^2 \\
&\leq \epsilon_1 (2\rho + 3\lambda_u \|K\|) \|x - \tilde{x}\|^2 + 2\epsilon_1 \lambda_u \|K\| (\|e\|^2 + \|\tilde{e}\|^2)
\end{aligned} \tag{4.93}$$

$$\begin{aligned}
2(e - \tilde{e})^\top P_2 [\bar{\Phi}(x, \hat{x}, u) - \bar{\Phi}(\tilde{x}, \tilde{\hat{x}}, \tilde{u})] &= 2\epsilon_2 \langle \bar{\Phi}(x, \hat{x}, u) - \bar{\Phi}(\tilde{x}, \tilde{\hat{x}}, \tilde{u}), e - \tilde{e} \rangle \\
&= 2\epsilon_2 [\langle \Phi(x, u) - \Phi(\hat{x}, u), e \rangle + \langle \Phi(\tilde{x}, \tilde{u}) - \Phi(\tilde{\hat{x}}, \tilde{u}), \tilde{e} \rangle \\
&\quad - \langle \Phi(x, u) - \Phi(\hat{x}, u), \tilde{e} \rangle - \langle \Phi(\tilde{x}, \tilde{u}) - \Phi(\tilde{\hat{x}}, \tilde{u}), e \rangle] \\
&\leq 2\epsilon_2 \rho (\|e\|^2 + \|\tilde{e}\|^2 + 2\|e\| \|\tilde{e}\|) \\
&\leq 4\epsilon_2 \rho (\|e\|^2 + \|\tilde{e}\|^2)
\end{aligned} \tag{4.94}$$

$$\begin{aligned}
2(e - \tilde{e})^\top P_2 L [\bar{h}(x, \hat{x}, u) - \bar{h}(\tilde{x}, \tilde{\hat{x}}, \tilde{u})] &\leq (e - \tilde{e})^\top G_2 G_2^\top (e - \tilde{e}) \\
&\quad + \|h(x, u) - h(\hat{x}, u) - (h(\tilde{x}, \tilde{u}) - h(\tilde{\hat{x}}, \tilde{u}))\|^2 \\
&\leq (e - \tilde{e})^\top G_2 G_2^\top (e - \tilde{e}) + \lambda_h^2 (\|e\|^2 + \|\tilde{e}\|^2 + 2\|e\| \|\tilde{e}\|) \\
&\leq (e - \tilde{e})^\top G_2 G_2^\top (e - \tilde{e}) + 2\lambda_h^2 (\|e\|^2 + \|\tilde{e}\|^2)
\end{aligned} \tag{4.95}$$

$$\|g(x, u) - g(\tilde{x}, \tilde{u})\|^2 \leq \lambda_g^2(1 + \|K\|)^2\|x - \tilde{x}\|^2 \quad (4.96)$$

According to LMIs (4.61)-(4.62), we have

$$G_1^\top G_1 < \sigma_1^2 I \rightarrow \|G_1\| < \sigma_1 \quad (4.97)$$

$$\sigma_2^2 R^\top R - I > 0 \rightarrow R^{-\top} R^{-1} < \sigma_2^2 I \rightarrow \|R^{-1}\| < \sigma_2 \quad (4.98)$$

thus, $\|K\| \leq \|G_1\| \|R^{-1}\| \leq \sigma_1 \sigma_2$. Now, considering (4.93)-(4.96) a sufficient condition for (4.92) is given by

$$\begin{aligned} J \leq & (x - \tilde{x})^\top [-Q_1 + \epsilon_1(2\rho + 3\lambda_u \sigma_1 \sigma_2)I + \lambda_g^2(1 + \sigma_1 \sigma_2)^2 I](x - \tilde{x}) \\ & + e^\top [-Q_2 + (4\epsilon_2 \rho + 2\epsilon_1 \lambda_u \sigma_1 \sigma_2 + 2\lambda_h^2)I + G_2 G_2^\top] e \\ & + \tilde{e}^\top [-Q_2 + (4\epsilon_2 \rho + 2\epsilon_1 \lambda_u \sigma_1 \sigma_2 + 2\lambda_h^2)I + G_2 G_2^\top] \tilde{e} \\ & - 2(x - \tilde{x})^\top P_1 B K e + 2(x - \tilde{x})^\top P_1 B K \tilde{e} + 2e^\top Q_2 \tilde{e} \\ & + 2(x - \tilde{x})^\top P_1 D_1 (w - \tilde{w}) + 2e^\top P_2 (D_1 - L D_2)(w - \tilde{w}) \\ & - 2\tilde{e}^\top P_2 (D_1 - L D_2)(w - \tilde{w}) - \mu(w - \tilde{w})^\top (w - \tilde{w}) \leq 0 \end{aligned} \quad (4.99)$$

with $\mu = \gamma^2$. It can be verified that using $P_1 B K = B G_1$, the definitions of $\Sigma_1, \Sigma_2, \Omega_1, \Omega_2, \Omega_3, \Omega_4$ and the Schur's complements, (4.99) is equivalent to (4.64). Note that based on the definitions of G_1 and G_2 , the optimal controller and observer gains are given by (4.71) and (4.72), respectively. This completes the proof. \blacksquare

Remark 4.12. *Since inequalities (4.71)-(4.72) put some bound on the feedback gain norm $\|K\|$, the values of σ_1 and σ_2 can be predetermined based on the system saturation level.*

4.3 Simulation Results

In order to illustrate the effectiveness of the proposed control techniques, four numerical examples are presented in this section. The first example investigates stabilizing of a certain nonlinear system while the second one deals with robust controller design for an uncertain Van der Pol oscillator. In the third example we design a tracking control scheme for a chaotic plant. The last example is serve to show the efficiency of the proposed observer-based control law in Section 4.2.

Example 4.3. The system dynamics which has the form of (4.9)-(4.10) is given by

$$\begin{cases} \dot{x}_1(t) = x_2 + 0.3 \sin(x_1 + u) + u + \theta(w) \\ \dot{x}_2(t) = x_1 - x_2 + \text{sat}(x_1 + x_2) + w \\ z = [x_1 \ x_2 \ u]^\top \end{cases} \quad (4.100)$$

where $\text{sat}(\cdot)$ is the standard saturation and $\theta(w)$ is a static piecewise linear function shown below

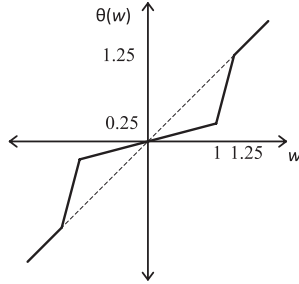


Figure 4.2: Disturbance nonlinearity

Clearly, the \mathcal{L}_2 -gain of $\theta(\cdot)$ is 1 while its incremental gain is equal to 4. The disturbance input is described by

$$w(t) = \begin{cases} 0.1 \sin 2t & 0 \leq t \leq 10 \\ 1.1 + 0.1 \sin 2t & 10 < t \end{cases}$$

It can be easily verified that the unforced plant, i.e. $u = 0$ and $w = 0$, is unstable. For the nonlinear system (4.100) we have

$$\begin{aligned} \left\| \begin{bmatrix} 0.3(\sin(x_1 + u) - \sin(\tilde{x}_1 + \tilde{u})) \\ \text{sat}(x_1 + x_2) - \text{sat}(\tilde{x}_1 + \tilde{x}_2) \end{bmatrix} \right\|^2 &\leq 0.09(x_1 + u - \tilde{x}_1 - \tilde{u})^2 + (x_1 + x_2 - \tilde{x}_1 - \tilde{x}_2)^2 \\ &\leq \tilde{X}^\top \underbrace{\begin{bmatrix} 1.09 & 1 & 0.09 \\ 1 & 1 & 0 \\ 0.09 & 0 & 0.09 \end{bmatrix}}_G \tilde{X} \leq \lambda_{\max}(G) \|\tilde{X}\|^2 \end{aligned}$$

where $\tilde{X}^\top = [x_1 - \tilde{x}_1 \ x_2 - \tilde{x}_2 \ u - \tilde{u}]$ and $\lambda_{\max}(G) = 2.0482$. Thus, Assumption 4.1 is satisfied globally with $\lambda_\Phi = \sqrt{2.0482}$. It was seen that achieving the minimum incremental disturbance attenuation of Corollary 4.1 results in undesirable large elements in the feedback gain. Hence, we set $\gamma = 1.3$ in our LMIs. By choosing $\alpha = 0.4$, $\epsilon_1 = 0.01$, and

$\epsilon_2 = 0.1$ and solving the LMIs the controller gain is obtained as $K = \begin{bmatrix} 10.668 & 6.483 \end{bmatrix}$. Figures 4.3-4.4 compare the incremental H_∞ controller designed by Corollary 4.1 with an H_∞ controller obtained based on the usual gain for the same attenuation level. It can be seen that the incremental control law forces the unstable states to converge to the origin in the presence of disturbance input. Moreover, it outperforms the usual H_∞ control law in the sense that reduces the amplification of the oscillations (output variations). This feature is still valid even when the operation region of the disturbances changes at $t = 10$ sec.

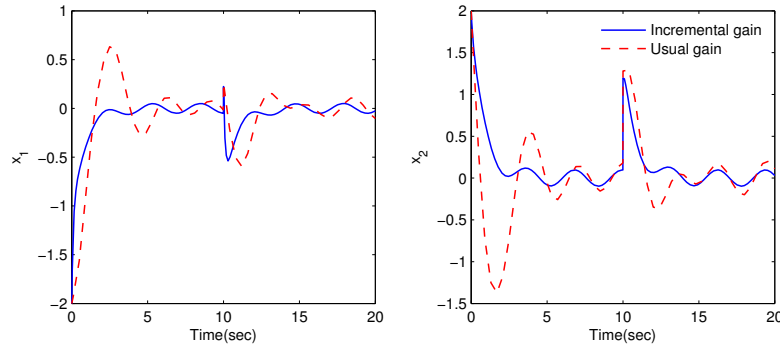


Figure 4.3: States responses in presence of the disturbance input with variable operation region

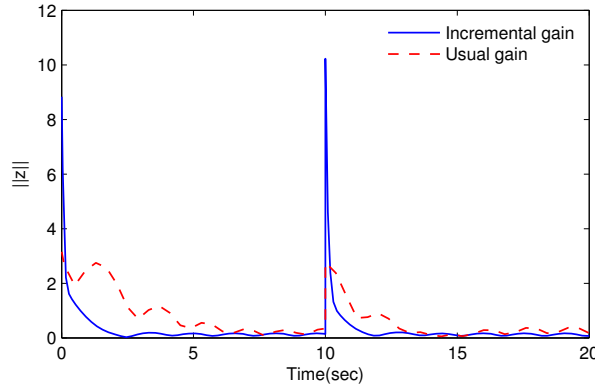


Figure 4.4: Norm of the penalty output

Example 4.4. Consider an uncertain model of the Van der Pol oscillator as follows

$$\begin{cases} \dot{x}_1(t) = (1 + \delta_1(t))x_2 + w \\ \dot{x}_2(t) = \rho(1 + 2\delta_2(t) - x_1^2)x_2 + x_1 + u + w \end{cases} \quad (4.101)$$

where $\rho > 0$ is a real number and $-1/2 < \delta_1(t) < 1/2$ and $-1 < \delta_2(t) < 1$ are unknown

time varying parameters. Assume that the disturbance signal $w(t)$ follows a uniform random distribution. Clearly, (4.101) can be written into (4.44) via

$$A = \begin{bmatrix} 0 & 1 \\ -1 & \rho \end{bmatrix}, \quad B = \begin{bmatrix} 0 \\ 1 \end{bmatrix}, \quad D = \begin{bmatrix} 1 \\ 1 \end{bmatrix},$$

$$\Delta A(t) = \begin{bmatrix} 0 & \delta_1(t) \\ 0 & 2\rho\delta_2(t) \end{bmatrix}, \quad \Phi = \begin{bmatrix} 0 \\ -\rho x_1^2 x_2 \end{bmatrix}$$

and

$$F(t) = \begin{bmatrix} \delta_1(t) \\ \delta_2(t) \end{bmatrix}, \quad M_a = \begin{bmatrix} 1 & 0 \\ 0 & 2\rho \end{bmatrix}, \quad N_a = \begin{bmatrix} 0 & 1 \end{bmatrix}$$

Note that the variation intervals of $\delta_1(t)$ and $\delta_2(t)$ imply $F^\top(t)F(t) < I$. Moreover, using Poincare-Bendixson theorem it can be concluded that the unforced system exhibits a limit cycle that is stable whenever $\delta_2(t) > -1/2$ and unstable for $\delta_2(t) < -1/2$, $\delta_1(t) > -1$. The system is locally Lipschitz on any compact subset of \mathbb{R}^2 but its Lipschitz constant depends on the compact region and can be computed as $\lambda_\Phi = \max \|\frac{\partial \Phi}{\partial x}\| = \max(\rho|x_1|\sqrt{4x_2^2 + x_1^2})$. Setting $\rho = 1$ and considering the operating region of the system we get $\lambda_\Phi = 31.58$.

Our purpose is to stabilize the system in the incremental sense for all admissible uncertainties. If we pick $\alpha = 0.3$, $\epsilon_1 = 0.0001$, and $\epsilon_2 = 0.001$ and $z = \begin{bmatrix} x_1 & x_2 & u \end{bmatrix}^\top$ as the penalty variable the minimization of Theorem 4.2 yields

$$\gamma^* = 1.673, \quad K = \begin{bmatrix} 4.342 & 2.85 \end{bmatrix}$$

Figure 4.5 shows the states responses with the initial condition $x_0 = \begin{bmatrix} 0.5 & -0.5 \end{bmatrix}^\top$. The control law is applied at $t = 25$ sec. It is clear that the states converge rapidly to the origin in presence of disturbance input as well as model uncertainties. The phase portrait of the controlled system is depicted in Figure 4-5.

Example 4.5. The proposed incremental-based controller can be modified appropriately such that it handles an input tracking problem. Consider again the system (4.9)-(4.10) accompanied by the measurement $y = Cx$. The nonlinearity Φ is assumed to be independent of the control input u and our tracking strategy is as below

$$u = -Kx + u_r \tag{4.102}$$

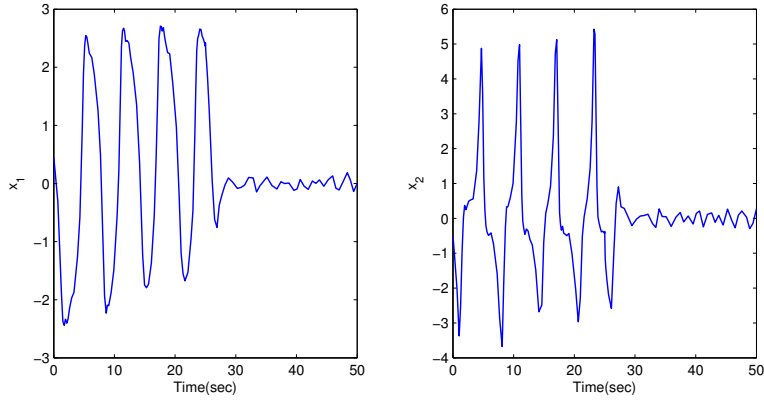


Figure 4.5: Time responses of the system states using the proposed robust incremental controller

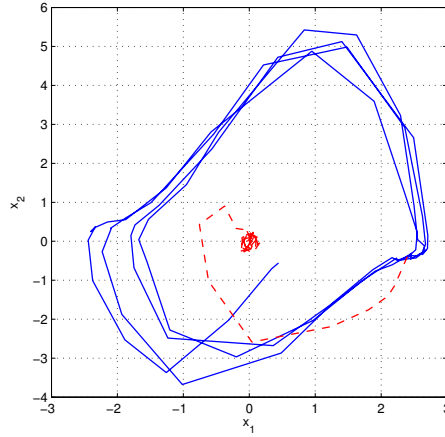


Figure 4.6: Phase portrait of the controlled Oscillator

with

$$\begin{aligned} u_r &= Kx_r - B^{-1}Ax_r - B^{-1}\Phi(x_r) + B^{-1}\dot{x}_r, \\ x_r &= C^{-1}r, \quad \dot{x}_r = C^{-1}\dot{r} \end{aligned} \quad (4.103)$$

where x_r and r are the reference state and desired output, respectively. The feedback gain K in (4.102) is obtained via an LMI optimization similar to that of Corollary 4.1.

Since chaos control has received substantial interest of research community, our result is applied on a chaotic physical system. The dynamics of a given Lorenz system with

control input $u(t) = [u_1 \quad u_2 \quad u_3]^\top$ and external disturbance $w(t)$ is expressed as

$$\begin{cases} \dot{x}_1(t) = a(x_2 - x_1) + u_1 + u_3 \\ \dot{x}_2(t) = rx_1 - x_2 - x_1x_3 + u_1 + w \\ \dot{x}_3(t) = -bx_3 + x_1x_2 + u_2 \end{cases} \quad (4.104)$$

where a and r are the so-called Prandtl and Rayleigh numbers, respectively and the parameter b depends on a geometric factor. It is well-known that the unforced plant behaves chaotically for $a = 10$, $b = 8/3$ and $r = 28$. The initial condition is taken as $x_0 = [10 \quad 10 \quad 10]^\top$.

This system is locally Lipschitz and its Lipschitz constant is given by $\max(\sqrt{2x_1^2 + x_2^2 + x_3^2})$ on any compact region around the origin. Using LMI optimization the following value of K is obtained for $\gamma = 0.5$

$$K = \begin{bmatrix} 3.28e-8 & 134.9 & 1.08e-9 \\ 3.35 & -0.33 & 136.54 \\ 129.2 & -97.23 & 3.26 \end{bmatrix}$$

The simulation results are plotted in Figures 4.7-4.8. The reference signal $r = [r_1 \quad r_2 \quad r_3]^\top$ is defined by

$$\begin{cases} r_1 = 5 \sin 3t \\ r_2 = 2 \cos 3t \\ r_3 = -4 \sin t \end{cases} \quad (4.105)$$

and the control input is applied at $t = 20$ sec. Note that here the whole state is assumed to be available in the output, i.e. $y = x$. It can be seen that the reference tracking objective is successfully achieved in Figure 4.7 and hence the proposed controller performs as expected. Trajectories of the controlled Lorenz system is shown in Figure 4.8.

Example 4.6. Consider a discontinuous system in the form of (4.56) with

$$A = \begin{bmatrix} -1 & 1 & -1 \\ 0 & -2 & 1 \\ 0 & 0 & 3 \end{bmatrix}, \quad B = \begin{bmatrix} 0 \\ 0 \\ 1 \end{bmatrix}, \quad C = \begin{bmatrix} 0 \\ 1 \\ -1 \end{bmatrix}^\top, \quad D_1 = [-0.5 \quad 0.5 \quad -1.5]^\top, \quad D_2 = 0.5$$

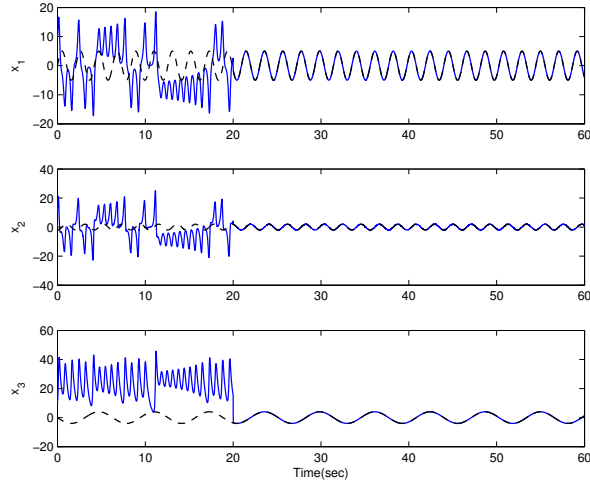


Figure 4.7: Reference tracking using the incremental H_∞ controller in presence of disturbance input

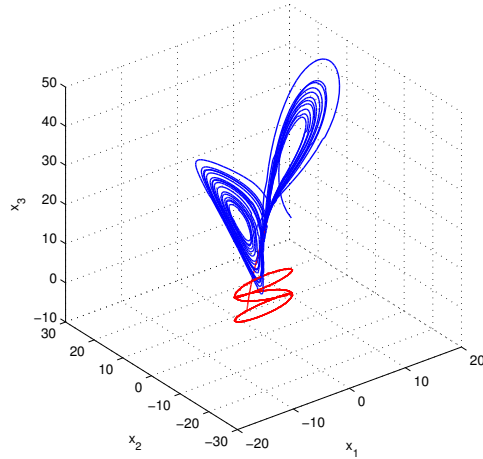


Figure 4.8: Phase portrait of the controlled Lorenz system

$$\Phi = \begin{bmatrix} -\operatorname{sgn}(x_1)\sqrt{|x_1|}u & 0 & -x_3^{1/3} \end{bmatrix}^\top$$

$$h = \sin(x_2 - x_3), \quad g = [x^\top u]^\top$$

where $\operatorname{sgn}(\cdot)$ denotes the sign (signum) function. Clearly, the unforced plant, i.e., when $u = 0$ and $w = 0$, is unstable, and none of the state variables is available in the measurement. By similar arguments as that of [61, Example 4.2], it is easy to confirm that $\Phi(x, u)$

is not Lipschitz. However, we have

$$\begin{aligned} & \langle -\operatorname{sgn}(x_1)\sqrt{|x_1|}u^* + \operatorname{sgn}(\hat{x}_1)\sqrt{|\hat{x}_1|}u^*, x_1 - \hat{x}_1 \rangle \\ & \leq -\frac{\|u^*\|}{\sqrt{|x_1|} + \sqrt{|\hat{x}_1|}}(x_1 - \hat{x}_1)^2 \\ & \langle -x_3^{1/3} + \hat{x}_3^{1/3}, x_3 - \hat{x}_3 \rangle \leq -\xi^{-2/3}(x_3 - \hat{x}_3)^2 \leq 0 \end{aligned}$$

where $\|u^*\|$ is chosen to be the infinity norm of any admissible control input u^* and $\xi \in (\min\{x_3, \hat{x}_3\}, \max\{x_3, \hat{x}_3\})$ is obtained from the mean value theorem. Consequently, Φ obeys the one-sided Lipschitz condition (2.9) with $\rho = -\|u^*\|/(2\sqrt{c})$ for $x_1 \in [-c, c]$. Moreover, it is Lipschitz with respect to u and can be written as $\Phi = E\Psi$ with

$$E = \begin{bmatrix} 1 & 0 & 0 \\ 0 & 0 & 1 \end{bmatrix}^T, \quad \Psi(x, u) = \begin{bmatrix} -\operatorname{sgn}(x_1)\sqrt{|x_1|}u \\ -x_3^{1/3} \end{bmatrix}$$

The functions h and g are also Lipschitz. Therefore, Assumptions 4.2-4.4 hold and Theorem 4.3 can be used to design a stabilizing control law. Using $\sigma_1 = 5$, $\sigma_2 = 2$, $E^\perp = [0 \ 1 \ 0]^T$, $\|u^*\| \leq 10$ and the operating region of x_1 as $[-5, 5]$, we get $\rho = -0.22$ and

$$\begin{aligned} \gamma^* &= 0.3, \quad K = \begin{bmatrix} -0.2304 & -2.4799 & 7.1347 \end{bmatrix}, \\ L &= \begin{bmatrix} 1.009 & -0.436 & -7.729 \end{bmatrix}^T \end{aligned}$$

Figure 4.9 shows the simulation results of the H_∞ output feedback control with the initial conditions $x(0) = [0 \ -1 \ 1]^T$ and $\hat{x}(0) = [0.5 \ 0 \ -0.5]^T$. Note that we assume a uniformly distributed random disturbance whose amplitude increases slowly within the time interval (5, 15). The control law that is applied at $t = 0.3$ sec forces the unstable states to converge to the origin asymptotically. It can be seen that our incremental gain-based controller performs satisfactory even in the presence of disturbances with many variations. Furthermore, the estimated states track the actual ones while the estimation error vanishes gradually.

4.4 Summary

In this chapter the \mathcal{L}_2 incremental gain is examined as a new performance measure to design a nonlinear H_∞ controller. Our result is expressed via a feasibility problem of some

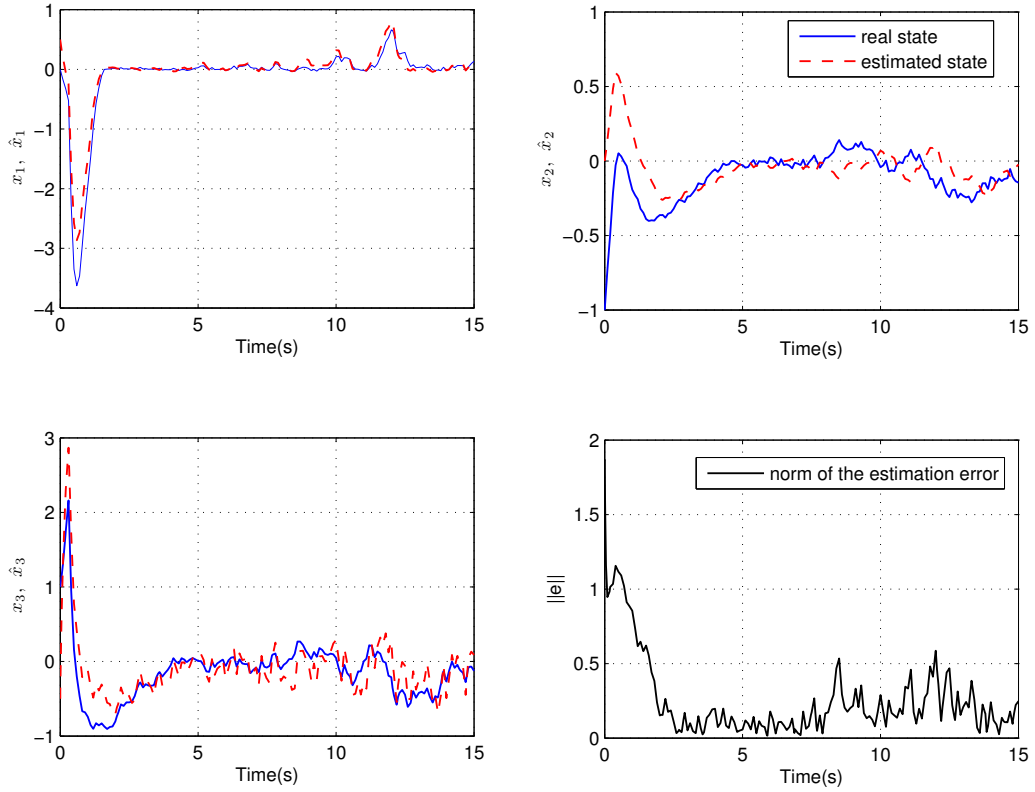


Figure 4.9: The simulation results for incremental observer-based H_∞ controller

linear matrix inequalities (LMIs) for a class of Lipschitz nonlinear plants and guarantees exponential stability with minimized incremental gain against model uncertainties and disturbance inputs.

Moreover, as an extensive class of nonlinear plants, the one-sided Lipschitz systems is investigated for H_∞ output feedback design in presence of disturbance inputs. We minimize the effect of disturbances through an incremental H_∞ performance criterion in an observer-based control scheme to obtain a stable closed-loop system. The simulation results make the proposed strategies practically viable.

Chapter 5

Input-to-Error Sampled-Data Nonlinear Observer

Throughout this chapter¹ we study sampled-data nonlinear observers, understood as observers for continuous-time systems implemented using a digital computer via sample and hold devices. We present two general estimation procedures for general nonlinear systems based on (i) discrete-time design (DTD), and (ii) continuous-time design (CTD) or emulation (see e.g., [3, 4] for more details). We show that, given a continuous-time nonlinear plant model, then under some standard assumptions and Lyapunov-ISS conditions, the proposed observers converge to the true plant state at each sampling instant in an input-to-state stable, semiglobal practical sense.

The second half of the chapter is dedicated to one specific type of nonlinearities, namely *one-sided Lipschitz*, in order to obtain constructive algorithms for a special class of systems. One-sided Lipschitz systems were inspired by recent advances in the mathematical literature in numerical analysis and can be viewed as a generalization of the popular Lipschitz condition that has received much attention in the control literature for the past 4 decades. All of the existing works focus on observer stability and make use of a modified one-sided Lipschitz condition in which the nonlinearity is scaled via a fixed symmetric matrix. This modification makes the design problem tractable, but affects the value of one-sided Lipschitz constant and brings additional constraints on the Lyapunov

¹The results of this chapter have been submitted for publication in the article: H. Beikzadeh and H. J. Marquez, “Input-to-Error Stable Observer for Nonlinear Sampled-Data Systems with Application to One-Sided Lipschitz Systems,” Submitted to *Automatica*, Sept. 2013.

function. Observer design for the original one-sided Lipschitz condition remains relatively unexplored. Very recently, the authors in [63] introduced an alternative approach which eliminates the need for scaling at the expense of an additional condition on the nonlinearity, known as *quadratically inner bounded*. This approach was further developed in [64] to obtain less conservative results and in [65] to address the discrete-time problem. In this chapter, we consider the the problem of sampled-data observer design for one-sided Lipschitz systems in the presence of disturbance inputs. We present two DTD and CTD (emulation)-based schemes that ensure *input-to-error stability* in terms of linear matrix inequalities (LMIs). Both of the proposed observers introduce refined Euler models by incorporating an integration parameter together with the sampling period to approximate the exact discrete-time models. We show that while the DTD observer necessitates the quadratically inner-bounded condition, the CTD observer does not. Instead, we employ a mild geometric condition on the plant nonlinearity and formulate the design procedure using a parameterization of the Lyapunov function [103].

The rest of the chapter is organized as follows. Section 5.1 introduces the family of input-to-error stable sample-data observers in presence of disturbances, and gives the relevant background. We provide sufficient conditions which guarantee semiglobal practical stability of the estimation error for general nonlinear plants using the DTD and CTD methods in sections 5.2 and 5.3, respectively. Our results is applied to one-sided Lipschitz systems in Section 5.4 and is verified via two appropriate simulation examples in Section 5.5. Eventually, some concluding remarks are drawn in the last section.

5.1 Definitions and Problem Setting

We consider the following nonlinear system:

$$G : \begin{cases} \dot{x}(t) = f(x(t), u(t), d(t)) \\ y(t) = g(x(t), u(t), d(t)) \end{cases} \quad (5.1)$$

where $x \in \mathbb{R}^n$, $u \in \mathbb{R}^m$, $d \in \mathbb{R}^q$ and $y \in \mathbb{R}^p$ are respectively the state vector, control input, exogenous disturbance and measured output and the nonlinear functions f and g are continuously differentiable vanishing at the origin. Assume that the continuous-time system G is connected to the ideal sampler \mathcal{S} and the (zero order) hold device \mathcal{H} with the

sampling period $T > 0$ in a sampled-data configuration. The exact discrete-time model of (1) is then given by

$$\begin{aligned} x(k+1) &= F_T^e(x[k], u(k), d[k]) \\ y(k) &= g(x(k), u(k), d(k)) \end{aligned} \quad (5.2)$$

where $F_T^e(x, u, \bar{d})$ is the solution of the differential equation in (5.1) over sampling interval $[kT, (k+1)T)$ with a constant input u . The need for a closed form solution of the differential equation (5.1) makes it impossible to obtain the model (5.2) in most practical cases. Therefore, consistent with the literature on nonlinear sampled-data systems, we refer to F_T^e as the exact discrete-time model of the system (5.1) and assume that it is unknown. Instead we employ a family of approximate discrete-time models $F_{T,h}^a(x(k), u(k), d[k])$, where h is a *modelling parameter* utilized to refine the approximate model for a given T .

Throughout the chapter the mismatch between the exact and approximate models is evaluated via the one-step consistency property of Definition 2.8. The one-step consistency can be checked using verifiable conditions based on the Euler approximation provided in [4, 13] without knowing the exact model F_T^e .

Considering the approximation $F_{T,h}^a$, we design a family of sampled-data observers of the form

$$\hat{x}(k+1) = F_{T,h}^a(\hat{x}(k), u(k), 0) + \ell_{T,h}(\hat{x}(k), y(k), u(k)), \quad (5.3)$$

where $\hat{x}(k)$ denotes the state estimate, $F_{T,h}^a(\hat{x}(k), u(k), 0)$ is the approximate model with zero disturbance and $\ell_{T,h}$ is zero at zero.

Our main question is under what conditions, and in what sense, an estimator like (5.3) guarantees convergence to the true plant state when applied to the exact model (5.2). Note that it is well established that, even in the absence of disturbance, an asymptotic convergence of an observer design based on the approximate model does not necessarily guarantee convergence of the true (exact) model (see [70]).

Definition 5.1. *The observer (5.3) is said to be input-to-error stable semiglobal in T and practical in h , if there exist $\beta \in \mathcal{KL}$ and $\gamma \in \mathcal{K}$ such that for any $\delta_1, \delta_2 > 0$ and compact sets $\mathcal{X} \in \mathbb{R}^n$, $\mathcal{U} \in \mathbb{R}^m$, we can find $T_1 > 0$ such that for any $T \in (0, T_1]$ and $\nu \in (0, \delta_1)$, there exists $h_1 \in (0, T]$ such that $\forall h \in (0, h_1]$,*

$$|x(0) - \hat{x}(0)| \leq \delta_1, \quad \|d\|_\infty \leq \delta_2 \quad (5.4)$$

and $x(k) \in \mathcal{X}$, $u(k) \in \mathcal{U}$, $\forall k \in \mathbb{Z}^+$ implies

$$|x(k) - \hat{x}(k)| \leq \beta(|x(0) - \hat{x}(0)|, kT) + \gamma(\|d\|_\infty) + \nu \quad (5.5)$$

This definition is a generalization of the notion of *semiglobal practical convergence* introduced by [70] when the plant is exposed to disturbance inputs. Note that for $d = 0$, Definition 5.1 reduces to [70, Definition 2(b)] where h is independent of T . The effect of the sampling period as well as the refining parameter on the residual observer error is investigated in Section 5.5.

5.2 Observer Design via Approximation and Input-to-State Stability

In this section, we derive conditions based on the approximate model that guarantee ISS observer convergence in the sense of Definition 5.1 for the exact model. From (5.2) and (5.3), the observer error $e := x - \hat{x}$ satisfies

$$e(k+1) = F_{T,h}^a(\hat{x}(k), u(k), 0) + \ell_{T,h}(\hat{x}(k), y(k), u(k)) - F_T^e(x(k), u(k), d[k]) \quad (5.6)$$

Adding and subtracting the approximate model $F_{T,h}^a(x(k), u(k), d[k])$, (5.6) can be rewritten as

$$e(k+1) = E_{T,h}(e(k), x(k), u(k)) + F_{T,h}^a(x(k), u(k), d[k]) - F_T^e(x(k), u(k), d[k]) \quad (5.7)$$

where

$$E_{T,h}(e, x, u) := F_{T,h}^a(\hat{x}, u, 0) + \ell_{T,h}(\hat{x}, y, u) - F_{T,h}^a(x, u, \bar{d}) \quad (5.8)$$

indicates the nominal estimation error dynamics for the approximate design, and $F_{T,h}^a - F_T^e$ is the mismatch between the approximate and exact plant models.

Theorem 5.1. *The observer error dynamics (5.6) is input-to-error stable if the following conditions hold:*

- (i) $F_{T,h}^a$ is one-step consistent with F_T^e as in Definition 2.8.
- (ii) There exists a family of Lyapunov functions $V_{T,h}(e)$, $\alpha_1(\cdot), \alpha_2(\cdot), \alpha_3(\cdot) \in \mathcal{K}_\infty$ and $\tilde{\gamma}(\cdot) \in \mathcal{K}$ with the following properties:

For any positive real numbers $(\delta_e, \delta_u, \delta_d)$, there exists $T^* > 0$ and $M > 0$ such that for each fixed $T \in (0, T^*]$ there exists $h^* \in (0, T]$ such that for all $e, e_1, e_2 \in B(\delta_e)$, $u \in B(\delta_u)$, $\|d\|_\infty \leq \delta_d$ and $h \in (0, h^*]$,

$$|V_{T,h}(e_1) - V_{T,h}(e_2)| \leq M|e_1 - e_2| \quad (5.9)$$

$$\alpha_1(|e|) \leq V_{T,h}(e) \leq \alpha_2(|e|) \quad (5.10)$$

$$\frac{\Delta V}{T} := \frac{V_{T,h}(E_{T,h}(e, x, u)) - V_{T,h}(e)}{T} \leq -\alpha_3(|e|) + \tilde{\gamma}(\|d\|_\infty) \quad (5.11)$$

In order to prove our main result, we need the following lemma.

Lemma 5.1. *Let $\alpha_1, \alpha_2, \alpha_3 \in \mathcal{K}_\infty$ and strictly positive real numbers (C_e, r, C_d) be such that $\|d\|_\infty \leq C_d$ and $\alpha_1(C_e) \geq r$. Assume that for $T_1 > 0$ and each fixed $T \in (0, T_1]$ there exists $h_1 \in (0, T]$ such that for any $h \in (0, h_1]$ there exists a function $V_{T,h} : \mathbb{R}^n \rightarrow \mathbb{R}^+$ with the following properties: we have $\alpha_1(|e|) \leq V_{T,h}(e) \leq \alpha_2(|e|)$ for all $e \in \mathbb{R}^n$ and $\max\{V_{T,h}(e(k+1)), V_{T,h}(e(k))\} \geq r$ for all $\|d\|_\infty \leq C_d$, $e \in \mathbb{R}^n$ with $|e| \leq C_e$ leads to $V_{T,h}(e(k+1)) - V_{T,h}(e(k)) \leq -\frac{T}{4}\alpha_3(|e|)$. Then, for all $|e(0)| \leq \alpha_2^{-1} \circ \alpha_1(R)$, $\|d\|_\infty \leq C_d$ we get $|e(k)| \leq C_e \quad \forall k \in \mathbb{Z}^+$, and furthermore the estimation error satisfies*

$$|e(k)| \leq \beta(|e(0)|, kT) + \alpha_1^{-1}(r) \quad (5.12)$$

Proof. The first part of the proof is analogous to that of [19, Claim 3]. Then, using an argument similar to the proof of Theorem 2 in [4], it can be concluded that there exists a class- \mathcal{KL} function $\beta_1(\cdot, \cdot)$ such that $V_{T,h}(e(k)) \leq \max\{\beta_1(V_{T,h}(e(0)), kT), r\}$. Then, (5.12) is obtained with $\beta(s, \tau) = \alpha_1^{-1}(\beta_1(\alpha_2(s), \tau))$. ■

Proof of Theorem 5.1: Let $(\delta_e, \delta_d, \nu) > 0$ be given and T_{11}, h_{11} come from Definition 2.8. First from (5.7) and (5.11) and using inequality (5.9) together with the consistency property (2.8), we obtain

$$\begin{aligned} V_{T,h}(e(k+1)) - V_{T,h}(e(k)) &\leq -T\alpha_3(|e|) + T\tilde{\gamma}(\|d\|_\infty) + V_{T,h}(e(k+1)) \\ &\quad - V_{T,h}(E_{T,h}(e(k), x(k), u(k))) \\ &\leq -T\alpha_3(|e|) + T\tilde{\gamma}(\|d\|_\infty) + TM\rho(h) \end{aligned} \quad (5.13)$$

for $T \in (0, T_{11}]$, $h \in (0, h_{11}]$. Define $\hat{\gamma} \in \mathcal{K}_\infty$ and positive real numbers (C_e, C_d, ε) as: $\hat{\gamma}(s) := \alpha_2 \circ \alpha_3^{-1}(4\tilde{\gamma}(s))$, $C_e := \delta_e$, $\varepsilon > 0$ is such that $\sup_{s \in [0, \delta_d]} \{\alpha_1^{-1}(\hat{\gamma}(s) + \varepsilon) - \alpha_1^{-1}(\hat{\gamma}(s))\} \leq \nu$, and $C_e := \max\{\alpha_1^{-1}(\hat{\gamma}(\delta_d) + \varepsilon), \alpha_1^{-1} \circ \alpha_2(\delta_e)\}$. These choices implies that $C_e \geq \alpha_1^{-1}(\hat{\gamma}(C_d) + \varepsilon)$ and $|e(0)| \leq \alpha_2^{-1} \circ \alpha_1(C_e)$. We now claim that there exists $T^* > 0$ such that for each $T \in (0, T^*]$ there exists $h^* \in (0, T]$ such that for all $h \in (0, h^*]$, $|e(0)| \leq \alpha_2^{-1} \circ \alpha_1(C_e)$, $\|d\|_\infty \leq C_d$ and all $k \in \mathbb{Z}^+$ it can be deduced that

$$\begin{aligned} \max\{V_{T,h}(e(k+1)), V_{T,h}(e(k))\} &\geq \hat{\gamma}(\|d\|_\infty) + \varepsilon \\ \Rightarrow V_{T,h}(e(k+1)) - V_{T,h}(e(k)) &\leq -\frac{T}{4}\alpha_3(|e(k)|) \end{aligned} \quad (5.14)$$

Let us define $\sigma_1 = \frac{1}{2}\alpha_2^{-1}(\frac{\varepsilon}{2})$ and $\sigma_2 = \alpha_2^{-1}(\frac{1}{2}\alpha_1(\sigma_1))$. Choose positive real numbers T_{12} , h_{12} , T_{13} , h_{13} , T_{14} , h_{14} such that: $T_{12}\rho(h_{12}) \leq \sigma_1$, $T_{13}(\frac{1}{4}\alpha_3(C_e) + \tilde{\gamma}(\|d\|_\infty) + M\rho(h_{13})) \leq \frac{\varepsilon}{2}$, $T_{14}\tilde{\gamma}(C_d) \leq \frac{1}{2}\alpha_1(\sigma_1)$, and $M\rho(h_{14}) \leq \frac{1}{2}\alpha_3(\sigma_2)$. Take $T^* = \min\{T_{11}, T_{12}, T_{13}, T_{14}\}$ and $h^* = \min\{h_{11}, h_{12}, h_{13}, h_{14}\}$ and consider any $T \in (0, T^*]$, $h \in (0, h^*]$, $|e(0)| \leq \alpha_2^{-1} \circ \alpha_1(C_e)$ and $\|d\|_\infty \leq C_d$. Now we consider two possible scenarios. First assume that $V_{T,h}(e(k+1)) \geq \hat{\gamma}(\|d\|_\infty) + \frac{\varepsilon}{2}$ and rewrite (5.13) as

$$\begin{aligned} V_{T,h}(e(k+1)) - V_{T,h}(e(k)) &\leq -\frac{T}{4}\alpha_3(|e(k)|) - \underbrace{\frac{T}{4}\alpha_3(\alpha_2^{-1}(V_{T,h}(e(k))))}_{(a)} + T\tilde{\gamma}(\|d\|_\infty) \\ &\quad - \underbrace{\frac{T}{2}\alpha_3(|e(k)|) + TM\rho(h)}_{(b)} \end{aligned} \quad (5.15)$$

therefore we conclude that $V_{T,h}(e(k+1)) \geq \hat{\gamma}(\|d\|_\infty) + \frac{\varepsilon}{2}$ implies $\hat{\gamma}(\|d\|_\infty) + \frac{\varepsilon}{2} \leq V_{T,h}(E_{T,h}(e, x, u)) - V_{T,h}(e(k)) + |V_{T,h}(e(k+1)) - V_{T,h}(E_{T,h}(e, x, u))| + V_{T,h}(e(k)) \leq -T\alpha_3(|e(k)|) + T\tilde{\gamma}(\|d\|_\infty) + MT(3\rho(h) + V_{T,h}(e(k)))$. By the choice of T_{13} and h_{13} , we get $\hat{\gamma}(\|d\|_\infty) + \frac{\nu}{2} \leq \frac{\nu}{2} + V_{T,h}(e(k))$.

Hence, it follows that

$$V_{T,h}(e(k+1)) \geq \hat{\gamma}(\|d\|_\infty) + \frac{\varepsilon}{2} \Rightarrow V_{T,h}(e(k)) \geq \hat{\gamma}(\|d\|_\infty). \quad (5.16)$$

Based on the definition of $\hat{\gamma}(\cdot)$, Term (a) ≤ 0 holds. By supposition $V_{T,h}(e(k+1)) \geq \hat{\gamma}(\|d\|_\infty) + \frac{\varepsilon}{2}$, we have $e(k+1) \geq \alpha_2^{-1}(\frac{\varepsilon}{2}) = 2\sigma_1$. Then our choice of T_{12} and h_{12} shows that $|E_{T,h}(e, x, u)| \geq |e(k+1)| - |e(k+1) - E_{T,h}(e, x, u)| \geq 2\sigma_1 - \sigma_1 = \sigma_1$. Using (5.11) and our choice of T_{14} , it yields that

$$\begin{aligned} \alpha_2(|e(k)|) &\geq V_{T,h}(E_{T,h}(e, x, u)) - T\tilde{\gamma}(C_d) \geq \alpha_1(|E_{T,h}(e, x, u)|) - T\tilde{\gamma}(C_d) \\ &\geq \alpha_1(\sigma_1) - \frac{1}{2}\alpha_1(\sigma_1) = \frac{1}{2}\alpha_1(\sigma_1) \end{aligned} \quad (5.17)$$

which implies $|e(k)| \geq \alpha_2^{-1}(\frac{1}{2}\alpha_1(\sigma_1)) = \sigma_2$. Then, from the choice of h_{14} , we have $|e(k)| \geq \sigma_2 \Rightarrow \text{Term(b)} \leq 0$. Consequently, $V_{T,h}(x(k+1), \hat{x}(k+1)) \geq \hat{\gamma}(\|d\|_\infty) + \frac{\nu}{2}$ results in $V_{T,h}(x(k+1), \hat{x}(k+1)) - V_{T,h}(x(k), \hat{x}(k)) \leq -\frac{T}{4}\alpha_3(|e(k)|)$.

Now Suppose that $V_{T,h}(e(k+1)) \leq \hat{\gamma}(\|d\|_\infty) + \frac{\varepsilon}{2}$ and $V_{T,h}(e(k)) \leq \hat{\gamma}(\|d\|_\infty) + \varepsilon$. From our choice of T_{13} and h_{13} , it follows that: $V_{T,h}(e(k+1)) - V_{T,h}(e(k)) \leq \hat{\gamma}(\|d\|_\infty) + \frac{\varepsilon}{2} - V_{T,h}(e(k)) + \frac{\varepsilon}{2} - \frac{\varepsilon}{2} \leq \hat{\gamma}(\|d\|_\infty) + \varepsilon - V_{T,h}(e(k)) - \frac{\varepsilon}{2} \leq -\frac{\varepsilon}{2} \leq \frac{T}{4}\alpha_3(|e(k)|)$. Therefore, (5.14) is valid under both cases.

With these prerequisites, we can finalize our proof. Taking the definitions of $\hat{\gamma} \in \mathcal{K}_\infty$, (C_e, C_d, ε) into account, assume that (5.14) holds with $T^* > 0, h^* > 0$. Let $r = \hat{\gamma}(\|d\|_\infty) + \varepsilon$, then we have $\alpha_1(C_e) \geq r$. With the definition of (C_e, r) , all the conditions of Lemma 5.1 are satisfied. Therefore, for all $h \in (0, h^*]$, $|e(0)| \leq \delta_e$ and $\|d\|_\infty \leq \delta_d$, we obtain

$$|e(k)| \leq \beta(|e(0)|, kT) + \alpha_1^{-1}(\hat{\gamma}(\|d\|_\infty) + \varepsilon) \leq \beta(|e(0)|, kT) + \gamma(\|d\|_\infty) + \nu \quad (5.18)$$

where $\gamma(s) := \alpha_1^{-1} \circ \hat{\gamma}(s)$. The proof of Theorem 5.1 is complete. \blacksquare

5.3 Observer Design via Emulation and Input-to-State Stability

Emulation is known as a common approach for sample-data implementation of controllers and observers, which consists of continuous-time discretization using approximate methods. Assume that we have a continuous-time observer described by

$$\dot{\hat{x}} = s(\hat{x}, y, u) \quad (5.19)$$

that is implemented with the approximate discrete-time model

$$\hat{x}(k+1) = S_{T,h}^a(\hat{x}(k), y(k), u(k)) \quad (5.20)$$

The function $s(\cdot, \cdot, \cdot)$ is assumed to be locally Lipschitz in all its arguments. We now provide a Lyapunov-ISS condition to guarantee the semiglobal practical convergence of the emulated observer (5.20).

Theorem 5.2. *The observer (5.20) is input-to-error stable if the following conditions hold:*

(i) $S_{T,h}^a$ is one-step consistent with S_T^e according to Definition 2.8, (y, u) as constant inputs during sampling intervals.

(ii) There exists a C^1 Lyapunov function V , $\alpha_1(\cdot), \alpha_2(\cdot), \alpha_3(\cdot) \in \mathcal{K}_\infty$ and $\tilde{\gamma}(\cdot) \in \mathcal{K}$ such that for all $x, \hat{x} \in \mathbb{R}^n$ and all $u \in \mathbb{R}^m$

$$\alpha_1(|e|) \leq V(e) \leq \alpha_2(|e|) \tag{5.21}$$

$$\frac{\partial V}{\partial x} f(x, u) + \frac{\partial V}{\partial \hat{x}} s(\hat{x}, y, u) \leq -\alpha_3(|e|) + \tilde{\gamma}(\|d\|_\infty) \tag{5.22}$$

with $e = x - \hat{x}$ as the estimation error.

Proof. The proof is analogous to that of Theorem 5.1 with the Lyapunov function $V_{T,h}$ replaced by V . The details are hence omitted. ■

5.4 Application: One-Sided Lipschitz Systems

In this section we apply the general input-to-state observer conditions of Sections 5.2 and 5.3 to the class of one-sided Lipschitz systems. Section 5.4.1 considers the DTD method and section 5.4.2 considers the same problem via emulation. We will show that both techniques are needed given the different challenges presented in the design.

5.4.1 DTD Method:

This section applies the general input-to-state observer convergence conditions of Theorem 5.1 to the problem of sampled-data observer design for one-sided Lipschitz nonlinear systems. In order to proceed, we need to specify some form of discrete-time model approximation. For this purpose, we focus on the Euler model because of its simplicity and also because it preserves the structure of the original nonlinear model.

Throughout the rest of this section we assume that the continuous-time system (5.1) can be put into the following form

$$\begin{aligned} \dot{x}(t) &= Ax(t) + \Phi(x(t), u(t)) + D_1 d(t) \\ y(t) &= Cx(t) + D_2 d(t) \end{aligned} \tag{5.23}$$

where A, C, D_1, D_2 are constant matrices of appropriate dimensions and the nonlinearity $\Phi(\cdot, \cdot)$ satisfies the one-sided Lipschitz assumption defined as follows: Φ is one-sided

Lipschitz in the region \mathcal{D} , i.e., for $\forall x, \hat{x} \in \mathcal{D}$ and any admissible control signal u^*

$$\langle \Phi(x, u^*) - \Phi(\hat{x}, u^*), x - \hat{x} \rangle \leq \mu \|x - \hat{x}\|^2 \quad (5.24)$$

where $\mu \in \mathbb{R}$ is the so-called one-sided Lipschitz constant.

Remark 5.1. Note that condition (5.24) is different from the nondecreasing (slope restricted) nonlinearities considered by [71, 104]. Slope restricted nonlinearities were the focus of much attention in the 1960's. A scalar function $\gamma(\cdot)$ is said to satisfy a sector condition if

$$\alpha \leq \frac{\gamma(v) - \gamma(\omega)}{v - \omega} \leq \beta \quad \forall v, \omega \in \mathbb{R}, \quad v \neq \omega, \quad \alpha, \beta \in \mathbb{R}$$

One-sided Lipschitz functions are vector-valued and therefore generalize the sector condition in a non-straightforward manner.

We need the following assumption previously made by [63, 65].

Assumption 5.1. Φ is quadratically inner-bounded in the region $\tilde{\mathcal{D}}$, i.e.,

$$(\Phi(x, u^*) - \Phi(\hat{x}, u^*))^\top (\Phi(x, u^*) - \Phi(\hat{x}, u^*)) \leq \eta \|x - \hat{x}\|^2 + \theta \langle x - \hat{x}, \Phi(x, u^*) - \Phi(\hat{x}, u^*) \rangle \quad (5.25)$$

for $\forall x, \hat{x} \in \tilde{\mathcal{D}}$ and $\eta, \theta \in \mathbb{R}$.

It is easy to verify that any Lipschitz function is also one-sided Lipschitz and quadratically inner bounded with $\theta = 0$ and $\eta > 0$. However the converse of these statements is not true ([63]). Thus, (5.23) with (5.24) constitutes a broad class of nonlinearities that include Lipschitz as a special case.

We first construct an approximate discrete-time model $F_{T,h}^a$ for the continuous-time system (5.23) through a refined Euler model as follows

$$\begin{cases} \varphi_h(i, x, u, d) := x + h(Ax + \Phi(x, u)) + \int_{kT+ih}^{kT+(i+1)h} d(\tau) d\tau, \\ \varphi_h^{i+1}(x, u, d) := \varphi_h(i+1, \varphi_h^i, u, d), \\ F_{T,h}^a(x(k), u(k), d[k]) := \varphi_h^N(x, u, d) \end{cases} \quad (5.26)$$

in which $\varphi_h^1 := x + h(Ax + \Phi(x, u)) + \int_{kT}^{kT+h} d(\tau) d\tau$ and $N = T/h$.

Proposition 5.1. The approximation (5.26) yields the following closed-form discrete-time model for (5.23)

$$\begin{aligned} x(k+1) &= A_h x(k) + \Phi_h(x(k), u(k)) + D_1 d_h[k] \\ y(k) &= C_h x(k) + D_2 d(k) \end{aligned} \quad (5.27)$$

with

$$\begin{aligned}
A_h &= (I + hA)^N, \quad C_h = C, \\
\Phi_h(x, u) &= \sum_{j=0}^{N-1} h(I + hA)^j \Phi(x, u), \\
d_h[k] &= \sum_{j=0}^{N-1} (I + hA)^{N-j-1} \int_{kT+jh}^{kT+(j+1)h} d(\tau) d\tau
\end{aligned} \tag{5.28}$$

Proof. The proof is straightforward and is thus omitted.

Let $H = \sum_{j=0}^{N-1} h(I + hA)^j$, then

$$\langle \Phi_h(x, u^*) - \Phi_h(\hat{x}, u^*), x - \hat{x} \rangle = \langle H\Phi(x, u^*) - H\Phi(\hat{x}, u^*), x - \hat{x} \rangle \leq \|H\|\mu\|x - \hat{x}\|^2$$

which states that Φ_h is also one-sided Lipschitz with the constant $\mu_h = \|H\|\mu$.

Remark 5.2. If $N \rightarrow 1$, then $A_h \rightarrow (I + AT)$, $\Phi_h \rightarrow T\Phi$ and (5.27) represents the original Euler model. Moreover, as $N \rightarrow \infty$, $A_h \rightarrow e^{AT}$ which is the zero-order hold equivalent of the linear part in (5.23).

Remark 5.3. It is straightforward that the approximation (5.27) is one-step consistent with the unknown exact discrete-time model of (5.23).

We now consider the following observer structure:

$$\hat{x}(k+1) = F_{T,h}^a(\hat{x}(k), u(k), 0) + L[y(k) - C_h\hat{x}(k)] \tag{5.29}$$

where $L \in \mathbb{R}^{n \times m}$ is the observer gain to be determined.

Theorem 5.3. Under Assumption 5.1, the observer (5.29) using the approximate model (5.27) is input-to-error stable according to Definition 5.1, if there exist matrices $P > 0$ and R and scalars $\zeta_1, \zeta_2 > 0$ such that the following LMI is feasible:

$$\begin{bmatrix}
-P + (\zeta_1\mu_h + \zeta_2\eta_h)I & Q + \frac{\zeta_2\theta_h - \zeta_1}{2}I & \sqrt{3}Q \\
* & 3P - \zeta_2I & 0 \\
* & * & -P
\end{bmatrix} < 0, \tag{5.30}$$

where $Q = A_h^\top P - C_h^\top R$, $\mu_h = \|H\|\mu$, $\eta_h = \|H\|^2\eta$ and $\theta_h = \|H\|^2\theta$. Then, the gain matrix L is given by $L = P^{-1}R^\top$.

Proof. To prove the result, let us pick the Lyapunov function candidate as $V_{T,h} = e^\top(k)Pe(k)$. From $\lambda_{\min}(P)|e|^2 \leq V_{T,h}(e) \leq \lambda_{\max}(P)|e|^2$, we have that (5.10) is satisfied. Besides,

$$|V_{T,h}(e_1) - V_{T,h}(e_2)| = |e_1^\top Pe_1 - e_2^\top Pe_2| = |[e_1 - e_2]P[e_1 + e_2]| \leq \lambda_{\max}(P)|e_1 + e_2||e_1 - e_2| \quad (5.31)$$

which implies (5.9) using the fact that $\exists M \in (0, \infty)$ such that $\lambda_{\max}|e_1 + e_2| \leq M$. Considering (5.27) and (5.29), the observer error dynamics is given by

$$\begin{aligned} e(k+1) := x(k+1) - \hat{x}(k+1) &= (A_h - LC_h)e(k) + \Delta\Phi_h(x(k), \hat{x}(k), u(k)) \\ &\quad + D_1d_h[k] - LD_2d(k) \end{aligned} \quad (5.32)$$

with $\Delta\Phi_h := \Phi_h(x(k), u(k)) - \Phi_h(\hat{x}(k), u(k))$. By virtue of (5.32), the difference of $V_{T,h}$ is calculated as

$$\begin{aligned} \Delta V &= V_{T,h}(e(k+1)) - V_{T,h}(e(k)) = e^\top(k+1)Pe(k+1) - e^\top(k)Pe(k) \\ &= e^\top[(A_h - LC_h)^\top P(A_h - LC_h) - P]e + \Delta\Phi_h^\top P\Delta\Phi_h + 2e^\top(A_h - LC_h)^\top P\Delta\Phi_h \\ &\quad + 2e^\top(A_h - LC_h)^\top PD_1d_h[k] - 2e^\top(A_h - LC_h)^\top PLD_2d(k) + 2\Delta\Phi_h^\top PD_1d_h[k] \\ &\quad - 2\Delta\Phi_h^\top PLD_2d(k) - 2d_h^\top[k]D_1^\top PLD_2d(k) \\ &\quad + d_h^\top[k]D_1^\top PD_1d_h[k] + d^\top(k)D_2^\top L^\top PLD_2d(k) \end{aligned} \quad (5.33)$$

Note that here $e(k+1)$ is indeed the nominal estimation error $E_{T,h}$ defined by (5.8) and hence, (5.33) calculates the Lyapunov function difference as used in (5.11). Employing the well-known matrix inequality

$$2\mathcal{X}^\top\mathcal{Y} \leq \mathcal{X}^\top P\mathcal{X} + \mathcal{Y}^\top P^{-1}\mathcal{Y} \quad (5.34)$$

for any positive definite matrix P and vectors $\mathcal{X}, \mathcal{Y} \in \mathbb{R}^n$, we obtain the following inequalities

$$2e^\top(A_h - LC_h)^\top PD_1d_h[k] \leq e^\top \tilde{A}_h e + d_h^\top[k]D_1^\top PD_1d_h[k] \quad (5.35)$$

$$-2e^\top(A_h - LC_h)^\top PLD_2d(k) \leq e^\top \tilde{A}_h e + d^\top(k)D_2^\top L^\top PLD_2d(k) \quad (5.36)$$

$$2\Delta\Phi_h^\top PD_1d_h[k] \leq \Delta\Phi_h^\top P\Delta\Phi_h + d_h^\top[k]D_1^\top PD_1d_h[k] \quad (5.37)$$

$$-2\Delta\Phi_h^\top PLD_2d(k) \leq \Delta\Phi_h^\top P\Delta\Phi_h + d^\top(k)D_2^\top L^\top PLD_2d(k) \quad (5.38)$$

where $\tilde{A}_h = (A_h - LC_h)^\top P(A_h - LC_h)$. Inserting (5.35)-(5.38) into (5.33), we have

$$\begin{aligned} \Delta V \leq & e^\top [3\tilde{A}_h - P]e + 3\Delta\Phi_h^\top P\Delta\Phi_h + 2e^\top (A_h - LC_h)^\top P\Delta\Phi_h + 3d_h^\top[k]D_1^\top PD_1 d_k[k] \\ & + 3d^\top(k)D_2^\top L^\top PLD_2 d(k) - 2d_h^\top[k]D_1^\top PLD_2 d(k) \end{aligned} \quad (5.39)$$

which can be written as

$$\begin{aligned} \Delta V/T \leq & \underbrace{\begin{bmatrix} e(k) \\ \Delta\Phi_h(k) \end{bmatrix}^\top \frac{1}{T} \begin{bmatrix} 3\tilde{A}_h - P & (A_h - LC_h)^\top P \\ * & 3P \end{bmatrix} \begin{bmatrix} e(k) \\ \Delta\Phi_h(k) \end{bmatrix}}_{(i)} \\ & + \underbrace{\begin{bmatrix} d_h[k] \\ d(k) \end{bmatrix}^\top \frac{1}{T} \begin{bmatrix} 3D_1^\top PD_1 & -D_1^\top PLD_2 \\ * & 3D_2^\top L^\top PLD_2 \end{bmatrix} \begin{bmatrix} d_h[k] \\ d(k) \end{bmatrix}}_{(ii)} \end{aligned} \quad (5.40)$$

Equation (5.24) can be rewritten in the form $\mu_h e^\top(k)e(k) - e^\top(k)\Delta\Phi_h \geq 0$. Therefore, for any positive scalar ζ_1

$$\frac{\zeta_1}{T} \begin{bmatrix} e(k) \\ \Delta\Phi_h(k) \end{bmatrix}^\top \begin{bmatrix} \mu_h I & -\frac{I}{2} \\ * & 0 \end{bmatrix} \begin{bmatrix} e(k) \\ \Delta\Phi_h(k) \end{bmatrix} \geq 0 \quad (5.41)$$

Similary, from (5.25), we have

$$\frac{\zeta_2}{T} \begin{bmatrix} e(k) \\ \Delta\Phi_h(k) \end{bmatrix}^\top \begin{bmatrix} \eta_h I & -\frac{\theta_h I}{2} \\ * & -I \end{bmatrix} \begin{bmatrix} e(k) \\ \Delta\Phi_h(k) \end{bmatrix} \geq 0 \quad (5.42)$$

for a positive scalar ζ_2 . Then, adding the left-side terms in (5.41) and (5.42) to term (i) in (5.39) leads to

$$\text{term (i)} \leq \begin{bmatrix} e(k) \\ \Delta\Phi_h(k) \end{bmatrix}^\top \Pi \begin{bmatrix} e(k) \\ \Delta\Phi_h(k) \end{bmatrix} \quad (5.43)$$

with

$$\Pi = \frac{1}{T} \begin{bmatrix} (3\tilde{A}_h - P) + (\zeta_1\mu_h + \zeta_2\eta_h)I & (A_h - LC_h)^\top P + \frac{\theta_h\zeta_2 - \zeta_1}{2}I \\ * & 3P - \zeta_2 I \end{bmatrix}$$

Using the Schur complement and notations $R = L^\top P$, $Q = A_h^\top P - C_h^\top R$, (5.30) is equivalent to $\Pi < 0$. Therefore, if LMI (5.30) holds a feasible solution, then for all $e(k) \neq 0$

$$\text{Term (i)} \leq \lambda_{max}(\Pi)(e^\top e + \Delta\Phi_h^\top \Delta\Phi_h) < -\alpha_3(\|e\|) < 0 \quad (5.44)$$

where $\alpha_3(\|e\|) = -\lambda_{max}(\Pi)\|e\|^2$. Regarding the second term of (5.40), it is easy to verify that

$$\begin{bmatrix} 3D_1^\top P D_1 & -D_1^\top P L D_2 \\ * & 3D_2^\top L^\top P L D_2 \end{bmatrix} = \begin{bmatrix} D_1 \\ D_2 \end{bmatrix}^\top \begin{bmatrix} 3P & -PL \\ * & 3L^\top P L \end{bmatrix} \begin{bmatrix} D_1 \\ D_2 \end{bmatrix} \quad (5.45)$$

is positive semi-definite which together with $\|d[k]\| \leq \|d\|_\infty$, $\|d(k)\| \leq \|d\|_\infty$ indicates that there always exists a function $\tilde{\gamma}(\cdot) \in \mathcal{K}$ such that Term (ii) $\leq \tilde{\gamma}(\|d\|_\infty)$. This inequality together with (5.44) results in (5.11). Considering Remark 5.3 all the conditions of Theorem 5.1 hold, and hence the observer (5.26) is input-to-error stable. This completes the proof. \blacksquare

Letting $\eta = 0$ and $\theta > 0$ in (5.25), the quadratically inner bounded condition reduces to the ‘‘sector constraint’’ as a special case discussed in [114], that is

$$(\Phi(x, u^*) - \Phi(\hat{x}, u^*))^\top (\Phi(x, u^*) - \Phi(\hat{x}, u^*)) \leq \theta \langle x - \hat{x}, \Phi(x, u^*) - \Phi(\hat{x}, u^*) \rangle \quad (5.46)$$

thus, we can derive the following corollary from Theorem 5.3.

Corollary 5.1. *Assume the one-sided Lipschitz system (5.23) under the sector constraint (5.46) with a constant $\theta > 0$. Then the observer (5.29) using the approximate model (5.27) is input-to-error stable, if there exist $P > 0$ and scalars $\zeta_1, \zeta_2, \varsigma > 0$ such that the following LMI is feasible*

$$\begin{bmatrix} -P + \zeta_1 \mu_h I & A_h^\top P - \frac{\sigma}{2} C_h^\top C_h + \frac{\zeta_2 \theta_h - \zeta_1}{2} I & \frac{\varsigma}{2} \sqrt{3} C_h^\top C_h \\ * & 3P - \zeta_2 I & 0 \\ * & * & -P \end{bmatrix} < 0, \quad (5.47)$$

the resulting matrix gain L is given by $L = \frac{\varsigma}{2} P^{-1} C^\top$.

Proof. Using the elimination of matrix variables introduced in [110] together with setting $\eta_h = 0$ in (5.30), we can obtain the matrix condition (5.47). Here the detailed proof is omitted. \blacksquare

Remark 5.4. *If we let $\mu_h = 0$ in (5.47), i.e., the plant is not necessarily one-sided Lipschitz, Corollary 5.1 presents a sampled-data design approach for the nonlinear systems with sector constraint nonlinearity [114].*

5.4.2 Emulation Method:

In this section we apply the general input-to-state observer convergence conditions of Theorem 5.2 to the problem of sampled-data observer design for one-sided Lipschitz nonlinear systems via emulation.

Before proceeding with the discussion, we note a significant difference between the emulation method discussed here and the direct discrete design of the previous section. In the direct discrete-time design, the quadratically inner bounded condition imposed by Assumption 5.1 seems to be inevitable. This fact is due to the challenging presence of the term $\Delta\Phi^\top P\Delta\Phi$ that appears in the derivation. We will see, however, that this condition is no longer needed for the emulation based design.

Consider again the one-sided Lipschitz plant (5.23) under the following assumption.

Assumption 5.2. *The nonlinearity Φ can be written as*

$$\Phi(x, u) = E\Psi(x, u) \quad (5.48)$$

where the full-column rank matrix $E \in \mathbb{R}^{n \times s}$ is the corresponding distribution of $\Psi(x, u)$ onto the nonlinear function $\Phi(x, u)$

Remark 5.5. *Assumption 5.2 places a geometric condition on the one-sided Lipschitz function Φ . Note that this condition affects neither the value of the one-sided Lipschitz constant nor the Lyapunov matrix in our synthesis (see Theorem 5.4).*

Throughout the rest of the section we assume that a continuous-time observer of the form:

$$\dot{\hat{x}}(t) = A\hat{x}(t) + \Phi(\hat{x}(t), u(t)) + L[y(t) - C\hat{x}(t)] \quad (5.49)$$

has already been designed for the continuous-time system (5.23)-(5.24), and construct $S_{T,h}^a$ in (5.20) using a refined Euler approximation similar to (5.26) as follows:

$$\hat{x}(k+1) = (I + h(A - LC))^N \hat{x}(k) + \sum_{j=0}^{N-1} h(I + h(A - LC))^j (\Phi(\hat{x}(k), u(k)) + Ly(k)) \quad (5.50)$$

Theorem 5.4. *Under Assumption 5.2, the discretized observer (5.50) obtained from the continuous-time observer (5.49) is input-to-error stable according to Definition 5.1, if there exist matrices $X = X^\top$ and R and scalar $\zeta > 0$ such that the following LMI feasibility*

problem has a solution:

$$Q + Q^\top + E^\perp X E^{\perp\top} + \zeta(2\mu + 1)I < 0 \quad (5.51)$$

$$E^\perp X E^{\perp\top} + \zeta I > I \quad (5.52)$$

in which $Q = A^\top E^\perp X E^{\perp\top} + \zeta A - RC$. If (5.51)-(5.52) has a feasible solution, then the observer gain is given by $L = (E^\perp X E^{\perp\top} + \zeta I)^{-1}R$.

The following lemma is needed in the proof of Theorem 5.4.

Lemma 5.2. For any symmetric matrix $P \in \mathbb{R}^{n \times n}$ and nonzero matrix $M \in \mathbb{R}^{n \times m}$, there exists a symmetric matrix $X \in \mathbb{R}^{m \times m}$ and a positive scalar $\zeta > 0$ such that P can be parameterized in the form $P = MXM^\top + \zeta I_n$.

Proof: The proof is analogous to that in [103, Lemma 4.1], and is omitted. \blacksquare

Proof of Theorem 5.4. From (5.23) and (5.49), the error dynamics of the continuous-time observer is

$$\dot{e}(t) = (A - LC)e(t) + \Phi(x(t), u(t)) - \Phi(\hat{x}(t), u(t)) + (D_1 - LD_2)d(t) \quad (5.53)$$

Choose $V(e) = e^\top(t)Pe(t)$ as the Lyapunov function candidate. Computing the left hand side of (5.22) yields

$$\begin{aligned} & \frac{\partial V}{\partial x} f(x, u) + \frac{\partial V}{\partial \hat{x}} s(\hat{x}, y, u) \\ &= 2e^\top(t)P(Ax(t) + \Phi(x(t), u(t)) + D_1d(t)) - 2e^\top(t)P(A\hat{x}(t) + \Phi(\hat{x}(t), u(t))) \\ &+ L[y(t) - C\hat{x}(t)] \\ &= e^\top(t)[(A - LC)^\top P + P(A - LC)]e(t) + 2e^\top(t)P[\Phi(x(t), u(t)) - \Phi(\hat{x}(t), u(t))] \\ &+ 2e^\top(t)P(D_1 - LD_2)d(t) \end{aligned} \quad (5.54)$$

that is indeed the time derivative of V along (5.53). In accordance with Lemma 5.2, assume that P can be parameterized as $P = E^\perp X E^{\perp\top} + \zeta I$, where X is an arbitrary weighting matrix, $\zeta > 0$ and E comes from Assumption 5.2. Now, using the geometric condition (5.48) and the one-sided Lipchitz property of Φ we get

$$\begin{aligned} e^\top(t)P[\Phi(x(t), u(t)) - \Phi(\hat{x}(t), u(t))] &= \langle PE\Psi(x(t), u(t)) - PE\Psi(\hat{x}(t), u(t)), x(t) - \hat{x}(t) \rangle \\ &= \zeta \langle E\Psi(x(t), u(t)) - E\Psi(\hat{x}(t), u(t)), x(t) - \hat{x}(t) \rangle \\ &\leq \zeta \mu e^\top(t)e(t) \end{aligned} \quad (5.55)$$

Also, based on the matrix inequality property (5.34) it follows that

$$2e^\top(t)P(D_1 - LD_2)d(t) \leq e^\top(t)Pe(t) + d^\top(t)(D_1 - LD_2)^\top(D_1 - LD_2)d(t) \quad (5.56)$$

Inserting (5.55)-(5.56) into (5.54) along with considering the parameterization of P gives rise to

$$\begin{aligned} \frac{\partial V}{\partial x}f(x, u) + \frac{\partial V}{\partial \hat{x}}s(\hat{x}, y, u) &= e^\top(t)[(A - LC)^\top(E^\perp XE^{\perp\top} + \zeta I) + (E^\perp XE^{\perp\top} + \zeta I)(A - LC) \\ &\quad + (E^\perp XE^{\perp\top} + \zeta I) + 2\zeta\mu I]e(t) + d^\top(t)(D_1 - LD_2)^\top(D_1 - LD_2)d(t) \end{aligned} \quad (5.57)$$

Since $d^\top(t)(D_1 - LD_2)^\top(D_1 - LD_2)d(t)$ is always positive semi-definite, (5.57) holds the form of (5.22) if $(A - LC)^\top(E^\perp XE^{\perp\top} + \zeta I) + (E^\perp XE^{\perp\top} + \zeta I)(A - LC) + (E^\perp XE^{\perp\top} + \zeta I) + 2\zeta\mu I < 0$. Using the definition of Q and L , we arrive at the linear matrix inequalities (5.51)-(5.52). Therefore, all the conditions of Theorem 5.2 are satisfied and the observer dynamics is input-to-error stable. This concludes the proof. \blacksquare

Remark 5.6. *Although the need for the quadratically inner bounded constraint was eliminated in Theorem 5.4, the direct discrete-time design of Theorem 5.3 usually brings better observer performance. This is mainly due to the fact that unlike the emulation approach, the DTD method deals with the sampling period directly (see also Example 2).*

5.5 Illustrative Examples

In this section we present two numerical examples showing the applicability of theorems 5.3 and 5.4 for sampled-data one-sided Lipschitz systems.

Example 1. [61] Consider the system (5.23), with

$$\begin{aligned} A &= \begin{bmatrix} -1 & -2 \\ 1 & -1.5 \end{bmatrix}, \quad C = \begin{bmatrix} 1 & 0 \end{bmatrix}, \quad D_1 = \begin{bmatrix} 0.5 \\ -1 \end{bmatrix}, \quad D_2 = 1 \\ \Phi(x(t), u(t)) &= \begin{bmatrix} \frac{1}{2}u(t) & \sin(x_1(t) - x_2(t)) - x_2^{\frac{1}{3}}(t) \end{bmatrix}^\top, \end{aligned}$$

$u(t) = \sin(t)$, and the disturbance input $d(t)$ follows a uniform random distribution. As discussed in the same reference, Φ is not a Lipschitz nonlinearity. It is, however, easy to

see that:

$$\begin{aligned}
\langle \Phi(x, u^*) - \Phi(\hat{x}, u^*), x - \hat{x} \rangle &= (\sin(x_1 - x_2) - \sin(\hat{x}_1 - \hat{x}_2) + \hat{x}_2^{\frac{1}{3}} - x_2^{\frac{1}{3}})(x_2 - \hat{x}_2) \\
&= \begin{bmatrix} \cos(\xi_1 - \xi_2) & -\cos(\xi_1 - \xi_2) \end{bmatrix} (x - \hat{x})(x_2 - \hat{x}_2) - \frac{1}{3}\xi_0^{-\frac{2}{3}}(x_2 - \hat{x}_2) \\
&\leq \left\| \begin{bmatrix} \cos(\xi_1 - \xi_2) & -\cos(\xi_1 - \xi_2) \end{bmatrix} \right\| \cdot \|(x - \hat{x})(x_2 - \hat{x}_2)\| \leq \sqrt{2}\|x - \hat{x}\|^2 \quad (5.58)
\end{aligned}$$

with $\xi_0 \in (\min(x_2, \hat{x}_2), \max(x_2, \hat{x}_2))$ and $\xi = (\xi_1, \xi_2) \in Co(x, \hat{x})$ (i.e., open convex set). It follows that Φ is one-sided Lipschitz with $\mu = \sqrt{2}$. Similarly, we have that

$$\begin{aligned}
\langle \Phi(x, u^*) - \Phi(\hat{x}, u^*), \Phi(x, u^*) - \Phi(\hat{x}, u^*) \rangle &= (\sin(x_1 - x_2) - \sin(\hat{x}_1 - \hat{x}_2) + \hat{x}_2^{\frac{1}{3}} - x_2^{\frac{1}{3}})^2 \\
&\leq (|\sin(x_1 - x_2) - \sin(\hat{x}_1 - \hat{x}_2)| + |\hat{x}_2^{\frac{1}{3}} - x_2^{\frac{1}{3}}|)^2 \\
&\leq (\sqrt{2} + \frac{1}{3}\xi_0^{-\frac{2}{3}})^2 \|x - \hat{x}\|^2. \quad (5.59)
\end{aligned}$$

Thus, Φ is quadratically inner bounded with $\eta = (\sqrt{2} + \frac{1}{3}r^{-\frac{2}{3}})$, and $\theta = 0$.

We now exploit the sampled-data observer (5.29) along with the approximation (5.27)-(5.28) to estimate system trajectories. Assuming $x \in \mathcal{D} = \{x \in \mathbb{R}^2 : \|x\| \leq r\}$, we have $\mu = \sqrt{2}, \eta = (\sqrt{2} + \frac{1}{3}r^{-\frac{2}{3}}), \theta = 0$. Taking $T = 0.5, N = 100$ and $r = 3$, and solving the LMI problem of Theorem 5.3 yields $L = [0.7052 \quad 0.1236]^\top$.

Figures 5.1-5.2 display the simulation results, where the initial conditions are set to $x(0) = [0.5 \quad 1]^\top$ and $\hat{x}(0) = x(0) = [1 \quad 0.5]^\top$. Evidently, the effect of state trajectory estimation is satisfactory and the estimation error diminishes as the sampling period T is decreased (see Figure 5.1). We also investigated the effect of refining parameter h for a fixed value of T on the performance of the sampled-data observer. We can see from Figure 5.2 that the residual error is reduced by increasing N (that is, decreasing h). However, h cannot be reduced indefinitely and there remains a residual estimation error since the sampling period T is fixed. This fact coincides with the semi-global practical convergence guaranteed by Theorem 5.1.

Example 2. Consider the normalized Chua's circuit with cubic nonlinearity given by

$$\begin{aligned}
\dot{x}_1(t) &= a(x_2(t) - x_1(t) - \mathcal{N}(x_1(t))) \\
\dot{x}_2(t) &= x_1(t) - x_2(t) + x_3(t) \\
\dot{x}_3(t) &= -bx_2(t) + u(t)
\end{aligned} \quad (5.60)$$

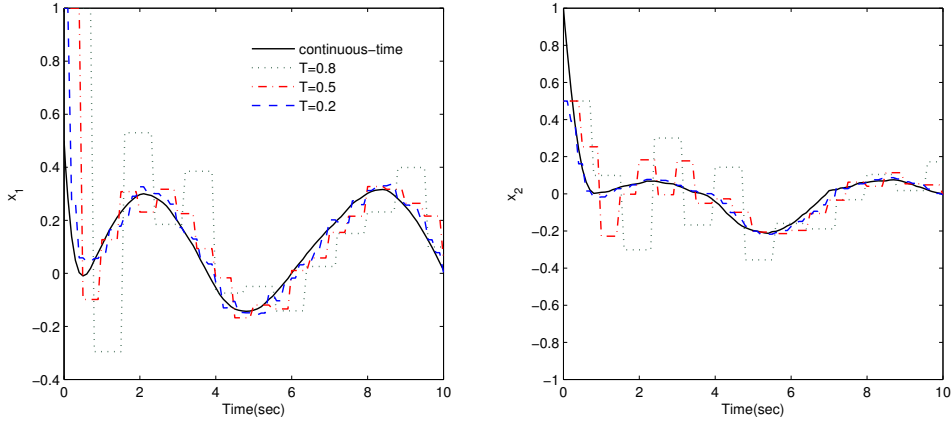


Figure 5.1: Estimated states for different values of T under uniformly random disturbance

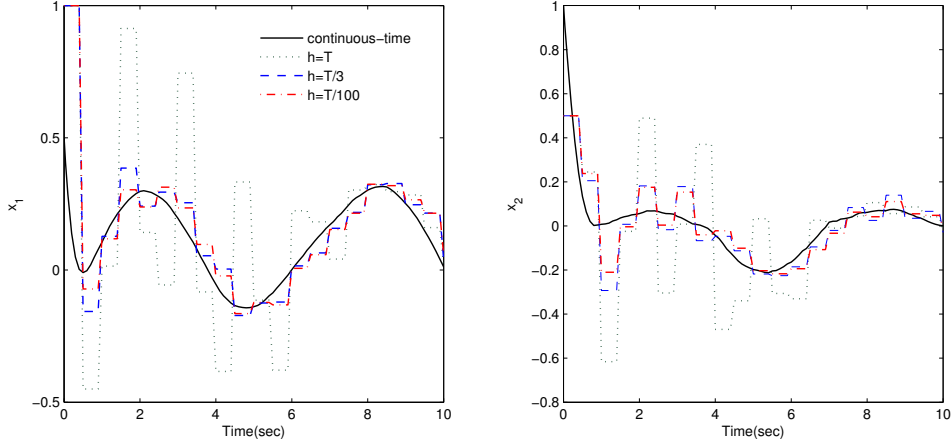


Figure 5.2: Estimated states for a fixed T and different values of h under uniformly random disturbance

which exhibits a family of chaotic attractors and can be easily implemented in laboratory as shown in Figure 3 (see e.g., [115] for an in-depth analysis). The state variables x_1 , x_2 and x_3 are the capacitors voltages and the inductor current, respectively, u stands for the control input, and the parameters $a, b > 0$ are determined by the circuit components. Also, $\mathcal{N}(x_1)$ is a cubic smooth function given as

$$\mathcal{N}(x_1) = m_0 x_1(t) + m_1 x_1^3(t), \quad m_0 < 0, \quad m_1 > 0 \quad (5.61)$$

describes the $i-v$ characteristic of the nonlinear resistor N_R used instead of the piecewise-linear characteristic of the canonical Chua's circuit. It is easy to see that if $m_0 < -1$, the equilibria of the unforced circuit are given by $x^e = \{[\pm\sqrt{-(m_0+1)/d} \quad 0 \quad \mp$

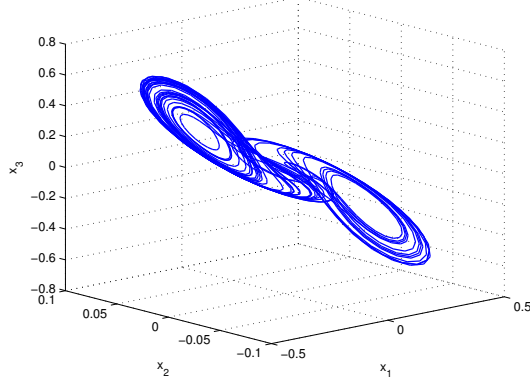
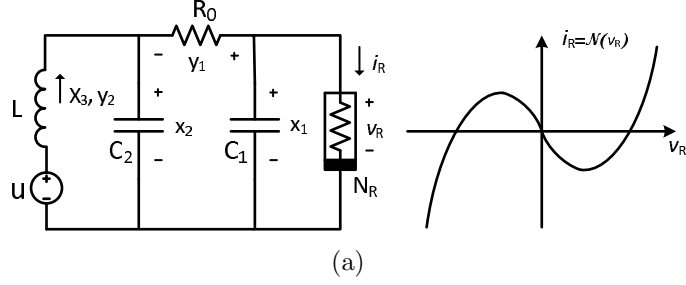


Figure 5.3: (a) Schematic of a Chua's circuit with cubic nonlinearity, (b) A chaotic behaviour of the circuit called double-scroll attractor

$\sqrt{-(m_0 + 1)/d}^\top, [0 \ 0 \ 0]^\top$. For $m \geq -1$ the origin is the only equilibrium of the system.

Assume now that our measurements are the voltage across the resistor R_0 and the current across the inductor L in Figure 5.3a, i.e.,

$$y(t) = \begin{bmatrix} y_1(t) \\ y_2(t) \end{bmatrix} = \begin{bmatrix} x_1(t) - x_2(t) \\ x_3(t) \end{bmatrix} + d(t). \quad (5.62)$$

The disturbance d in (5.62) represents the effect of white noise. We design the DTD and CTD-based sampled-data observers introduced in Section 5.4 to estimate the inaccessible states in the presence of disturbance inputs. To this end, first note that the chaotic equations (5.60) can be written in the form (5.23) with

$$A = \begin{bmatrix} -a(m_0 + 1) & a & 0 \\ 1 & -1 & 1 \\ 0 & -b & 0 \end{bmatrix}, \quad \Phi = \begin{bmatrix} -am_1 x_1^3(t) \\ 0 \\ u(t) \end{bmatrix}, \quad C = \begin{bmatrix} 1 & -1 & 0 \\ 0 & 0 & 1 \end{bmatrix}.$$

It can be easily shown that $\Phi(x, u)$ is locally Lipschitz with a region based Lipschitz

constant and is globally one-sided Lipschitz with $\mu = 0$:

$$\begin{aligned}\langle \Phi(x, u^*) - \Phi(\tilde{x}, u^*), x - \tilde{x} \rangle &= -am_1(x_1^3 - \hat{x}_1^3)(x_1 - \hat{x}_1) \\ &= -am_1(x_1 - \hat{x}_1)^2(x_1^2 + x_1\hat{x}_1 + \hat{x}_1^2) \\ &\leq -\frac{am_1}{2}(x_1 - \hat{x}_1)^2(x_1^2 + \hat{x}_1^2) \leq 0\end{aligned}$$

The quadratically inner-bounded property of Φ is not global and the constants η, θ in (5.25) depend on the region of operation of the circuit. Thus, in this example we prefer the emulation method which does not require the use of the quadratically inner-bounded assumption.

For the sake of numerical simulations, the parameters of the Chua's circuit are chosen as $a = 10$, $b = 16$, $m_0 = -1.5$, $m_1 = 1$, and the input voltage is set to $u = \sin t$. We also take $T = 0.1$ and $h = 100$ for the sampling period and the integration period, respectively. Solving the LMI feasibility problem of Theorem 5.3 with $\mu = 0$ and $\eta = -1, \theta = -0.5$ results in

$$P = \begin{bmatrix} 2.0205 & -1.3626 & 2.5546 \\ -1.3626 & 6.2141 & 0.9220 \\ 2.5546 & 0.9220 & 5.1111 \end{bmatrix},$$

$$R^\top = \begin{bmatrix} 2.8245 & 1.9271 \\ -1.6215 & 1.0771 \\ 3.8332 & 4.5576 \end{bmatrix}, L = \begin{bmatrix} 1.0897 & -1.4128 \\ -0.0539 & -0.3838 \\ 0.2150 & 1.6671 \end{bmatrix}$$

The function Φ satisfies the geometric condition of Assumption 5.2 with $\Psi = -am_1x_1^3$, $E = \begin{bmatrix} 1 & 0 & 0 \end{bmatrix}^\top$. Therefore, applying Theorem 5.4 the observer gain is obtained as

$$E^\perp = \begin{bmatrix} 0 & 0 & 1 \\ 0 & 1 & 1 \end{bmatrix}, X = \begin{bmatrix} -1.9382 & 1.7036 \\ 1.7036 & 21.8019 \end{bmatrix},$$

$$R = \begin{bmatrix} 132.4673 & -350.3288 \\ 376.5884 & -281.8653 \\ 373.8343 & 66.6209 \end{bmatrix}, L = \begin{bmatrix} 6.5112 & -17.2199 \\ 5.9406 & -10.7797 \\ 5.3696 & 7.3369 \end{bmatrix}$$

Figure 5.4 compares the behaviour of the DTD and CTD sampled-data observers designed above under the same values of T and h originated from the initial conditions $x(0) = \begin{bmatrix} 0.2 & -0.5 & 0.4 \end{bmatrix}^\top$ and $\hat{x}(0) = \begin{bmatrix} 0.1 & -0.2 & 0.1 \end{bmatrix}^\top$. Both observers provide estimates closed

to the actual state trajectories in spite of the fact that their parameters were not modified during the operation of disturbances. This is in agreement with the concept of input-to-error stability in the semiglobal practical sense. Moreover, Figure 5.5 shows that the DTD observer outperforms the emulated one with a smaller estimation error with faster decay rate.

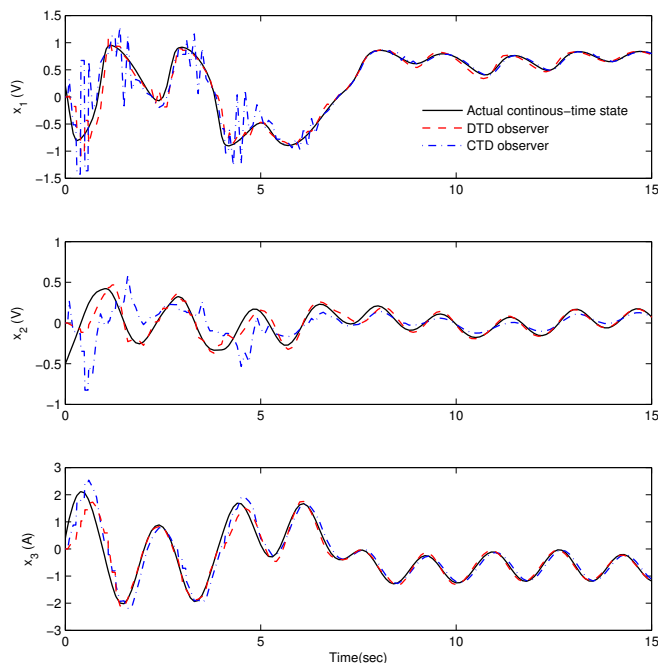


Figure 5.4: Sampled-data state estimation of a chaotic circuit from noisy measurements using DTD and CTD observers

5.6 Summary

In this chapter the notion of input-to-state stability (ISS) was adopted to design nonlinear observers for sampled-data systems subject to disturbance inputs and intrinsic discretization error due to unknown exact discrete-time model. A general framework was presented based on the discrete-time approximation (DTD) as well as the emulation (CTD) approach with guaranteed semiglobal practical ISS from exogenous disturbances to the estimation error, under some standard assumptions.

The second half of the chapter considers the application of the theoretical framework

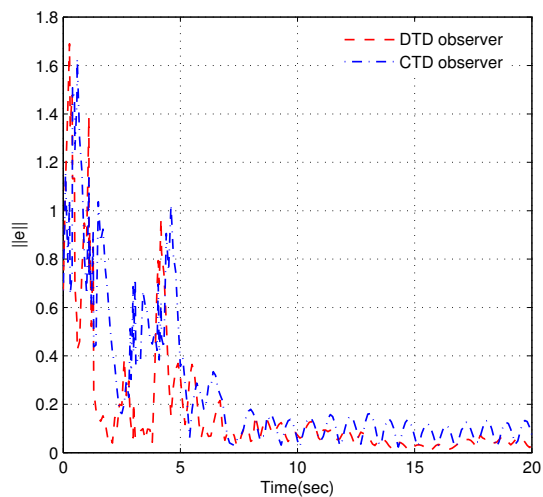


Figure 5.5: Comparison of the estimation error for two sampled-data observers

for sampled-data observers to the important case of one-sided Lipschitz systems. We show that for this class of systems DTD and CTD present distinct and unique challenges. Indeed, the DTD presents some structural limitations that require the use of additional assumptions on the nonlinearities in order to proceed. We resolved these difficulties by imposing the additional condition of quadratic inner boundedness on the nonlinearity. Unlike the DTD-based scheme, the CTD-based design does not require this condition but instead a mild geometric condition.

Simulation results suggest that the DTD method is usually preferable and has the advantage of having a smaller estimation errors and better intersample behavior compared with the CTD method.

Chapter 6

Multirate Observer Design via Discrete-Time Approximation

In this chapter¹, we tackle the observer design problem for nonlinear MSD systems under the effect of disturbance inputs. This chapter can be viewed as a multirate version of the previous chapter. Our main purpose is to layout a general framework for multirate observer synthesis. The main idea is to introduce a fast-rate sampler that reconstructs the inter-sample outputs between measured samples using an approximate discrete-time model of the plant together with the system output function and a modified hold device that assigns each control input to its previous measured value during the corresponding sampling interval. The outputs of the modified sample and hold devices are then fed to a single-rate observer working at the base sampling period of the plant. Taking the disturbances as the input and the estimation error as the state, the notion of input-to-state stability (ISS) is adopted to analyze the convergence of the estimation error. We show that if the single-rate observer is input-to-state stable, then under some standard assumptions and Lyapunov-ISS conditions, the proposed multirate observer is input-to-state stable in the semiglobal practical sense. It is worth noticing that the concept of input-to-state stability, initially characterized by Sontag [100], was previously applied for observer design of continuous-time systems with slope-restricted nonlinearities by [104] and Lipschitz continuity condition in [72].

¹The results of this chapter have been accepted for publication in the article: H. Beikzadeh and H. J. Marquez, “Multirate Observers for Nonlinear Sampled-Data Systems Using Input-to-State Stability and Discrete-Time Approximation,” *IEEE Transactions on Automatic Control*, Accepted on Jan. 2014.

Our approach deals explicitly with (i) the model mismatch induced by the discrete-time approximation (discussed in [70] for single-rate sampled-data observers), and (ii) the effect of disturbances and consequent deviations of the model estimates from true plant outputs. Our proposed sampled-data scheme is not restricted to either the high gain observers used in [22] or to the dual-rate case studied in [21] and covers the “low measurement rate” case addressed in [17–21] as a special case. We also emphasize that our primary goal in this chapter is to study observer convergence properties under multirate sampling independently of the use of the observer as part of a feedback law. These results are, of course, applicable in observer-based multirate controller as well as fault detection.

The outline of this chapter is as follows. Section 6.1 provides the general configuration of a multirate nonlinear plant together with a sample-data observer structure in presence of disturbances, and gives the relevant definitions and notations. We introduce a multirate observer scheme and prove our main result in Section 6.2. Section 6.3 verifies the efficiency of the proposed multirate state estimation through a benchmark model of the planar vertical takeoff and landing (PVTOL) aircraft. Also, it is compared with the single-rate observer designed in Chapter refch5 by implementing on a one-sided Lipschitz system. Eventually, some concluding remarks are drawn in the last section.

6.1 Multirate System and Preliminaries

Consider the general nonlinear plant represented by

$$G : \begin{cases} \dot{x}(t) = f(x(t), u(t), d(t)) \\ y(t) = g(x(t), u(t), d(t)) \end{cases} \quad (6.1)$$

where $x \in \mathbb{R}^n$, $u \in \mathbb{R}^m$, $d \in \mathbb{R}^q$ and $y \in \mathbb{R}^p$ are respectively the state vector, control input, exogenous disturbance and measured output, and f and g are continuously differentiable functions vanishing at the origin. Assume that the continuous-time system G is connected to an ideal sampler \mathcal{S} and a (zero order) hold device \mathcal{H} with different sampling rates in a multirate sampled-data configuration. Precisely, the p channels of y are sampled periodically at sampling instances $a_i T$, $a_i \in \mathbb{Z}^+ \forall i = 1, \dots, p$, via \mathcal{S} and the m channels of u are kept constant with periods $b_j T$, $b_j \in \mathbb{Z}^+ \forall j = 1, \dots, m$, via \mathcal{H} . Note that the sample and hold operators are synchronized at $t = 0$ and T is a real number referred to

as the base sampling period of the system. Any common factors among a_i and b_j can be absorbed into T , and thus we can assume without loss of generality that a_i and b_j are relatively prime. This setup has been extensively utilized in the literature for stabilization of linear multirate plants (see e.g., [34]).

Consider now a single-rate zero-order hold discretization of the system G with sampling period T . The exact discrete-time model of (6.1) is given by

$$x(k+1) = x(k) + \int_{kT}^{(k+1)T} f(x(\tau), u(k), d(\tau))d\tau := F_T^e(x[k], u(k), d[k]) \quad (6.2)$$

$$y(k) = g(x(k), u(k), d(k)). \quad (6.3)$$

Finding an explicit solution for (6.2) is impossible in most practical cases, thus consistent with the literature on nonlinear sampled-data systems, F_T^e will be assumed to be unknown. It is realistic, however, to use a family of approximate discrete-time models $F_{T,h}^a(x(k), u(k), d[k])$, where h can be interpreted as the *integration period* of the numerical schemes used to generate the approximate model.

Remark 6.1. *The approximate model $F_{T,h}^a$ can be obtained using different numerical integration methods such as the classical Euler model with $T = h$. However, as illustrated by many authors (see e.g., [13, 18]) it is usually more appropriate to choose h different from T . We will also employ this scheme that appears to be much more reasonable for multirate systems.*

Throughout the chapter the mismatch of the exact and approximate models is expressed via consistency property of Definition 2.7, that was extended to multirate case by [17]. It is worth mentioning that the one-step consistency can be checked using verifiable sufficient conditions provided in [4, 13] and [20] without knowing the exact model F_T^e . In order to propose a multirate observer strategy, we first consider a family of sampled-data observers governed by

$$\hat{x}(k+1) = \mathcal{O}_{T,h}(\hat{x}, y, u) := F_{T,h}^a(\hat{x}, u, 0) + \ell_{T,h}(\hat{x}, y, u) \quad (6.4)$$

where $F_{T,h}^a(\hat{x}(k), u(k), 0)$ is the approximate model with zero disturbance and $\ell_{T,h}$ is zero at zero.

Definition 6.1. *The correction term $\ell_{T,h}$ of the observer dynamic (6.4) is said to be uniformly locally Lipschitz if given $\delta_1 > 0$ there exist $L_\ell > 0$ and $T_1 > 0$ such that for each*

fixed $T \in (0, T_1]$, there exists $h_1 \in (0, T]$ such that $|\ell_{T,h}(\xi_1) - \ell_{T,h}(\xi_2)| \leq L_\ell |\xi_1 - \xi_2|$ for all $\xi_1, \xi_2 \in \mathcal{B}(\delta_1)$ and $h \in (0, h_1]$, where $\xi := (\hat{x}', y', u)'$.

Remark 6.2. *The local Lipschitz continuity condition of Definition 6.1 constitutes a mild assumption that is readily satisfied in most practical cases.*

The main question is that under what conditions, and in what sense, an estimator like (6.4) guarantees convergence when applied to the exact model (6.2)-(6.3). In this work following the lines of [100], we use the following input-to-state stability (ISS) notion to analyze the convergence of the estimation error.

Definition 6.2. *The observer (6.4) is said to be input-to-state stable semiglobal in T and practical in h , if there exist $\beta \in \mathcal{KL}$ and $\gamma \in \mathcal{K}$ such that for any $\delta_1, \delta_2 > 0$ and compact sets $\mathcal{X} \in \mathbb{R}^n$, $\mathcal{U} \in \mathbb{R}^m$, we can find $T_1 > 0$ such that for any $T \in (0, T_1]$ and $\nu \in (0, \delta_1)$, there exists $h_1 \in (0, T]$ such that $\forall h \in (0, h_1]$, $|e(0)| \leq \delta_1$, $\|d\|_\infty \leq \delta_2$ and $x(k) \in \mathcal{X}$, $u(k) \in \mathcal{U}$ implies $\forall k \in \mathbb{Z}^+$*

$$|e(k)| \leq \beta(|e(0)|, kT) + \gamma(\|d\|_\infty) + \nu \quad (6.5)$$

This definition is a generalization of the *semiglobal practical* convergence presented by [70] when the plant exposed to disturbance inputs. We now present the concept of Lyapunov-ISS observer which can be used to investigate the stability property of Definition 6.2.

Definition 6.3. *The family of observers $\hat{x}(k+1) = \tilde{\mathcal{O}}_{T,h}(\hat{x}, y, u)$ is Lyapunov-ISS for the difference equation $x(k+1) = \tilde{F}_{T,h}(x, u, \bar{d})$ if there exists a family of Lyapunov functions $V_{T,h}(x, \hat{x})$, $\alpha_1(\cdot), \alpha_2(\cdot), \alpha_3(\cdot) \in \mathcal{K}_\infty$ and $\tilde{\gamma}(\cdot) \in \mathcal{K}$ with the following properties:*

For any positive real numbers $(\delta_1, \delta_2, \delta_3)$, there exist $T_1 > 0$ and $M > 0$ such that for each fixed $T \in (0, T_1]$ there exists $h_1 \in (0, T]$ such that for all $x, x_1, x_2 \in \mathcal{B}(\delta_1)$, $\hat{x} \in \mathcal{B}(\delta_2)$, $\|d\|_\infty \leq \delta_3$ and $h \in (0, h_1]$,

$$|V_{T,h}(x_1, \hat{x}) - V_{T,h}(x_2, \hat{x})| \leq M|x_1 - x_2| \quad (6.6)$$

$$\alpha_1(|e|) \leq V_{T,h}(x, \hat{x}) \leq \alpha_2(|e|) \quad (6.7)$$

$$\frac{\Delta V}{T} := \frac{V_{T,h}(\tilde{F}_{T,h}(x, u, \bar{d}), \tilde{\mathcal{O}}_{T,h}(\hat{x}, y, u)) - V_{T,h}(x, \hat{x})}{T} \leq -\alpha_3(|e|) + \tilde{\gamma}(\|d\|_\infty) \quad (6.8)$$

6.2 Multirate Nonlinear Observer

In this section we formulate a general observer framework for the multirate sampled-data system introduced in the previous section. We assume that an ISS single-rate observer is given and design a multirate observer which preserves similar stability features in a specific sense. The main idea is the following: we exploit a fast rate observer based on the family (6.4), that uses a periodic switch to reconstruct the missing outputs between measured samples together with a switch to keep input channels constant during intervals smaller than their corresponding sampling intervals. More precisely, our multirate nonlinear observer is defined by

$$\hat{x}(k\tau_o + \tau_o) = F_{T,h}^a(\hat{x}(k\tau_o), u_c(k\tau_o), 0) + \ell_{T,h}(\hat{x}(k\tau_o), y_c(k\tau_o), u_c(k\tau_o)) \quad (6.9)$$

where τ_o is the observer sampling time that is here assumed to be equal to T for the sake of simplicity (see Remark 6.3), and $y_c = [y_{c1} \ \dots \ y_{cp}]'$ and $u_c = [u_{c1} \ \dots \ u_{cm}]'$ are the output of appropriate periodic switches as below

$$y_{c_i}(k) = \begin{cases} y_i(k), & \text{if } k = l_i a_i \ \exists l_i \in \mathbb{Z}^+ \\ g_i(F_{T,h}^a(\hat{x}(k-1), u_c(k-1), 0), u_c, 0), & \text{otherwise} \end{cases} \quad (6.10)$$

$$u_{c_j}(k) = \begin{cases} u_j(k), & \text{if } k = r_j b_j \ \exists r_j \in \mathbb{Z}^+ \\ u_{c_j}(k-1), & \text{otherwise} \end{cases} \quad (6.11)$$

This sampled-data configuration is depicted in Figure 6.1. It can be seen that the i^{th} component of the modified output vector y_c connects to the actual measurement y_i when it is available, otherwise it uses the output mapping model g , the approximate model $F_{T,h}^a$ and the state estimates to compensate for unmeasured intersample outputs. Likewise, the j^{th} channel of the modified hold \mathcal{H}_f applies the actual input u_j at its sampling instances while keeping it constant during the subintervals.

Remark 6.3. *It is usually desired to choose the estimation sampling period τ_o much faster than the system sampling times. However, in some applications one may study a slow-rate observer in which τ_o is limited by the measurement sampling times, i.e., $\tau_o = \inf\{a_1 T, \dots, a_p T\}$. For the general case of τ_o , the observer structure will be obtained by*

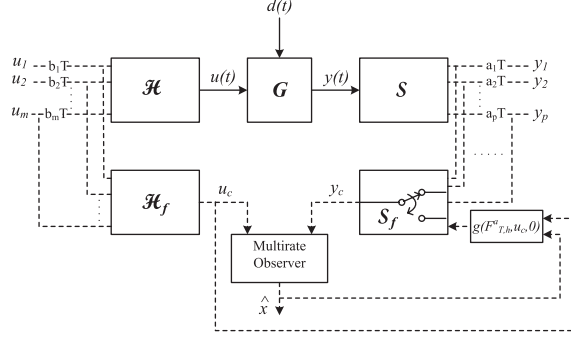


Figure 6.1: A schematic of the multirate nonlinear sampled-data observer.

reformulating (6.10)-(6.11) as follows

$$y_{ci}(k\tau_o) = \begin{cases} y_i(\lfloor \frac{k\tau_o}{a_i T} \rfloor a_i T), & \text{if } k\tau_o \geq l_i a_i T \ \& \ (k-1)\tau_o < l_i a_i T \ \text{for } l_i \in \mathbb{Z}^+ \\ g_i(F_{T,h}^a(\hat{x}((k-1)\tau_o), u_c((k-1)\tau_o), 0), u_c(k\tau_o), 0), & \text{otherwise} \end{cases}$$

$$u_{cj}(k\tau_o) = \begin{cases} u_j(\lfloor \frac{k\tau_o}{b_j T} \rfloor b_j T), & \text{if } k\tau_o \geq r_j b_j T \ \& \ (k-1)\tau_o < r_j a_j T \ \text{for } r_j \in \mathbb{Z}^+ \\ u_{cj}((k-1)\tau_o), & \text{otherwise} \end{cases}$$

For our analysis we first note that considering (6.2) and (6.11), the exact discrete-time model of the original multirate plant (6.1) can be expressed as

$$x(k+1) = F_T^e(x(k), u_c(k), d[k]) \quad (6.12)$$

in which the integral is taken over similar time intervals, but u is replaced by u_c . It is clear from (6.11) that although each component of the modified input u_c is updated at different instances the whole vector is constant during sampling intervals $[kT, (k+1)T)$. By virtue of (6.9) and (6.12), the observer error dynamics is given by

$$\begin{aligned} e(k+1) &= F_{T,h}^a(\hat{x}, u_c, 0) + \ell_{T,h}(\hat{x}, y_c, u_c) - F_T^e(x, u_c, \bar{d}) \\ &= E_{T,h}(e, x, u_c) + F_{T,h}^a(x, u_c, \bar{d}) - F_T^e(x, u_c, \bar{d}) \end{aligned} \quad (6.13)$$

where

$$E_{T,h}(e, x, u_c) = F_{T,h}^a(\hat{x}, u_c, 0) + \ell_{T,h}(\hat{x}, y_c, u_c) - F_{T,h}^a(x, u_c, \bar{d}) \quad (6.14)$$

indicates the nominal error dynamics for the approximate design, and $F_{T,h}^a - F_T^e$ is the mismatch between the approximate and exact plant models. We now address the stability of the proposed multirate scheme under the following assumptions.

Assumption. (i) The single-rate observer (6.4) is Lyapunov-ISS for $F_{T,h}^a$ according to Definition 6.3. (ii) The approximate model $F_{T,h}^a$ is one-step consistent with the exact discrete-time model F_T^e based on Definition 6.1. (iii) The function $\ell_{T,h}(\cdot, \cdot, \cdot)$ is uniformly locally Lipschitz based on Definition 6.2 and the control input u is locally Lipschitz and bounded. (iv) Each input signal is held at a frequency greater than its corresponding Nyquist frequency, i.e., $\frac{1}{b_j T} \geq 2\omega_{maxj} \forall j = 1, \dots, m$, where ω_{maxj} is the highest frequency content present in the j^{th} input channel.

Remark 6.4. Assumption (iv) is made to enforce a bound on the input variations which appears in our derivation (see the proof of Theorem 1). It simply ensures perfect reconstruction of each input from the sampled data. Assumption (iv) can, however, be ignored in the special cases of single-rate input channel, closed-loop systems as well as “low measurement rate”.

Theorem 6.1. Under Assumptions (i)-(iv), the multirate observer (6.9)-(6.11) is ISS stable for the exact discrete-time model of the multirate system (6.1) in the sense of Definition 6.3.

The following lemmas are needed in the proof of our main result.

Lemma 6.1. Given any $\varepsilon_1 > 0$ there exists $T_1 > 0$ such that for all $T \in (0, T_1]$ the fast rate control inputs u and u_c satisfies $|u_c(k) - u(k)| \leq \varepsilon_1$.

Proof. Let $T_1 > 0$ be such that $T_1 L_u \sqrt{b_1^2 + \dots + b_m^2} < \varepsilon_1$ with L_u as the Lipschitz constant of u , and suppose $T \in (0, T_1]$. Based on (6.11) we get

$$|u_c(k) - u(k)|^2 = \sum_{j=1}^m \sigma_j^k |u_j(k) - u_j(r_j b_j)|^2 \quad (6.15)$$

where $\sigma_j^k \in \{0, 1\}$ and $\sigma_j^k = 0$ whenever the j^{th} channel of u_c is sampled at a sampling instance that is an integer multiple of $b_j T$, otherwise σ_j^k is equal to 1. Note that if $\sigma_j^k = 1 \forall j = 1, \dots, m$, i.e., the worst case scenario, the right hand side of (6.15) represents the control input variations between different sampling instances. Using the continuity of $u(\cdot)$ together with Assumption (iv), it can be easily shown that in this case

$$|u_c(k) - u(k)|^2 \leq \sum_{j=1}^m L_u^2 T^2 ((r_j + 1)b_j - r_j b_j)^2 \quad (6.16)$$

with $r_j b_j < k < (r_j + 1)b_j$. From (6.16) we have $|u_c(k) - u(k)| \leq TL_u \sqrt{b_1^2 + \dots + b_m^2}$ which by the choice of T proves Lemma 6.1. \blacksquare

Lemma 6.2. *Consider the exact discrete-time model (6.12) and (6.9)-(6.11). Given any strictly positive real numbers $(D_1, D_3, \varepsilon_2)$, there exists $T_2 > 0$ such that for any fixed $T \in (0, T_2]$ there exists $h_2 \in (0, T]$ such that for all $h \in (0, h_2]$, $|x(0)| \leq D_1$, $|\hat{x}(0)| \leq D_1$, and $\|d\|_\infty \leq D_3$ the following holds: if $\max_{i \in \{0, 1, \dots, k\}} |x(i)| \leq D_1$ and $\max_{i \in \{0, 1, \dots, k\}} |\hat{x}(i)| \leq D_1$ for some $k \in \mathbb{Z}^+$, then for some $\lambda > 0$ the output of the single-rate plant (6.2)-(6.3) and the switch output y_c satisfies:*

$$|y_c(k) - y(k)| \leq T\varepsilon_2 + T\lambda(\|d\|_\infty + |u_c - u| + |u_c^- - u^-| + |e^-|) \quad (6.17)$$

Proof. Let $(D_1, D_3, \varepsilon_2) \in \mathbb{R}^+$ be given. By Assumption (iii), we know that $|u(k)| < D_u$ for some $D_u > 0$, and hence from Lemma 6.1 $|u_c(k)| < D_u + \varepsilon_1 = D_2$. Let $L_f, L_g > 0$ be the Lipschitz constants of the functions f and g on the compact sets Ω_f and $\Omega_g \subset \mathbb{R}^{n \times m \times q}$, respectively, such that $\mathcal{B}(D_1) \times \mathcal{B}(D_2) \times \mathcal{B}(D_3) \subset \Omega_f \cap \Omega_g$. Define $D_4 = L_g(D_1 + D_2 + D_3) + \varepsilon_2 + 1$ and assume that $T_{21}, h_{21} > 0$ and $\rho(\cdot) \in \mathcal{K}$ come from Assumption (ii) corresponding to $(\delta_1, \delta_2, \delta_3) = (D_1, D_2, D_3)$. Denoting $a_{max} = \max\{a_1, \dots, a_p\}$ choose $T_{22}, h_{22} > 0$ such that $L_g \rho(h_{22})(e^{L_f(a_{max}-1)T_{22}} - 1)/(e^{L_f T_{22}} - 1) < \varepsilon_2$. Also, let $T_{23} > 0$, $\lambda > 0$ be such that $L_g e^{L_f(a_{max}-1)T} \leq \lambda T$ for any $T \in (0, T_{23}]$. Finally, we define $T_2 = \min\{T_{21}, T_{22}, T_{23}\}$ and $h_2 = \min\{h_{21}, h_{22}\}$. Suppose $T \in (0, T_2]$, $h \in (0, h_2]$, $\max_{i \in \{0, 1, \dots, k\}} |x(i)| \leq D_1$ and $\max_{i \in \{0, 1, \dots, k\}} |\hat{x}(i)| \leq D_1$ for some $k \in \{0, 1, \dots\}$. First, we claim that the Lipschitz property of g yields $\max_{i \in \{0, 1, \dots, k\}} |y(i)| \leq L_g(D_1 + D_2 + D_3)$ for some $k \in \{0, 1, \dots\}$ and then $|y_c(k)| \leq D_4$ follows by induction. Now taking (6.3), (6.10) into account, we have that

$$|y_c(k) - y(k)|^2 = \sum_{i=1}^p \mu_i^k |g_i(F_{T,h}^a(\hat{x}^-, u_c^-, 0), u_c, 0) - g_i(F_T^e(x^-, u^-, d[k-1]), u, d)|^2 \quad (6.18)$$

where $\mu_i^k \in \{0, 1\}$ depends on the current sampling instant and varies between different outputs. Indeed, it is equal to 0 when the measurement is available at the i^{th} output channel otherwise it is equal to 1. Clearly, no matter what the sampling instant kT is, it

can be inferred that

$$\begin{aligned} |y_c(k) - y(k)| &\leq |g(F_{T,h}^a(\hat{x}^-, u_c^-, 0), u_c, 0) - g(F_T^e(x^-, u^-, d[k-1]), u, d)| \\ &\leq L_g |F_{T,h}^a(\hat{x}^-, u_c^-, 0) - F_T^e(x^-, u^-, d[k-1])| + L_g |u_c - u| + L_g \|d\|_\infty \end{aligned} \quad (6.19)$$

represents the worst upper bound for (6.18), where we have used the Lipschitz property of g along with $|d(k)| \leq \|d\|_\infty$. Let us assign a hypothetical periodic switch to a certain measurement channel y_i as

$$x_c^i(k) = \begin{cases} x(k), & \text{if } k = l_i a_i \quad \exists l_i \in \mathbb{Z}^+ \\ F_{T,h}^a(\hat{x}^-, u_c^-, 0), & \text{otherwise} \end{cases} \quad (6.20)$$

Now k can be considered in three different cases. If $k = l_i a_i$ for some $l_i \in \{0, 1, \dots\}$, then it is obvious that $|x_c^i(k) - x(k)| = 0$. If $k = l_i a_i + 1$ then using Assumption (ii), Gronwal-Bellman and triangle inequalities we get $|x_c^i(k) - x(k)| = |F_{T,h}^a(\hat{x}(l_i a_i), u_c(l_i a_i), 0) - F_T^e(x(l_i a_i), u(l_i a_i), d[l_i a_i])| \leq T\rho(h) + |F_T^e(\hat{x}(l_i a_i), u_c(l_i a_i), 0) - F_T^e(x(l_i a_i), u(l_i a_i), d[l_i a_i])| \leq T\rho(h) + (e^{L_f T} - 1)(\|d\|_\infty + |u_c(l_i a_i) - u(l_i a_i)| + |e^-|)$. Based on induction and geometric series formulas, it can be concluded that

$$\begin{aligned} |x_c^i(k) - x(k)| &\leq e^{L_f T} |x_c^{i-} - x^-| + (e^{L_f T} - 1)(\|d\|_\infty + |u_c^- - u^-| + |e^-|) \\ &\leq T\rho(h) \frac{e^{(k-l_i a_i)L_f T} - 1}{e^{L_f T} - 1} + (e^{(k-l_i a_i)L_f T} - 1)(\|d\|_\infty + |u_c^- - u^-| + |e^-|) \end{aligned} \quad (6.21)$$

holds for all $k \in \{l_i a_i + 2, \dots, (l_i + 1)a_i - 1\}$ as the third case. Inequality (6.21) and the definition of a_{max} leads to $|F_{T,h}^a(\hat{x}^-, u_c^-, 0) - F_T^e(x^-, u^-, d[k-1])| \leq T\rho(h)(e^{L_f(a_{max}-1)T} - 1)/(e^{L_f T} - 1) + (e^{L_f(a_{max}-1)T} - 1)(\|d\|_\infty + |u_c^- - u^-| + |e^-|)$ for the first term on right hand side of (6.19). Consequently, from (6.19) and the choice of T and h (6.17) is obtained, which completes the proof of Lemma 6.2. \blacksquare

Lemma 6.3. *Let $\alpha_1, \alpha_2, \alpha_3 \in \mathcal{K}_\infty$ and strictly positive real numbers (R, r, C_d) be such that $\|d\|_\infty \leq C_d$ and $\alpha_1(R) \geq r$. Assume that for $T_3 > 0$ and each fixed $T \in (0, T_3]$ there exists $h_3 \in (0, T]$ such that for any $h \in (0, h_3]$ there exists a function $V_{T,h} : \mathbb{R}^{2n} \rightarrow \mathbb{R}^+$ with the following properties: we have $\alpha_1(|e|) \leq V_{T,h}(x, \hat{x}) \leq \alpha_2(|e|)$ for all $x, \hat{x} \in \mathbb{R}^n$ and $V_{T,h}(x(k+1), \hat{x}(k+1)) - V_{T,h}(x, \hat{x}) \leq -\frac{T}{4}\alpha_3(|e|)$ holds for all $\|d\|_\infty \leq C_d$, $x, \hat{x} \in \mathbb{R}^n$ with $|x| \leq R, |\hat{x}| \leq R$ and $\max\{V_{T,h}(x(k+1), \hat{x}(k+1)), V_{T,h}(x, \hat{x})\} \geq r$. Then, for all*

$|e(0)| \leq \alpha_2^{-1} \circ \alpha_1(R)$, $\|d\|_\infty \leq C_d$ we get $|e(k)| \leq R \quad \forall k \in \mathbb{Z}^+$, and furthermore the estimation error satisfies

$$|e(k)| \leq \beta(|e(0)|, kT) + \alpha_1^{-1}(r) \quad (6.22)$$

Proof. The definitions of r and R imply $|e(0)| \leq \max\{\alpha_1^{-1} \circ V_{T,h}(e(0)), \alpha_1^{-1}(r)\}$. So either $V_{T,h}(x(1), \hat{x}(1)) \geq r$ which from the conditions of Lemma 3, implies $V_{T,h}(x(1), \hat{x}(1)) \leq V_{T,h}(x(0), \hat{x}(0))$ or else $V_{T,h}(x(1), \hat{x}(1)) \leq r$. In either case, $V_{T,h}(x(1), \hat{x}(1)) \leq \max\{V_{T,h}(x(0), \hat{x}(0)), r\}$. Thus $V_{T,h}(x, \hat{x}) \leq \max\{V_{T,h}(x(0), \hat{x}(0)), r\}$ follows by induction and $|e(k)| \leq R$ holds as well. Using an argument similar to the proof of Theorem 2 in [4] (see also [70, Theorem 1]), we can conclude that there exists a class- \mathcal{KL} function $\beta_1(\cdot, \cdot)$ such that $V_{T,h}(x, \hat{x}) \leq \max\{\beta_1(V_{T,h}(x(0), \hat{x}(0)), kT), r\}$. Then, (6.22) is obtained with $\beta(s, \tau) = \alpha_1^{-1}(\beta_1(\alpha_2(s), \tau))$. \blacksquare

Lemma 6.4. Consider the exact model (6.12) and the multirate observer (6.9)-(6.11). There exists $\hat{\gamma} \in \mathcal{K}_\infty$ such that for any strictly positive real numbers (C_e, C_d, v) with $C_e \geq \alpha_1^{-1}(\hat{\gamma}(C_d) + v)$, we can find $T_4 > 0$ such that for each $T \in (0, T_4]$ there exists $h_4 \in (0, T]$ such that for all $h \in (0, h_4]$, $|e(0)| \leq \alpha_2^{-1} \circ \alpha_1(C_e)$, $\|d\|_\infty \leq C_d$ and all $k \in \mathbb{Z}^+$, if $\max\{V_{T,h}(x(k+1), \hat{x}(k+1)), V_{T,h}(x, \hat{x})\} \geq \hat{\gamma}(\|d\|_\infty) + v$ we have

$$\Rightarrow V_{T,h}(x(k+1), \hat{x}(k+1)) - V_{T,h}(x, \hat{x}) \leq -\frac{T}{4}\alpha_3(|e|) \quad (6.23)$$

Proof. Let positive real numbers (C_e, C_d, v) be given. Assume that T_{41} comes from Lemma 6.1 corresponding to ε_1 such that $|u_c - u| \leq \varepsilon_1, |u_c^- - u^-| \leq \varepsilon_1$, and $\mu > 0$ is a number such that $L_\ell + 2e^{L_f(a_{max}-1)T} - 2 \leq \mu T$ for any $T \in (0, T_{42}]$. Let $(C_e, C_d, \varepsilon_2)$ generate T_{43}, h_{43} and λ as in Lemma 6.2. Define $\varepsilon_3 = \frac{1}{2}\alpha_2^{-1}(\frac{v}{2})$, $\varepsilon_4 = \alpha_2^{-1}(\frac{1}{2}\alpha_1(\varepsilon_3))$. Also, take $\varepsilon_1, \varepsilon_2, \lambda > 0$ such that $ML_\ell(2\lambda\varepsilon_1 + \varepsilon_2) \leq \frac{1}{4}\alpha_3(\varepsilon_4)$ where L_ℓ is the Lipschitz constant of $\ell_{T,h}(\cdot)$ according to Definition 6.2. Let positive real numbers $T_{44}, T_{45}, T_{46}, T_{47}$ and h_{44}, h_{45}, h_{46} be such that: $T_{44}(3\rho(h_{44}) + L_\ell(\varepsilon_2 + \lambda\|d\|_\infty) + (2L_\ell\lambda + \mu)\varepsilon_1 + L_\ell\lambda|e^-|) \leq \varepsilon_3$, $T_{45}(\frac{1}{4}\alpha_3(C_e) + \tilde{\gamma}(\|d\|_\infty) + M(3\rho(h_{45}) + L_\ell(\varepsilon_2 + \lambda\|d\|_\infty) + (2L_\ell\lambda + \mu)\varepsilon_1 + L_\ell\lambda|e^-|)) \leq \frac{v}{2}$, $M(3\rho(h_{46}) + \mu\varepsilon_1 + T_{46}L_\ell\lambda|e^-|) \leq \frac{1}{4}\alpha_3(\varepsilon_4)$, and $T_{47}\tilde{\gamma}(C_d) \leq \frac{1}{2}\alpha_1(\varepsilon_3)$. Define $\hat{\gamma}(s) = \alpha_2 \circ \alpha_3^{-1}(4(\tilde{\gamma}(s) + ML_\ell\lambda s))$. Taking $T_4 = \min\{T_{41}, T_{42}, T_{43}, T_{44}, T_{45}, T_{46}, T_{47}\}$ and $h_4 =$

$\min\{h_{43}, h_{44}, h_{45}, h_{46}\}$, we consider any $T \in (0, T_4]$, $h \in (0, h_4]$, $|e(0)| \leq \alpha_2^{-1} \circ \alpha_1(C_e)$ and $\|d\|_\infty \leq C_d$.

By Assumption (i) and Definition 6.3, for the single-rate observer (6.4), a Lyapunov function $V_{T,h}$ exists which satisfies $\Delta V = V_{T,h}(F_{T,h}^a(x, u, \bar{d}), F_{T,h}^a(\hat{x}, u, 0) + \ell(\hat{x}, y, u)) - V_{T,h}(x, \hat{x}) \leq -T\alpha_3(|e|) + T\tilde{\gamma}(\|d\|_\infty)$. Therefore, for the multirate setup we have

$$\begin{aligned} V_{T,h}(x^+, \hat{x}^+) - V_{T,h}(x, \hat{x}) &\leq -T\alpha_3(|e|) + T\tilde{\gamma}(\|d\|_\infty) + M|F_T^e(x, u_c, \bar{d}) - F_{T,h}^a(x, u, \bar{d})| \\ &\quad + M|E_{T,h}(e, x, u_c) + F_{T,h}^a(x, u_c, \bar{d}) - F_{T,h}^a(\hat{x}, u, 0) - \ell(\hat{x}, y, u)| \end{aligned} \quad (6.24)$$

in which $E_{T,h}$ comes from (6.14). Adding and subtracting $F_T^e(x, u, \bar{d})$ to the third and $F_T^e(\hat{x}, u_c, 0) + F_T^e(\hat{x}, u, 0)$ to the forth term on the right hand side of (6.24) and using the triangle inequalities, it can be written as

$$\begin{aligned} V_{T,h}(x^+, \hat{x}^+) - V_{T,h}(x, \hat{x}) &\leq -T\alpha_3(|e|) + T\tilde{\gamma}(\|d\|_\infty) \\ &\quad + M(|F_T^e(x, u, \bar{d}) - F_{T,h}^a(x, u, \bar{d})| + |F_T^e(x, u_c, \bar{d}) - F_T^e(x, u, \bar{d})| \\ &\quad + |F_{T,h}^a(\hat{x}, u_c, 0) - F_T^e(\hat{x}, u_c, 0)| + |F_T^e(\hat{x}, u_c, 0) - F_T^e(\hat{x}, u, 0)| \\ &\quad + |F_T^e(\hat{x}, u, 0) - F_{T,h}^a(\hat{x}, u, 0)| + |\ell(\hat{x}, y_c, u_c) - \ell(\hat{x}, y, u)|) \end{aligned} \quad (6.25)$$

Applying assumptions (ii)-(iii), the choice of T_{41} and T_{43}, h_{43} , and comparison lemma we see that $V_{T,h}(x^+, \hat{x}^+) - V_{T,h}(x, \hat{x}) \leq -T\alpha_3(|e|) + T\tilde{\gamma}(\|d\|_\infty) + M(3T\rho(h) + L_\ell T(\varepsilon_2 + \lambda\|d\|_\infty) + (2L_\ell T\lambda + 2e^{L_f(amax-1)T} - 2 + L_\ell)\varepsilon_1 + L_\ell T\lambda|e^-|)$. Now our choice of T_{42} with the positive number μ results in $V_{T,h}(x^+, \hat{x}^+) - V_{T,h}(x, \hat{x}) \leq -T\alpha_3(|e|) + T\tilde{\gamma}(\|d\|_\infty) + TM(3\rho(h) + L_\ell(\varepsilon_2 + \lambda\|d\|_\infty) + (2L_\ell\lambda + \mu)\varepsilon_1 + L_\ell\lambda|e^-|)$. Let us consider two possible scenarios. First assume that $V_{T,h}(x^+, \hat{x}^+) \geq \hat{\gamma}(\|d\|_\infty) + \frac{\nu}{2}$ and denote $\pi_1 := ML_\ell(2\lambda\varepsilon_1 + \varepsilon_2)$, $\pi_2 := M(3\rho(h) + \mu\varepsilon_1 + L_\ell\lambda|e^-|)$, and $\kappa(s) := \tilde{\gamma}(s) + ML_\ell\lambda s$, then we have

$$\begin{aligned} &V_{T,h}(x^+, \hat{x}^+) - V_{T,h}(x, \hat{x}) \\ &\leq -\frac{T}{4}\alpha_3(|e|) - \underbrace{\frac{T}{4}\alpha_3(\alpha_2^{-1}(V_{T,h}(x, \hat{x})))}_{(*)} + T\kappa(\|d\|_\infty) \\ &\quad - \underbrace{\frac{T}{4}\alpha_3(|e|) + T\pi_1}_{(**)} - \underbrace{\frac{T}{4}\alpha_3(|e|) + T\pi_2}_{(***)} \end{aligned} \quad (6.26)$$

It is easy to see that $V_{T,h}(x^+, \hat{x}^+) \geq \hat{\gamma}(\|d\|_\infty) + \frac{\nu}{2}$ indicates $\hat{\gamma}(\|d\|_\infty) + \frac{\nu}{2} \leq V_{T,h}(F_{T,h}^a(x, u, \bar{d}), F_{T,h}^a(\hat{x}, u, 0) + \ell(\hat{x}, y, u)) - V_{T,h}(x, \hat{x}) + |V_{T,h}(x^+, \hat{x}^+) - V_{T,h}(F_{T,h}^a(x, u, \bar{d}), F_{T,h}^a(\hat{x}, u, 0) +$

$\ell(\hat{x}, y, u)| + V_{T,h}(x, \hat{x}) \leq -T\alpha_3(|e|) + T\hat{\gamma}(\|d\|_\infty) + MT(3\rho(h) + L_\ell(\varepsilon_2 + \lambda\|d\|_\infty) + (2L_\ell\lambda + \mu)\varepsilon_1 + L_\ell\lambda|e^-|) + V_{T,h}(x, \hat{x})$. From the choice of T_{45} and h_{45} , we get $\hat{\gamma}(\|d\|_\infty) + \frac{v}{2} \leq \frac{v}{2} + V_{T,h}(x, \hat{x})$. Hence, it follows that: $V_{T,h}(x^+, \hat{x}^+) \geq \hat{\gamma}(\|d\|_\infty) + \frac{v}{2} \Rightarrow V_{T,h}(x, \hat{x}) \geq \hat{\gamma}(\|d\|_\infty)$. Based on the definition of $\hat{\gamma}(\cdot)$, Term $(*) \leq 0$ holds. Under the same supposition $V_{T,h}(x^+, \hat{x}^+) \geq \hat{\gamma}(\|d\|_\infty) + \frac{v}{2}$, we have $|x^+ - \hat{x}^+| \geq \alpha_2^{-1}(\frac{v}{2}) = 2\varepsilon_3$. Then our choice of T_{44} and h_{44} shows that $|F_{T,h}^a(x, u, \bar{d}) - F_{T,h}^a(\hat{x}, u, 0) - \ell(\hat{x}, y, u)| \geq |x^+ - \hat{x}^+| - |(x^+ - \hat{x}^+) - (F_{T,h}^a(x, u, \bar{d}) - F_{T,h}^a(\hat{x}, u, 0) - \ell(\hat{x}, y, u))| \geq 2\varepsilon_3 - \varepsilon_3 = \varepsilon_3$. Using our choice of T_{47} and (6.7), it yields that

$$\begin{aligned} \alpha_2(|e|) &\geq V_{T,h}(F_{T,h}^a(x, u, \bar{d}), F_{T,h}^a(\hat{x}, u, 0) + \ell(\hat{x}, y, u)) - T\hat{\gamma}(C_d) \\ &\geq \alpha_1(|F_{T,h}^a(x, u, \bar{d}) - F_{T,h}^a(\hat{x}, u, 0) - \ell(\hat{x}, y, u)|) - T\hat{\gamma}(C_d) \\ &\geq \alpha_1(\varepsilon_3) - \frac{1}{2}\alpha_1(\varepsilon_3) = \frac{1}{2}\alpha_1(\varepsilon_3) \end{aligned} \quad (6.27)$$

which implies $|e| \geq \alpha_2^{-1}(\frac{1}{2}\alpha_1(\varepsilon_3)) = \varepsilon_4 \geq \alpha_3^{-1}(4\pi_1)$ and then Term $(**) \leq 0$. Moreover, from the choice of T_{45} and h_{45} , we have $|e| \geq \varepsilon_4 \Rightarrow -\frac{T}{4}\alpha_3(|e|) + T\pi_2 \leq 0$. Consequently, under $V_{T,h}(x^+, \hat{x}^+) \geq \hat{\gamma}(\|d\|_\infty) + \frac{v}{2}$, it is derived that $V_{T,h}(x^+, \hat{x}^+) - V_{T,h}(x, \hat{x}) \leq -\frac{T}{4}\alpha_3(|e(k)|)$. Now Suppose that $V_{T,h}(x^+, \hat{x}^+) \leq \hat{\gamma}(\|d\|_\infty) + \frac{v}{2}$ and $V_{T,h}(x, \hat{x}) \leq \hat{\gamma}(\|d\|_\infty) + v$. From our choice of T_{45} and h_{45} , it yields that: $V_{T,h}(x^+, \hat{x}^+) - V_{T,h}(x, \hat{x}) \leq \hat{\gamma}(\|d\|_\infty) + \frac{v}{2} - V_{T,h}(x, \hat{x}) + \frac{v}{2} - \frac{v}{2} \leq \hat{\gamma}(\|d\|_\infty) + v - V_{T,h}(x, \hat{x}) - \frac{v}{2} \leq -\frac{v}{2} \leq -\frac{T}{4}\alpha_3(|e|)$. ■

Proof of Theorem 1. With these prerequisites, we can finalize our proof. Let all the conditions in Theorem 6.1 hold and $\hat{\gamma} \in \mathcal{K}_\infty$ come from Lemma 6.4. Choose (C_e, C_d, v) as: $C_d := \delta_d$, $\nu > 0$ is such that $\sup_{s \in [0, \delta_d]} [\alpha_1^{-1}(\hat{\gamma}(s) + v) - \alpha_1^{-1}(\hat{\gamma}(s))] \leq \nu$, $C_e := \max\{\alpha_1^{-1}(\hat{\gamma}(\delta_d) + v), \alpha_1^{-1} \circ \alpha_2(\delta_e)\}$. These choices imply that $C_e \geq \alpha_1^{-1}(\hat{\gamma}(C_d) + v)$ and $|e(0)| \leq \alpha_2^{-1} \circ \alpha_1(C_e)$. Assume that (C_e, C_d, v) generate $T^* > 0$, $h^* > 0$ as in Lemma 6.4 such that (6.23) holds. Define $R = C_e$ and $r = \hat{\gamma}(\|d\|_\infty) + v$, then we have $\alpha_1(R) \geq r$. With the definition of (R, r) , all the conditions of Lemma 6.3 are satisfied. Therefore, for all $h \in (0, h^*]$, $|e(0)| \leq \delta_e$ and $\|d\|_\infty \leq \delta_d$, we obtain

$$\begin{aligned} |e(k)| &\leq \beta(|e(0)|, kT) + \alpha_1^{-1}(\hat{\gamma}(\|d\|_\infty) + v) \\ &\leq \beta(|e(0)|, kT) + \gamma(\|d\|_\infty) + \nu \end{aligned} \quad (6.28)$$

where $\gamma(s) := \alpha_1^{-1} \circ \hat{\gamma}(s)$. This concludes the proof of the theorem. ■

6.3 Simulation Examples

6.3.1 PVTOL

To illustrate the features of the multi rate observer, consider the planar vertical takeoff and landing (PVTOL) aircraft without velocity measurements. This is an interesting example in the area of visual-based control of autonomous vehicles which usually demands input and measurement channels with different sampling rates. The simplified continuous-time model of the PVTOL aircraft is described as [116]

$$\begin{cases} \dot{x}_1 = x_2 \\ \dot{x}_2 = -\frac{u_1}{m} \sin(x_5) + \epsilon \frac{u_2}{m} \cos(x_5) + d_s \\ \dot{x}_3 = x_4 \\ \dot{x}_4 = \frac{u_1}{m} \cos(x_5) + \epsilon \frac{u_2}{m} \sin(x_5) - g + d_s \\ \dot{x}_5 = x_6 \\ \dot{x}_6 = \frac{u_2}{J} + d_s \end{cases} \quad (6.29)$$

$$y = \begin{bmatrix} x_1 & x_3 & x_5 \end{bmatrix}^\top + d_m \quad (6.30)$$

where x_1, x_3, x_5 stand for the horizontal and vertical coordinates and roll angle, x_2, x_4, x_6 are the horizontal, vertical and angular velocities of the aircraft, the control variables u_1, u_2 correspond to the thrust and the rolling moment, respectively. The disturbance signal d_s follows a uniform random distribution and the output y is corrupted by the additive white noise vector d_m . Also, m is the mass, J the moment of inertia, g the gravitational acceleration and ϵ represents a small positive coefficient giving the coupling between the rolling moment and the lateral acceleration of the aircraft. We assume that the velocities are not available in the measurement and only the coordinates and the roll angle can be measured.

We construct the approximate discrete-time model $F_{T,h}^a$ of (6.29) via a refined Euler model as follows

$$\begin{cases} f_h(i, x, u, d) := x + hf(x, u, 0) + \int_{iT+ih}^{(i+1)T+ih} d_s(\tau) d\tau, \\ f_h^{i+1}(x, u, d) := f_h(i+1, f_h^i, u, d), \\ F_{T,h}^a(x(k), u(k), d[k]) := f_h^N(x, u, d) \end{cases} \quad (6.31)$$

in which $f_h^1 := x + hf(x, u, 0) + \int_{kT}^{kT+h} d_s(\tau) d\tau$ and $N = T/h$. Note that here $d = [d_s \ d_m^\top]^\top$ is the disturbance vector although the state equation is only affected by d_s . The consistency of our approximate scheme can be simply verified in a way analogous to the arguments of [20, Lemma 1] and [19, Example]. Inspired by [117], we propose the following Luenberger-type for the sampled-data observer (6.4)

$$\begin{aligned} \hat{x}(k+1) &= F_{T,h}^a(\hat{x}(k), u(k), 0) \\ &+ \begin{bmatrix} l_{11} & l_{12} & 0 & 0 & 0 & 0 \\ 0 & 0 & l_{23} & l_{24} & 0 & 0 \\ 0 & 0 & 0 & 0 & l_{35} & l_{36} \end{bmatrix}^\top \begin{bmatrix} y_1 - \hat{x}_1 \\ y_2 - \hat{x}_3 \\ y_3 - \hat{x}_5 \end{bmatrix} \end{aligned} \quad (6.32)$$

Taking $V_{T,h} = (x - \hat{x})^\top(x - \hat{x})$, it is not difficult to show that (6.32) is a Lyapunov-ISS observer for $F_{T,h}^a$. Moreover, since it possesses a Luenberger-like structure we can easily verify the uniformly locally Lipschitz condition in Assumption (iii).

We now assume that the PVTOL is placed in a sampled-data setup with various sampling rates. More precisely, the sampling periods of the input and output channels are set to $\{0.2, 0.5\}$ *sec* and $\{3, 1.5, 0.3\}$ *sec*, respectively. The discrete-time observer (6.32) was put into the multirate configuration of (6.11)-(6.13) and we studied the implementation of the single-rate observer (6.32) as well as our proposed multirate observer in presence of disturbance inputs. For numerical simulations, the systems parameters are chosen as follows: $m = 0.5$ *kg*, $J = 0.1$ *Nm²*, $g = 9.81$ *m/s²*, $\epsilon = 0.8$ *Nm*. The initial conditions are: $x(0) = [5 \ 0.2 \ 5 \ 0.2 \ 0.2 \ 0.2]^\top$, $\hat{x}(0) = [3 \ 0 \ 3 \ 0 \ 0.1 \ 0]^\top$. The input signals are $u_1 = \sin t$ and $u_2 = 0.1 \sin 2t$, which satisfy Assumption (iv) considering their sampling rates. Also, the basic sampling period and the numerical integration period are $T = 0.1$ and $h = 0.001$, respectively. Finally, we pick the observer gains $l_{11} = 1$, $l_{12} = 0.5$, $l_{23} = 1$, $l_{24} = 0.25$, $l_{35} = 1$, $l_{36} = 0.5$ and the observer sampling rate $\tau_o = T = 0.1$ for both the single-rate and multirate implementations.

Figure 6.2 displays the simulation results. As can be seen in the figure, the single-rate observer fails to track the actual states. On the other hand, the proposed multirate observer performs successfully and presents sampled-data estimates that are almost identical to the continuous-time states. This fact can also be verified using the norm of the estimation errors depicted in Figure 6.3. Our simulation results were examined for different values of τ_o as well as h . Roughly speaking, increasing the value of τ_o or h has destructive

effects on the performance of our proposed multirate scheme.

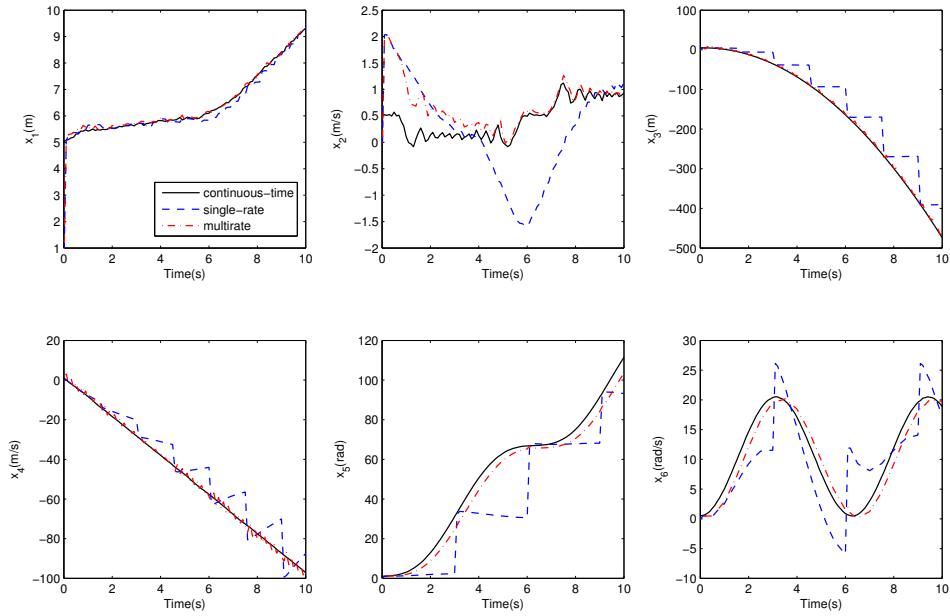


Figure 6.2: Sampled-data state estimation of PVTOL with different sampling rates using single-rate and multirate observers

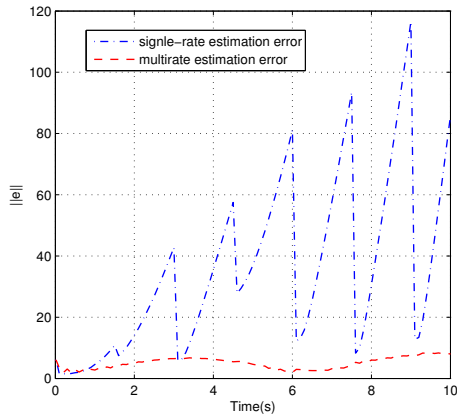


Figure 6.3: Norm of the estimation error for single-rate and multirate observers

6.3.2 A One-Sided Lipschitz System

The purpose of this section is to illustrate the applicability of Theorems 5.3 and 6.1 for single-rate and multirate systems. Consider a nonlinear dynamical system borrowed

from [61] in the form of (5.23) with

$$A = \begin{bmatrix} 0 & 100 & & \\ -48.6 & -1.26 & 48.6 & 0 \\ 0 & 0 & 0 & 10 \\ 1.95 & 0 & -1.95 & -0.01 \end{bmatrix}, \quad C = \begin{bmatrix} 1 & 0 \\ 0 & 1 \\ 0 & 0 \\ 0 & 0 \end{bmatrix}^\top,$$

$$\Phi(x, u) = \begin{bmatrix} 0 & 21.6u & 0 & -x_4^{\frac{1}{3}} \end{bmatrix}^\top,$$

$$D_1 = \begin{bmatrix} 0.5 & -1 & 1 & 0.5 \end{bmatrix}^\top, \quad D_2 = \begin{bmatrix} -0.5 & 0.5 \end{bmatrix}^\top,$$

$u = \sin(t)$, and the disturbance input $d(t)$ follows a uniform random distribution. As discussed in [61], Φ is not a Lipschitz nonlinearity, but it holds the one-sided Lipschitz condition (2.26) with $\mu = 0$. Moreover, using the mean value theorem it is easy to confirm that Φ is quadratically inner bounded for $\eta = 0$, $\theta \geq \frac{1}{9}\xi_0^{-4/3}$ where $\xi_0 \in (\min(x_4, \hat{x}_4), \max(x_4, \hat{x}_4))$.

We now study sampled-data observer design under two different scenarios. First a single-rate case is treated. If we choose $T = 0.2$, $N = 100$ and $\theta = 1$, then solving the feasibility problem of Theorem 5.3 yields

$$L = \begin{bmatrix} -0.1135 & -9.3931 & -0.5555 & 0.0580 \\ 0.3362 & 1.9142 & 0.3240 & 0.0262 \end{bmatrix}^\top$$

Figures 6.4-6.5 display the simulation results, where the initial conditions are set to $x(0) = [2 \ 0 \ 2 \ 2]^\top$ and $\hat{x}(0) = [0 \ 1 \ -1 \ 1]^\top$. Evidently, the effect of state trajectory estimation is satisfactory and the residual error can be reduced either by decreasing T or increasing N for a fixed value of T . However, it cannot be reduced arbitrarily and always an estimation error remains. This fact coincides with the semi-global practical ISS in Definitions 5.1 and 6.2.

Second a more practical situation (multirate case) is considered. The sampling periods of the input and output channels are chosen as $\{0.4\}$ and $\{3, 1.5\}$ seconds, respectively. Clearly, the sampling rate of the sinusoidal input signal satisfies the conditions of Theorem 6.1. Picking $T = 0.1$ and $h = 100$, we implemented both the single-rate observer (5.29), which incorrectly assumes all the signals have the same sampling rate, and the multirate observer (6.9)-(6.11). It can be seen in Figure 6.6, while the single-rate observer fails to track the actual states, the proposed multirate observer performs successfully and presents sampled-data estimates that are almost identical to the actual continuous-time states.

Similar to single-rate case, our simulation results were also examined for different values of T and h . Roughly speaking, increasing the value of T or h has destructive effects on the performance of the proposed multirate scheme.

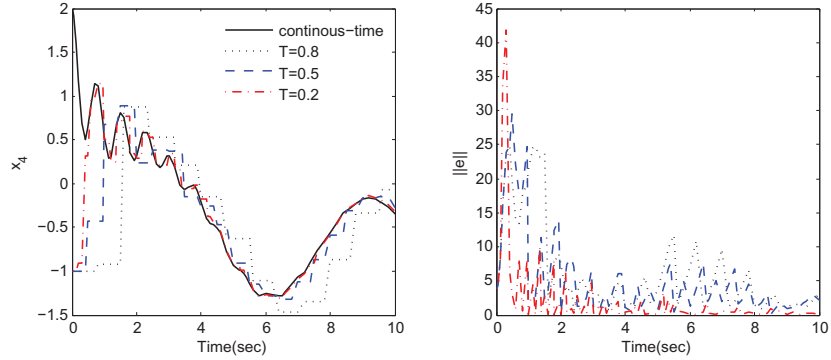


Figure 6.4: Estimate of x_4 and norm of the observer error for different values of T under uniformly random disturbance

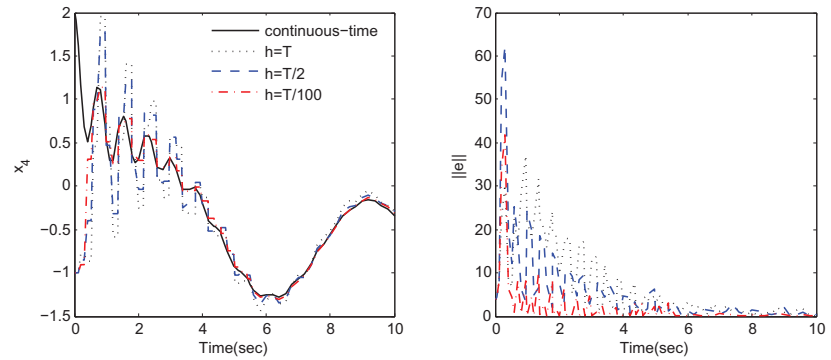


Figure 6.5: Estimate of x_4 and norm of the observer error for a fixed T and different values of h under uniformly random disturbance

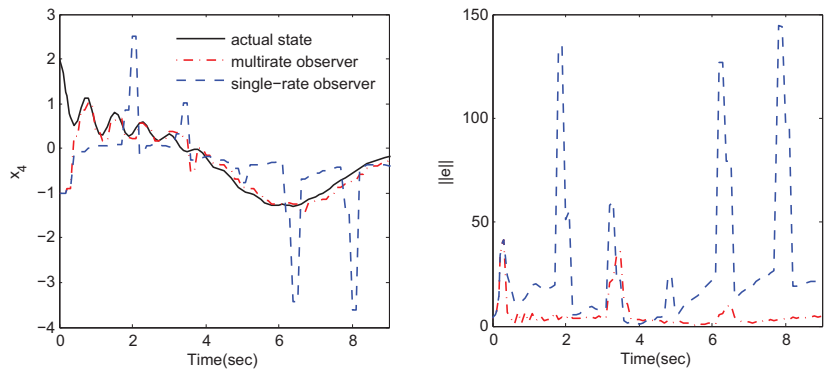


Figure 6.6: Estimate of x_4 and norm of the observer error for single-rate and multirate observer under uniformly random disturbance and multirate sampling

6.4 Summary

In this chapter a general multirate nonlinear observer is developed under the effect of disturbances and the convergence properties of the error dynamics is analyzed in terms of input-to-state stability (ISS) theory. The proposed estimation method consists of an ISS single-rate observer working at a certain sampling time supplied by artificial fast-rate sample and hold switches which reconstruct the missing outputs and inputs between sampling instances. We also emphasize that although our primary goal in this chapter is to study observer convergence properties under multirate sampling independently of the feedback design task, the proposed approach is, of course, applicable in observer-based multirate controller and fault detection plans as future works.

Chapter 7

Multirate Output Feedback NCS via Discrete-Time Approximation

In this chapter¹ we study output feedback sampled-data stabilization of nonlinear multirate NCSs in the face of disturbance inputs. Inspired by the theory of robust control, network constraints in both the forward and backward paths are represented via signal-to-error ratio (SER) and received signal-to-error ratio (R-SER) models employed by [97, 98], which introduce multiplicative uncertainties to the plant. A major benefit of this modelling is that it captures different unknown transmission errors as well as possible sensors and actuators inaccuracy. Also, it does not require a priori information about the probability distributions of network delays. Considering a general description of nonlinear sampled-data systems, we propose a multirate dynamic output feedback law that is composed of a periodic switch and a single-rate sampled-data controller. The main idea is to reconstruct the intersample outputs between measured samples using an approximate discrete-time model of the plant together with the system output mapping by means of the periodic switch (fast-rate sampler) and then fed the switch output to the single-rate controller being updated at the base sampling period of the plant. It is shown that if the nominal NCS with the single-rate output feedback satisfies a certain discrete-time dissipation inequality (see [118]), then under some standard assumptions the uncertain multirate NCS with the proposed controller is also dissipative with respect to similar supply rate deteriorated by

¹The results of this chapter have been submitted for publication in the article: H. Beikzadeh and H. J. Marquez, “Multirate Output Feedback Control of Nonlinear Networked Control Systems,” Submitted to *IEEE Transactions on Automatic Control*, Jan. 2014.

some additive terms, in spite of channels uncertainties and disturbances. The effect of these terms may be degraded by picking the sampling period or the integration period of the discrete-time approximation small enough. Preservation of dissipativity using the state feedback control and emulation method has been investigated for single-rate and multirate nonlinear plants in [9] and [20], respectively. Therefore, this work generalizes the results of [20] to obtain a framework for output feedback stabilization of multirate nonlinear sampled-data systems via discrete-time design and in presence of a communication network.

As a general feature covering a wide range of important system theoretic properties, including stability, input-to-state stability (ISS), passivity, L_p -stability, etc., dissipativity and the proposed framework is applied to analyze the stability of the multirate NCS. First for a disturbance driven system, input-to-state stability of the proposed multirate NCS is guaranteed, in a simiglobal practical sense. Then, explicit conditions on channels sampling rates and uncertainties are provided under which the disturbance free system with the network-based output feedback multirate controller is locally exponentially stable. Unlike the discrete-time single-rate framework in [91], we do not assume that all the state variables are measurable. The validity of our results for both the SER and R-SER channel models along with the potential ability of the R-SER model to handle larger uncertainties has been pointed out throughout the chapter. Comparing with the literature on multirate nonlinear sampled-data systems, our approach is not restricted to either the high gain observers used in [22] or to the dual-rate case studied in [19, 21] and covers the “low measurement rate” case addressed in [17–21] as a special case.

The outline of this chapter is as follows. In Section 7.1, after presenting a model for the multirate nonlinear NCS under network constrains and some preliminary backgrounds the problem is formulated. Section 7.2 contains the main contribution of the chapter by developing an output feedback multirate sampled-data control scheme and analyzing the dissipativity of the uncertain NCS. Input-to-state stability (ISS) and exponential stability of the multirate NCS is ensured using the proposed output feedback structure in Section 7.3. The results are illustrated via simulation examples in Section 7.4. Finally, concluding remarks are given in Section 7.5.

7.1 Multirate Nonlinear NCS: Modelling and Problem Setting

Consider the output feedback multirate NCS displayed in Figure 7.1. It consists of a continuous-time nonlinear plant described by

$$G : \begin{cases} \dot{x}(t) = f(x(t), u(t), d(t)) \\ y(t) = g(x(t), d(t)) \end{cases} \quad (7.1)$$

where $x(t) \in \mathbb{R}^n$ is the state, $u(t) \in \mathbb{R}^m$ the control input, $y(t) \in \mathbb{R}^p$ the measured output, $d(t) \in \mathbb{R}^q$ the exogenous disturbance, and f and g are locally Lipschitz nonlinear functions vanishing at the origin. The physical plant is connected to ideal sampler and (zero-order) hold devices of different sampling rates. Precisely, the p channels of y are sampled periodically at sampling instances $a_i T$, $a_i \in \mathbb{Z}^+ \forall i = 1, \dots, p$ and the m channels of u are kept constant with periods $b_j T$, $b_j \in \mathbb{Z}^+ \forall j = 1, \dots, m$, where a_i and b_j are relatively prime. Assume that the sample and hold circuits are synchronized at $t = 0$ and $T > 0$ is a real number referred to as the *base sampling period* of the system. Finally, the feedback loop is closed via a communication network and a sampled-data output feedback controller K to be designed.

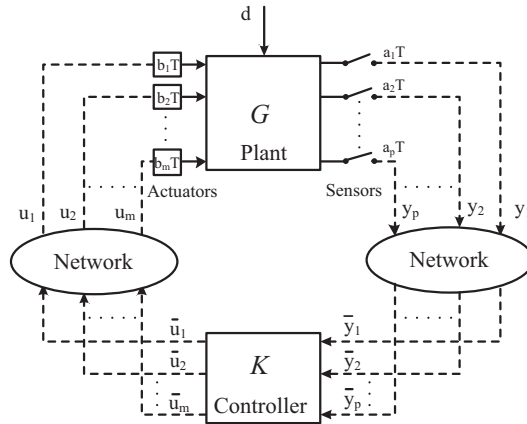


Figure 7.1: Structure of the multirate NCS with output feedback controller

We assume that in Figure 7.1 each element of the measured output $y_i(ka_i T)$ and the control signal $u_j(kb_j T)$ is separately transmitted through an independent channel of the network to the controller and actuators, respectively. This corresponds to parallel

transmission strategy where the sensors and actuators are located separately from each other and from the controller. All the communications between the controller and the plant in both the forward and backward paths are subject to network-induced constraints such as transmission delays, data packet dropout and signal quantization. To model the effect of these constraints mathematically, we adopt the idea of signal-to-error ratio (SER) and received signal-to-error ratio (R-SER) proposed by [98] (see Figure 7.2). Basically, our results are based on the SER model and will be extended to the R-SER case in an analogous fashion (see also Remark 7.1). Each channel is modelled by an ideal transmission channel together with an additive norm-bounded uncertainty, as depicted in Figure 7.2a. The uncertainties Δ_{u_j} , Δ_{y_i} can be nonlinear, time varying and dynamic systems. Our only assumption is that for all $i = 1, \dots, p$ and $j = 1, \dots, m$ $\Delta_{y_i}(0) = 0$, $\Delta_{u_j}(0) = 0$ and their ℓ_2 induced norm admit some bounds

$$\|\Delta_{u_j}\|_\infty = \sup_{\bar{u}_j \in \ell_2} \frac{\|e_{u_j}\|_2}{\|\bar{u}_j\|_2} \leq \delta_{u_j}, \quad \|\Delta_{y_i}\|_\infty = \sup_{y_i \in \ell_2} \frac{\|e_{y_i}\|_2}{\|y_i\|_2} \leq \delta_{y_i} \quad (7.2)$$

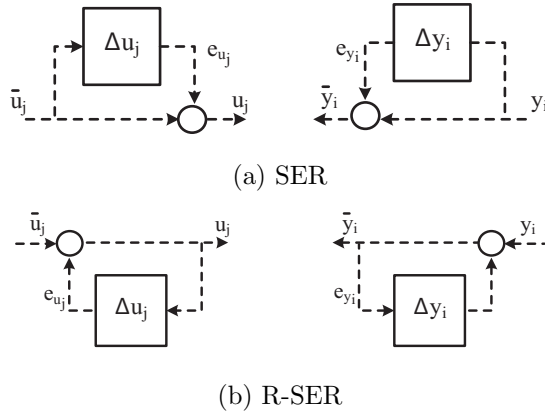


Figure 7.2: Channels model

As elaborated in [97], this channel model, motivated by the logarithmic quantization of [119], introduces a multiplicative uncertainty to the plant which can be used to capture unknown transmission errors as well as possible sensors and actuators inaccuracy. Moreover, the inverse norm bounds $\delta_{u_j}^{-1}$, $\delta_{y_i}^{-1}$ can be regarded as the worst case signal-to-error ratios.

Remark 7.1. *In the R-SER model shown in Figure 7.2b, each channel is the combination of an ideal transmission and a feedback norm-bounded uncertainty which introduces a*

relative uncertainty instead of a multiplicative uncertainty. Thus, the two channel models imply different physical meanings (see [97] for more details).

The following example shows how the effect of packet losses and network delays are covered by the SER channel model.

Example 7.1. Let the i^{th} plant output at the updating instant $t_k^i = ka_iT$ experience a time-varying bounded delay τ_k^i passing through the network, i.e., $0 \leq \tau_k^i \leq \bar{\tau}^i$ that is a natural assumption in this context. Also, there exists ℓ_k^i packet dropout at time t_k^i owing to link failure. The number of consecutive data losses is assumed to be bounded, i.e., $0 \leq \ell_k^i \leq \bar{\ell}^i$. Combining the effect of communication delay and packet dropout, the i^{th} input of the output feedback controller can be given as

$$\bar{y}_i(t_k^i) = y_i(t_k^i - (\lceil \frac{\tau_k^i}{a_i T} \rceil + \ell_k^i)a_i T) = (1 + \Delta_{y_i})y_i(t_k^i) \quad (7.3)$$

which holds the form of the SER model. Note that $\lceil \cdot \rceil$ represents the ceiling function (smallest integer larger than or equal to the argument) and the H_∞ norm of the uncertainty Δ_{y_i} depends on the values of $\bar{\tau}^i, \bar{\ell}^i$

Before proceeding to stabilize the multirate NCS, let us consider the single-rate system analogous to G in Figure 7.1 connected to the nominal network without uncertainties, i.e., $\bar{u} = u, \bar{y} = y$. Then, the exact discrete-time model is given by

$$x(k+1) = x(k) + \int_{kT}^{(k+1)T} f(x(\tau), u(k), d(\tau))d\tau := F_T^c(x[k], u(k), d[k]) \quad (7.4)$$

$$y(k) = g(x(k), d(k)). \quad (7.5)$$

in which T is the sampling period and the control input $u(k)$ is transmitted over the network and kept constant during the interval $[kT, (k+1)T)$. In general, it is impossible to compute explicitly the exact discrete-time model (7.4)-(7.5) even for the nominal sampled-data signals. Instead, we deal with a family of approximate discrete-time plant model (using a discretization method) of the form $x(k+1) = F_{T,h}^a(x(k), u(k), d[k])$, where the refining parameter h can be interpreted as the *integration period* of the numerical schemes used to generate the approximate model (see e.g., [13, 18]). In the sequel, we denote $d[k]$ (whenever needed) as d_f instead of \bar{d} to avoid confusion with uncertainties.

Next, we assume $u(k)$ is obtained via a dynamic output feedback controller expressed as

$$\xi(k+1) = Z_{T,h}(\xi(k), y(k)) \quad (7.6)$$

$$u(k) = U_{T,h}(\xi(k), y(k)) \quad (7.7)$$

where $\xi \in \mathbb{R}^s$ stands for the controller state, and $Z_{T,h}, U_{T,h}$ are zero at zero. Throughout the chapter the mismatch of the exact and approximate models is measured via the consistency properties explained in Chapter 2.

Definition 7.1. *The approximate model $F_{T,h}^a$ is said to be one step consistent with F_T^e , if there exist $\rho(\cdot) \in \mathcal{K}$ and $T^* > 0$ such that given any strictly positive numbers $(\sigma_1, \sigma_2, \sigma_3)$ and each fixed $T \in (0, T^*]$, there exists $h^* \in (0, T]$ such that*

$$|F_T^e(x, u, d_f) - F_{T,h}^a(x, u, d_f)| \leq T\rho(h) \quad (7.8)$$

for all $x \in B(\sigma_1)$, $u \in B(\sigma_2)$, $\|d\|_\infty \leq \sigma_3$ and $h \in (0, h^*]$. Moreover, $F_{T,h}^a$ is said to be multi-step consistent with F_T^e if given $L, \eta > 0$ there exist $\alpha : \mathbb{R}^+ \times \mathbb{R}^+ \rightarrow \mathbb{R}^+$ and $T^{**} > 0$ such that for each fixed $T \in (0, T^{**}]$, we can find $h^{**} \in (0, T]$ such that

$$\{x_1, x_2 \in B(\sigma_1), |x_1 - x_2| \leq \varsigma\} \Rightarrow |F_T^e(x_1, u, d_f) - F_{T,h}^a(x_2, u, d_f)| \leq T\alpha(\varsigma, h) \quad (7.9)$$

for all $u \in B(\sigma_2)$, $\|d\|_\infty \leq \sigma_3$ and $h \in (0, h^{**}]$, where

$$k \leq L/h \Rightarrow \alpha^k(0, h) := \overbrace{\alpha(\dots \alpha(\alpha(0, h), h) \dots, h)}^k \leq \eta \quad (7.10)$$

It is shown by simple examples in [4] that, in general, one-step and multi-step consistency do not imply each other. While the one-step consistency is a measure of the closeness of solutions starting from the same initial condition over one step, the multi-step consistency can be used to evaluate the closeness of solutions starting from different initial conditions over multiple steps.

Remark 7.2. *The notion of one-step consistency can be checked using verifiable sufficient conditions provided in [4, 13] (the multirate version can be found in [17, 20] based on the Euler approximation without knowing the exact model F_T^e). Besides, the multi-step consistency is guaranteed by one-step consistency plus a type of Lipschitz condition on either the exact or the approximate discrete-time model (see [4, Lemma 3]).*

The problem addressed in the chapter can now be formulated as follows. Given a non-linear plant and a single-rate output-feedback controller designed for nominal transmitted signals, we aim to design a multirate controller using an approximate discrete-time model such that the resulting sampled-data NCS guarantees certain stability properties in the face of channels uncertainties and for the unknown exact discrete-time plant model.

7.2 Multirate Networked Output-Feedback Stabilization

7.2.1 Controller Design

In this section, we propose a multirate sampled-data scheme to stabilize the NCS introduced in the previous section. The main idea is to design the single-rate controller (7.6)-(7.7) holding a certain stability property for nominal network channels and exploit it in a multirate structure that preserves similar feature in a specific sense for real channels with uncertainties. Precisely, our multirate nonlinear controller (K in Figure 7.1) consists of a fast-rate output feedback law based on (7.6)-(7.7) as below

$$\xi(k+1) = Z_{T,h}(\xi(k), y_c(k)) \quad (7.11)$$

$$\bar{u}(k) = U_{T,h}(\xi(k), y_c(k)) \quad (7.12)$$

where T is chosen as the controller sampling time for the sake of simplicity (see Remark 7.3), $\bar{u} = [\bar{u}_1 \dots \bar{u}_m]'$ is the controller output, and $y_c = [y_{c_1} \dots y_{c_p}]'$ is the output of a periodic switch defined by

$$\mathcal{S}_f : y_{c_i}(k) = \begin{cases} \bar{y}_i(k), & \text{if } k = l_i a_i \quad \exists l_i \in \mathbb{Z}^+ \\ g_i(x_c, 0), & \text{otherwise} \end{cases} \quad (7.13)$$

with x_c approximated by $F_{T,h}^a$ with zero disturbance, i.e.,

$$x_c(k+1) = F_{T,h}^a(x_c, \bar{u}, 0) \quad (7.14)$$

Figure 7.3 shows this multirate sampled-data configuration. It can be seen that the i^{th} component of the modified output vector y_c connects to the actual measurement \bar{y}_i when it is available, otherwise it uses the output mapping function g and the approximate model $F_{T,h}^a$ to compensate for unmeasured intersample outputs. The single-rate control signal \bar{u} is transmitted through the multi-channel network to obtain the multirate control input u that is delivered to various hold devices with different sampling rates in Figure 7.1.

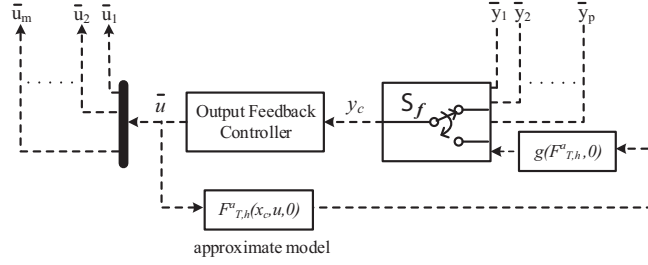


Figure 7.3: Output feedback multirate controller

Remark 7.3. *It is a natural supposition to pick T as the sampling period of the controller (7.11)-(7.12). However, in some applications one may desire a different sampling rate. Our multirate structure can be easily reformulated to cope with this case.*

Remark 7.4. *Alternatively, we can generate the multirate control law by putting the hold devices of Figure 7.1 right after the single-rate signal \bar{u} in Figure 7.3. It can be shown that no matter what structure is used, our results obtained thereafter are always valid.*

7.2.2 Dissipativity of the Multirate NCS

Now we investigate stability of the proposed multirate NCS under network constraints. As spelled out before, the first step is to assume a certain property is ensured by the single-rate controller (7.6)-(7.7) or equivalently (7.11)-(7.12). For this purpose, we employ the theory of dissipativity to characterize the properties of the closed-loop sampled-data system. The following definition is inspired from [118, Definition 2.1] which was presented for discrete-time dissipative systems.

Definition 7.2. *The discrete-time model*

$$\begin{aligned} x(k+1) &= \mathcal{F}_T(x, u, d_f) \\ y(k) &= g(x, d) \end{aligned} \tag{7.15}$$

with the control input $u(k)$ given by (7.6)-(7.7) is said to be dissipative with respect to the supply rate $w(x(k), \xi(k), d(k))$ if there exists $V_{T,h} : \mathbb{R}^{n+s} \rightarrow \mathbb{R}^+$ with $V_{T,h}(0, 0) = 0$, called the storage function, such that given any strictly positive numbers $(\sigma_1, \sigma_2, \sigma_3)$ there exists $T^ > 0$ such that for each fixed $T \in (0, T^*]$ there exists $h^* \in (0, T]$ such that*

$$\frac{V_{T,h}(\mathcal{F}_T(x, U_{T,h}(\xi, y), d_f), Z_{T,h}(\xi, y)) - V_{T,h}(x, \xi)}{T} \leq w(x, \xi, d) \tag{7.16}$$

for all $x \in B(\sigma_1)$, $u \in B(\sigma_2)$, $\|d\|_\infty \leq \sigma_3$ and $h \in (0, h^]$.*

Remark 7.5. Basically, the supply rate is expressed as a function of input and output (or a penalty variable in some applications), i.e., $w(d, u, y)$, that for the case of closed-loop system with state-dependent output can be taken as used in (7.16) (see (V, w) -dissipativity in [9]).

In the sequel, given a discrete-time model \mathcal{F} (exact or approximate), we use a bar, i.e., $\bar{\mathcal{F}}$, to distinguish the uncertain model concerning with the network constraints from the nominal model \mathcal{F} . Also for notational convenience, we denote $\tilde{x} := [x' \ \xi']'$, $\chi := [\xi' \ y']'$. Let us make the following assumptions.

Assumption 7.1. The approximate discrete-time model $F_{T,h}^a$ together with the single-rate controller (7.6)-(7.7) is dissipative according to Definition 7.2.

Assumption 7.2. The associated storage function $V_{T,h}$ is locally Lipschitz, i.e., for all $\tilde{x}_1, \tilde{x}_2 \in B(\sigma_1)$, there exist $L_v > 0$ and $T^* > 0$ such that for each fixed $T \in (0, T^*]$ there exists $h^* \in (0, T]$ such that $|V_{T,h}(\tilde{x}_1) - V_{T,h}(\tilde{x}_2)| \leq L_v |\tilde{x}_1 - \tilde{x}_2|$ for all $h \in (0, h^*]$.

Assumption 7.3. $F_{T,h}^a$ is one-step and also multi-step consistent with the exact discrete-time model F_T^e based on Definition 7.2.

Assumption 7.4. The controller (7.6)-(7.7) is uniformly locally Lipschitz, i.e., for any $\sigma_1 > 0$ there exist $L_z, L_u > 0$ and $T^* > 0$ such that for each fixed $T \in (0, T^*]$ there exists $h^* \in (0, T]$ such that for all $\chi_1, \chi_2 \in B(\sigma_1)$ and $h \in (0, h^*]$, we have $|Z_{T,h}(\chi_1) - Z_{T,h}(\chi_2)| \leq L_z |\chi_1 - \chi_2|$, $|U_{T,h}(\chi_1) - U_{T,h}(\chi_2)| \leq L_u |\chi_1 - \chi_2|$.

Assumption 7.5. Each input signal u_j is held at a frequency greater than its corresponding Nyquist frequency, i.e., $\frac{1}{b_j T} \geq 2\omega_{maxj} \ \forall j = 1, \dots, m$, where ω_{maxj} is the highest frequency content present in the j^{th} input channel.

Note that Assumptions 7.1-7.4 are natural extensions of the well-known assumptions used in the area of nonlinear sampled-data systems (see e.g., [4,9]). Assumption 7.1 implies that the single-rate output-feedback controller (7.6)-(7.7) is designed such that under the network channels without uncertainties, i.e., $\Delta_{u_j} = \Delta_{y_i} = 0 \ \forall 0 \leq j \leq m, 0 \leq i \leq p$, the approximate nominal discrete-time plant model satisfies a dissipation inequality. Assumption 7.3 bounds the difference between the approximate and exact nominal discrete-time

plant models starting from the same as well as different initial conditions, whereas Assumption 7.4 places uniform bounds on the control inputs (see [19, Remark 1]). Finally, Assumption 7.2 indicates continuity of the storage function.

Remark 7.6. *Assumption 7.5 simply ensures perfect reconstruction of each input from the sampled data. It imposes some bounds on the difference of the single-rate and multirate input signals which appears in our derivations (see the proof of Theorem 1). Assumption 7.5 can, however, be ignored in the special cases of single-rate input channel and “low measurement rate” constraint.*

In order to perform our analysis, we first need a description for the exact discrete-time model of the multirate plant (7.1). Associated with the transmitted input vector u which is held at different sampling rates, we define a fictitious zero-order hold device to create the single-rate vector $u_c = [u_{c_1} \dots u_{c_m}]'$ as

$$\mathcal{H}_f : u_{c_j}(k) = \begin{cases} u_j(k), & \text{if } k = r_j b_j \exists r_j \in \mathbb{Z}^+ \\ u_{c_j}(k-1), & \text{otherwise} \end{cases} \quad (7.17)$$

which connects to the actual input u_j at its sampling instances and keeps it constant during the subintervals. Now, considering (7.4) and (7.17) the exact discrete-time model of multirate NCS under network uncertainties can be written as

$$x(k+1) = \bar{F}_T^e(x(k), u_c(k), d[k]) \quad (7.18)$$

It is clear from (7.17) that although each component of the modified input u_c is updated at a different time instance the whole vector is constant during sampling intervals $[kT, (k+1)T)$.

We now state and prove our main result. Theorem 7.1 derives sufficient conditions under which the closed-loop uncertain NCS using the proposed multirate output feedback setup (7.11)-(7.14) is also dissipative in a semiglobal practical sense.

Theorem 7.1. *Consider the multirate nonlinear NCS shown in Figure 7.1 controlled by (7.11)-(7.12) with (7.13)-(7.14). Under Assumptions 7.1-7.5 and the channels uncertainties satisfying (7.2), given any positive real numbers $(\sigma_{\tilde{x}}, \sigma_d, \varsigma_c, \nu, \kappa_1, \kappa_2)$ there exists $T^* > 0$ such that for each $T \in (0, T^*]$, all $|\tilde{x}(0)| \leq \sigma_{\tilde{x}}$, $\|d\|_\infty \leq \sigma_d$, $|x(0) - x_c(0)| \leq \varsigma_c$,*

there exists $h^* \in (0, T]$ such that for all $h \in (0, h^*]$ the uncertain exact discrete-time system (7.18) fulfills the following dissipation inequality

$$\frac{V_{T,h}(\tilde{x}(k+1)) - V_{T,h}(\tilde{x}(k))}{T} \leq w(\tilde{x}, d) + T(\kappa_1|\tilde{x}| + \kappa_2\|d\|_\infty) + \nu \quad (7.19)$$

Proof. Let us study the evolution of the storage function $V_{T,h}$ along the solutions of the exact model (7.18) and the controller (7.11)-(7.12):

$$V_{T,h}(\tilde{x}(k+1)) - V_{T,h}(\tilde{x}(k)) = V_{T,h}(\bar{F}_T^e(x, u_c, d_f), Z_{T,h}(\xi, y_c)) - V_{T,h}(x, \xi) \quad (7.20)$$

Adding and subtracting $V_{T,h}(F_{T,h}^a(x, U(\xi, y), d_f), Z_{T,h}(\xi, y))$ and considering Assumptions 7.1-7.2, we get

$$\begin{aligned} & V_{T,h}(\tilde{x}(k+1)) - V_{T,h}(\tilde{x}(k)) \\ & \leq Tw(\tilde{x}, d) + L_v \underbrace{|\bar{F}_T^e(x, u_c, d_f) - F_{T,h}^a(x, U(\xi, y), d_f)|}_{(i)} + L_v \underbrace{|Z_{T,h}(\xi, y_c) - Z_{T,h}(\xi, y)|}_{(ii)} \end{aligned} \quad (7.21)$$

Denoting $\Delta u = \text{diag}\{\Delta u_1, \Delta u_2, \dots, \Delta u_m\}$, the fast rate control input (before being delivered to the hold devices in Figure 7.1) under network uncertainties is given by

$$u(k) = (I + \Delta u)\bar{u}(k) = (I + \Delta u)U(\xi(k), y_c(k)) \quad (7.22)$$

Now, by adding and subtracting $\bar{F}_T^e(x, u, d_f) + F_T^e(x, U(\xi, y), d_f)$ to term (i) of (7.21) and then using the one-step consistency condition of Assumption 7.3 as well as triangle inequalities, also by virtue of Assumption 7.4 for term (ii) in (7.21), it is obtained that for any $T \in (0, T_1^*]$ and $h \in (0, h_1^*]$

$$\begin{aligned} & V_{T,h}(\tilde{x}(k+1)) - V_{T,h}(\tilde{x}(k)) \\ & \leq Tw(\tilde{x}, d) + L_v \left(T\rho(h) + |\bar{F}_T^e(x, u_c, d_f) - \bar{F}_T^e(x, u, d_f)| \right. \\ & \quad \left. + |\bar{F}_T^e(x, u, d_f) - F_T^e(x, U(\xi, y), d_f)| \right) + L_v L_z |y_c - y| \end{aligned} \quad (7.23)$$

where $T_1^*, h_1^* > 0$ and $\rho(\cdot)$ come from the one-step consistency in Assumption 7.3. Application of the Gronwal-Bellman inequality together with the control input expansion in

(7.22) yield

$$\begin{aligned}
& V_{T,h}(\tilde{x}(k+1)) - V_{T,h}(\tilde{x}(k)) \\
& \leq Tw(\tilde{x}, d) + L_v \left(T\rho(h) + (e^{L_f T} - 1)(|u_c - u| \right. \\
& \quad \left. + |(I + \Delta u)U(\xi, y_c) - U(\xi, y)|) \right) + L_v L_z |y_c - y| \\
& \leq Tw(\tilde{x}, d) + L_v \left(T\rho(h) + (e^{L_f T} - 1)(|u_c - u| + |\Delta u U(\xi, y_c)|) \right. \\
& \quad \left. + (L_z + L_u(e^{L_f T} - 1))|y_c - y| \right) \tag{7.24}
\end{aligned}$$

where L_f is the Lipschitz constant of f , and we have used the uniform continuity of $U_{T,h}(\cdot, \cdot)$ in Assumption 7.4. The following lemmas address, in turn, the critical terms $|u_c - u|$ and $|y_c - y|$.

Lemma 7.1. *Given any $\varepsilon_1 > 0$, there exists $T_1 > 0$ such that for any $T \in (0, T_1]$ there exists $h_1 \in (0, T]$ such that for all $h \in (0, h_1]$, the fast rate control inputs u and u_c satisfies $|u_c(k) - u(k)| \leq \varepsilon_1$.*

Proof. Let $T_1 > 0$ be such that $T_1 L_u \sqrt{b_1^2 + \dots + b_m^2} < \varepsilon_1$, where L_u comes from Assumption 7.4 for $(T^*, h^*) = (T_1, h_1)$, and suppose $T \in (0, T_1]$. Based on (7.17) we get

$$|u_c(k) - u(k)|^2 = \sum_{j=1}^m \vartheta_j^k |u_j(k) - u_j(r_j b_j)|^2 \tag{7.25}$$

with $\vartheta_j^k \in \{0, 1\}$ and $\vartheta_j^k = 0$ whenever the j^{th} channel of u_c is sampled at a sampling instance that is an integer multiple of $b_j T$, otherwise ϑ_j^k is equal to 1. Note that if $\vartheta_j^k = 1 \forall j = 1, \dots, m$ at the sampling instance $t = kT$, i.e., the worst case scenario, the right hand side of (7.25) represents the control input variations between different sampling times. Using the continuity of $u(\cdot)$ together with Assumption 7.5, it can be easily shown that in this case

$$|u_c(k) - u(k)|^2 \leq \sum_{j=1}^m L_u^2 T^2 (k - r_j b_j)^2 \leq \sum_{j=1}^m L_u^2 T^2 ((r_j + 1)b_j - r_j b_j)^2 \tag{7.26}$$

for $r_j b_j < k < (r_j + 1)b_j$. Form (7.26) we have $|u_c(k) - u(k)| \leq T L_u \sqrt{b_1^2 + \dots + b_m^2}$ which by the choice of T proves Lemma 7.1. ■

Lemma 7.2. *Given any strictly positive real numbers $(C_{\tilde{x}}, C_d, C_c, \varepsilon_2)$, there exists $T_2 > 0$ such that for any fixed $T \in (0, T_2]$ there exists $h_2 \in (0, T]$ such that for all $h \in (0, h_2]$,*

$|\tilde{x}(0)| \leq C_{\tilde{x}}$, $\|d\|_\infty \leq C_d$, $|x(0) - x_c(0)| \leq C_c$ the following holds: if $\max_{i \in \{0,1,\dots,k\}} |\tilde{x}(i)| \leq C_{\tilde{x}}$ for some $k \in \mathbb{Z}^+$ then the difference between the switch output y_c in (7.13) and the output of the analogous single-rate plant (7.6)-(7.7) satisfies:

$$|y_c(k) - y(k)| \leq T(\varepsilon_2 + \lambda_1|y(k)| + \lambda_2\|d\|_\infty) \quad (7.27)$$

for some $\lambda_1, \lambda_2 > 0$.

Proof. Let $(C_{\tilde{x}}, C_d, C_c, \varepsilon_2) \in \mathbb{R}^+$ be given. Let $L_f, L_g > 0$ be the Lipschitz constants of the functions f and g , respectively, and define $C_y = L_g(C_{\tilde{x}} + C_d) + \varepsilon_2 + 1$. By Assumption 7.4 and the property that $U_{T,h}$ is zero at zero, we have that for any positive numbers (C_u, C_y) there exists $T_{21} > 0$ and $h_{21} > 0$ such that $U(\xi, y_c) < C_u$ holds for all $\chi \in B(C_y)$ and $h \in (0, h_{21}]$. Assume that $T_{22}, h_{22} > 0$ and $\alpha(\cdot, \cdot)$ come from the multi-step consistency in Assumption 7.3 corresponding to $(\sigma_1, \sigma_2, \sigma_3, \varsigma) = (C_{\tilde{x}}, C_d, C_u, C_c)$. Denoting $a_{max} = \max\{a_1, \dots, a_p\}$ and $\delta_{y_{max}} = \max\{\delta_{y_1}, \dots, \delta_{y_p}\}$, choose $T_{23}, h_{23} > 0$ such that $\sqrt{p}L_g\alpha(\varsigma, h_{23})((L_g(e^{L_f T_{23}} - 1))^{a_{max}-1} - 1)/(L_g e^{L_f T_{23}} - L_g - 1) \leq \varepsilon_2$. Also, let $T_{24}, T_{25} > 0$, $\lambda_1, \lambda_2 > 0$ be such that $\sqrt{p}L_u L_g^{a_{max}-1}(e^{L_f T} - 1)^{a_{max}-1} \delta_{y_{max}} \leq \lambda_1 T$ and $\sqrt{p}L_g e^{L_f T}((L_g(e^{L_f T} - 1))^{a_{max}-1} - 1)/(L_g e^{L_f T} - L_g - 1) \leq \lambda_2 T$ for any $T \in (0, T_{24}]$ and $T \in (0, T_{25}]$, respectively. Finally, we define $T_2 = \min\{T_{21}, T_{22}, T_{23}, T_{24}, T_{25}\}$ and $h_2 = \min\{h_{21}, h_{22}, h_{23}\}$.

Suppose $T \in (0, T_2]$, $h \in (0, h_2]$, $\max_{i \in \{0,1,\dots,k\}} |\tilde{x}(i)| \leq C_{\tilde{x}}$ for some $k \in \{0, 1, \dots\}$. First, we claim that the Lipschitz property of g yields $\max_{i \in \{0,1,\dots,k\}} |y(i)| \leq C_y$ $k \in \{0, 1, \dots\}$ and then $|y_c(k)| \leq C_y$ follows by induction. Now taking (7.7), (7.13) as well as the channel model of Figure 7.2a into account, we have that

$$|y_c(k) - y(k)|^2 = \sum_{i=1}^p \mu_i^k |g_i(x_c, 0) - g_i(x, d)|^2 + (1 - \mu_i^k) |\Delta_{y_i} y_i|^2 \quad (7.28)$$

where $\mu_i^k \in \{0, 1\}$ depends on the current sampling instant and varies from one output channel to another. Indeed, it is equal to 0 when the measurement is available at the i^{th} output channel otherwise it is equal to 1. In particular, corresponding to the i^{th} measurement channel, k can be considered in three different cases. If $k = l_i a_i$ for some $l_i \in \{0, 1, \dots\}$, then it is obvious that $|y_{c_i}(k) - y_i(k)| = |\Delta_{y_i} y_i(l_i a_i)| \leq \delta_{y_i} |y_i(l_i a_i)|$. If $k = l_i a_i + 1$, then using the Lipschitz property of g , the fact that $|d(k)| \leq \|d\|_\infty$, the multi-step consistency in Assumption 7.3, uniform condition of Assumption 7.4, and triangle

inequalities we get

$$\begin{aligned}
|y_{c_i}(l_i a_i + 1) - y_i(l_i a_i + 1)| &\leq L_g(|F_{T,h}^a(x_c(l_i a_i), \bar{u}(l_i a_i), 0) - F_T^c(x(l_i a_i), u(l_i a_i), d[l_i a_i])|) \\
&+ L_g \|d\|_\infty \leq L_g T \alpha(\varsigma, h) + L_g |F_T^c(x(l_i a_i), \bar{u}(l_i a_i), 0) - F_T^c(x(l_i a_i), u(l_i a_i), d[l_i a_i])| + L_g \|d\|_\infty \\
&\leq L_g T \alpha(\varsigma, h) + L_g (e^{L_f T} - 1) [|U(\xi(l_i a_i), y_c(l_i a_i)) - U(\xi(l_i a_i), y(l_i a_i))| + \|d\|_\infty] + L_g \|d\|_\infty \\
&\leq L_g T \alpha(\varsigma, h) + L_g L_u (e^{L_f T} - 1) \delta_{y_i} |y_i(l_i a_i)| + L_g e^{L_f T} \|d\|_\infty \tag{7.29}
\end{aligned}$$

Note that the Gronwal-Bellman inequality (comparison lemma) has been exploited in the third inequality of (7.29). Otherwise, it can be concluded by induction and geometric series formulas that

$$\begin{aligned}
|y_{c_i}(k) - y_i(k)| &\leq L_g (\alpha(\varsigma, h) + (e^{L_f T} - 1) (\|d\|_\infty + |y_{c_i}(k-1) - y_i(k-1)|)) + L_g \|d\|_\infty \\
&\leq L_g \frac{(L_g (e^{L_f T} - 1))^{k-l_i a_i} - 1}{L_g (e^{L_f T} - 1) - 1} T \alpha(\varsigma, h) + L_u L_g^{k-l_i a_i} (e^{L_f T} - 1)^{k-l_i a_i} \delta_{y_i} |y_i(l_i a_i)| \\
&+ L_g e^{L_f T} \frac{(L_g (e^{L_f T} - 1))^{k-l_i a_i} - 1}{L_g (e^{L_f T} - 1) - 1} \|d\|_\infty \tag{7.30}
\end{aligned}$$

holds for all $k \in \{l_i a_i + 2, \dots, (l_i + 1) a_i - 1\}$, if $T \neq \frac{1}{L_f} \ln(\frac{L_g + 1}{L_g})$ (that can always be avoided by choosing L_f, L_g appropriately). Inequality (7.30), the definitions of a_{max} , $\delta_{y_{max}}$ together with the fact that $\max_{1 \leq i \leq p} |y_i| \leq |y|$ lead to

$$\begin{aligned}
|y_c(k) - y(k)| &= \left(\sum_{i=1}^p |y_{c_i}(k) - y_i(k)|^2 \right)^{\frac{1}{2}} \\
&\leq \Phi(T, a_{max}) T \alpha(\varsigma, h) + \nabla(T, \delta_{y_{max}}, a_{max}) |y| + e^{L_f T} \Phi(T, a_{max}) \|d\|_\infty \tag{7.31}
\end{aligned}$$

which implies the worst upper bound for (7.28) with

$$\Phi(T, a_{max}) = \sqrt{p} L_g ((L_g (e^{L_f T} - 1))^{a_{max}-1} - 1) / (L_g e^{L_f T} - L_g - 1) \tag{7.32}$$

$$\nabla(T, \delta_{y_{max}}, a_{max}) = \sqrt{p} L_u L_g^{a_{max}-1} (e^{L_f T} - 1)^{a_{max}-1} \delta_{y_{max}} \tag{7.33}$$

Consequently, inequality (7.27) is obtained from (7.31) and by the choice of T and h . The proof of Lemma 7.2 is complete. \blacksquare

With these prerequisites, the proof of Theorem 7.1 can be finalized as follows. Let $T_2^*, h_2^* > 0$ come from Lemma 7.1 and $(C_{\bar{x}}, C_d, C_c) = (\sigma_{\bar{x}}, \sigma_d, \varsigma_c)$ together with $\varepsilon_2 > 0$ generate $T_3^*, h_3^* > 0$ according to Lemma 7.2 with $\lambda_1, \lambda_2 > 0$. Define $\delta_{u_{max}} = \max\{\delta_{u_1}, \dots, \delta_{u_m}\}$.

Also, choose $(T_4^*, h_4^*, T_5^*, T_6^*) \in \mathbb{R}^+$ such that

$$L_v \left(\rho(h_4^*) + (e^{L_f T_4^*} - 1)(\varepsilon_1 + (1 + \delta_{u_{max}})L_u \varepsilon_2) + L_z \varepsilon_2 \right) \leq \nu, \quad (7.34)$$

$$L_v \left(L_g L_z \lambda_1 + L_u (e^{L_f T} - 1)(\delta_{u_{max}} + \delta_{u_{max}} \lambda_3 L_g + \lambda_1 L_g) \right) \leq \kappa_1 T \quad \forall T \in (0, T_5^*], \quad (7.35)$$

$$L_v \left(L_z \lambda_2 + L_u (e^{L_f T} - 1)((1 + \delta_{u_{max}})\lambda_2 + L_g(\delta_{u_{max}} \lambda_3 + \lambda_1)) \right) \leq \kappa_2 T \quad \forall T \in (0, T_6^*]. \quad (7.36)$$

Assume $\lambda_3 > 0$ be a number such that $\lambda_1 T + 1 \leq \lambda_3 T$ for any $T \in (0, T_7^*]$. Finally, given positive numbers $(\sigma_{\tilde{x}}, \sigma_d, \varsigma_c, \kappa_1, \kappa_2)$, we pick the sampling and integration periods as $T^* = \min\{T_1^*, T_2^*, T_3^*, T_4^*, T_5^*, T_6^*, T_7^*\}$ and $h^* = \min\{h_1^*, h_2^*, h_3^*, h_4^*\}$.

First note that from Assumption 7.4 and the fact that $|\Delta u| \leq \delta_{u_{max}}$, we have

$$|\Delta u U(\xi, y_c)| \leq \delta_{u_{max}} L_u (|\xi| + |y_c|) \leq \delta_{u_{max}} L_u (|\xi| + |y - y_c| + |y|) \quad (7.37)$$

Suppose $T \in (0, T^*]$ and $h \in (0, h^*]$. Substituting the result of Lemma 7.1, inequalities (7.27) and (7.37) into (7.24) give rise to

$$\begin{aligned} & V_{T,h}(\tilde{x}(k+1)) - V_{T,h}(\tilde{x}(k)) \\ & \leq T w(\tilde{x}, d) + L_v T \left(\rho(h) + (e^{L_f T} - 1)\varepsilon_1 + (e^{L_f T} - 1)\delta_{u_{max}} L_u (|\xi| + \varepsilon_2 + \lambda_3 |y| + \lambda_2 \|d\|_\infty) \right. \\ & \quad \left. + (L_z + L_u (e^{L_f T} - 1))(\varepsilon_2 + \lambda_1 |y| + \lambda_2 \|d\|_\infty) \right) \end{aligned} \quad (7.38)$$

The Lipschitz condition of the output mapping g indicates that $|y| \leq L_g(|x| + \|d\|_\infty)$.

Therefore, after rearranging the terms in (7.38), it can be rewritten as

$$\begin{aligned} & V_{T,h}(\tilde{x}(k+1)) - V_{T,h}(\tilde{x}(k)) \\ & \leq T w(\tilde{x}, d) + L_v T \left(\rho(h) + (e^{L_f T} - 1)(\varepsilon_1 + (1 + \delta_{u_{max}})L_u \varepsilon_2) + L_z \varepsilon_2 \right) \\ & \quad + L_v L_g T \left(L_z \lambda_1 + L_u (e^{L_f T} - 1)(\delta_{u_{max}} \lambda_3 + \lambda_1) \right) |x| + L_v L_u T (e^{L_f T} - 1) \delta_{u_{max}} |\xi| \\ & \quad + L_v T \left(L_z \lambda_2 + L_u (e^{L_f T} - 1)((1 + \delta_{u_{max}})\lambda_2 + L_g(\delta_{u_{max}} \lambda_3 + \lambda_1)) \right) \|d\|_\infty \end{aligned} \quad (7.39)$$

If we divide both sides of (7.39) by T and take into account the conditions (7.34)-(7.36) on ν, κ_1, κ_2 and the choice of T^* and h^* , then the dissipation inequality (7.19) is verified readily. This concludes the proof of Theorem 7.1. \blacksquare

Remark 7.7. *The dissipation inequality (7.19) is similar to the strong form of (V, w) -dissipativity in [9] which is useful for a large class of applications such as input-to-state*

stability, where the disturbance input is only assumed to be a measurable (not necessarily Lipschitz) function of time.

Remark 7.8. *It can be shown that the result of Theorem 7.1 is also valid for the R-SER channel model displayed in Figure 7.2b.*

Theorem 7.1 conveys how the proposed multirate output feedback controller preserves the closed-loop dissipativity, in a semiglobal practical sense, in spite of network constraints as well as disturbance inputs. Explicit conditions on the channels uncertainties and sampling rates will be derived in the next section to guarantee the asymptotic stability of the multirate nonlinear NCS. It can be inferred from (7.19) that, although the supply rate has been deteriorated slightly by some additive terms, in most applications this deterioration can be degraded by adjusting the parameters T and h . Moreover, the approach presented by [9, Corollary 5.3] might be used to cancel ν and $T(\kappa_1|\tilde{x}| + \kappa_2\|d\|_\infty)$ in properties like passivity or H_∞ control [20, Corollary 1].

It should be mentioned that, the dissipation rate w may have various forms, each of which refers to a specific theoretic property. For instance, nonlinear H_∞ control is covered by taking $w(\tilde{x}, d) = \frac{\gamma}{2}|d(k)|^2 - \frac{\gamma}{2}|\tilde{x}(k)|^2$ for $\gamma > 0$ (see [20]) and input-to-state stability (ISS) corresponds to $w(\tilde{x}, d) = -\alpha_3(|\tilde{x}|) + \tilde{\gamma}(\|d\|_\infty)$ for $\alpha_3 \in \mathcal{K}_\infty$, $\tilde{\gamma} \in \mathcal{K}$ (see next section for in-depth discussion).

7.3 Stability of the Multirate NCS

This section applies the general dissipativity property supplied by Theorem 7.1 to analyze the stability of the proposed multirate networked controller in both the disturbance driven and disturbance (noise) free situations. While the role of the network constraints and different sampling was encapsulated in terms of κ_1, κ_2, ν in (7.19), their effect on the closed-loop behaviour will be made more clear in this section.

7.3.1 Input-to-State Stability

Input-to-state stability (ISS) is an effective tool for stability investigation, when the plant is exposed to disturbance inputs. Roughly, the difference equation $x(k+1) = \mathcal{F}(x, u, d_f)$ is said to be input-to-state stable if there exist $\beta \in \mathcal{KL}$, $\gamma \in \mathcal{K}$ such that $|x(k)| \leq$

$\beta(|x(0)|, kT) + \gamma(\|d\|_\infty)$ (see e.g., [19] for accurate definition). The following corollary demonstrates ISS preservation for the multirate NCS in a semiglobal practical sense.

Corollary 7.1. *In Theorem 7.1, set $w(\tilde{x}, d) = \alpha_3(|\tilde{x}|) + \tilde{\gamma}(\|d\|_\infty)$ and assume $\alpha_1(|\tilde{x}|) \leq V_{T,h} \leq \alpha_2(|\tilde{x}|)$ for $\alpha_1, \alpha_2, \alpha_3 \in \mathcal{K}_\infty$, $\tilde{\gamma} \in \mathcal{K}$. Then, under similar assumptions and given any positive real numbers $(\sigma_{\tilde{x}}, \sigma_d, \varsigma_c, \nu)$ there exist $\beta \in \mathcal{KL}$, $\gamma \in \mathcal{K}$ and $T^* > 0$ such that for each $T \in (0, T^*]$, all $|\tilde{x}(0)| \leq \sigma_{\tilde{x}}$, $\|d\|_\infty \leq \sigma_d$, $|x(0) - x_c(0)| \leq \varsigma_c$, there exists $h^* \in (0, T]$ such that for all $h \in (0, h^*]$, the solutions of multirate sampled-data NCS controlled by (7.11)-(7.14) satisfy:*

$$|\tilde{x}(k)| \leq \beta(|\tilde{x}(0)|, kT) + \gamma(\|d\|_\infty) + \nu, \quad \forall k \in \mathbb{Z}^+ \quad (7.40)$$

provided that $\tilde{\alpha}(|\tilde{x}|) - T\kappa_1|\tilde{x}| \in \mathcal{K}_\infty$, where κ_1 comes from (7.35).

Proof. From Theorem 7.1 and inequality (7.19), we get

$$\frac{V_{T,h}(\tilde{x}(k+1)) - V_{T,h}(\tilde{x}(k))}{T} \leq \underbrace{-\tilde{\alpha}(|\tilde{x}|) + T\kappa_1|\tilde{x}|}_{(i)} + \underbrace{\tilde{\gamma}(\|d\|_\infty) + T\kappa_2\|d\|_\infty}_{(ii)} + \nu \quad (7.41)$$

Obviously, term (ii) is always a class \mathcal{K} function but term (i) is of class \mathcal{K}_∞ only if $\tilde{\alpha}(|\tilde{x}|) - T\kappa_1|\tilde{x}| > 0$. The rest of the proof follows directly the proof of [9, Corollary 5.1], thus omitted. \blacksquare

There is no need to emphasize that Corollary 7.1 is also applicable for the R-SER channel model. Only the description of κ_1 , κ_2 and ν will be changed.

7.3.2 Exponential Stability

Throughout the rest of this section we let the effect of disturbances be negligible, i.e., $d = 0$, and exploit the following Lyapunov characterization to formulate stability conditions. Moreover, for the sake of simplicity the input channels are assumed to be held at a same sampling period equal to T , i.e., $b_j = 1 \forall j = 1, \dots, m$. This imposes the “low measurement rate” constraint that is widely used in the literature on multirate systems [17].

Definition 7.3. *The parametrized discrete-time model (7.15) with zero disturbance together with output feedback control (7.6)-(7.7) is said to be exponentially stable, if there exists a family of Lyapunov functions $V_{T,h} : \mathbb{R}^{n+s} \rightarrow \mathbb{R}^+$ and $T^* > 0$ such that for each*

fixed $T \in (0, T^*]$ there exists $h^* \in (0, T]$ such that

$$c_1 |\tilde{x}|^r \leq V_{T,h}(\tilde{x}) \leq c_2 |\tilde{x}|^r \quad (7.42)$$

$$\frac{V_{T,h}(\mathcal{F}_T(x, U_{T,h}(\xi, y), 0), Z_{T,h}(\xi, y)) - V_{T,h}(x, \xi)}{T} \leq -c_3 |\tilde{x}|^r \quad (7.43)$$

for some $1 \leq r < \infty$ and $\forall \tilde{x} \in B(\sigma_1) \subset \mathbb{R}^{n+s}$, $h \in (0, h^*]$. with $c_i > 0$, $i = 1, 2, 3$

Note that this definition provides well-know Lyapunov conditions for exponential stability (see e.g., [48]), which has been recently used in the context of nonlinear networked control systems by [91]. We now modify in turn Assumptions 7.1-7.3 in the form of Assumptions 7.6-7.8 to be applicable for the purpose of this section.

Assumption 7.6. *The approximate discrete-time model $F_{T,h}^a$ together with the single-rate controller (7.6)-(7.7) is exponentially stable in the sense of Definition 7.3.*

Assumption 7.7. *The associated Lyapunov function $V_{T,h}$ is locally Lipschitz and satisfies: $\sup\{\partial V_{T,h}/\partial \tilde{x}\} \leq L_v |\tilde{x}|^{r-1}$ for $L_v > 0$, $\tilde{x} \in B(\sigma_1)$, and r in accordance with Assumption 7.6.*

Assumption 7.8. *$F_{T,h}^a$ is one-step and also multi-step consistent with the exact discrete-time model F_T^e according to Definition 7.1, where inequalities (7.8) and (7.9) are, respectively, replaced by (7.44) and (7.45) defined below*

$$|F_T^e(x, u, 0) - F_{T,h}^a(x, u, 0)| \leq T\rho(h)(|x| + |u|) \quad (7.44)$$

$$|F_T^e(x_1, u, 0) - F_{T,h}^a(x_2, u, 0)| \leq T\alpha(\varsigma, h)(|u|) \quad (7.45)$$

Remark 7.9. *The stronger form of consistency introduced in Assumption 7.8 is known to hold for a large class of Runge-Kutta methods (see for instance [120, Theorem 4.6.7]). Also, integration schemes satisfying (7.44) are available in [121] and have been utilized by [91] for stabilization of single-rate NCS.*

Theorem 7.2. *The multirate nonlinear NCS with SER channel model controlled by (7.11)-(7.14) is locally exponentially stable, if given positive real numbers $(\sigma_{\tilde{x}}, \varsigma_c)$ there exists $T \in (0, T^*]$ such that for each $T \in (0, T^*]$, all $|\tilde{x}(0)| \leq \sigma_{\tilde{x}}$, $|x(0) - x_c(0)| \leq \varsigma_c$, there*

exists $h^* \in (0, T]$ such that for all $h \in (0, h^*]$ Assumptions 7.6-7.8 and 7.4 hold, and the following inequality is satisfied

$$\frac{(n+s)^{\frac{r}{2}}}{T^*} \Pi^{r-1} (\Omega_1 + \Omega_2 + \Omega_3) \leq (1-\theta)c_3 \quad (7.46)$$

for some $0 < \theta < 1$, where

$$\begin{aligned} \Pi &= T^* \rho(h^*) (L_u L_g + L_u + 1) + e^{L_f T^*} \\ &\quad + (L_z + L_u (e^{L_f T^*} - 1)) (L_g \nabla^* + (L_g + 1) (1 + L_u T^* \Phi^* \alpha(\varsigma_c, h^*))) \end{aligned} \quad (7.47)$$

$$\Omega_1 = T^* \rho(h^*) (L_u L_g + L_u + 1) \quad (7.48)$$

$$\Omega_2 = L_z (L_g \nabla^* + (L_g + 1) L_u T^* \Phi^* \alpha(\varsigma_c, h^*)) \quad (7.49)$$

$$\begin{aligned} \Omega_3 &= L_u (e^{L_f T^*} - 1) (\delta_{u_{max}} + 1) (L_g \nabla^* + (L_g + 1) L_u T^* \Phi^* \alpha(\varsigma_c, h^*)) \\ &\quad + L_u L_g (e^{L_f T^*} - 1) \delta_{u_{max}} \end{aligned} \quad (7.50)$$

and $\Phi^* = \Phi(T^*, a_{max})$, $\nabla^* = \nabla(T^*, \delta_{y_{max}}, a_{max})$ defined by (7.32) and (7.33), respectively.

Proof. First by supposition that all the input channels have the same sampling rate, the application of H_f is redundant here. Therefore, $u_c = u = (I + \Delta u)\bar{u}$ and the uncertain exact discrete-time model is given by $\bar{F}_T^e(x, u, 0)$. Similar to the proof of Theorem 7.1, we start by evaluation of the Lyapunov function increment along the closed-loop solutions of the uncertain system:

$$V_{T,h}(\tilde{x}(k+1)) - V_{T,h}(\tilde{x}(k)) := V_{T,h}(\bar{F}_T^e(x, u, 0), Z_{T,h}(\xi, y_c)) - V_{T,h}(x, \xi) \quad (7.51)$$

Adding and subtracting $V_{T,h}(F_{T,h}^a(x, U(\xi, y), 0), Z_{T,h}(\xi, y))$ and then using the mean value theorem along with Assumption 7.7 gives

$$\begin{aligned} V_{T,h}(\tilde{x}(k+1)) - V_{T,h}(\tilde{x}(k)) &\leq -a_3 T |\tilde{x}|^r \\ &\quad + L_v \left(\max\{|\bar{F}_T^e(x, u, 0)| + |Z_{T,h}(\xi, y_c)|, |F_{T,h}^a(x, U(\xi, y), 0)| + |Z_{T,h}(\xi, y)|\} \right)^{r-1} \\ &\quad \times (|\bar{F}_T^e(x, u, 0) - F_{T,h}^a(x, U(\xi, y), 0)| + |Z_{T,h}(\xi, y_c) - Z_{T,h}(\xi, y)|) \end{aligned} \quad (7.52)$$

where we used $V_{T,h}(\tilde{x}_1) - V_{T,h}(\tilde{x}_2) \leq L_v (\max\{|\tilde{x}_1|, |\tilde{x}_2|\})^{r-1} |\tilde{x}_1 - \tilde{x}_2|$ and $||x \ \xi|| \leq |x| + |\xi|$. Before proceeding to investigate the second term in (7.52), note that from (7.31)-(7.33) in Lemma 7.2 and the multi-step strong consistency in Assumption 7.8, we have that

$$\begin{aligned} |y_c(k) - y(k)| &\leq \Phi(T, a_{max}) T \alpha(\varsigma, h) |U(\xi, y)| + \nabla(T, \delta_{y_{max}}, a_{max}) |y| \\ &\leq L_u \Phi(T, a_{max}) T \alpha(\varsigma, h) |\xi| + L_g (\nabla(T, \delta_{y_{max}}, a_{max}) + L_u \Phi(T, a_{max}) T \alpha(\varsigma, h)) |x| \end{aligned} \quad (7.53)$$

in which Assumption 7.4 and the Lipschitz property of g were applied to derive the second inequality. Now, we upperbound $|\bar{F}_T^e|$, $|F_{T,h}^a|$, $|Z_{T,h}(\xi, y_c)|$, $|Z_{T,h}(\xi, y)|$ as follows. Using the Gronwall-Bellman inequality, Assumption 7.4 and the SER model, we obtain

$$\begin{aligned} |\bar{F}_T^e| &\leq |x| + (e^{L_f T} - 1)(|x| + (I + \Delta u)U(\zeta, y_c)) \\ &\leq e^{L_f T} |x| + L_u(e^{L_f T} - 1)(1 + \delta_{y_{max}})(|\zeta| + |y_c|) \end{aligned} \quad (7.54)$$

Inequality (7.53) and the fact that $|y_c| \leq |y_c - y| + |y|$ yields

$$\begin{aligned} |\bar{F}_T^e| &\leq \underbrace{\left(e^{L_f T} + L_u L_g (e^{L_f T} - 1)(1 + \delta_{y_{max}})(1 + \nabla + T L_u \Phi \alpha) \right)}_{\pi_{e_1}} |x| \\ &\quad + \underbrace{L_u (e^{L_f T} - 1)(1 + \delta_{y_{max}})(1 + T L_u \Phi \alpha)}_{\pi_{e_2}} |\xi| \end{aligned} \quad (7.55)$$

where the arguments of ∇, Φ, α are dropped for notational convenience. Hence,

$$|\bar{F}_T^e| \leq \max\{\pi_{e_1}, \pi_{e_2}\}(|x| + |\xi|) \leq \pi_e |\tilde{x}| \quad (7.56)$$

with $\pi_e := \sqrt{n+s}(\pi_{e_1} + \pi_{e_2}) = \sqrt{n+s} \left(e^{L_f T} + L_u (e^{L_f T} - 1)(L_g \nabla + (L_g + 1)(1 + T L_u \Phi \alpha)) \right)$. In exactly the similar way, for the exact discrete-time model without uncertainty, i.e., $F_T^e(x, U(\zeta, y), 0)$, it can be written

$$|F_T^e| \leq (e^{L_f T} + L_u L_g (e^{L_f T} - 1))|x| + L_u (e^{L_f T} - 1)|\xi| \quad (7.57)$$

Note that (7.57) can be verified by setting $\delta_{y_{max}} = \nabla = \Phi = 0$ in (7.55). It is clear from (7.57) and (7.55) that $|F_T^e| \leq \pi_e |\tilde{x}|$. Consequently, by the one-step strong consistency governed by (7.44) and Assumption 7.4, $|F_{T,h}^a|$ can be upperbounded as

$$\begin{aligned} |F_{T,h}^a - F_T^e| &\leq T\rho(h)(|x| + |U(\xi, y)|) \leq T\rho(h)((L_u L_g + 1)|x| + L_u |\xi|) \\ \Rightarrow |F_{T,h}^a| &\leq (\pi_e + T\rho(h)\sqrt{n+s}(L_u + L_u L_g + 1))|\tilde{x}| = \pi_a |\tilde{x}| \end{aligned} \quad (7.58)$$

Again owing to Assumption 7.4 and (7.53), we can upperbound $|Z_{T,h}(\xi, y_c)|$, $|Z_{T,h}(\xi, y)|$ as

$$|Z_{T,h}(\xi, y)| \leq L_z L_g |x| + L_z |\xi| \quad (7.59)$$

$$|Z_{T,h}(\xi, y_c)| \leq L_z L_g (1 + \nabla + T L_u \Phi \alpha) |x| + L_z (1 + T L_u \Phi \alpha) |\xi| \quad (7.60)$$

Let us define $\pi_z = \sqrt{n + s}L_z(L_g\nabla + (L_g + 1)(1 + TL_u\Phi\alpha))$. It is straightforward to see that $|Z_{T,h}(\xi, y_c)|, |Z_{T,h}(\xi, y)| \leq \pi_z|\tilde{x}|$. Finally, combining (7.56), (7.58), the bound on $|Z_{T,h}|$, and the fact that $\max\{\pi_e, \pi_a, \pi_z\} \leq \pi_a + \pi_z$ leads to

$$(\max\{|\bar{F}_T^e| + |Z_{T,h}(\xi, y_c)|, |F_{T,h}^a| + |Z_{T,h}(\xi, y)|\})^{r-1} \leq (n + s)^{\frac{r-1}{2}}\Pi^{r-1}|\tilde{x}|^{r-1} \quad (7.61)$$

for $\Pi(T, h, \delta_{y_{max}}, a_{max})$ defined in (7.47). Next, we address the term $|\bar{F}_T^e - F_{T,h}^a| + |Z_{T,h}(\xi, y_c) - Z_{T,h}(\xi, y)|$ in (7.52). Following the same procedure used to bound terms (i), (ii) in the proof of Theorem 7.1 and employing Assumption 7.8 we get

$$\begin{aligned} |\bar{F}_T^e - F_{T,h}^a| + |Z_{T,h}(\xi, y_c) - Z_{T,h}(\xi, y)| &\leq T\rho(h)(|x| + U(x, y)) \\ &+ (e^{L_f T} - 1)|\Delta u U(\xi, y_c)| + (L_z + L_u(e^{L_f T} - 1))|y_c - y| \end{aligned} \quad (7.62)$$

Direct but lengthy manipulations based on Assumption 7.4 and (7.53) show that

$$|\bar{F}_T^e - F_{T,h}^a| + |Z_{T,h}(\xi, y_c) - Z_{T,h}(\xi, y)| \leq \sqrt{n + s}(\Omega_1 + \Omega_2 + \Omega_3)|\tilde{x}| \quad (7.63)$$

with $\Omega_1, \Omega_2, \Omega_3$ given by (7.48)-(7.50). Putting (7.61), (7.63) and the condition (7.46) together, the Lyapunov function increment in (7.52) admits

$$\frac{V_{T,h}(\tilde{x}(k+1)) - V_{T,h}}{T} \leq -c_3\theta|\tilde{x}|^r \quad (7.64)$$

Therefore, the conditions of Definition 7.3 hold under multirate sampling and network uncertainties, which confirms exponential stability of the uncertain exact discrete-time model. \blacksquare

Theorem 7.2 can be interpreted as follows. If the single-rate output feedback controller exponentially stabilizes the nominal approximate discrete-time model, then under some standard continuity and closeness assumptions and the satisfaction of condition (7.46), the proposed multirate NCS is also locally exponentially stable. Note that (7.46) includes three different terms:

- Ω_1 , which reflects the effect of discrete-time approximation via the one-step consistency property,
- Ω_2 , which stands for only the output channels uncertainty,
- and Ω_3 , which consists of both the input and output channels uncertainty.

Also, the effect of different sampling rates and the multi-step consistency are reflected by $L_g \nabla(T^*, \delta_{y_{max}}, a_{max}) + (L_g + 1)L_u T^* \Phi(T^*, a_{max}) \alpha(\zeta_c, h^*)$, which exists in both terms Ω_2 and Ω_3 . It is worth mentioning that, c_3 on the right hand side of (7.46) can be regarded as a margin of stability of the approximate nominal closed-loop system that should dominate the effects of $\Omega_1, \Omega_2, \Omega_3$ introduced above.

Remark 7.10. *Similar discussions to those after [91, Theorem 2] can be carried out regarding the feasibility of condition (7.46) and the related possible bottlenecks. However, since the left hand side of (7.46) can always be made arbitrarily small by an appropriate choice of T^*, h^* , uncertainties bounds as well as various sampling rates, we can easily formulate conditions under which (7.46) is guaranteed by choosing these parameters sufficiently small (see [91, Theorem 3] that is intended for similar purpose).*

Remark 7.11. *Theorem 7.2 can be applied to the same problem with the R-SER channel model. The only difference is that, in our derivations $\delta_{y_{max}}$ and $\delta_{u_{max}}$ should be replaced by $1/(1+\delta_{y_{max}})$ and $1/(1+\delta_{u_{max}})$, respectively. However, as stressed by [97, 98], application of R-SER model is usually preferred to SER model due to introducing a more flexible optimization problem. It can be shown that the fulfillment of (7.46) under the R-SER model provides a bigger stability margin compared with the SER case.*

7.4 Case Study

This section is serve to illustrate some of the main results in this chapter by output feedback stabilization of an elementary example in a multirate network-based setup. The first part is dedicated to the ISS property and the second part studies the exponential stability. In order to evaluate the effect of network uncertainties in our simulations, we will use the total network capacity defined as $\mathcal{C} = \sum_{i=1}^p \frac{1}{a_i T} \ln \delta_{y_i}^{-1} + \sum_{j=1}^m \frac{1}{b_j T} \ln \delta_{u_j}^{-1}$. This is taken from [97] for linear multirate NCS, and measures how much information per time unite can be transmitted through the whole network.

Consider the continuous-time plant [19]

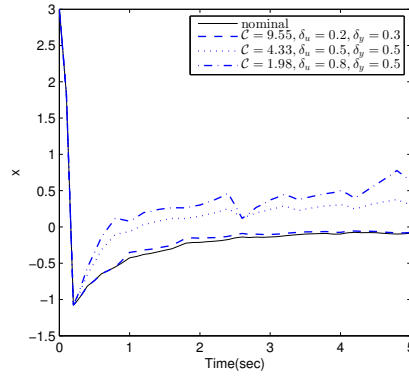
$$\begin{aligned} \dot{x}(t) &= x^3(t) + u(t) + d(t) \\ y(t) &= x(t) + d(t) \end{aligned} \tag{7.65}$$

with the approximate discrete-time model $F_{T,h}^a$ generated by

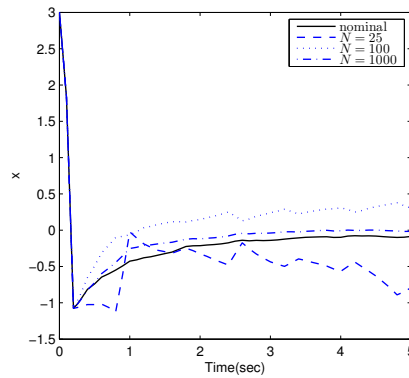
$$\begin{cases} f_h(i, x, u, d) := x + h(x^3 + u) + \int_{kT+ih}^{kT+(i+1)h} d(\tau) d\tau, \\ f_h^{i+1}(x, u, d) := f_h(i+1, f_h^i, u, d), \\ F_{T,h}^a(x, u, d_f) := f_h^N(x, u, d), \quad N = \frac{T}{h} \end{cases} \quad (7.66)$$

that is a refined Euler model utilized in several references, e.g., [18–20]. One-step and multi-step consistency of (7.66) with the exact discrete-time model of (7.65) was already checked in [19]. Also, by taking $V_{T,h} = |x|$, $\alpha_3(|x|) = |x|$, and $\tilde{\gamma}(\|d\|_\infty) = \|d\|_\infty$, it follows that the digital static controller $u(k) = -y(k) - y^3(k)$ (that is here state feedback) makes the approximate model $F_{T,h}^a$ input-to-state stable. Hence, Assumptions 7.1-7.4 can be easily validated. We now study the “low measurement rate” situation in Figure 7.1 with $b_1 = 1$, $a_1 = 4$ and under the SER model for input and out channels with bounded δ_u and δ_y . If we pick $T = 0.2$, that is enough to satisfy Assumption 7.5, simglobal practical ISS of the dual-rate NCS using the digital controller $u(k) = -y_c(k) - y_c^3(k)$ with (7.13)-(7.14) is obtained from Corollary 7.1. The simulation results are shown in Figure 7.4 for a randomly distributed disturbance input. It can be inferred from Figure 7.4a that although the ISS property is maintained under different channel uncertainties, increasing δ_u or δ_y (decreasing the network capacity \mathcal{C}) has destructive effects and may lead to divergence. Figure 7.4b reveals the effect of the integration period h on the closed-loop performance for a given value of \mathcal{C} .

We now set the disturbance input d to zero in (7.65) and analyze the exponential stability using Theorem 7.2 (and in particular condition (7.46)). Similar to the arguments of [91, Section 4], we can conclude that the controller $u(k) = -y(k)^3 - y(k) - hy(k)$ with the Lyapunov function $V_{T,h} = |x|$ makes the approximate discrete-time model (7.66) exponentially stable. Besides, it is straightforward to verify Assumptions 7.7-7.8. The proposed multirate control setup was implemented for different sampling rates as well as various channel uncertainties. For simulation purposes, we choose $T = 0.1$, $N = 100$, $b_1 = 1$, and the output channel uncertainty is fixed such that $\delta_y = 0.2$. Figure 7.5 displays the minimum required input channel capacity \mathcal{C}_u (maximum allowable input uncertainty) to prevent instability versus the measurement sampling frequency $\frac{1}{a_1 T}$ for both the SER and R-SER models. It can be perceived that for the R-SER model the multirate controller can tolerate larger uncertainties (see Remark 7.11), and in this case we may expect an



(a)



(b)

Figure 7.4: State evolution of the multirate NCS (a) under different network uncertainties and $N = 100$ (b) under different values of integration period $h = T/N$ and $C = 4.33$.

improvement in terms of the required network capacity to preserve stability.

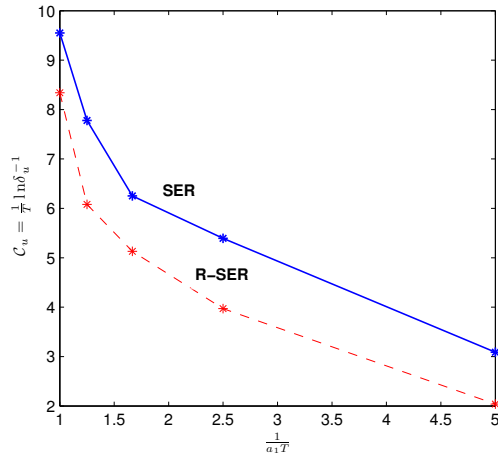


Figure 7.5: Bounds on the channel uncertainty for exponential stability under SER and R-SER models

7.5 Summary

In this chapter we developed a general output feedback stabilization for multirate NCS within the context of sampled-data systems and using discrete-time approximation. This framework is the combination of a single-rate output feedback controller previously designed and purposeful periodic switches which reconstruct the missing intersample outputs between measured sampled data. The network channels are modelled as multiplicative and relative uncertainties to the plant signals, called SER and R-SER models. These models can account for different network-induced constraints with different physical meanings. It is shown that the proposed multirate structure is capable of preserving the dissipation inequalities, in presence of disturbances and under both channel models, with some additive terms depending on various sampling rates, channel uncertainties and the integration period. As special cases of dissipativity with practical importance, we derived explicit sufficient conditions to first guarantee input-to-state stability (ISS) of the disturbance driven multirate NCS and then exponential stability of the disturbance free multirate networked-based controller for both the SER and R-SER models. Simulation results validate how the proposed multirate strategy can stabilize the nonlinear NCS under much lower transmission data rate leading to significance saving in the required bandwidth. Moreover, in coincide with our theoretical expectations the R-SER model provides more robustness against channel uncertainties compared with the SER model.

Chapter 8

Conclusions and Future Works

This thesis studies nonlinear sampled-data systems with input and output channels of various sampling rates. While the main focus is on the design problem, important issues on the stability analysis of multirate nonlinear plants are also investigated mainly within the context of dissipativity. In addition to providing general frameworks for multirate controller and observer designs, a new performance criterion based on the incremental gain is proposed, and multirate nonlinear networked control systems (NCSs) are analyzed as an application with practical significance. The major contributions of this thesis can be categorized as follows:

1. In chapter 3 we considered a nonlinear plant connected to multirate sample and hold devices when the output sampling rates are lower than the input sampling rates. This refers to the “low measurement rate” constraint with several applications since D/A converters are usually faster than A/D converters. An inferential state feedback control setup was developed using the emulation (CTD) method and the theory of dissipative dynamical systems was exploited to analyze the stability of the closed-loop sampled-data system. We proved that the proposed multirate inferential setup preserves dissipativity in a semiglobal practical sense for both the static and dynamic feedback cases. Considering this main result, a general approach for multirate nonlinear H_∞ control was then proposed based on an emulated controller together with an approximate discrete-time model of the plant.
2. In chapter 4 the \mathcal{L}_2 incremental gain was introduced as a novel performance index

for designing nonlinear H_∞ controllers. The advantages of the new technique comparing with the well-known H_∞ control design based on the usual \mathcal{L}_2 gain is that it quantifies whether or not small changes in exogenous inputs such as disturbances or noise will result in small changes at the output. Moreover, it ensures not only closed loop stability but also existence and uniqueness of the solution of the system equations. We first designed a state feedback incremental H_∞ control scheme for a class of Lipschitz nonlinear plants in terms of linear matrix inequalities (LMIs). The proposed strategy is exponentially stable in the absence of disturbances and minimizes the \mathcal{L}_2 incremental gain from the disturbances to the controlled output under the effect of exogenous inputs. Our results were then extended to a more practical case where only some (or maybe none) of the state variables are measurable and also a more general class of nonlinearities called one-sided Lipschitz. Precisely, an observer-based output feedback controller was presented using tractable linear matrix inequalities (LMIs) that is shown to be asymptotically stable with minimized incremental gain from the disturbance inputs to the penalty variable.

3. Chapter 5 tackles the problem of sampled-data observer design in presence of system and measurement disturbance signals which indeed provides a background for the multirate results of chapter 6. We constructed a family of observers using CTD and DTD methods and discrete-time approximation, and adopted the notion of input-to-state stability (ISS) to analyze the convergence of the estimation error. It was shown that under some standard continuity and consistency assumptions both the CTD and DTD-based observers are input-to-state stable from disturbances to the estimation error in a semiglobal practical sense for the unknown exact discrete-time plant model. Considering the one-sided Lipschitz condition as a broad class of nonlinear systems together with a refined Euler approximate model, systematic approaches for sampled-data observers were derived that can be cast into feasibility of certain LMIs. Although the DTD method usually exhibits better performance compared with the CTD technique, it necessitates a second assumption called quadratically inner bounded condition. Instead, the CTD-based design requires only a mild geometric condition.
4. Chapter 6 extends the results of chapter 5 to MSD systems. We considered a general

description of nonlinear plants and established a prescriptive framework for multi-rate sampled-data observer design in presence of disturbance inputs. The proposed structure consists of a single-rate observer working at the base sampling period of the system that is fed by two periodic switches. These switches are, respectively, a modified sampler to reconstruct the missing intersample outputs using an approximate discrete-time model together with the output mapping function and a modified hold device that assigns each control input to its previous measured value during the corresponding sampling interval. We proved that if the single-rate observer is designed (using the materials of chapter 5) to be input-to-state stable then under some standard assumptions and Lyapunov-ISS conditions, the proposed multirate observer is input-to-state stable in a semiglobal practical sense.

5. Finally, in chapter 7 we addressed an important application of multirate sampling by developing an output feedback stabilizing scheme for nonlinear networked-control systems (NCSs) with communication channels of various sampling rates. Two uncertainty based channel models called signal-to-error ratio (SER) and relative signal-to-error ratio (R-SER) model, respectively, were utilized to capture different network constraints such as delays, data loss, etc. as well as sensors and actuators inaccuracies. Then, we proposed a multirate dynamic NCS which includes a single-rate discrete-time output feedback controller together with a periodic switch to predict the intersample outputs using an approximate discrete time plant model and the output mapping function. It was shown that if the single-rate stabilizer satisfies a certain dissipation inequality, then under some continuity and consistency assumptions the closed-loop multirate NCS will be also dissipative with respect to similar supply rate impaired by some additive terms, for the unknown exact discrete-time plant model and in presence of channel uncertainties as well as disturbance inputs. Our result is valid for both the SER and R-SER channel models. Moreover, the stability of the disturbance driven and disturbance free multirate NCS was guaranteed using the notions of input-to-state stability (ISS) and exponential stability, respectively, by deriving explicit conditions on network uncertainties and different sampling rates. We showed that, no matter which channel model is considered, the proposed multirate output feedback NCS can lead to significant saving in the required com-

munication bandwidth compared with the corresponding single-rate NCS. However, simulation results verify that R-SER model exhibits more robustness against the network uncertainties under the same sampling rates pattern.

The followings are some areas that could be pursued in future research.

- **Discrete-time incremental H_∞ controllers:**

We have considered the development of incremental gain-based controllers for continuous time systems. This result can be only applied in the emulation method for sampled-data design where a continuous-time controller is discretized. One important direction that can be followed in future is to present analogous formulations for discrete-time systems. This will enable us to take the advantages of incremental gain in the direct DTD method for nonlinear sampled-data control design as well. Again Lipschitz and one-sided Lipschitz conditions can be employed to derive constructive LMI-based solutions.

- **Multirate nonlinear sampled-data fault detection and isolation:**

Faulty signals can exist in actuators, sensors and process components that can deteriorate normal operation or even lead to instability. Therefore, fault detection and isolation (FDI) has found prominent application in most industrial processes. The main purpose is take immediate and appropriate actions in order to preserve safe operation while avoiding the possibly of catastrophic damages. This problem will be more challenging when input and output signals are sampled at different rates. There exists a large number articles dealing with multirate FDI for linear systems, however, there is no similar work in the literature on the nonlinear counterpart that fully takes the technical bottlenecks of nonlinear sampled-data systems into account. Also, the multirate FDI has been recently proposed as a technique capable of prompt fault detection (see e.g., [33]). Considering these facts, Another interesting subject that can be suggested as a future work is to construct multirate nonlinear FDI. Since we have already developed a framework for multirate sample-data observer design in chapter 6 and the observer-based method is one of the well-know techniques for FDI, this task can be successfully conducted considering our results in this thesis.

- **Observer-based multirate nonlinear NCS:**

Although the dynamic output feedback NCS proposed in chapter 7 possesses a close structure to observer-based control schemes, designing an explicit multirate observer-based nonlinear NCS can be considered as a challenging future work. The new output feedback NCS may contain a partially state/output controller that is fed by a multirate sampled-data observer previously designed using the framework of chapter 6. The most difficult part is to find a way the *separation principle* that is no longer valid for nonlinear systems, by choosing the sampling periods of the observer and controller appropriately. By this means we will obtain a more general form of the results presented in [21,22] which is not restricted to dual-rate case or high-gain observers and is also applicable in the area of networked-control systems.

- **Multirate nonlinear teleoperation control systems:**

Teleoperation or in particular telerobotics is an important application of networked-control systems (NCSs) where there is a teleoperator, a human operator, and a remote environment (communication network). Passivity-based approach has been recently studied in the literature to stabilize teleoperation systems governed by linear equations. Since passivity is a special case of dissipativity and in chapter 7 we have established a general stabilization framework using the theory of dissipativity, another potential perspective is to apply our results to obtain multirate sampled-data teleoperation systems in which teleoperator passivity is maintained under certain sufficient conditions.

- **Multirate event-driven sampled-data control systems:**

Recently, event-triggered control has received a great deal of attention from research community as an effective way to reduce unnecessary energy consumption and save limited network resources. In event-triggered control, the measurement transmission and the control tasks are executed only when a certain predefined event condition is violated. This will be an interesting idea to extend the multirate sampled-data frameworks of this thesis especially the networked-based results to the case of event-triggered systems where several open and challenging issues exist.

Bibliography

- [1] T. Chen and B. Francis, *Optimal Sampled-Data Control Systems*. London: Springer, 1995.
- [2] D. Nesić and A.R. Teel, “Sampled-data control of nonlinear systems: An overview of recent results,” in *Perspective on robust control*. New York: Springer, 2001, pp. 221–239.
- [3] D. S. Laila and D. Nesić and A. Astolfi, “Sampled-data control of nonlinear systems,” in *Advanced Topics in Control Systems Theory: Lecture notes in control and information sciences*. London: Springer-Verlag, 2006, pp. 91–137.
- [4] D. Nesić and A.R. Teel and P.V. Kokotović, “Sufficient conditions for stabilization of sampled-data nonlinear systems via discrete-time approximations,” *Syst. Control Lett.*, vol. 38, pp. 259–270, 1999.
- [5] B. Castillo, S. Di Gennaro, S. Monaco and D. Normand-Cyrot, “On regulation under sampling,” *IEEE Trans. Autom. Control*, vol. 42, pp. 864–868, 1997.
- [6] D.H. Owens, Y. Zheng and S.A. Billings, “Fast sampling and stability of nonlinear sampled-data systems: Part 1. Existence theorems,” *IMA J. Math. Contr. Inform.*, vol. 7, pp. 1–11, 1990.
- [7] A.R. Teel, D. Nesić and P.V. Kokotović, “A note on input-to-state stability of sampled-data nonlinear systems,” in *Proc. of the 37th IEEE Conf. Dec. Control*, Tampa, Florida, 1998, pp. 2473–2478.

- [8] D. Nesić and D.S. Laila, “On preservation of dissipation inequalities under sampling,” in *Proc. 39th IEEE Conf. Dec. Control*, Sydney, Australia, 2000, pp. 2472–2477.
- [9] D. S. Laila and D. Nesić and A. R. Teel, “Open and closed loop dissipation inequalities under sampling and controller emulation,” *European J. of Control*, vol. 8, no. 2, pp. 109–125, 2002.
- [10] D.S. Laila and D. Nesić, “A note on preservation of dissipation inequalities under sampling: the dynamic feedback case,” in *Proc. 2001 Amer. Control Conf.*, Arlington, VA, 2001, pp. 2822–2827.
- [11] D. Nesić and A.R. Teel, “Stabilization of sampled-data nonlinear systems via backstepping on their Euler approximate model,” *Automatica*, vol. 42, pp. 1801–1808, 2006.
- [12] —, “Set stabilization of sampled-data nonlinear differential inclusions via their approximate discrete-time models,” in *Proc. of the 39th IEEE Conf. Dec. Control*, Sydney, Australia, 2000, pp. 2112–2117.
- [13] —, “A framework for stabilization of nonlinear sampled-data systems based on their approximate discrete-time models,” *IEEE Trans. Autom. Control*, vol. 49, no. 7, pp. 1103–1122, 2004.
- [14] V. Feliu, J.A. Cerrada and C. Cerrada, “A method to design multirate controllers for plants sampled at a low rate,” *IEEE Trans. Autom. Control*, vol. 35, pp. 57–60, 1990.
- [15] G. M. Kranc, “Input-output analysis of multirate feedback systems,” *IRE Trans. Autom. Control*, vol. 3, no. 1, pp. 21–28, 1957.
- [16] M. F. Sågfors and H. T. Toivonen, “ H_∞ and LQG control of asynchronous sampled-data systems,” *Automatica*, vol. 33, no. 9, pp. 1663–1668, 1997.
- [17] I. Polushin and H. J. Marquez, “Multirate Versions of Sampled-Data Stabilization of Nonlinear Systems,” *Automatica*, vol. 40, pp. 1035–1041, 2004.

- [18] X. Liu and H. J. Marquez, “Preservation of input-to-state stability under sampling and emulation: multi-rate case,” *Int. J. Control*, vol. 80, no. 12, pp. 1944–1953, 2007.
- [19] X. Liu and H. J. Marquez and Y. Lin, “Input-to-state stabilization for nonlinear dual-rate sampled-data systems via approximate discrete-time model,” *Automatica*, vol. 44, no. 12, pp. 3157–3161, 2008.
- [20] H. Beikzadeh and H. J. Marquez, “Dissipativity of nonlinear multirate sampled-data systems under emulation design,” *Automatica*, vol. 49, pp. 308–312, 2013.
- [21] A. Üstüntürk, “Output feedback stabilization of nonlinear dual-rate sampled-data systems via an approximate discrete-time model,” *Automatica*, vol. 48, no. 8, pp. 1796–1802, 2012.
- [22] J. H. Ahrens and T. Xiaobo and H. K. Khalil, “Multirate sampled-data output feedback control with application to smart material actuated systems,” *IEEE Trans. Autom. Control*, vol. 54, no. 11, pp. 2518–2529, 2009.
- [23] U. Halldorsson and M. Fikar and H. Unbehauen, “Nonlinear predictive control with multirate optimisation step length,” *IEE Proc. Control Theory Appl.*, vol. 152, no. 3, pp. 273–284, 2005.
- [24] I. Izadi and Q. Zhao and T. Chen, “An optimal scheme for fast rate fault detection based on multirate sampled data,” *J. Process Contr.*, vol. 15, no. 3, pp. 307–319, 2005.
- [25] M. Zhong and Y. Hao and S.X. Ding and G. Wang, “Observer-Based Fast Rate Fault Detection for a Class of Multirate Sampled-Data Systems,” *IEEE Trans. Autom. Control*, vol. 52, no. 3, pp. 520–525, 2007.
- [26] Y. Shi and F. Ding and T. Chen, “Multirate crosstalk identification in xDSL systems,” *IEEE Trans. Commun.*, vol. 54, no. 10, pp. 1878–1886, 2006.
- [27] S. C. Kadu and M. Bhushan and R. D. Gudi, “Optimal sensor network design for multirate systems,” *J. Process Contr.*, vol. 18, no. 6, pp. 594–609, 2008.

- [28] T. Chen and P.P. Vaidyanathan, "Recent developments in multidimensional multi-rate systems," *IEEE Trans. Circuits Syst. Video Technol.*, vol. 3, no. 2, pp. 116–137, 1993.
- [29] Y. Yamamoto and H. Fujioka and P.P. Khargonekar, "Signal reconstruction via sampled-data control with multirate filter banks," in *36rd IEEE Conf. Dec. Control*, San Diego, CA, 1997, pp. 3395–3400.
- [30] J. Ding and Y. Shi and H. Wang and F. Ding, "A modified stochastic gradient based parameter estimation algorithm for dual-rate sampled-data systems," *Digit. Signal Process.*, vol. 20, no. 4, pp. 1238–1247, 2010.
- [31] D. Glasson, "Development and applications of multirate digital control," *IEEE Control Syst. Mag.*, vol. 3, pp. 2–8, 1983.
- [32] H. M. Al-Rahmani and G. F. Franklin, "Techniques in multirate digital control," *Control and Dynamic System*, vol. 70, pp. 1–24, 1995.
- [33] I. Izadi, T. Chen and Q. Zhao, " H_∞ performance comparison of single-rate and multirate sampled-data systems," in *Proc. 2006 Amer. Control Conf.*, Minneapolis, MN, 2006, pp. 183–187.
- [34] T. Chen and L. Qiu, " H_∞ design of general multirate sampled-data control systems," *Automatica*, vol. 30, no. 7, pp. 1139–1152, 1994.
- [35] M. F. Sãgfors and H. T. Toivonen and B. Lennartson, " H_∞ control of multirate sampled-data systems: A state space approach," *Automatica*, vol. 34, no. 4, pp. 415–428, 1998.
- [36] S. Longhi, "Structural properties of multirate sampled-data systems," *IEEE Trans. Autom. Control*, vol. 39, pp. 692–696, 1994.
- [37] D.G. Meyer, "A parametrization of stabilizing controllers for multirate sampled-data systems," *IEEE Trans. Autom. Control*, vol. 35, pp. 233–236, 1990.
- [38] A.M. Azad, T. Hesketh, " H_∞ -optimal control of multi-rate sampled-data systems," in *Proc. 2002 Amer. Control Conf.*, Anchorage, AK, 2002, pp. 459–464.

- [39] A.J. van der Schaft, “ L_2 -gain Analysis of Nonlinear Systems and Nonlinear State Feedback H_∞ Control,” *IEEE Trans. Autom. Control*, vol. 37, pp. 770–784, 1992.
- [40] —, “ L_2 -gain and passivity techniques in nonlinear control,” in *Communications and Control Engineering series*. London: Springer-Verlag, 2000.
- [41] W. Lin and C. I. Byrnes, “ H_∞ -control of discrete-time nonlinear systems,” *IEEE Trans. Autom. Control*, vol. 41, pp. 494–510, 1996.
- [42] H.D. Tuan and S. Hosoe, “On robust H_∞ control for nonlinear discrete and sampled-data systems,” *IEEE Trans. Autom. Control*, vol. 43, pp. 715–718, 1998.
- [43] S.K. Nguang and P. Shi, “ H_∞ control of nonlinear sampled-data systems,” in *Proc. 1999 Amer. Control Conf.*, San Diego, CA, 1999, pp. 1289–1293.
- [44] J.C. Willems, “Dissipative dynamical systems: part I, part II,” *Arch. Ration. Mech. Anal.*, vol. 45, pp. 321–393, 1972.
- [45] G. Zames, “On the input-output stability of time-varying nonlinear feedback systems Part I: Conditions derived using concepts of loop gain, conicity, and positivity,” *IEEE Trans. Autom. Control*, vol. AC-11, pp. 228–238, 1966.
- [46] I.W. Sandberg, “On the L_2 -boundedness of solutions of nonlinear functional equations,” *Bell Syst. Tech. J.*, vol. 43, pp. 1581–1599, 1964.
- [47] C.A. Desoer and M. Vidyasagar, *Feedback Systems: Input-Output Properties*. New York: Academic Press, 1975.
- [48] M. Vidyasagar, *Nonlinear Systems Analysis*. NJ: Prentice-Hall, Englewood Cliffs, 1993.
- [49] H.J. Marquez, *Nonlinear Control Systems: Analysis and Design*. New York: Wiley, 2003.
- [50] G. Zames, “Feedback and optimal sensitivity: Model reference transformations, multiplicative seminorms and approximate inverse,” *IEEE Trans. Autom. Control*, vol. AC-26, pp. 301–320, 1981.

- [51] T.T. Georgiou, “Differential stability and robust control of nonlinear systems,” *Math. Control Signals Systems*, vol. 6, pp. 289–306, 1993.
- [52] T.T. Georgiou and M.C. Smith, “Robustness analysis of nonlinear feedback systems: An input-output approach,” *IEEE Trans. on Automatic Control*, vol. 42, pp. 1200–1221, 1997.
- [53] D. Angeli, “A Lyapunov approach to incremental stability properties,” *IEEE Trans. Autom. Control*, vol. 47, pp. 410–421, 2002.
- [54] Q.-C. Pham, N. Tabareau, and J.-J. Slotine, “A contraction theory approach to stochastic incremental stability,” *IEEE Trans. Autom. Control*, vol. 54, pp. 816–820, 2009.
- [55] Y. Chitour, W. Liu, and E.D. Sontag, “On the continuity and incremental-gain properties of certain saturated linear feedback loops,” *Int. J. Robust Nonlinear Control*, vol. 5, pp. 413–440, 1995.
- [56] B.G. Romanchuk and M.R. James, “Characterization of the incremental L_p gain for nonlinear systems,” in *Proc. of the 36th IEEE Conf. Dec. Control*, Kobe, Japan, 1996, pp. 3270–3275.
- [57] B.G. Romanchuk, “Analytic comparison of nonlinear H_∞ bounding techniques for low order systems with saturation,” in *Proc. of the 34th IEEE Conf. Dec. Control*, New Orleans, LA, 1995, pp. 963–968.
- [58] B.G. Romanchuk and M.C. Smith, “Incremental gain analysis of piecewise linear systems and application to the antiwindup problem,” *Automatica*, vol. 35, pp. 1275–1283, 1999.
- [59] G.-D. Hu, “Observers for one-sided Lipschitz non-linear systems,” *IMA J. Math. Control Inform.*, vol. 23, pp. 395–401, 2006.
- [60] —, “A note on observer for one-sided Lipschitz non-linear systems,” *IMA J. Math. Control Inform.*, vol. 25, no. 3, pp. 297–303, 2008.
- [61] Y. Zhao and J. Tao and N.-Z. Shi, “A note on observer design for one-sided Lipschitz nonlinear systems,” *Syst. Control Lett.*, vol. 59, pp. 66–71, 2010.

- [62] F. Fu and M. Hou and G. Duan, “Stabilization of quasi-one-sided Lipschitz nonlinear systems,” *IMA J. Math. Control Inform.*, vol. 30, pp. 169–184, 2013.
- [63] M. Abbaszadeh and H. J. Marquez, “Nonlinear observer design for one-sided Lipschitz systems,” in *2010 Amer. Control Conf.*, Baltimore, MD, 2010, pp. 5284–5289.
- [64] W. Zhang and H.S. Su and Y. Liang and Z.-Z. Han, “Non-linear observer design for one-sided Lipschitz systems: An linear matrix inequality approach,” *IET Control Theory Appl.*, vol. 6, no. 9, pp. 1297–1303, 2012.
- [65] M. Benallouch and M. Boutayeb and M. Zasadzinski, “Observer design for one-sided Lipschitz discrete-time systems,” *Syst. Control Lett.*, vol. 61, pp. 879–886, 2012.
- [66] A. Radke and Z. Gao, “A Survey of State and Disturbance Observers for Practitioners,” in *2006 Amer. Control Conf.*, Minneapolis, MN, 2006, pp. 5183–5188.
- [67] P.E. Moraal and J.W. Grizzle, “Observer design for nonlinear systems with discrete-time measurements,” *IEEE Trans. Autom. Control*, vol. 40, no. 3, pp. 295–404, 1995.
- [68] E. Biyik and M. Arcak, “A hybrid redesign of Newton observers in the absence of an exact discrete-time model,” *Syst. Control Lett.*, vol. 55, no. 6, pp. 429–436, 2006.
- [69] A. M. Dabroom and H. K. Khalil, “Output feedback sampled-data control of nonlinear systems using high-gain observers,” *IEEE Trans. Autom. Control*, vol. 46, no. 11, pp. 1712–1725, 2001.
- [70] M. Arcak and D. Nesić, “A framework for nonlinear sampled-data observer design via approximate discrete-time models and emulation,” *Automatica*, vol. 40, no. 11, pp. 1931–1938, 2004.
- [71] M. Arcak and P.V. Kokotović, “Nonlinear observers: a circle criterion design and robustness analysis,” *Automatica*, vol. 37, no. 12, pp. 1923–1930, 2001.
- [72] A. Alessandri, “Observer design for nonlinear systems by using input-to-state stability,” in *43rd IEEE Conf. Dec. Control*, Atlantis, Bahamas, 2004, pp. 3892–3897.
- [73] H. Ishii and B. A. Francis, *Limited Data Rate in Control Systems with Networks*. Berlin: Springer-Verlag, 2002.

- [74] P. Örgren and E. Fiorelli and N. E. Leonard, “Cooperative control of mobile sensor networks: Adaptive gradient climbing in a distributed environment,” *IEEE Trans. Autom. Control*, vol. 49, pp. 1292–1302, 2004.
- [75] P. Seiler and R. Sengupta, “Analysis of communication losses in vehicle control problems,” in *Proc. 2001 Amer. Control Conf.*, Arlington, VA, 2001, pp. 1491–1496.
- [76] —, “An H_∞ approach to networked control,” *IEEE Trans. Autom. Control*, vol. 50, pp. 356–364, 2005.
- [77] L. Moreau, “Stability of multiagent systems with time-dependent communication links,” *IEEE Trans. Autom. Control*, vol. 50, no. 2, pp. 169–182, 2005.
- [78] P. J. Antsaklis, “Special issue on networked control systems,” *IEEE Trans. Autom. Control*, vol. 49, no. 9, 2004.
- [79] —, “Special issue on technology of networked control systems,” *Proc. IEEE*, vol. 95, no. 1, pp. 5–8, 2007.
- [80] Y. Tipsuwan and M. Chow, “Control methodologies in networked control systems,” *Control Engg. Practice*, vol. 11, no. 10, pp. 1099–1111, 2003.
- [81] J. P. Hespanha and P. Naghshtabrizi and Y. Xu, “A survey of recent results in networked control systems,” *Proc. IEEE*, vol. 95, no. 1, pp. 138–162, 2007.
- [82] M. Yu and L. Wang and T. Chu, “Sampled-data stabilisation of networked control systems with nonlinearity,” *IEE Proc. Control Theory Appl.*, vol. 152, no. 6, pp. 609–614, 2005.
- [83] J. Cao and S. Zhong and Y. Hu, “Novel delay-dependent stability conditions for a class of MIMO networked control systems with nonlinear perturbations,” *Appl. Math. Comput.*, vol. 197, no. 2, pp. 797–809, 2008.
- [84] D. Muñoz de la Peña and P. D. Christofides, “Lyapunov-based model predictive control of nonlinear systems subject to data losses,” *IEEE Trans. Autom. Control*, vol. 53, no. 9, pp. 2076–2089, 2008.

- [85] A. V. Savkin and T. M. Cheng, “Detectability and output feedback stabilizability of nonlinear networked control systems,” *IEEE Trans. Autom. Control*, vol. 52, no. 4, pp. 730–735, 2007.
- [86] T. M. Cheng and A. V. Savkin, “Output feedback stabilisation of nonlinear networked control systems with non-decreasing nonlinearities,” in *Proc. 2006 Amer. Control Conf.*, Minneapolis, MN, 2006, pp. 2795–2800.
- [87] W. P. M. H. Heemels and A. R. Teel and N. van de Wouw and D. Nesić, “Networked control systems with communication constraints: tradeoffs between transmission intervals, delays and performance,” *IEEE Trans. Autom. Control*, vol. 55, no. 8, pp. 1781–1796, 2010.
- [88] D. Nesić and A. R. Teel, “Input-output stability properties of networked control systems,” *IEEE Trans. Autom. Control*, vol. 49, no. 10, pp. 1650–1667, 2004.
- [89] G. C. Walsh and O. Belidman and L. G. Bushnell, “Asymptotic behavior of nonlinear networked control systems,” *IEEE Trans. Autom. Control*, vol. 46, no. 7, pp. 1093–1097, 2001.
- [90] I. G. Polushin and P. X. Liu and C.-H. Lung, “On the model-based approach to nonlinear networked control systems,” *Automatica*, vol. 44, no. 9, pp. 2409–2414, 2008.
- [91] N. van de Wouw and D. Nesić and W. P. M. H. Heemels, “A discrete-time framework for stability analysis of nonlinear networked control systems,” *Automatica*, vol. 48, no. 6, pp. 1144–1153, 2012.
- [92] M. C. F. Donkers and W. P. M. H. Heemels and N. van de Wouw and L. Hetel, “Stability analysis of networked control systems using a switched linear systems approach,” *IEEE Trans. Autom. Control*, vol. 56, no. 9, pp. 2101–2115, 2011.
- [93] L. A. Montestruque, P. J. Antsaklis, “On the model based control of networked control systems,” *Automatica*, vol. 39, no. 10, pp. 1837–1843, 2003.

- [94] —, “Networked control systems: A model-based approach,” in *The Handbook of networked and embedded systems*, Hristu and Levine ed. Boston: Birkhauser, 2005, pp. 601–626,.
- [95] H. Ishii and S. Hara, “A subband coding approach to control under limited data rates and message losses,” *Automatica*, vol. 44, no. 4, pp. 1141–1148, 2008.
- [96] Y. Zou and T. Chen and S. Li, “Network-based predictive control of multirate systems,” *IET Control Theory and Appl.*, vol. 4, no. 7, pp. 1145–1156, 2010.
- [97] W. Chen and L. Qiu, “Stabilization of networked control systems with multirate sampling,” *Automatica*, vol. 49, no. 6, pp. 1528–1537, 2013.
- [98] L. Qiu and W. Chen, “Stabilization of networked multi-input systems with channel resource allocation,” *IEEE Trans. Autom. Control*, vol. 58, no. 3, pp. 554–568, 2013.
- [99] B. Brogliato and R. Lozano and B. Maschke and O. Egeland, *Dissipative Systems Analysis and Control. Theory and Applications*, 2nd ed. London: Springer Verlag, 2007.
- [100] E.D. Sontag and Y. Wang, “On characterizations of the input-to-state stability property,” *Syst. Control Lett.*, vol. 24, no. 5, pp. 351–359, 1995.
- [101] K. Dekker and J. G. Verwer, *Stability of Runge-Kutta Methods for Stiff Nonlinear Differential Equation*. North-Holland, 1984.
- [102] J.A. Ball, J.W. Helton and M. Walker, “ H_∞ control for nonlinear systems via output feedback,” *IEEE Trans. Autom. Control*, vol. AC-38, pp. 546–559, 1993.
- [103] R. Raoufi, “Nonlinear robust observers for simultaneous state and fault estimation,” Ph.D. dissertation, Department of Electrical and Computer Engineering, University of Alberta, Edmonton, Canada, 2010.
- [104] M. Arcak and P.V. Kokotović, “Observer-based control of systems with slope-restricted nonlinearities,” *IEEE Trans. Autom. Control*, vol. 46, pp. 1146–1150, 2001.
- [105] L.O. Chua, C.A. Desoer, and E.S. Kuh, *Linear and Nonlinear Circuits*. New York: McGraw-Hill, 1987.

- [106] C.-H. Lien, K.-W. Yu, Y.-F. Lin, Y.-J. Chung, and L.-Y. Chung, “Robust reliable H_∞ control for uncertain nonlinear systems via LMI approach,” *Appl. Math. Comput.*, vol. 198, pp. 453–462, 2008.
- [107] M. Rehan, K.-S. Hong, and S.S. Ge, “Stabilization and tracking control for a class of nonlinear systems,” *Nonlinear Anal.-Real*, vol. 12, pp. 1786–1796, 2011.
- [108] M. Abbaszadeh and H.J. Marquez, “LMI optimization approach to robust H_∞ observer design and static output feedback stabilization for discrete-time nonlinear uncertain systems,” *Int. J. Robust Nonlinear Control*, vol. 19, pp. 313–340, 2009.
- [109] Y. Wang, L. Xie, and C.E. de Souza, “Robust control of a class of uncertain nonlinear systems,” *Syst. Control Lett.*, vol. 19, pp. 139–149, 1992.
- [110] S.P. Boyd, L.E. Ghaoufi, E. Feron, and V. Balakrishnan, *Linear Matrix Inequalities in System and Control Theory*. Philadelphia: SIAM, 1994.
- [111] M. Abbaszadeh and H.J. Marquez, “Robust H_∞ observer design for sampled-data Lipschitz nonlinear systems with exact and Euler approximate models,” *Automatica*, vol. 44, pp. 799–806, 2008.
- [112] P.P. Khargonekar, I.R. Petersen, and K. Zhou, “Robust stabilization of uncertain linear systems: Quadratic stabilizability and H_∞ control theory,” *IEEE Trans. on Automatic Control*, vol. 35, pp. 356–361, 1998.
- [113] S. Xu, “Robust H_∞ filtering for a class of discrete-time uncertain nonlinear systems with state delay,” *IEEE Trans. Circuits Syst. I, Fundam. Theory Appl.*, vol. 49, pp. 1853–1859, 2002.
- [114] A. Howell and J.K. Hedrick, “Nonlinear observer design via convex optimization,” in *2002 Amer. Control Conf.*, Anchorage, AK, 2002, pp. 2088–2093.
- [115] G.-Q. Zhong, “Implementation of Chua’s circuit with a cubic nonlinearity,” *IEEE Trans. Circuits Syst. I, Fundam. Theory Appl.*, vol. 41, no. 12, pp. 934–941, 1994.
- [116] J. Hauser and S. Sastry and G. Meyer, “Nonlinear control design for slightly non-minimum phase systems: Application to V/STOL aircraft,” *Automatica*, vol. 28, no. 4, pp. 665–679, 1992.

- [117] K. D. Do and Z. P. Jiang and J. Pan, “On global tracking control of a VTOL aircraft without velocity measurements,” *IEEE Trans. Autom. Control*, vol. 48, no. 12, pp. 2212–2217, 2003.
- [118] C. I. Byrnes and W. Lin, “Losslessness, feedback equivalence, and the global stabilization of discrete-time nonlinear systems,” *IEEE Trans. Autom. Control*, vol. 39, no. 1, pp. 83–98, 1994.
- [119] N. Elia and S. Mitter, “Stabilization of linear systems with limited information,” *IEEE Trans. Autom. Control*, vol. 46, no. 9, pp. 1384–1400, 2001.
- [120] A. M. Stuart and A. R. Humphries, *Dynamical Systems and Numerical Analysis*. Cambridge: Cambridge University Press, 1996.
- [121] N. van de Wouw and D. Nesić and W. P. M. H. Heemels, “A discrete-time framework for stability analysis of nonlinear networked control systems,” Eindhoven University of Technology, Tech. Rep. D&C.2010.043, 2010.